VOLUME II

DIAGENETIC PROCESSES IN ORE FORMATION WITH SPECIAL REFERENCE TO THE ZAMBIAN COPPERBELT AND PERMIAN MARL SLATE

(2 VOLUMES)

BY

MICHAEL ALEXANDER SWEENEY

Thesis submitted for the degree of

Doctor of Philosophy

at the

University of Aston in Birmingham

February 1985

VOLUME II

LIST OF TABLES

FIGURES

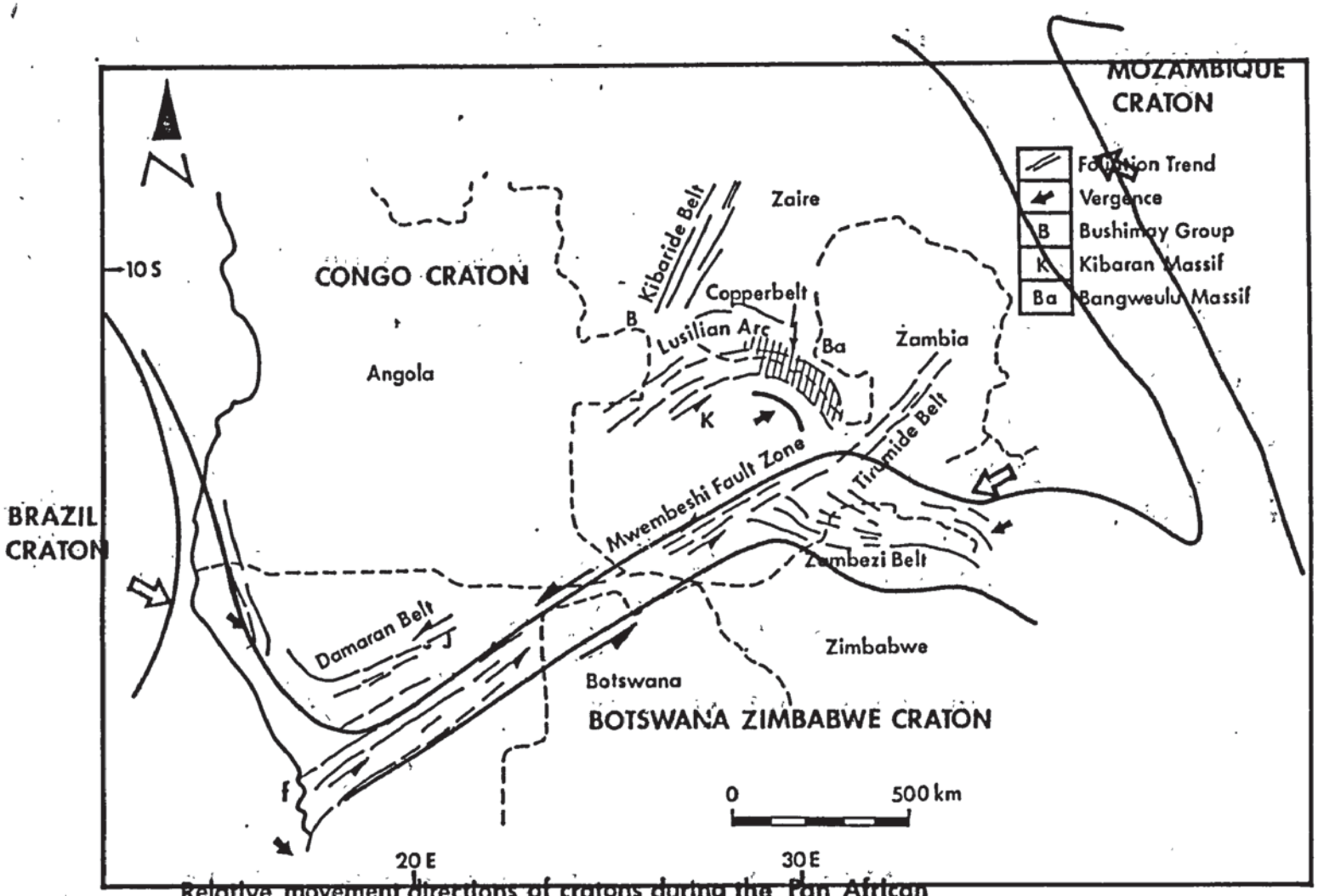

Relative movement directions of cratons during the Pan African

Fig. 2.1 Location of the Copperbelt in relation to tectonic structures, showing the different shear senses and movement directions. (Modified after Coward and Daly, 1984)

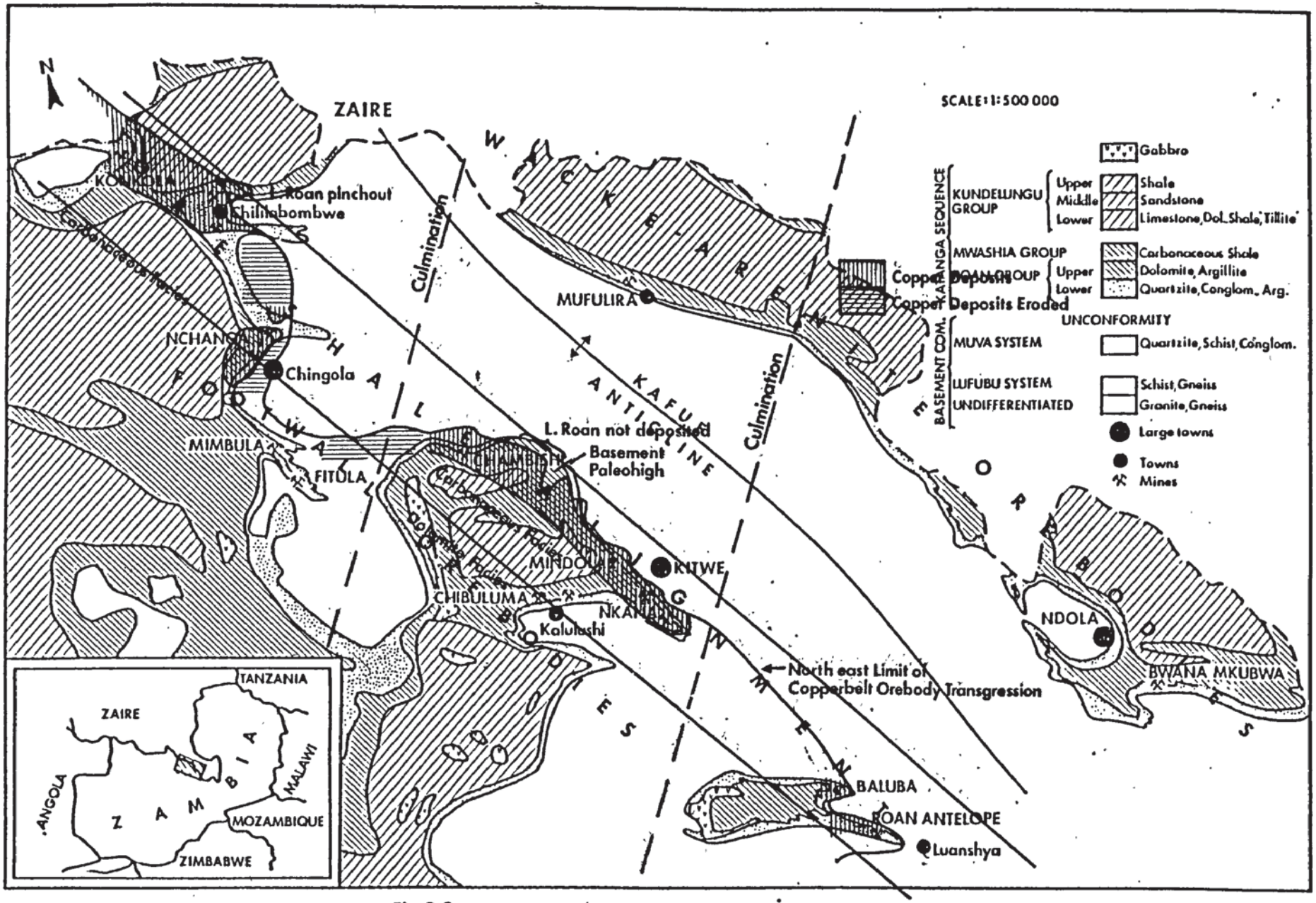

Fig 2.2 Geological Map of the Zambian Copperbelt

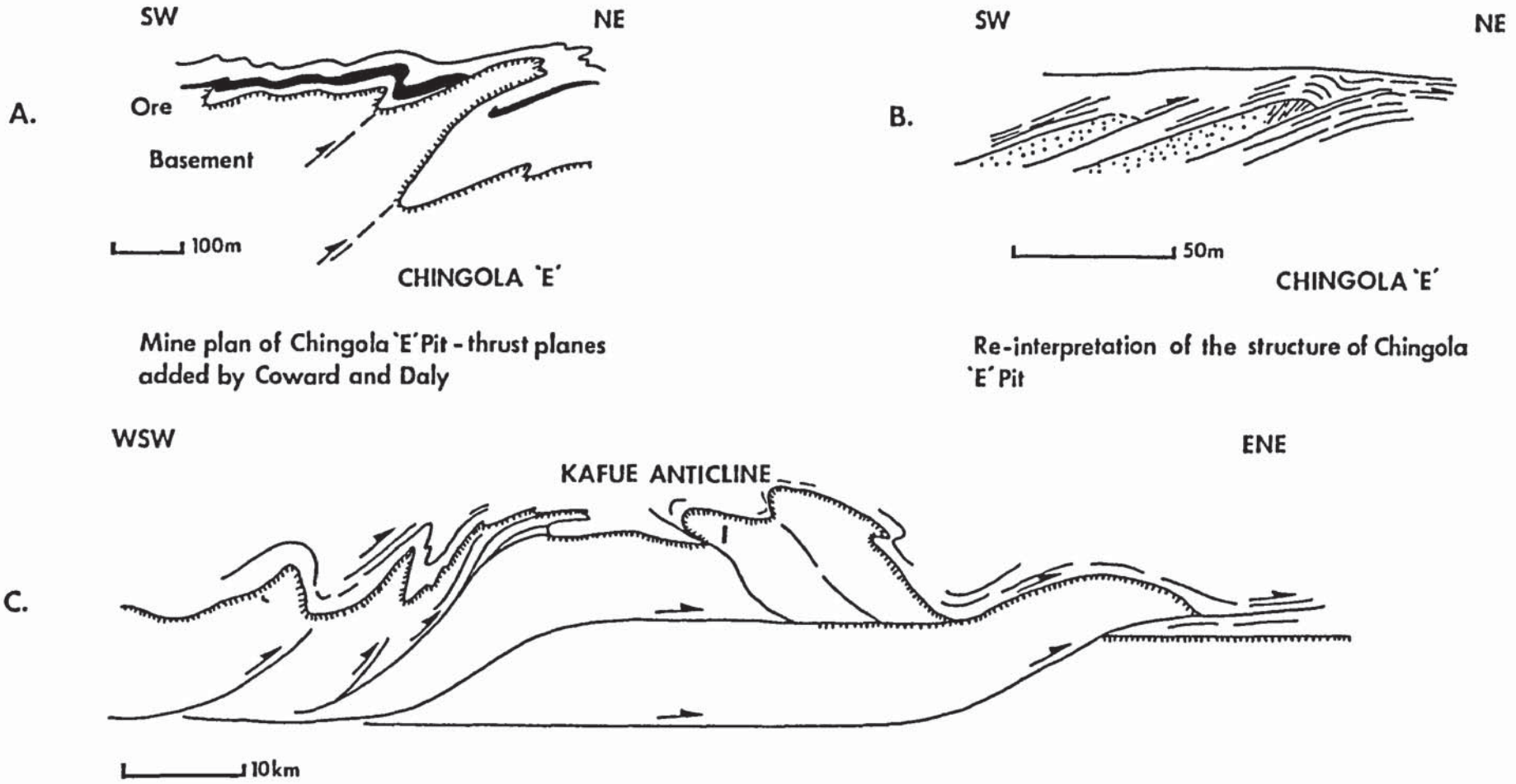

Mine plan of Chingola 'E' Pit - thrust planes added by Coward and Daly

Re-interpretation of the structure of Chingola 'E' Pit

Cross section through the Kafue Anticline showing the anticline to be the product of uplift on thrust ramps

Fig. 2.3

Re-interpretation of Copperbelt structures in terms of a thrusting model (after Coward and Daly, 1984)

YORK-WILLIAMSON LEAST SQUARES FIT

Line	87Rb/86Sr	s.d.	87Sr/86Sr	s.d.	rho	Wresidual	Sample
1	10.2506	.0513	.812140	.000081	0.00	.1	337/5a
2	13.2810	.0664	.838122	.000084	0.00	40.2	337/5b
3	9.4147	.0471	.805412	.000081	0.00	.8	337/6
4	4.5287	.0226	.768792	.000077	0.00	.1	337/7
5	17.5556	.0878	.863859	.000086	0.00	24.3	337/8
6	14.8334	.0742	.846180	.000085	0.00	.6	377/9

No. of cycles 3
Centroid is 7.795 0.79351
Slope= 0.007545 ±0.000034(1-sigma)
Intercept= 0.734695 ± 0.000604(2-sigma)
MSWD= 16.52
AGE= 529.34 ± 4.81 Ma (2-sigma)

DATA STORED UNDER FILENAME MIKE/S

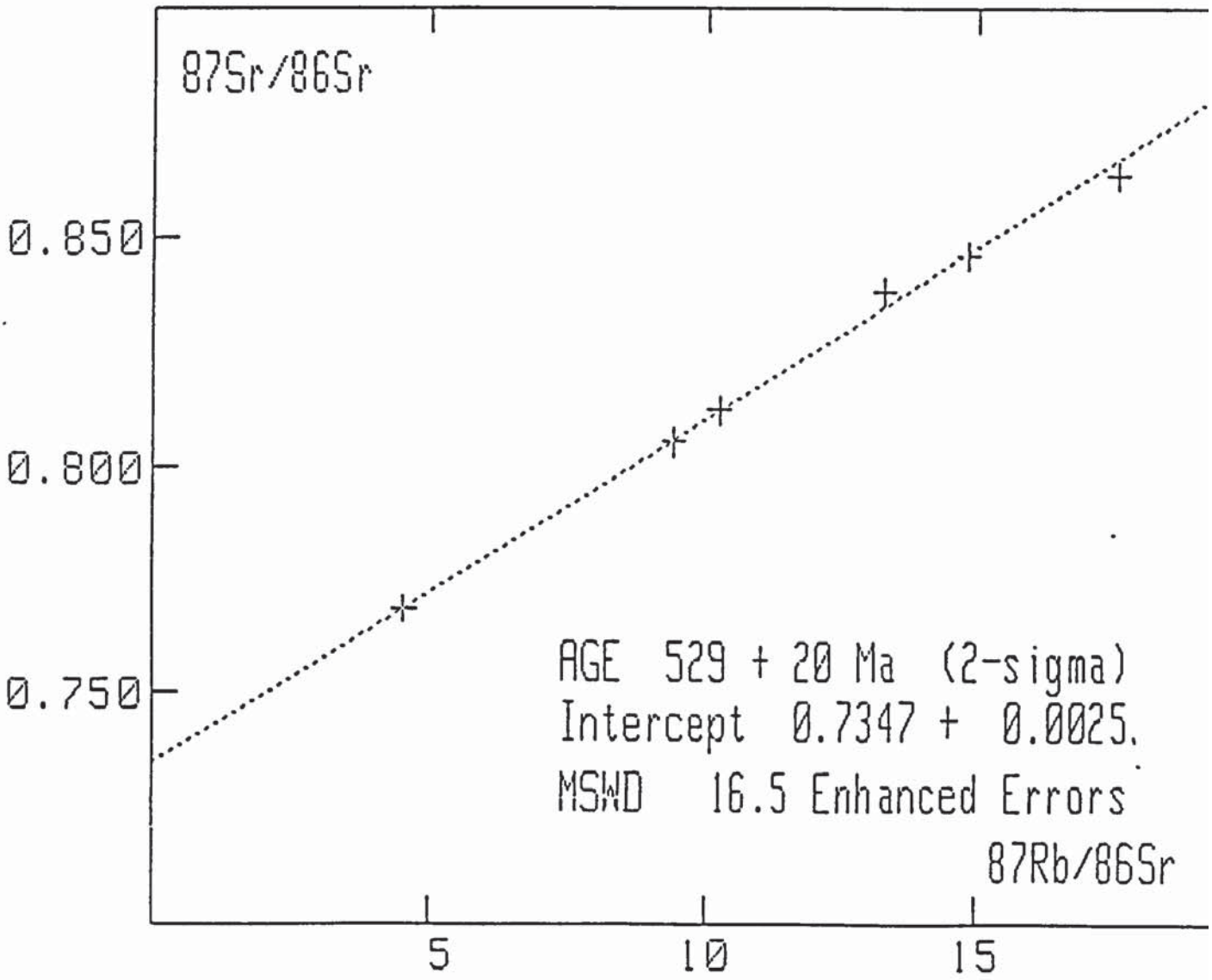

Figure 2.4 Rb-Sr isochron diagram for samples of Ore-Shale

YORK-WILLIAMSON LEAST SQUARES FIT

Line	87Rb/86Sr	s.d.	87Sr/86Sr	s.d.	rho	Wresidual	Sample
1	10.2506	.0513	.812140	.000081	0.00	.1	337/5a
2	13.2810	.0664	.838122	.000084	0.00	40.2	337/5b
3	9.4147	.0471	.805412	.000081	0.00	.8	337/6
4	4.5287	.0226	.768792	.000077	0.00	.1	337/7
5	17.5556	.0878	.863859	.000086	0.00	24.3	337/8
6	14.8334	.0742	.846180	.000085	0.00	.6	377/9

No. of cycles 3
Centroid is 7.795 0.79351
Slope= 0.007545 ±0.000034(1-sigma)
Intercept= 0.734695 ± 0.000604(2-sigma)
MSWD= 16.52
AGE= 529.34 ± 4.81 Ma (2-sigma)

DATA STORED UNDER FILENAME MIKE/S

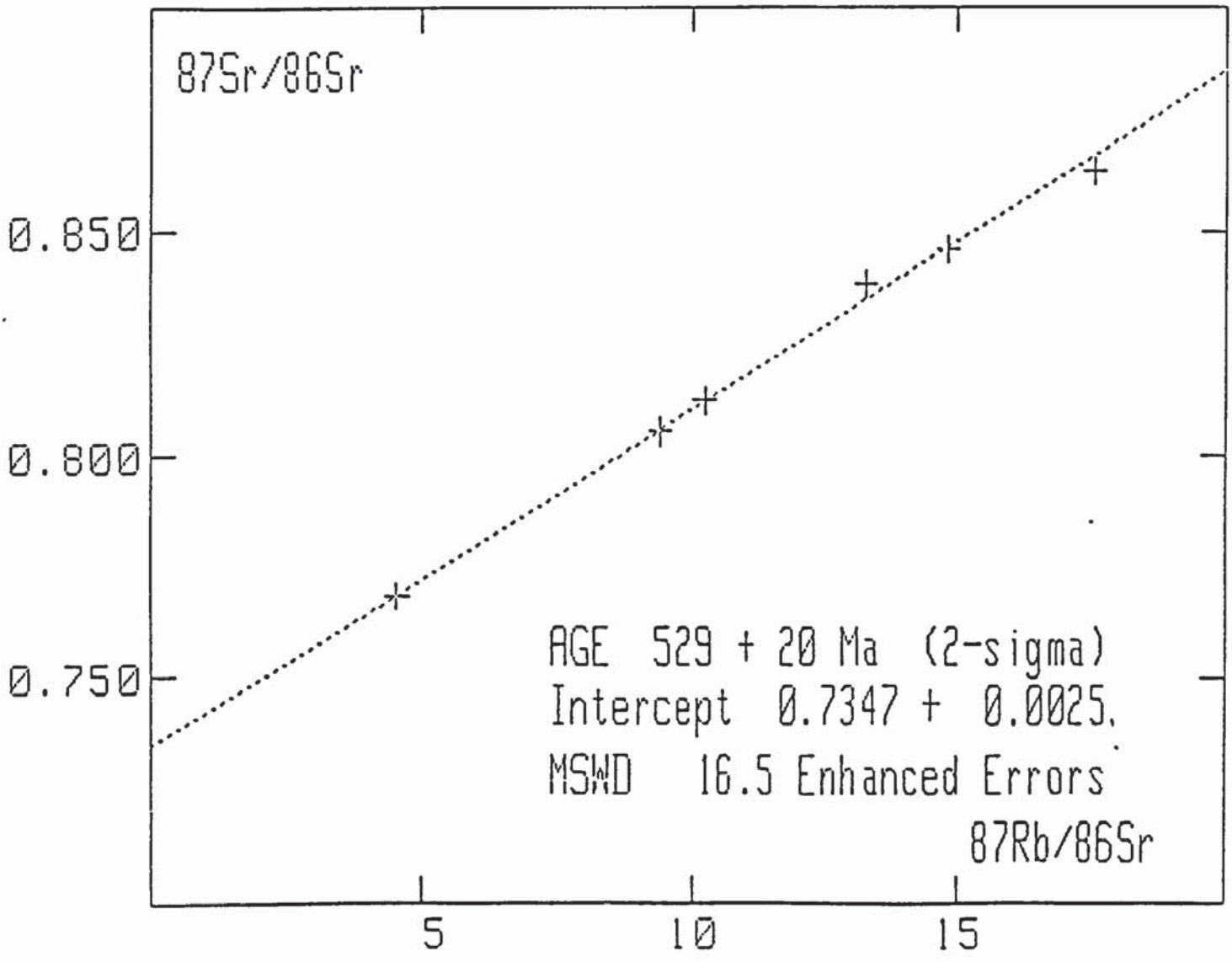

Figure 2.4 Rb-Sr isochron diagram for samples of Ore-Shale

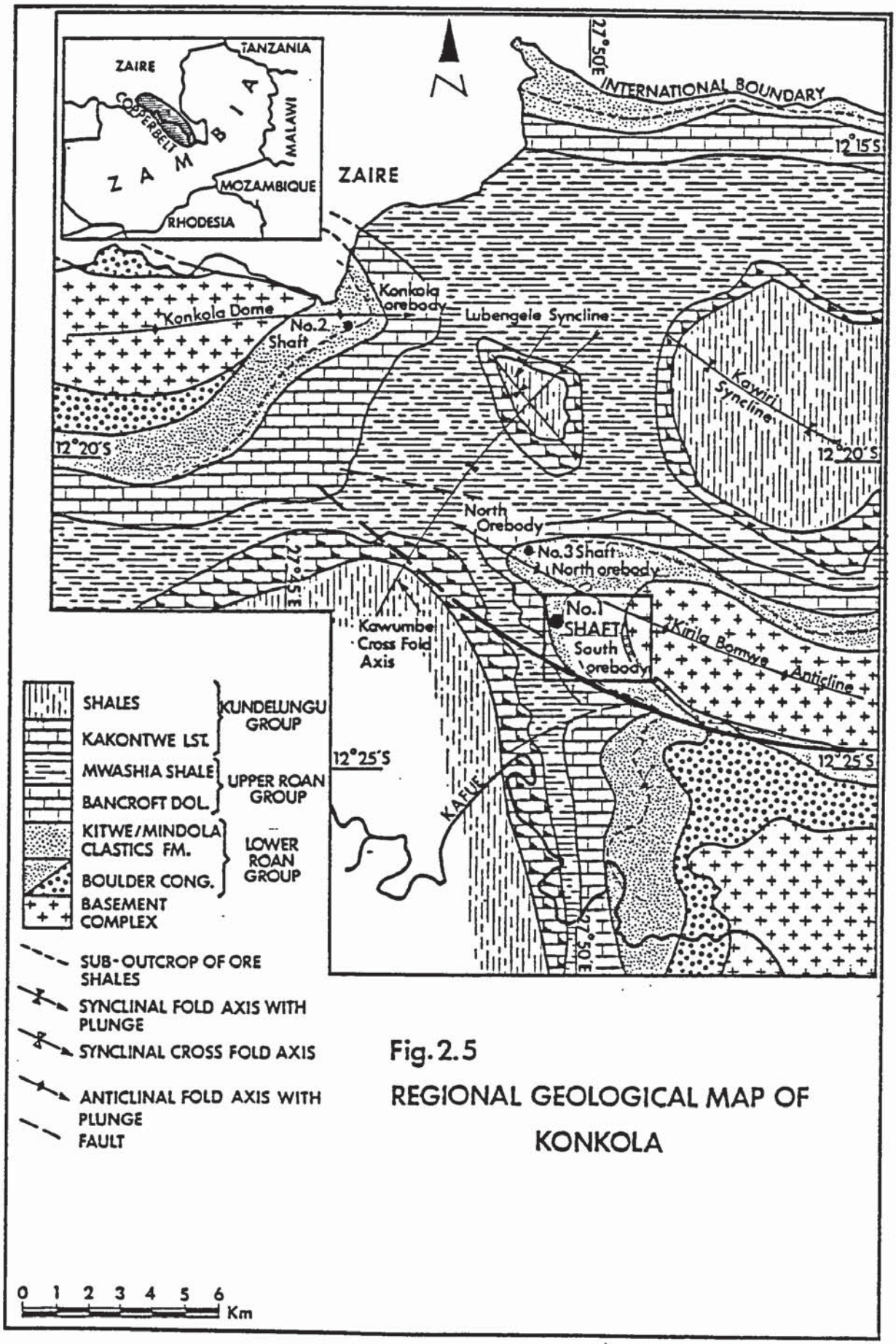

Fig. 2.5

REGIONAL GEOLOGICAL MAP OF KONKOLA

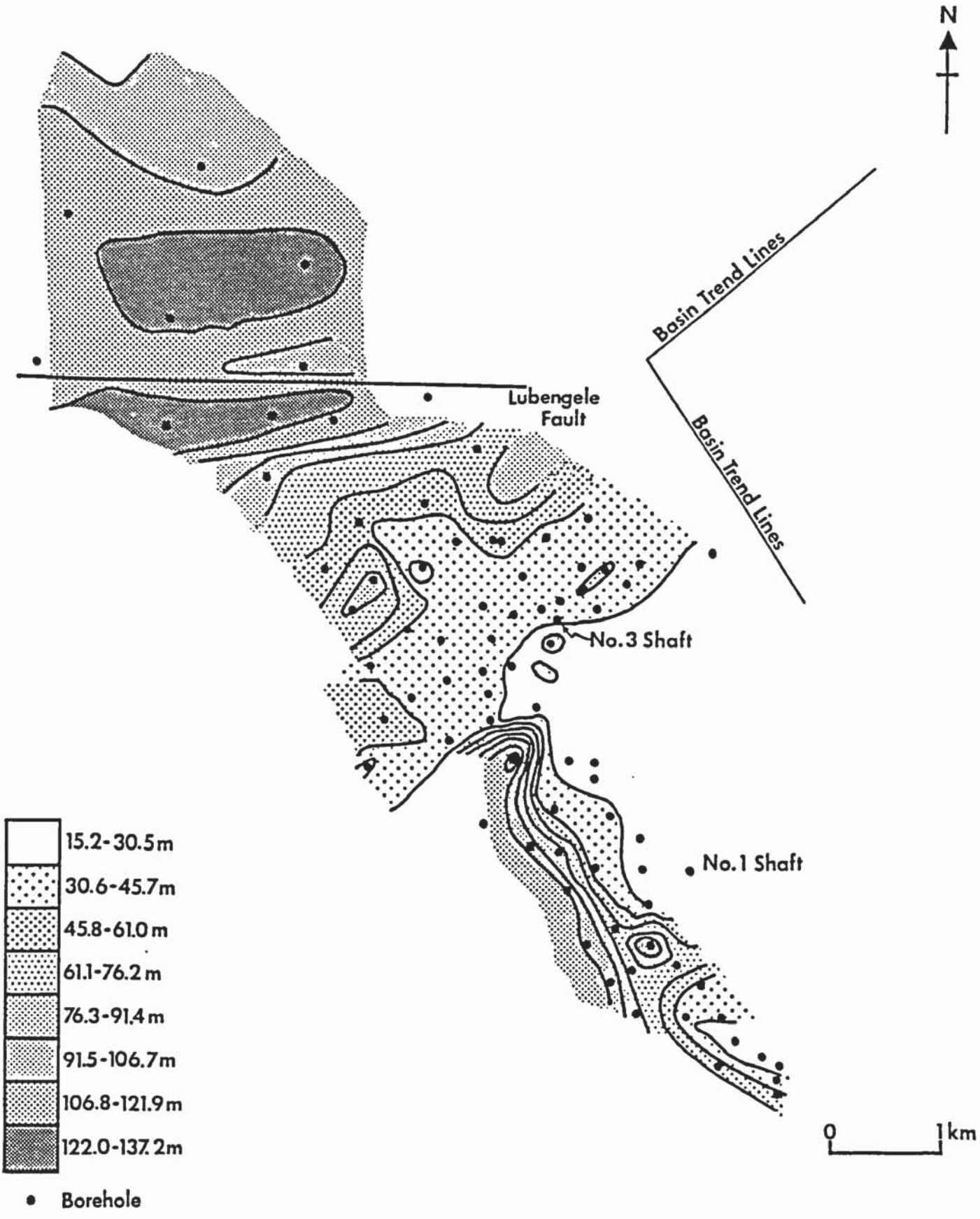

Fig. 2.6

Isopach map of the Hangingwall Quartzite (Nchanga Quartzite Member) after Naish, 1973

Formation		Lithology	Tectono-Thermal Event	Effect of Tectono-Thermal Event
Kundelungu	U	Shale	Lifilian Orogeny 656-456 Ma	Regional deformation and metamorphism. Production of drag folds and thrusting (duplication at the south Orebody). Bedding parallel thrusting and folding of the Hangingwall Aquifer.
	M	Sandstone	Lusakan Folding 840 Ma	
	L	Limestone	Lomanian Orogeny 950 Ma	
Upper Roan		Tillite Mwashia Sh. Upper Roan Dolomite		General 'tightening' of depositional basins. Development of joint pattern minor faulting and formation of pegmatites (840 Ma).
		Shale with Grit Upper Hangingwall Aquifer Lower Hangingwall Aquifer Hangingwall Quartzite Ore Shale	1055 Ma	Possible movement along Luansobe and Lubengele faults.
	5	Footwall Conglomerate Footwall Sst	Basin subsidence, possibly tectonically influenced, along Basement controlled directions.	Marked effect on sedimentation, pinchouts againts palaeohighs, subsidence reflected in isopachyte pattern. Slump folding soft sediment boudination and slide sheets occur. Numerous depositional unconformities.
	4	Porous Conglomerate		
	3	Argillaceous Sst. Footwall Quartzite		
	2	Lower Porous Conglomerate		
	1	Boulder Conglomerate		
Basement Complex		Muva Lufuba Granites	Kibaran (Irumide 1310 Ma) resulting in NE trending folds Formation of N-NW trending hills and valleys.	Syntaxis of Basement deformation controlled the location and extent of Roan depositional basins.

Figure 2.7 Generalised chronology and effect of Tectono-Thermal Events.

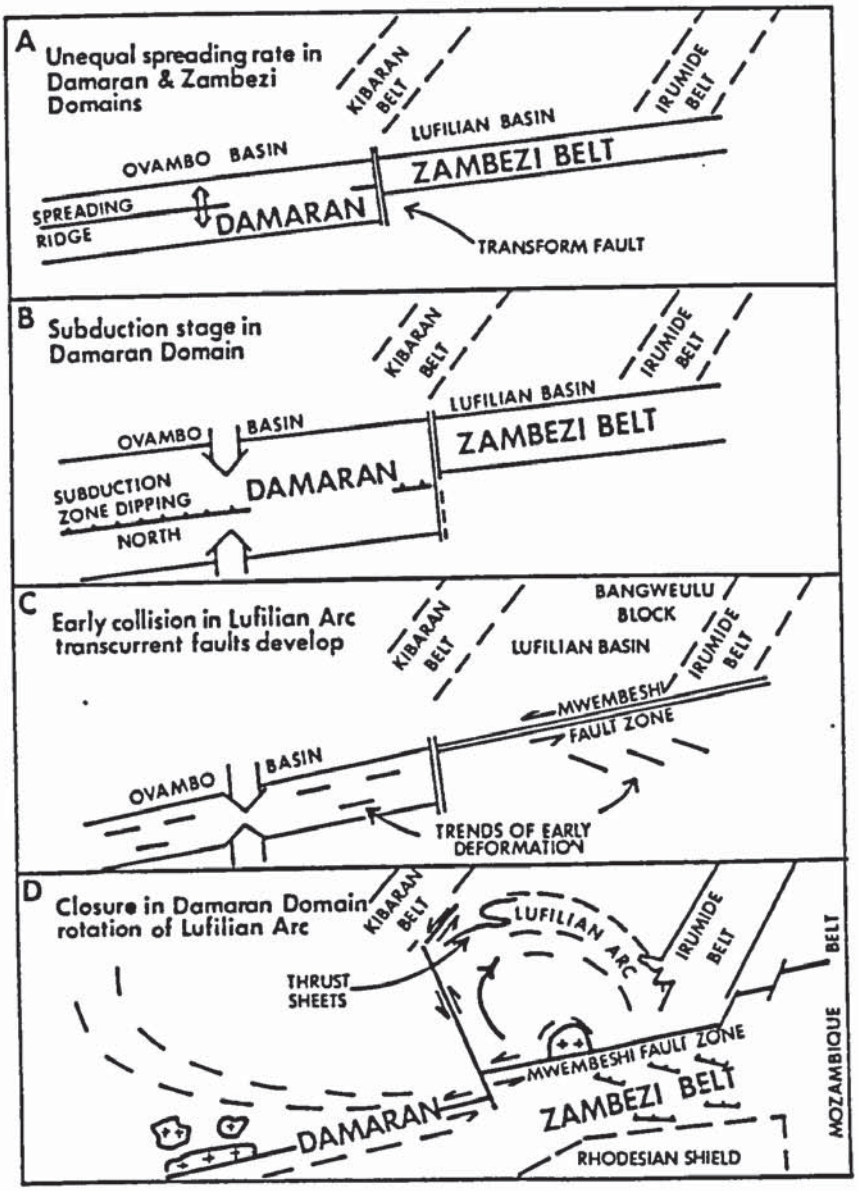

Fig. 2.8

Reconstruction of events leading to the formation of the Lufilian Arc (after Unrug 1983)

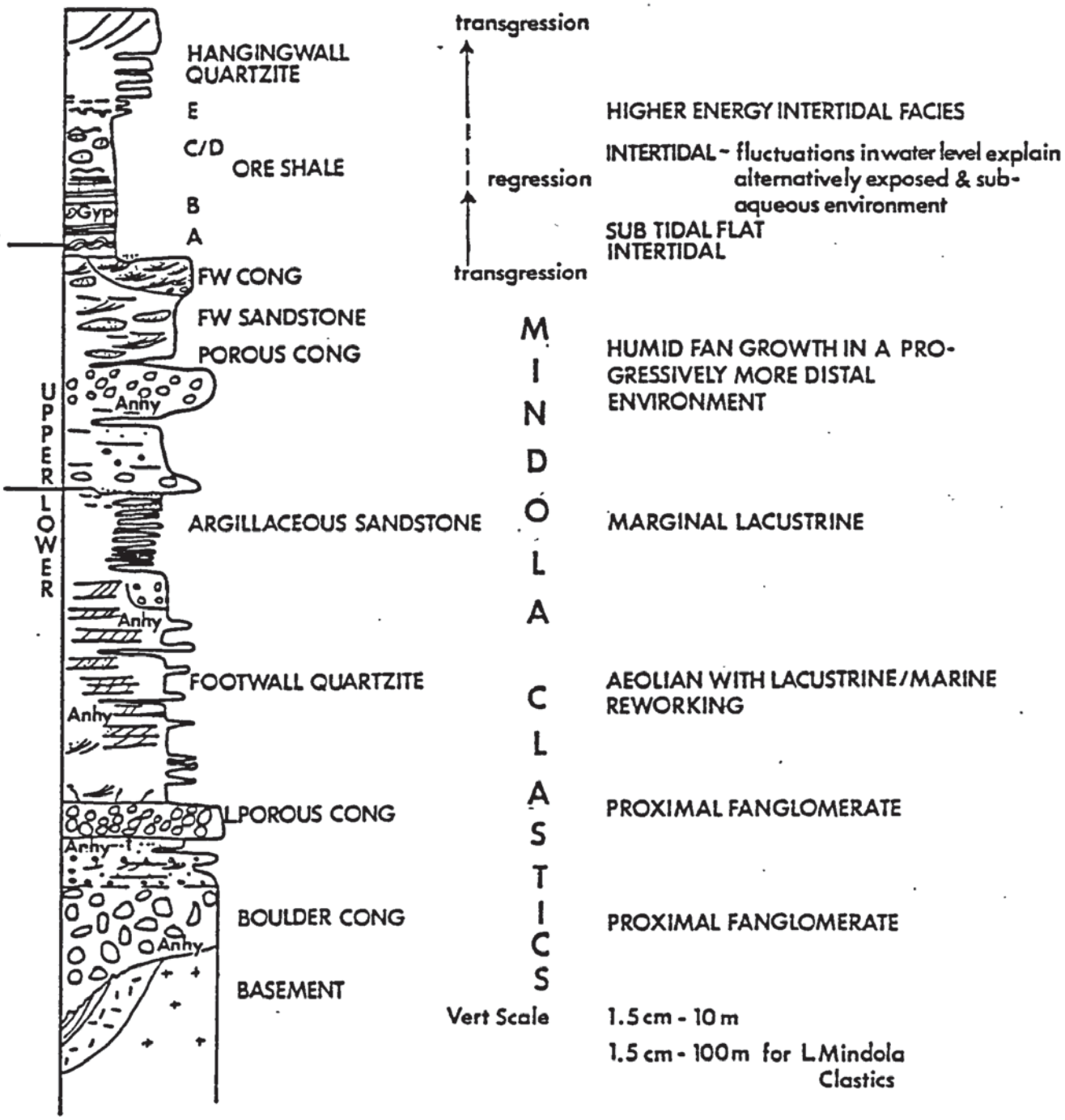

Fig.3.1 DIAGRAMMATIC LOG OF THE MINDOLA CLASTIC & LOWER KITWE FORMATIONS

Boulder Conglomerate } Proximal Fan
Lower Porous Conglomerate }
Pebble Conglomerate – Distal Fan (stream flood)
Footwall Quartzite – Aeolian with lacustrine and marine reworking
Argillaceous Sst. – Marginal lacustrine

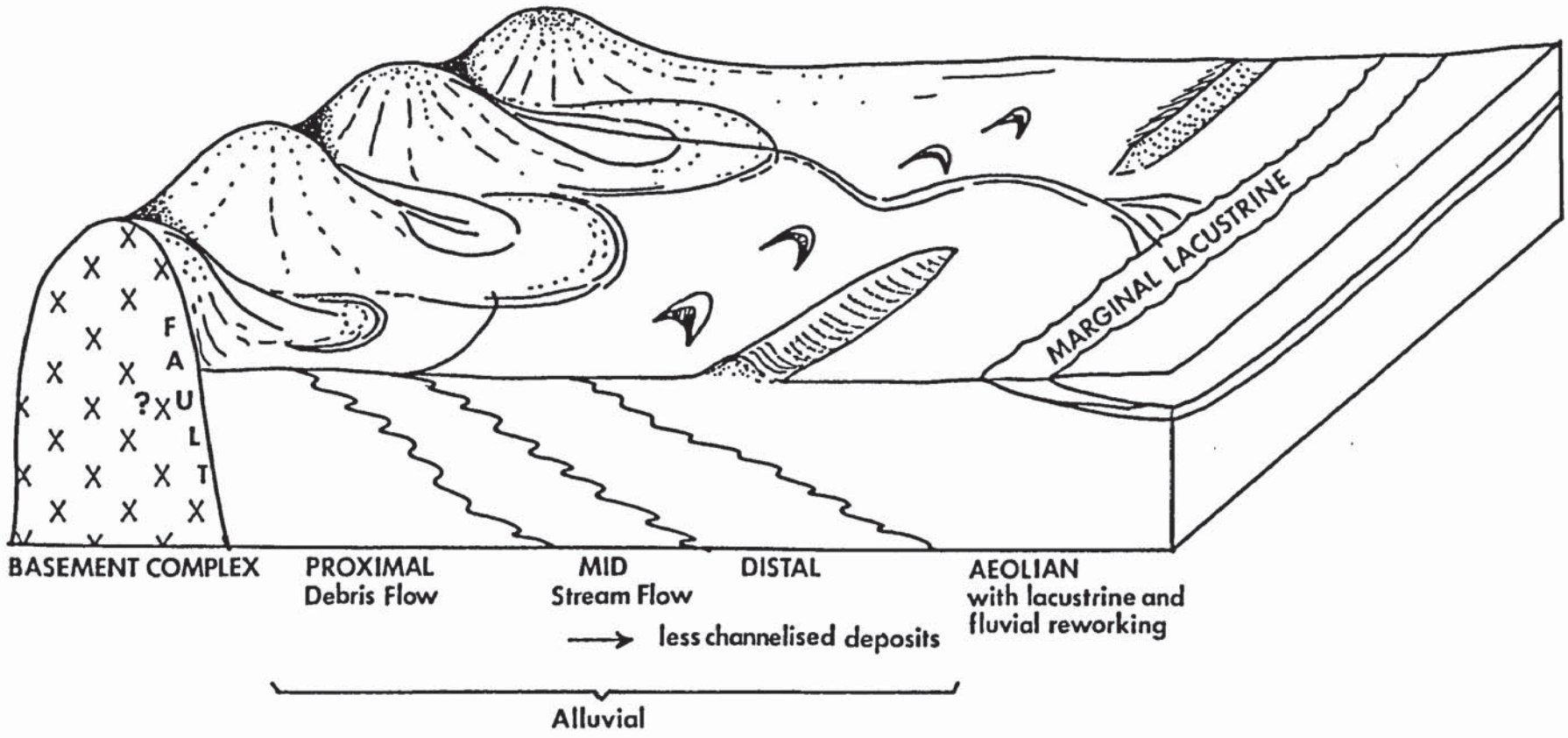

Fig. 3.2
Schematic Diagram of the Depositional Environment of units of the Bancroft Quartzite Member

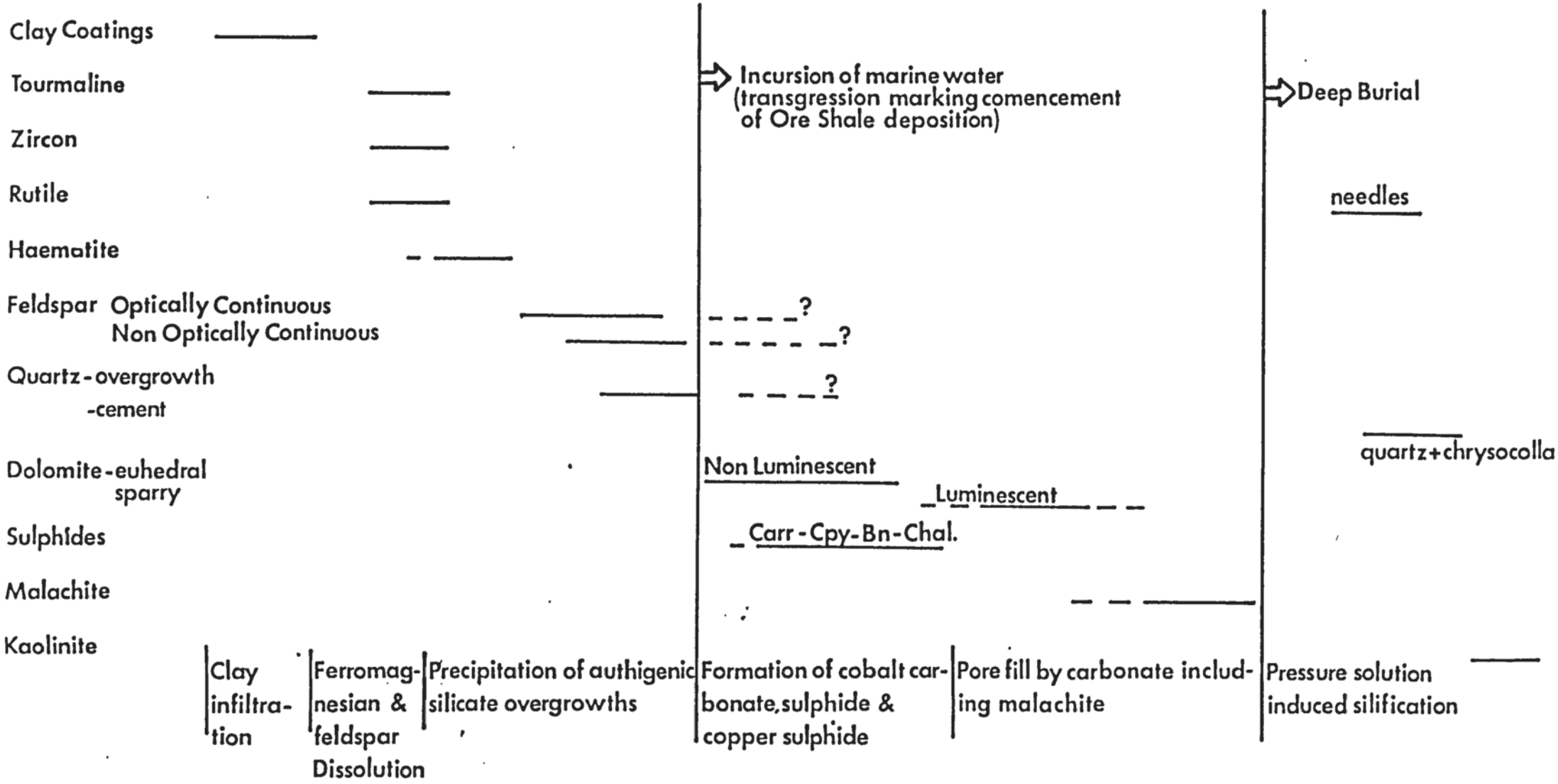

Fig. 4.1

Suggested Paragenetic Sequence of Diagenetic Events in Footwall Rocks

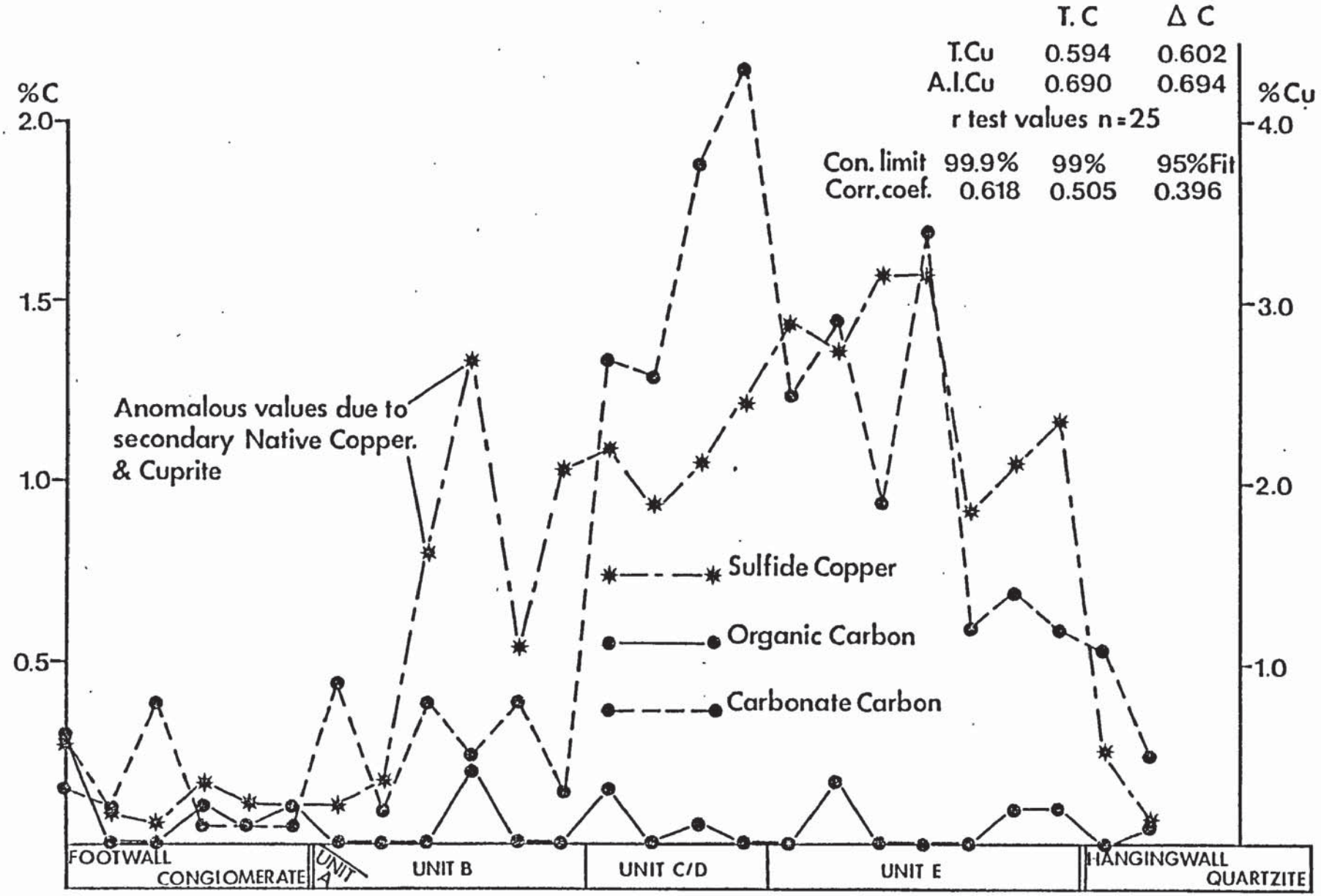

Fig. 4.2

Correlation between Carbon and Copper (Borehole CP 337)

MINERAL	%Cu	%Co	%Ni	%S	%Fe	Total
Pyrite (core)	0.31	7.29	0.06	52.57	39.58	99.81
Pyrite (rim)	1.08	10.12	0.07	52.81	36.43	100.51
Chalcopyrite	31.16	1.56	0.08	35.03	30.22	98.05
Carrollite	15.18	42.44	0.59	41.34	1.54	101.09

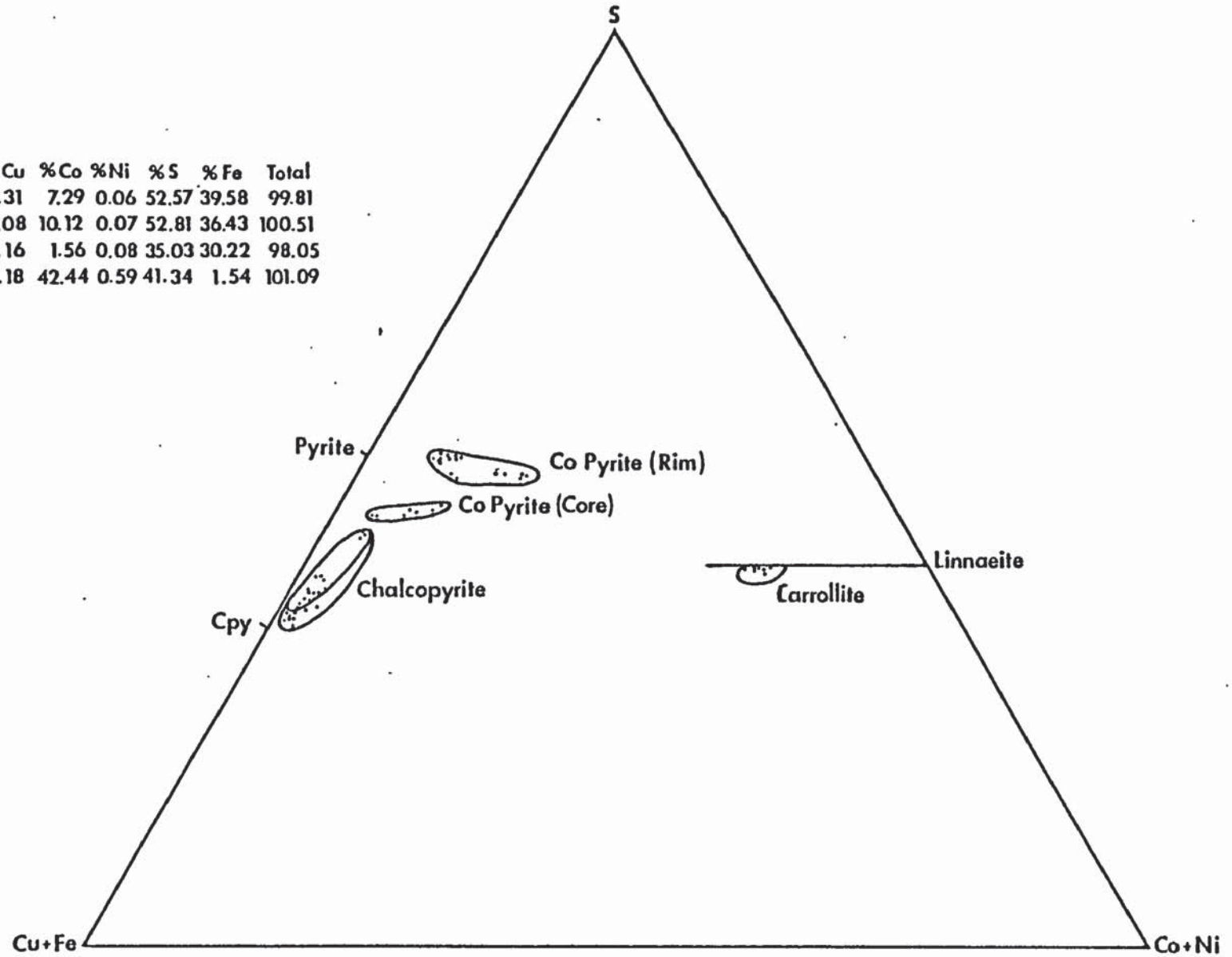

Fig. 4.3 Plot of Cobaltiferous Pyrite, Chalcopyrite and Carrollite compositions

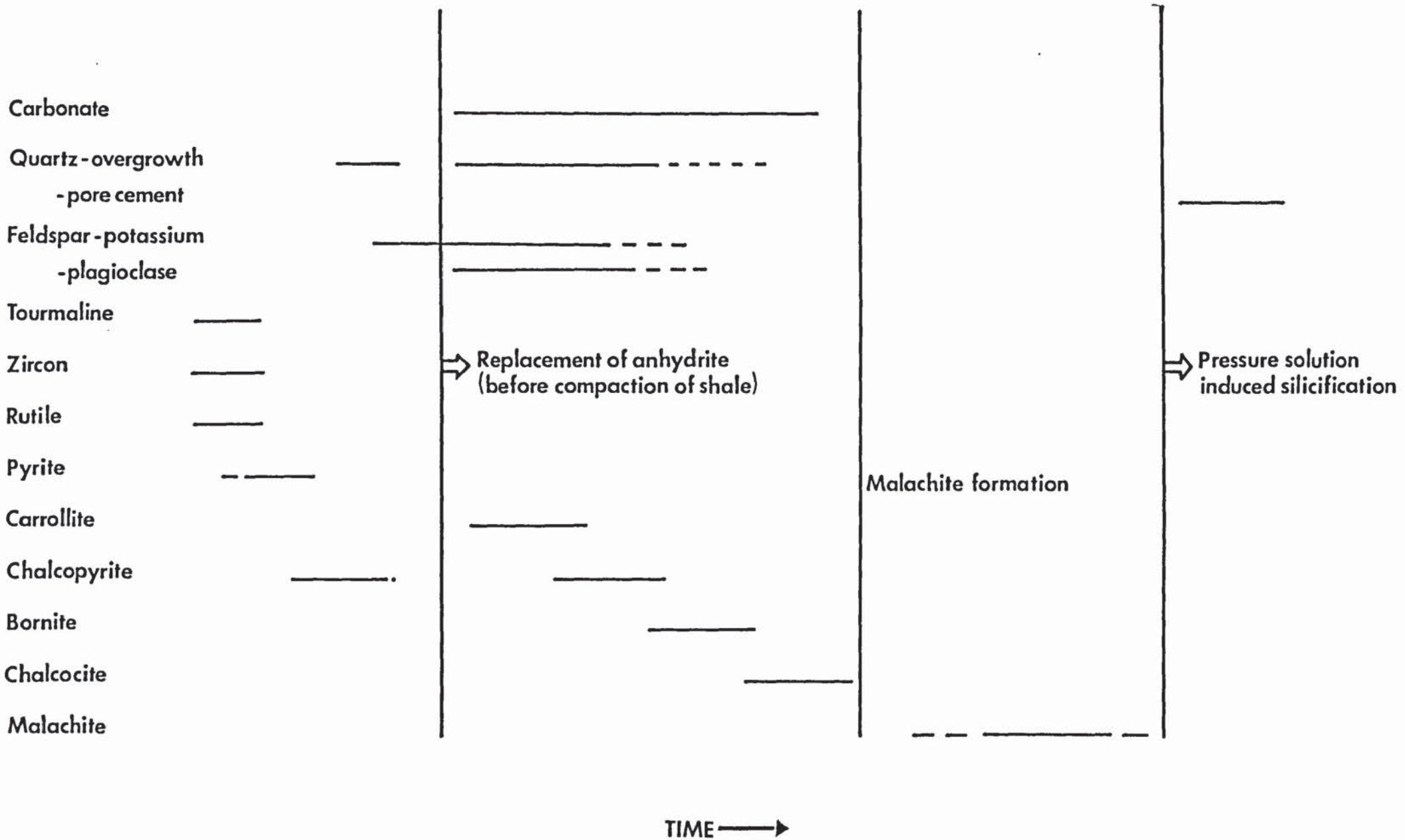

Fig. 4.4

Suggested Paragenetic Sequence of Diagenetic Events in the Copperbelt Orebody Member (Ore Shale)

WEATHERING AT SOURCE

TRANSPORTATION

FOOTWALL CONGLOMERATE AND SANDSTONE		COPPERBELT OREBODY MEMBER
Clay Infiltration Ferromagnesian Minerals Ilmenite to Haematite Plagioclase to Clays	DISSOLUTION REPLACEMENT	Feldspars (possibly during weathering and transport) Ilmenite to pyrite
	AUTHIGENIC MINERAL TRANSPORTATION	
Tourmaline Zircon Rutile Haematite Quartz Feldspar	Early Diagenesis	Clays (now represented by muscovite) Tourmaline Zircon and Rutile Pyrite and Chalcopyrite Quartz Feldspar
Carbonate (Cobaltian) Silicates Sulphides (Carrollite - Chalcopyrite - Bornite - Chalcocite)	Association with Sulphate Reduction (pre-sediment compaction)	Cabonate Quartz and Feldspar Sulphides (Carrollite - Chalcopyrite - Bornite - Chalcocite)
Malachite Dolomite	Pore fill by Carbonate	Carbonate
Quartz and Rutile Chrysocolla Kaolinite	Deep Burial (1000 m)	Quartz Alteration of original clays.

Figure 4.5 Summary of the diagenetic stages in the formation of the Copperbelt Orebody Member and the Footwall Conglomerate and Sandstone

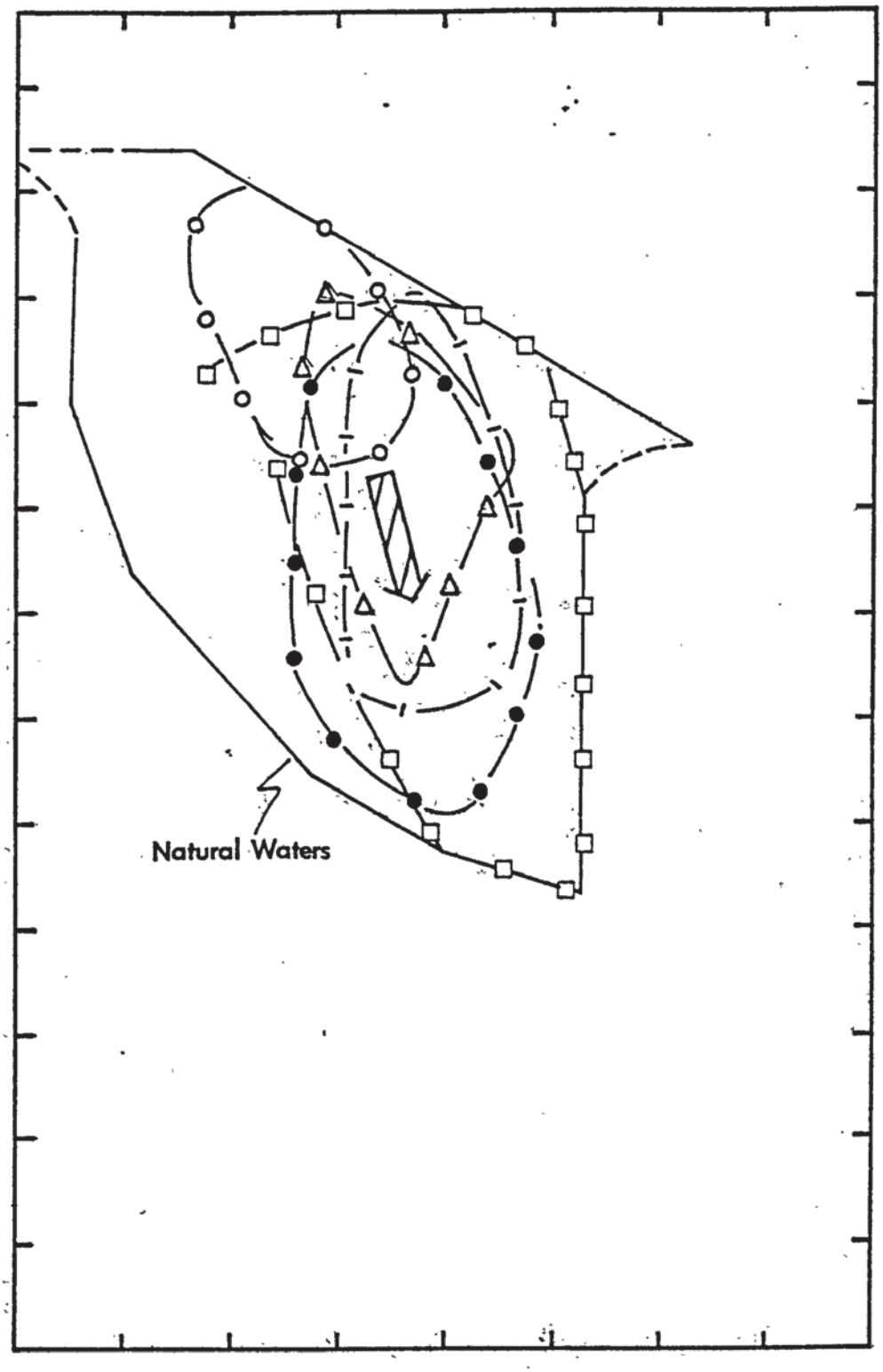

Fig. 4.6b

Summary of Eh - pH fields for waters pertinent to Copperbelt Orebody Member and 'footwall rocks' diagenesis (after Becking et al, 1960)

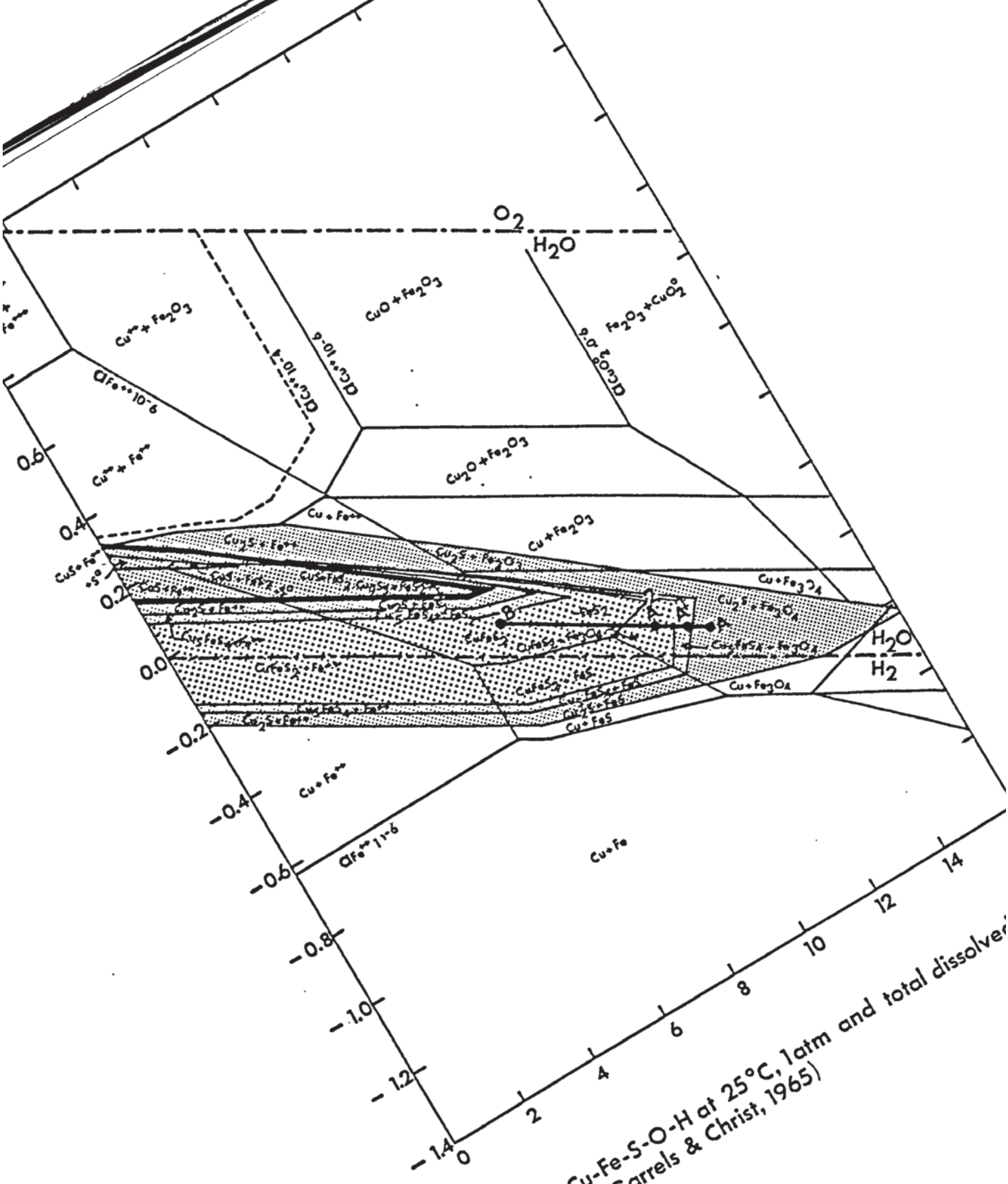

Fig. 4.6a The system Cu-Fe-S-O-H at 25°C, 1atm and total dissolved
=10-4m (after Garrels & Christ, 1965)

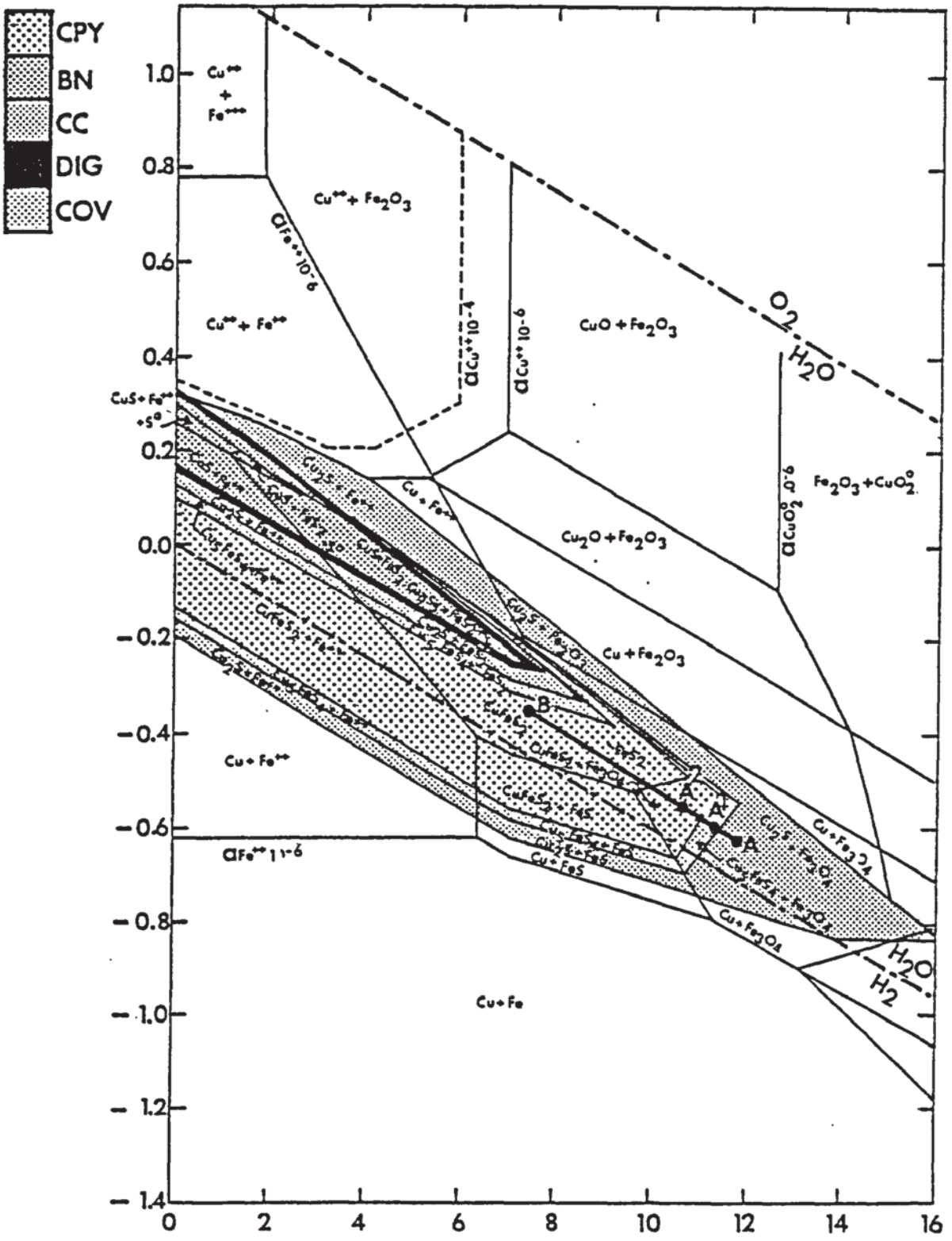

Fig. 4.6a

The system Cu-Fe-S-O-H at 25°C, 1atm and total dissolved sulphur $=10^{-4}$m (after Garrels & Christ, 1965)

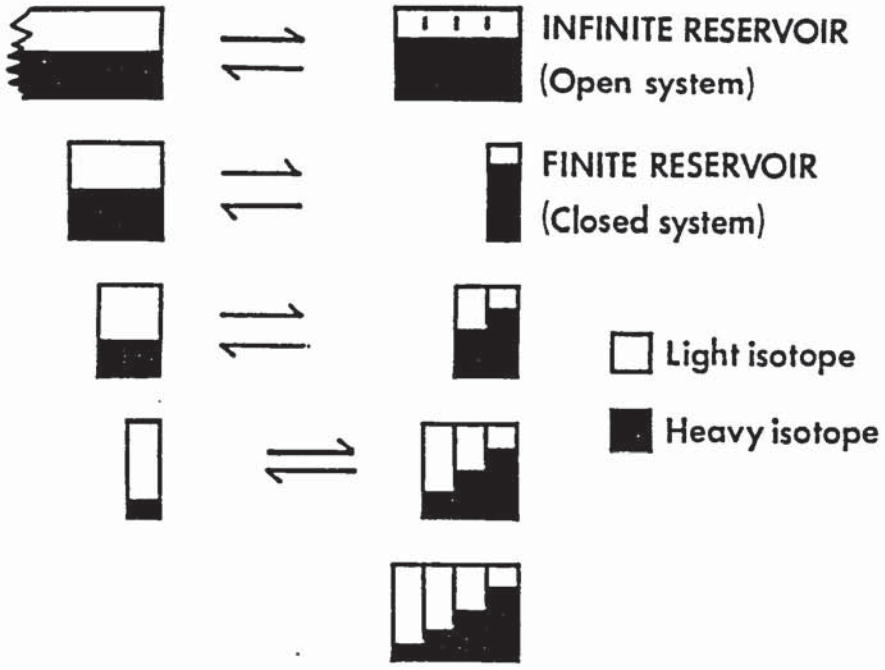

Fig. 5.1
The Reservoir Effect: showing schematically successive aliquots in equilibrium with the reservoir. (After Coleman, 1977)

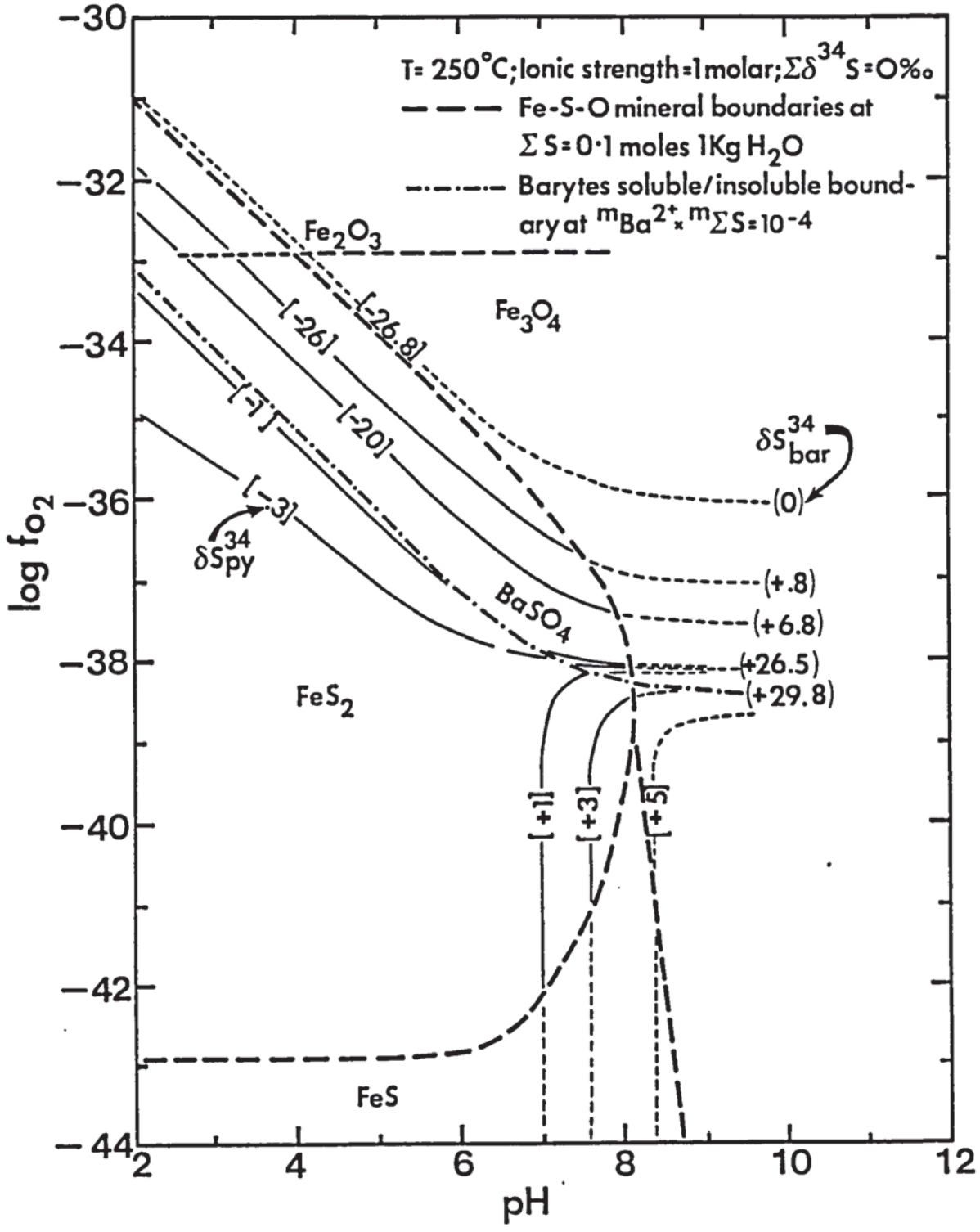

Fig. 5.2
Variation of $\delta^{34}S$ as a function of fO_2 and ph. (After Ohmoto, 1972)

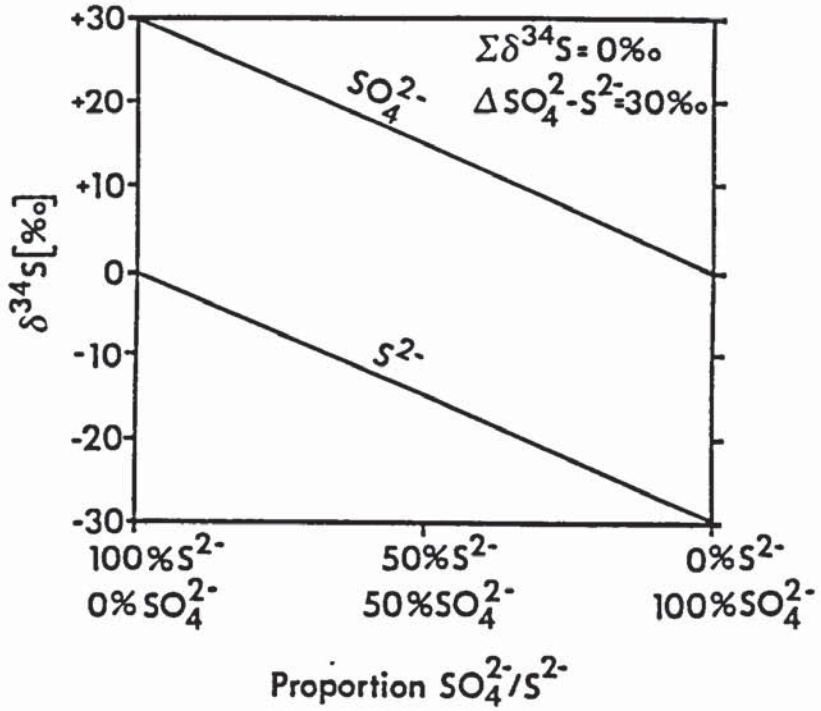

Fig. 5.3
Variation of $\delta^{34}S$ with sulphide/sulphate ratio. (After Coleman, 1977)

ZONE	DEPTH (m) Boundary Limiting Factor	*TEMP°C Porosity %	REACTIONS	MINERALS FORMED	^{13}C (per mil PDB) of HCO_3^-
a	0	0	Bacterial Oxidation	Upward diffusion of	
I	0_2 Diffusion		$CH_2O+O_2 \rightleftharpoons HCO_3^- + H^+$	bicarbonate means low	-25
	10^{-2}		Bacterial Reduction	probability of carbonate	
b	10^{-1}	80	$CH_2O+2Fe_2O_3+3H_2O \rightleftharpoons$ $HCO_3^-+4Fe^{2+}+7OH^-$	supersaturation, therefore carbonate formation unlikely	-25
	10m	0.2	Bacterial Sulphate Reduction	Sulphides	
II	SO_4^{2-} Diffusion		$2CH_2O+ SO_4^{2-} \rightleftharpoons$	Low iron calcite/dolomite	
		75	$2HCO_3^- +H_2S^-$	(Iron used to form sulphides)	-20 to -30
	1000m		Bacterial Fermentation		
	Increase in	30	$2CH_2O$	High Iron Carbonates	+10
III	temperature or	30	$\rightleftharpoons HCO_3^- + CH_4 + H^+$	Calcite Dolomite Ankerite	to
	lack of O.M.		$+H_2O$	Siderite	+15
		75	Abiotic Reactions		
IV			$R.CO_2H \rightleftharpoons R.H.+HCO_3^- + H^+ + H_2^+0$	Siderite	-10 to -25
		15	Thermal Degradation		

* A Thermal gradient of 22.5° C/Km below sediment/water interface has been used.
O.M. = Organic Matter.

Figure 5.4 Diagentic zones of carbonate formation during sediment (Mudstone) burial (after Curtis, 1977; Irwin et al. 1977 and Benmore, 1983).

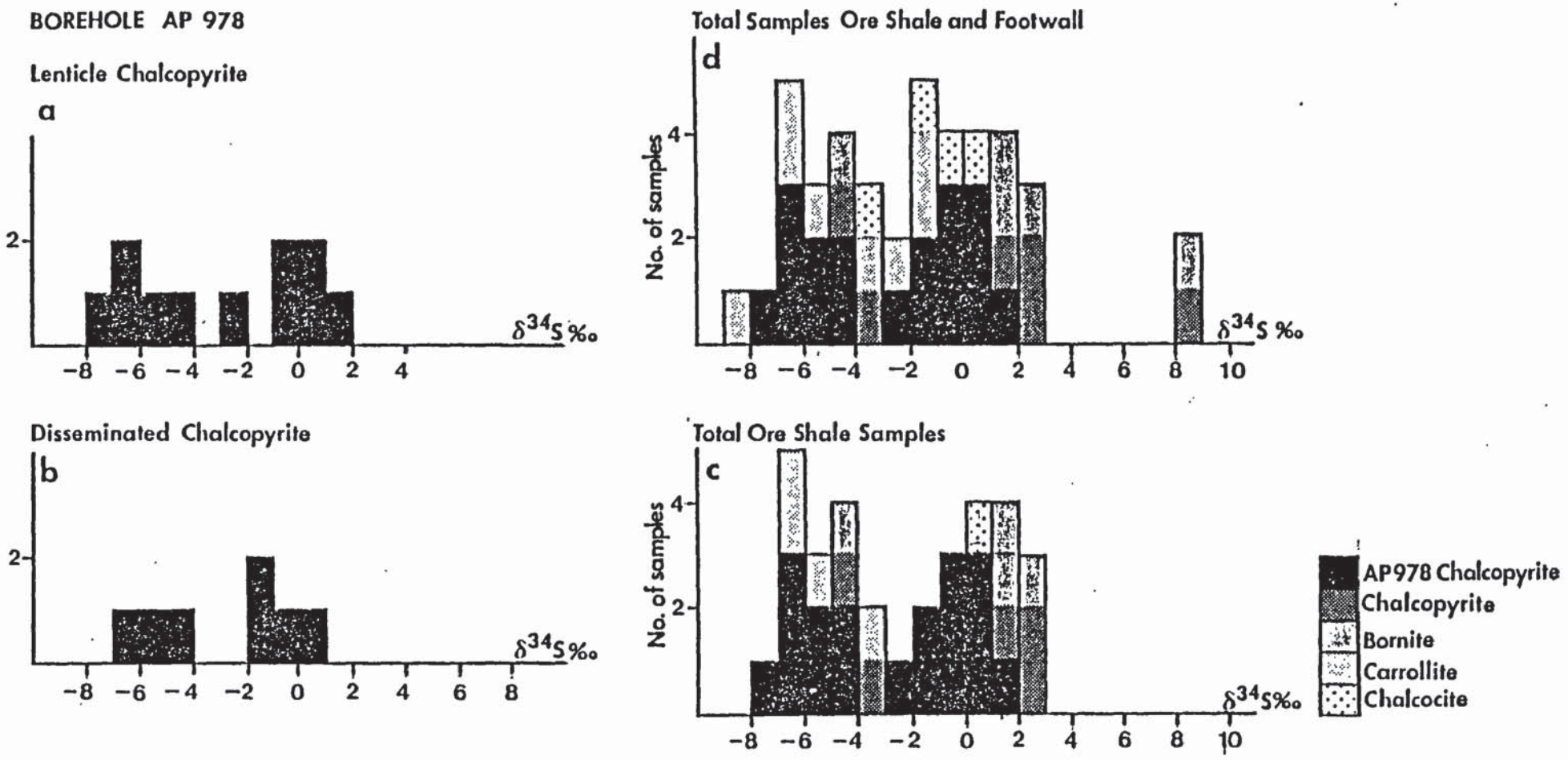

Fig.6.1

Histogram showing the frequency distribution of orebody $\delta^{34}S$ values

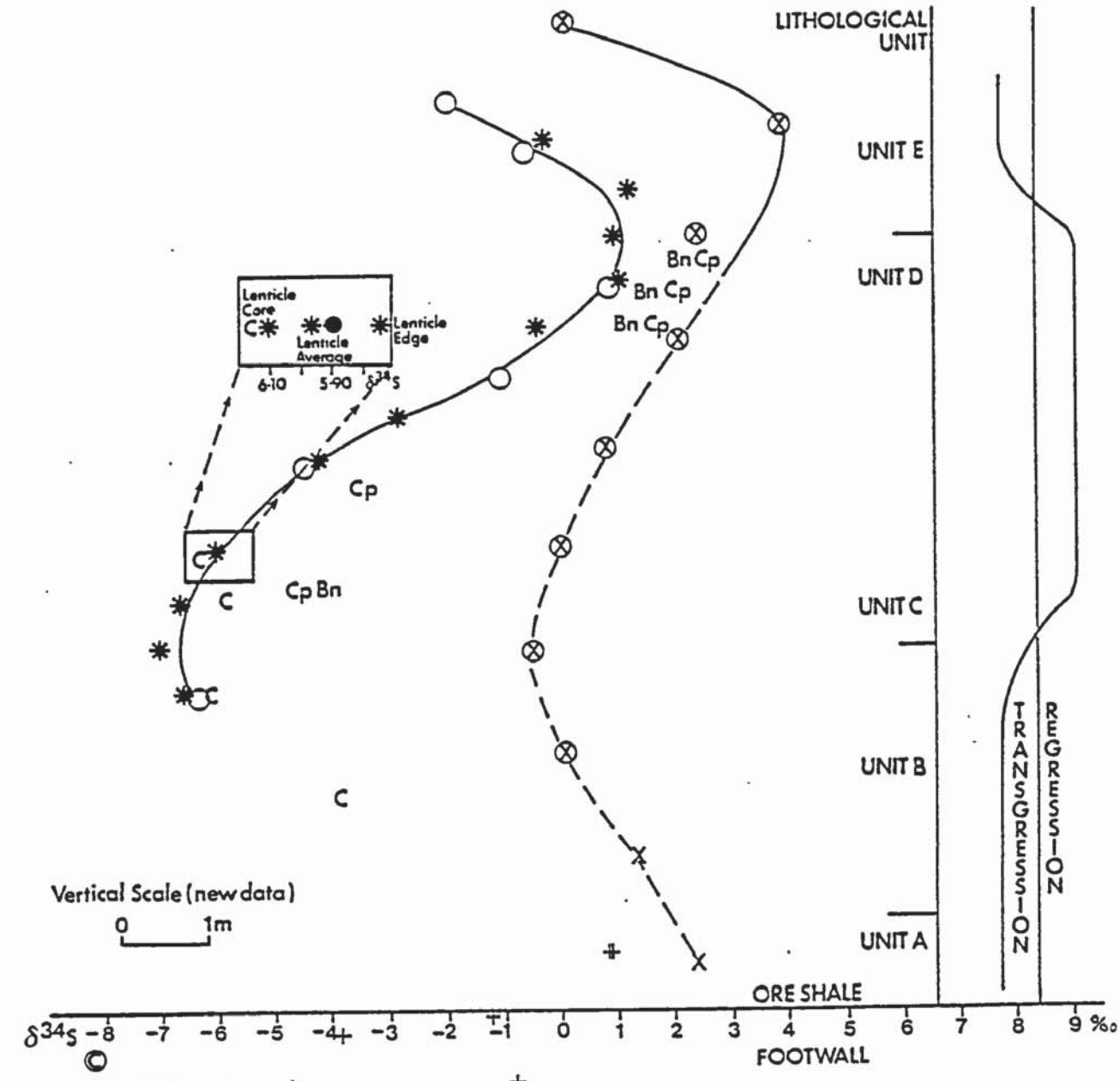

✱ Lenticular Chalcopyrite
○ Disseminated Chalcopyrite
} AP 978

C Carrolite

⊗ Chalcocite/Bornite
X Chalcocite
} After Dechow & Jensen 1965

\+ Chalcocite

Carrolite

Bn Bornite

Cp Chalcopyrite

BnBnCp

Fig. 6.2 Combined $\delta^{34}S$ values plotted against lithology

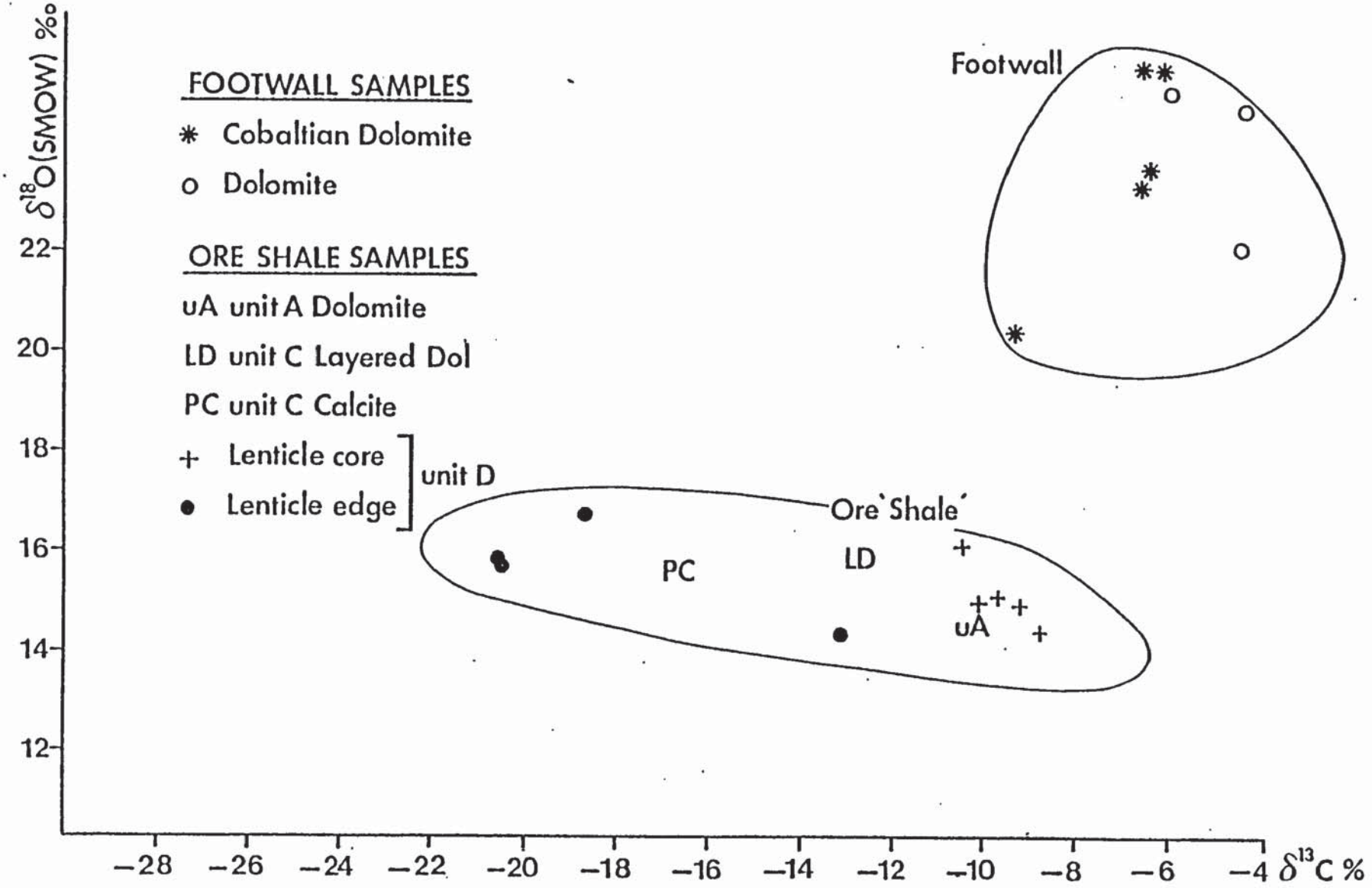

Fig.6.3

Plot of $\delta^{18}O$ versus $\delta^{13}C$ results for Footwall and Ore - Shale Samples

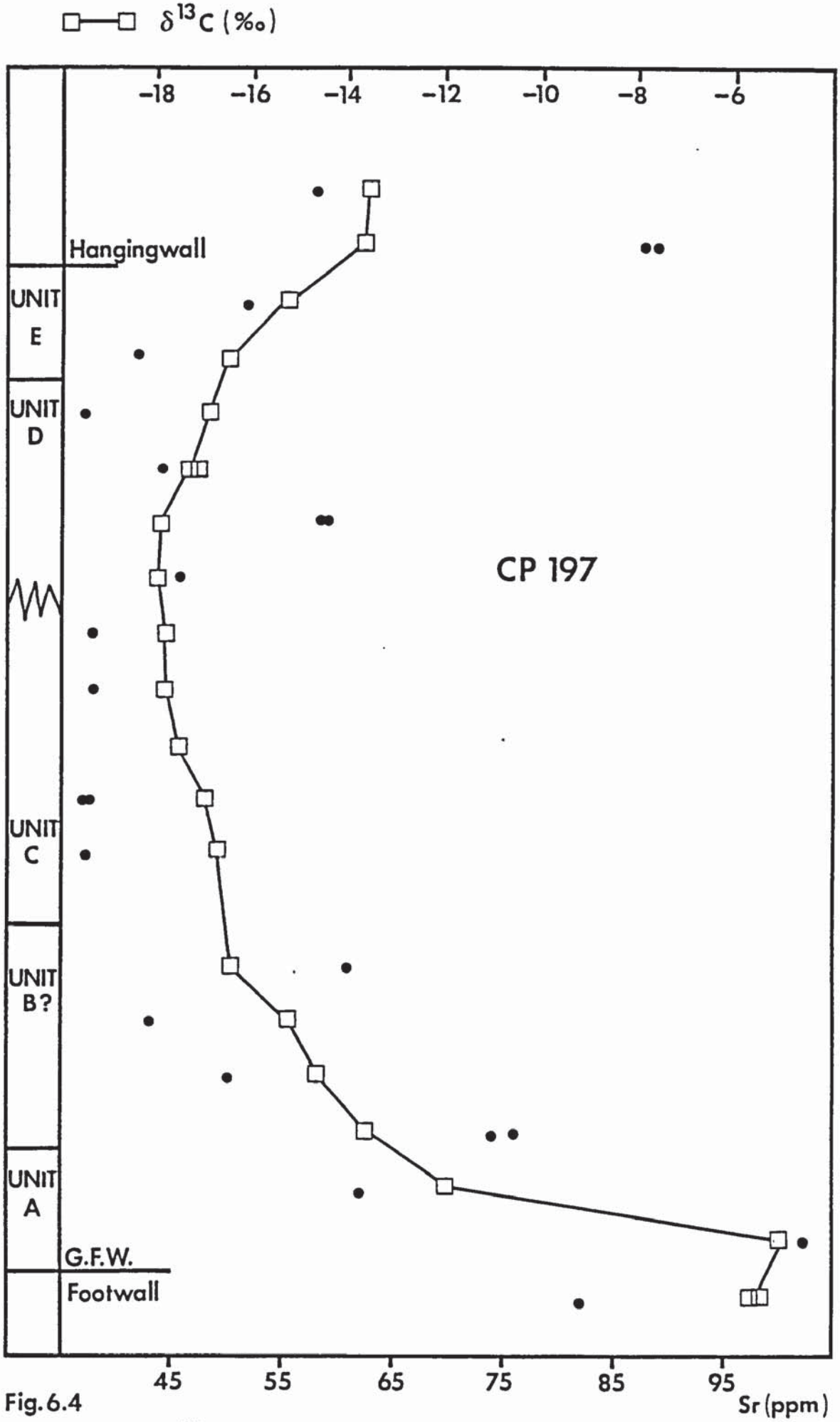

Fig. 6.4 Plot of $\delta^{13}C$ and ppm Sr against lithology for Borehole CP 197

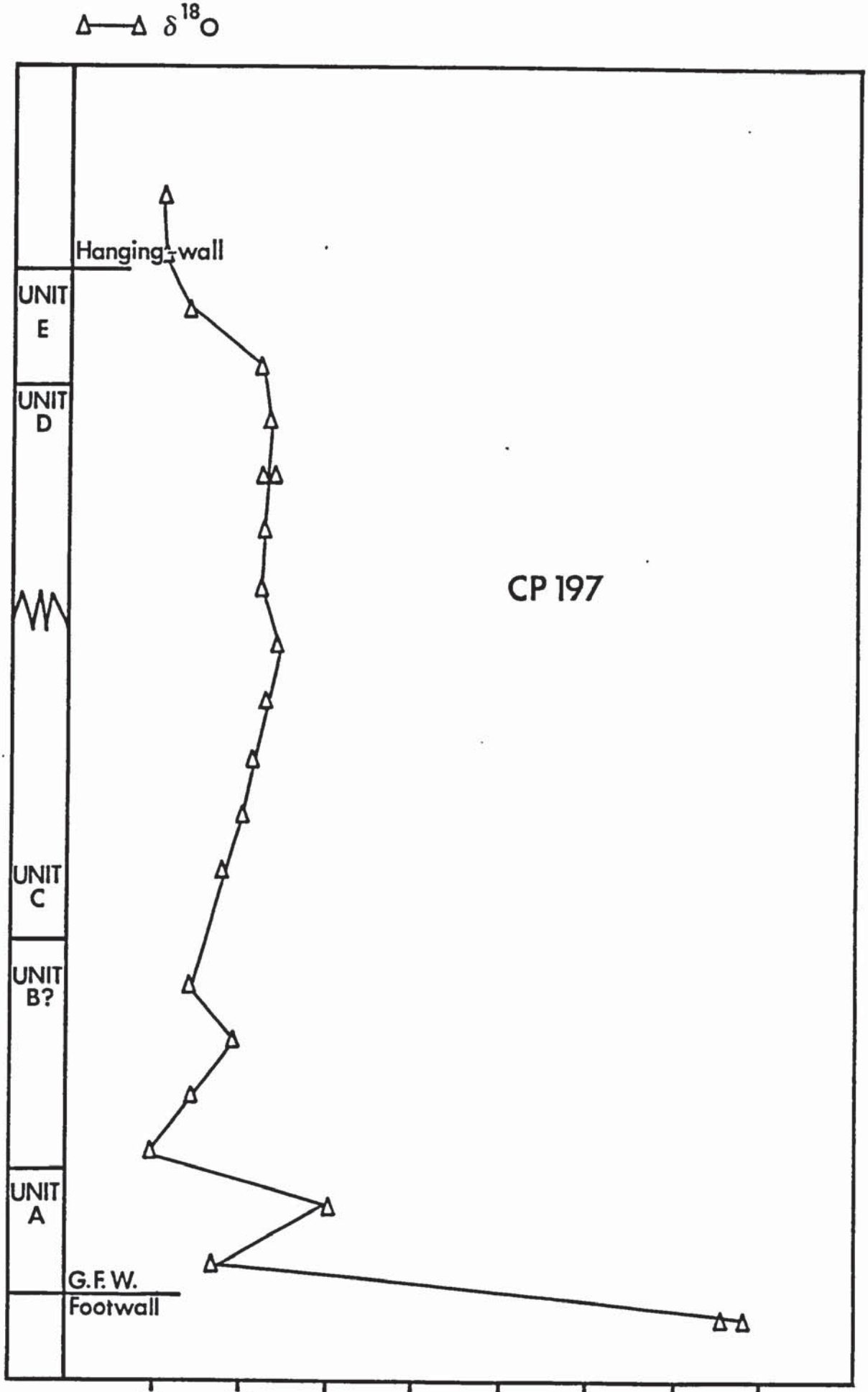

Fig. 6.5

Plot of $\delta^{18}O$ against lithology for samples from CP 197

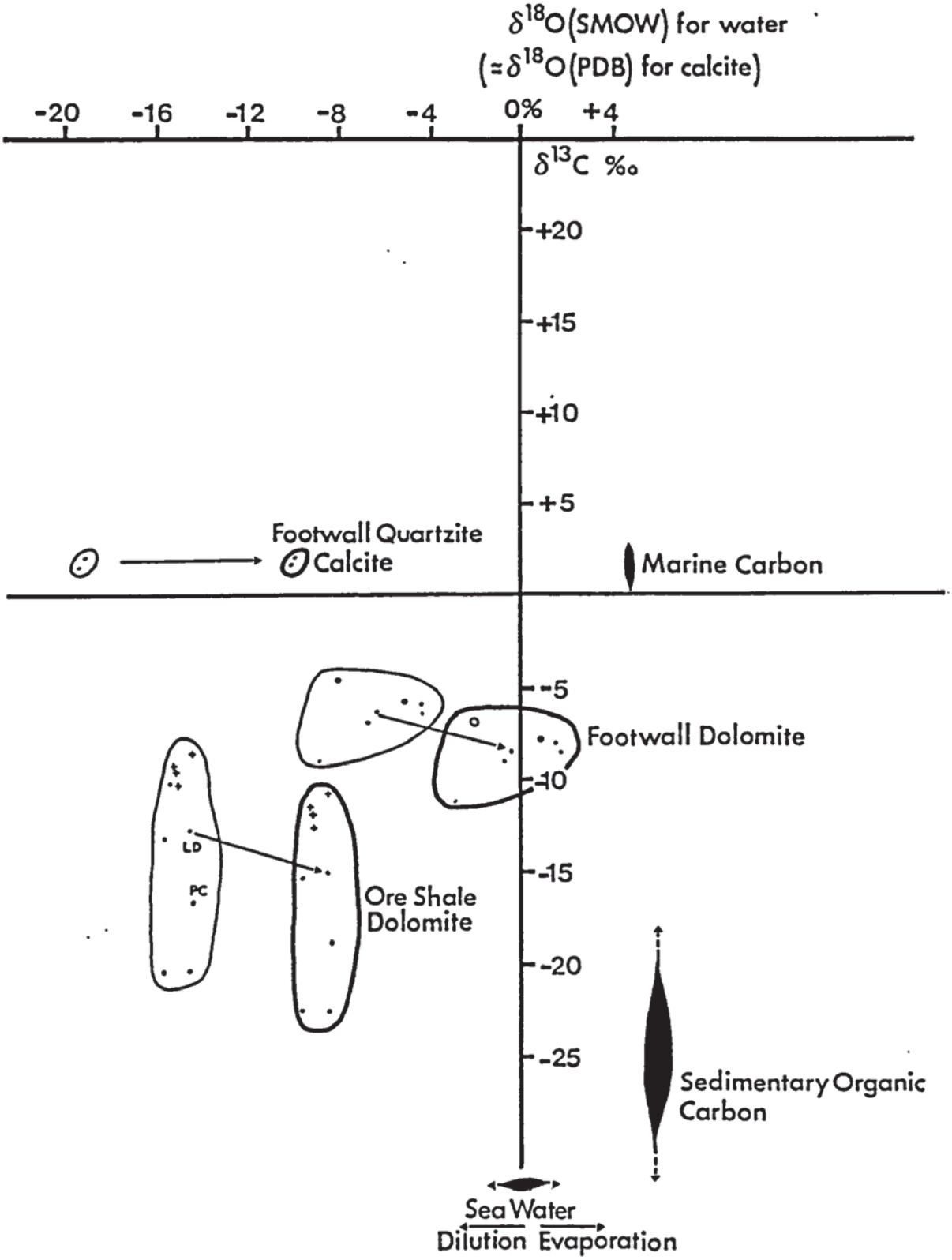

Fig. 6.6

CARBON & OXYGEN ISOTOPE COMPOSITION FOR CORRECTED PRECAMBRIAN CALCITE VALUES.(MODIFIED AFTER HUDSON.1977)

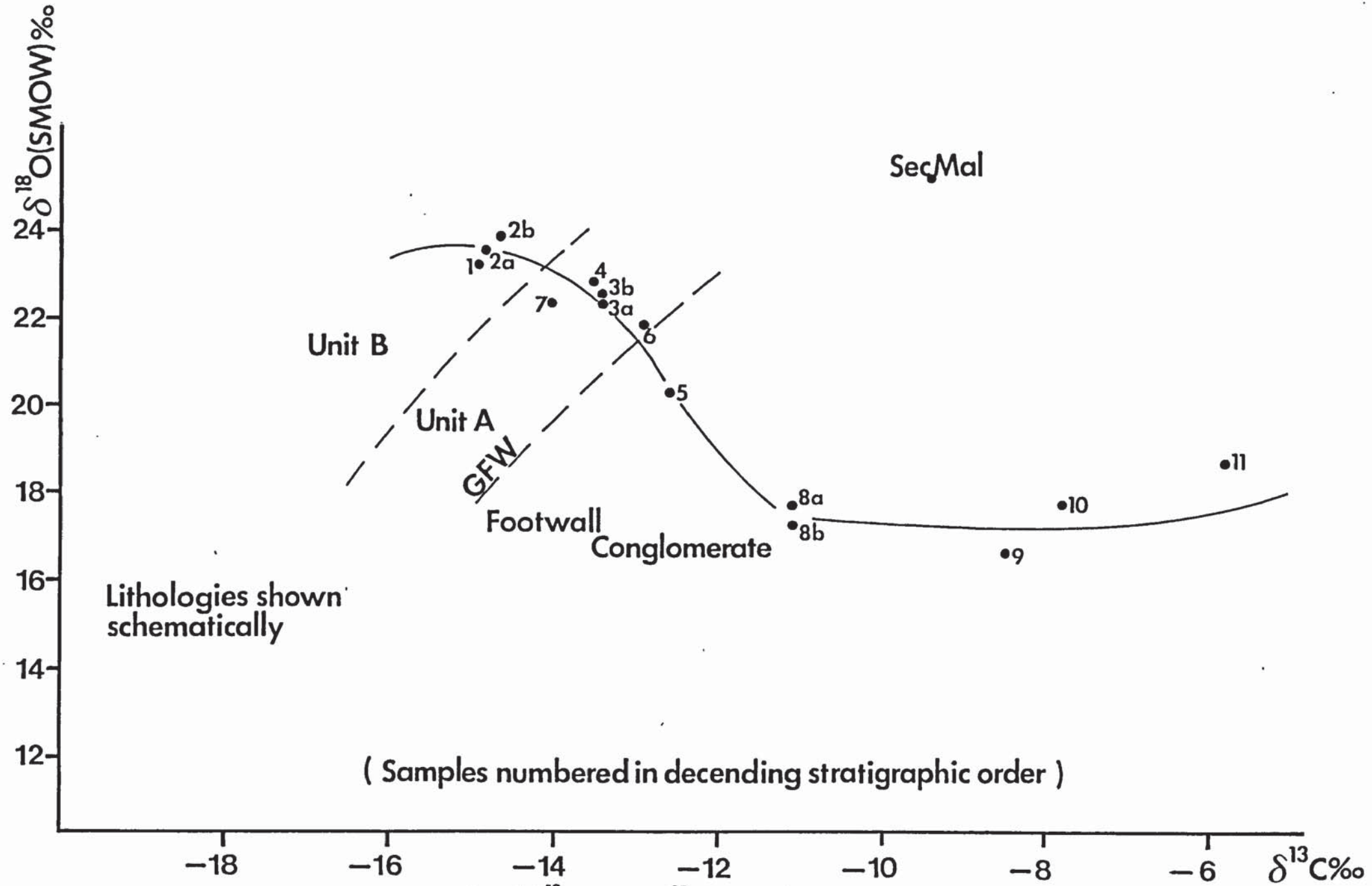

Fig. 6.7 Plot of $\delta^{18}O$ versus $\delta^{13}C$ for Malachite Samples

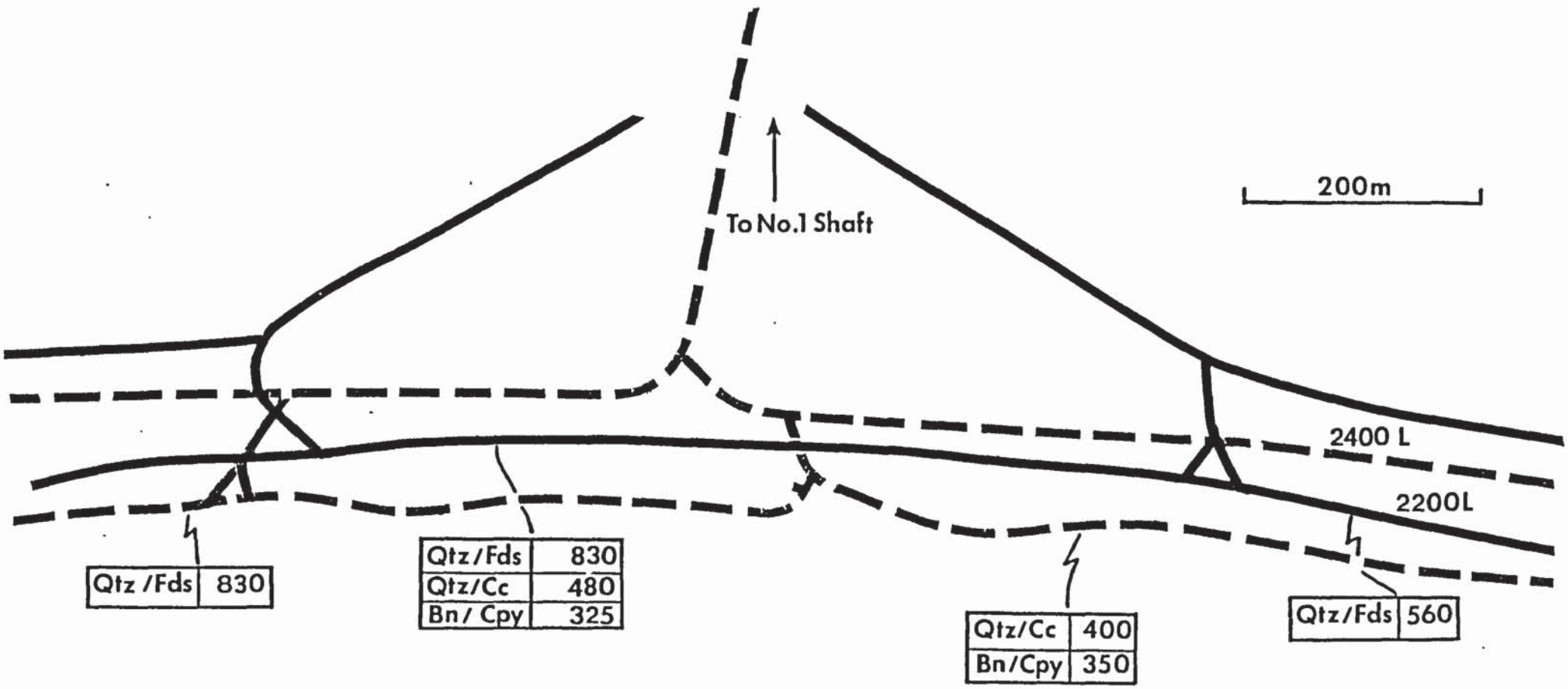

Ledgend

Coexisting Pair	Temp °C

Qtz	Quartz
Fds	Alkali Feldspar
Cc	Calcite
Bn	Bornite
Cpy	Chalcopyrite

Fig. 6.8 TEMPERATURE DISTRIBUTION No. 1 SHAFT
(Calculated from coexisting mineral pair)

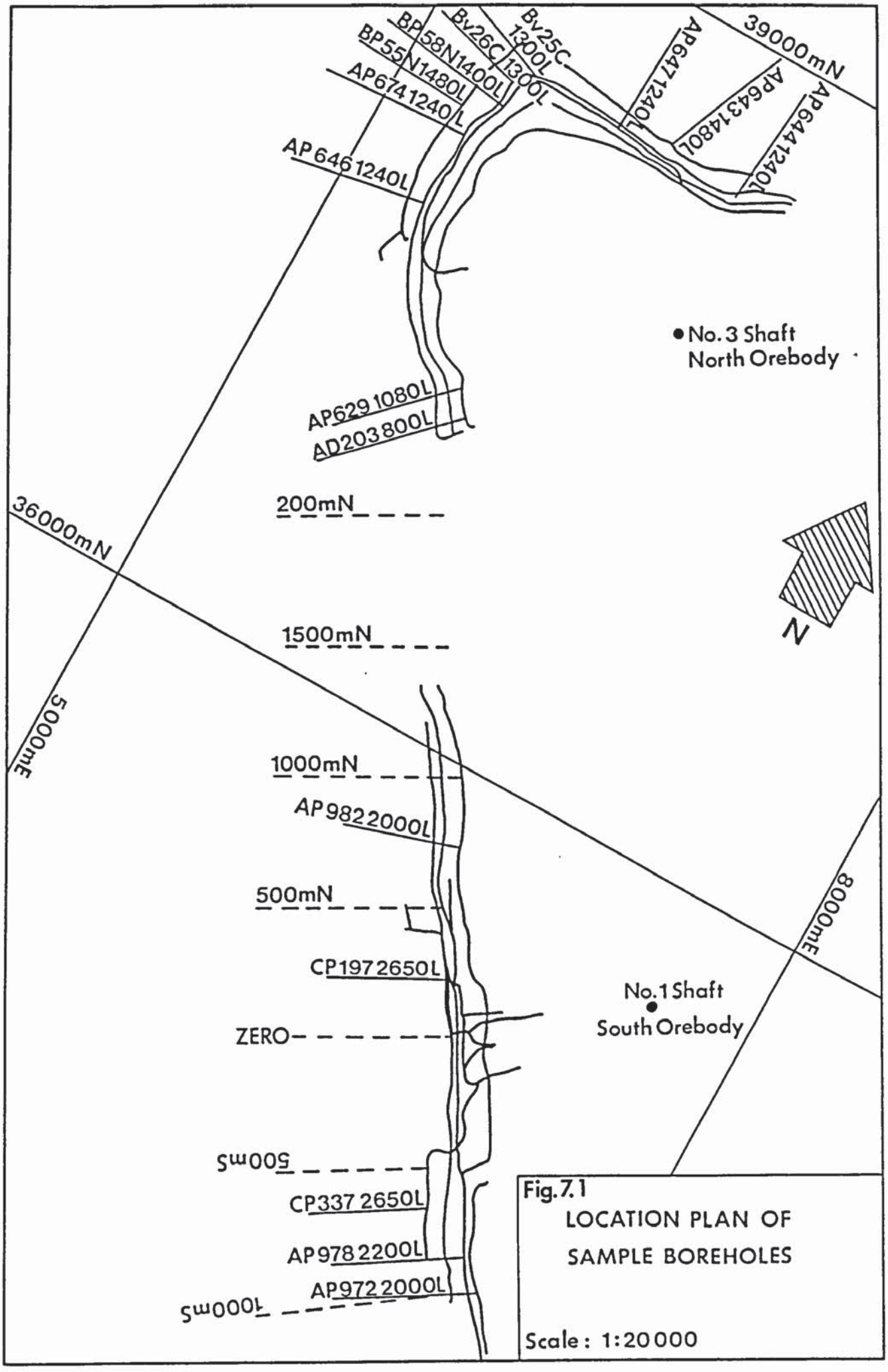

Fig. 7.1
LOCATION PLAN OF
SAMPLE BOREHOLES

Scale : 1:20000

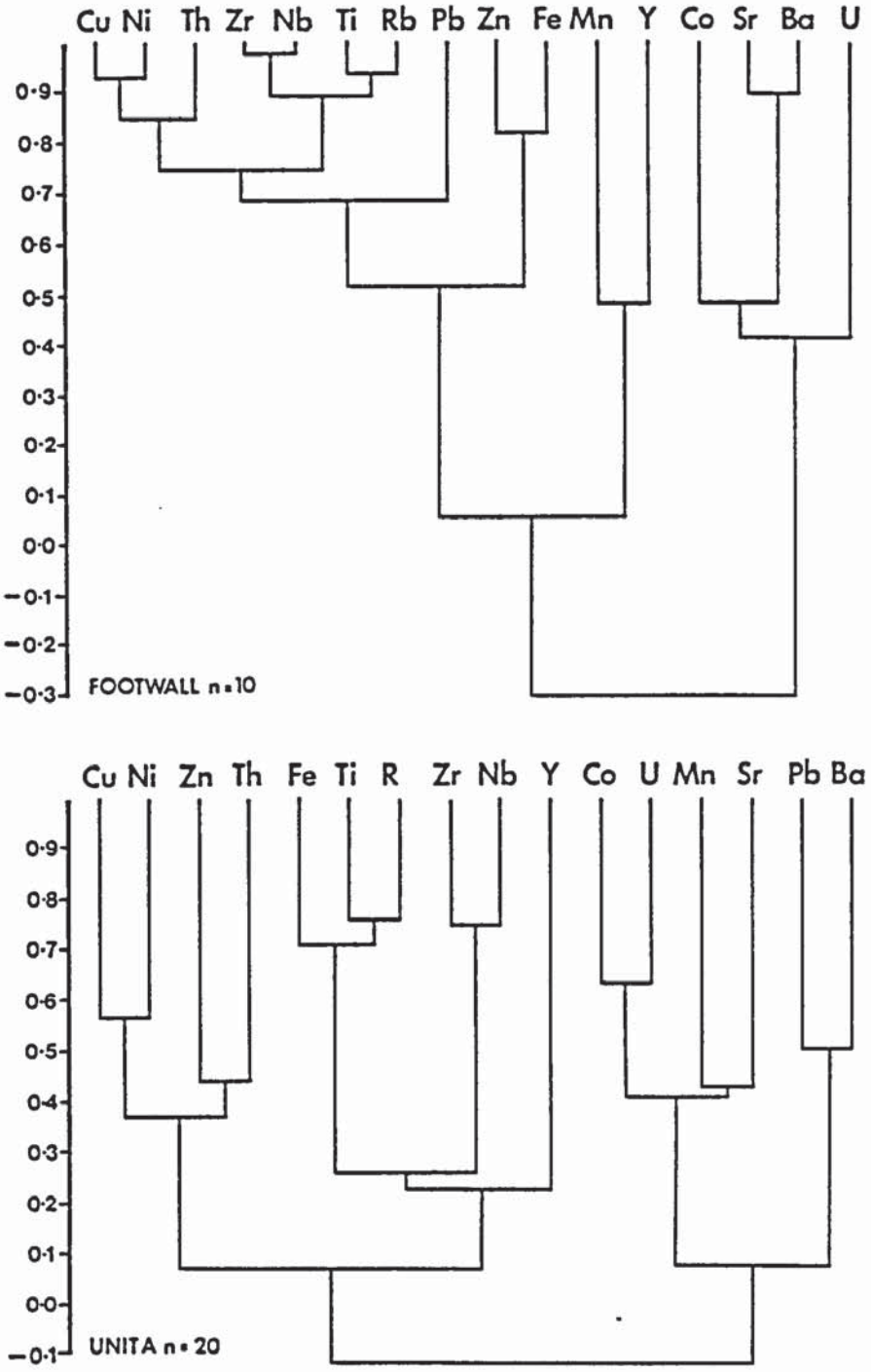

Fig. 7.2

Element Dendrogram for samples from the Footwall and Unit A of the Ore - Shale

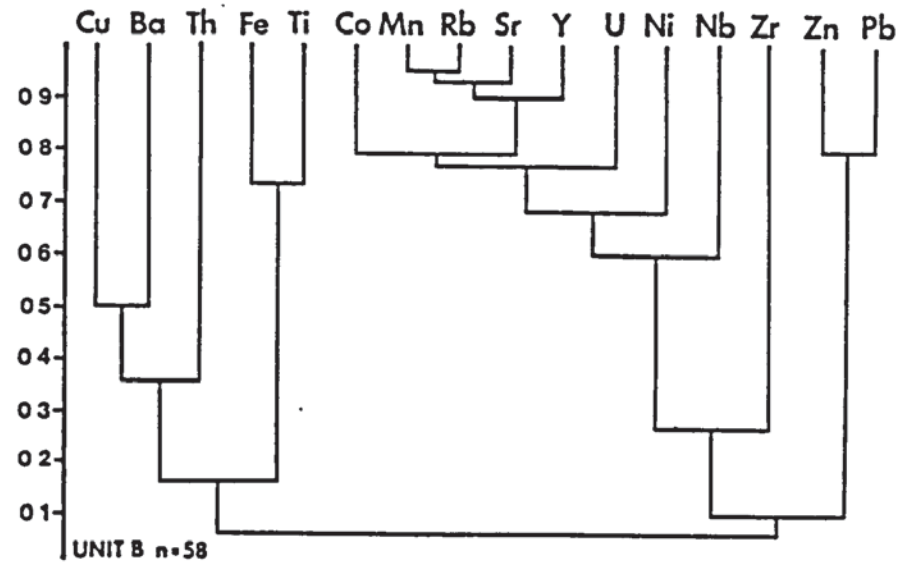

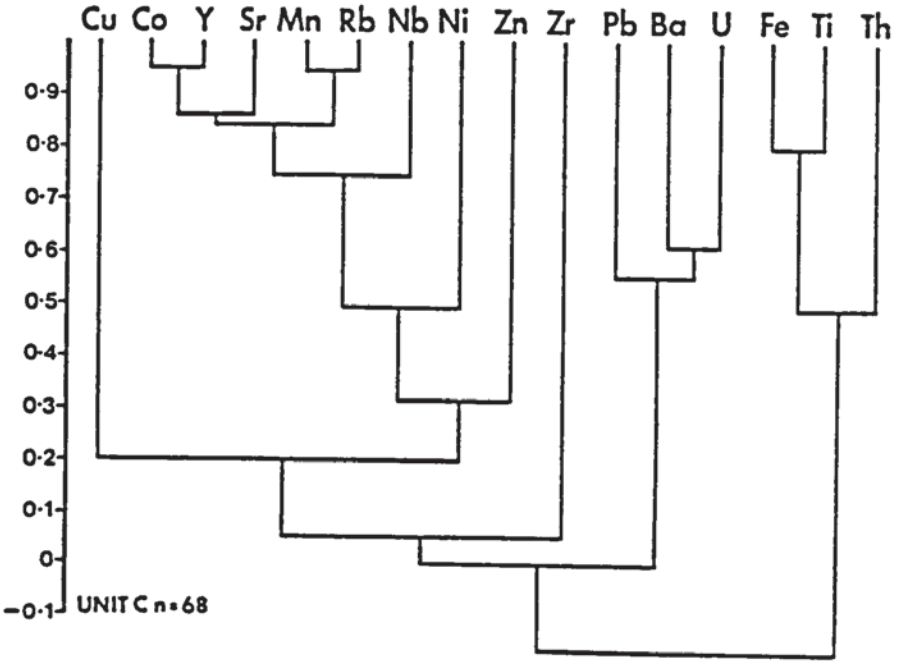

Fig. 7.3

Element Dendrogram for samples from Unit B and C of the Ore-Shale

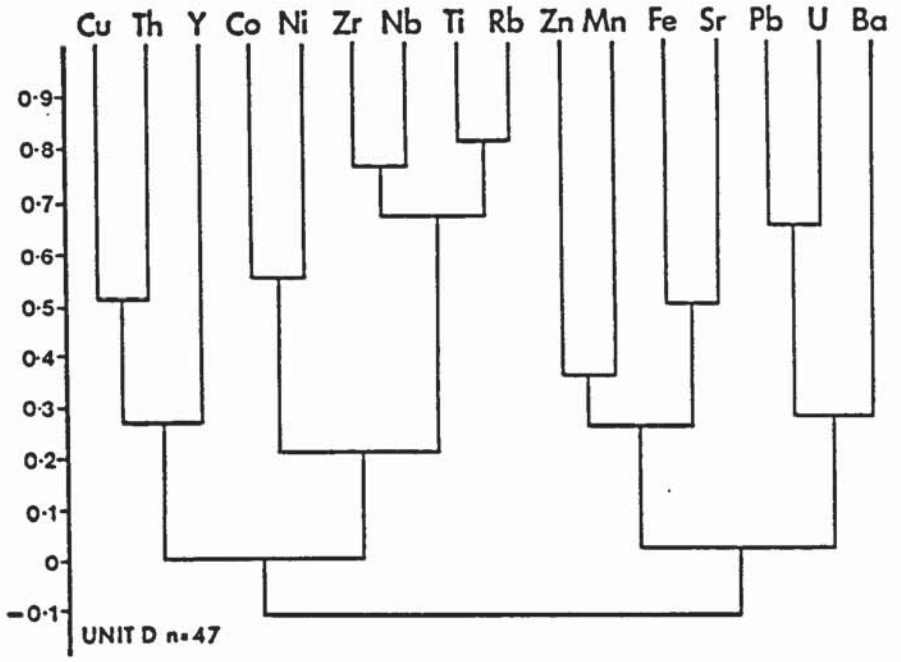

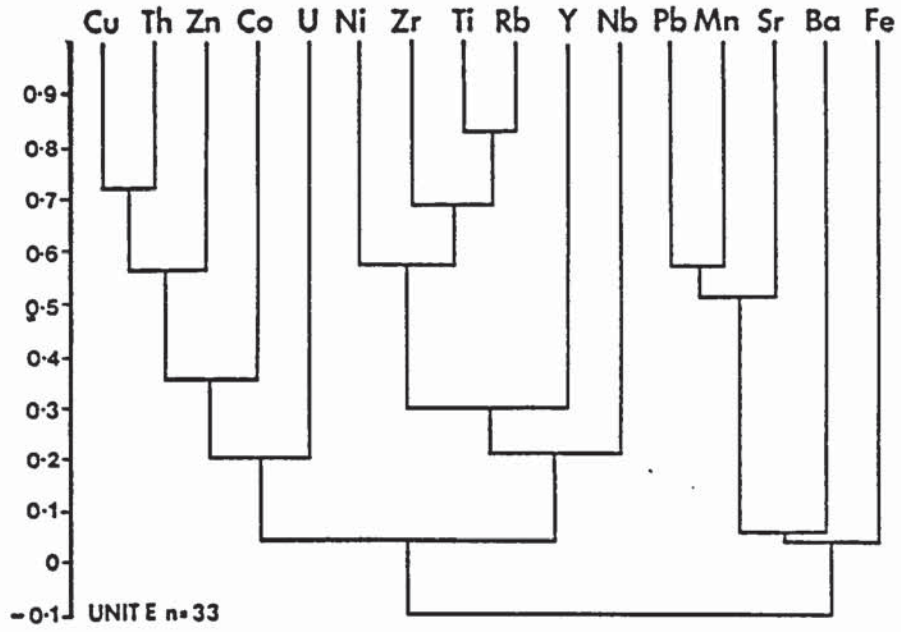

Fig 7.4

Element Dendrogram for samples from Units D and E of the Ore Shale

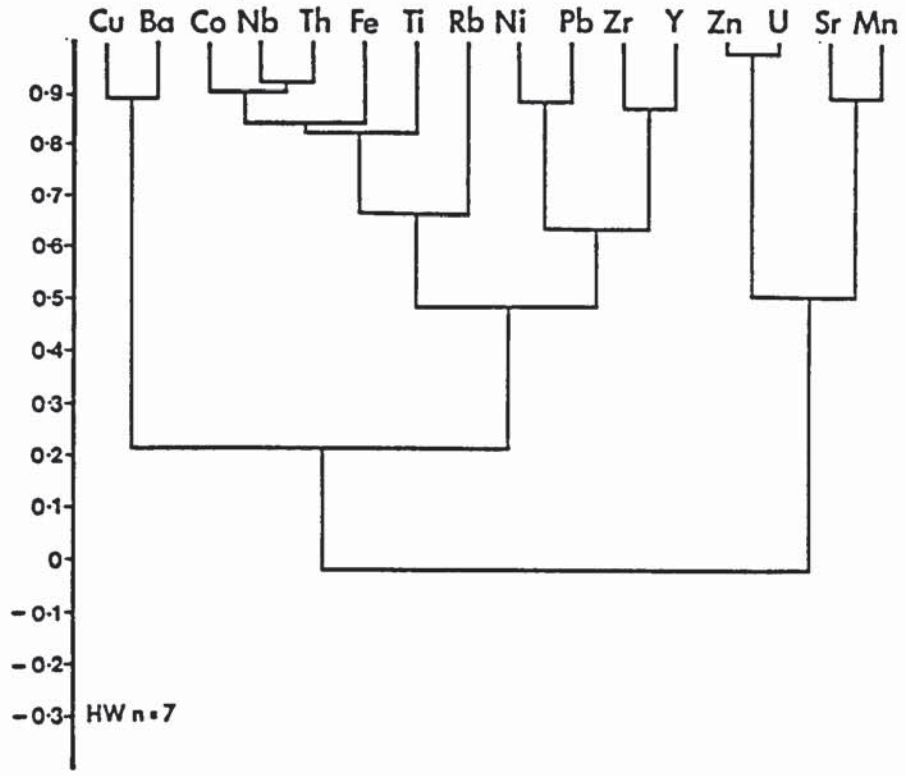

Fig. 7.5

Element Dendrogram for samples from the Hangingwall Quartzite

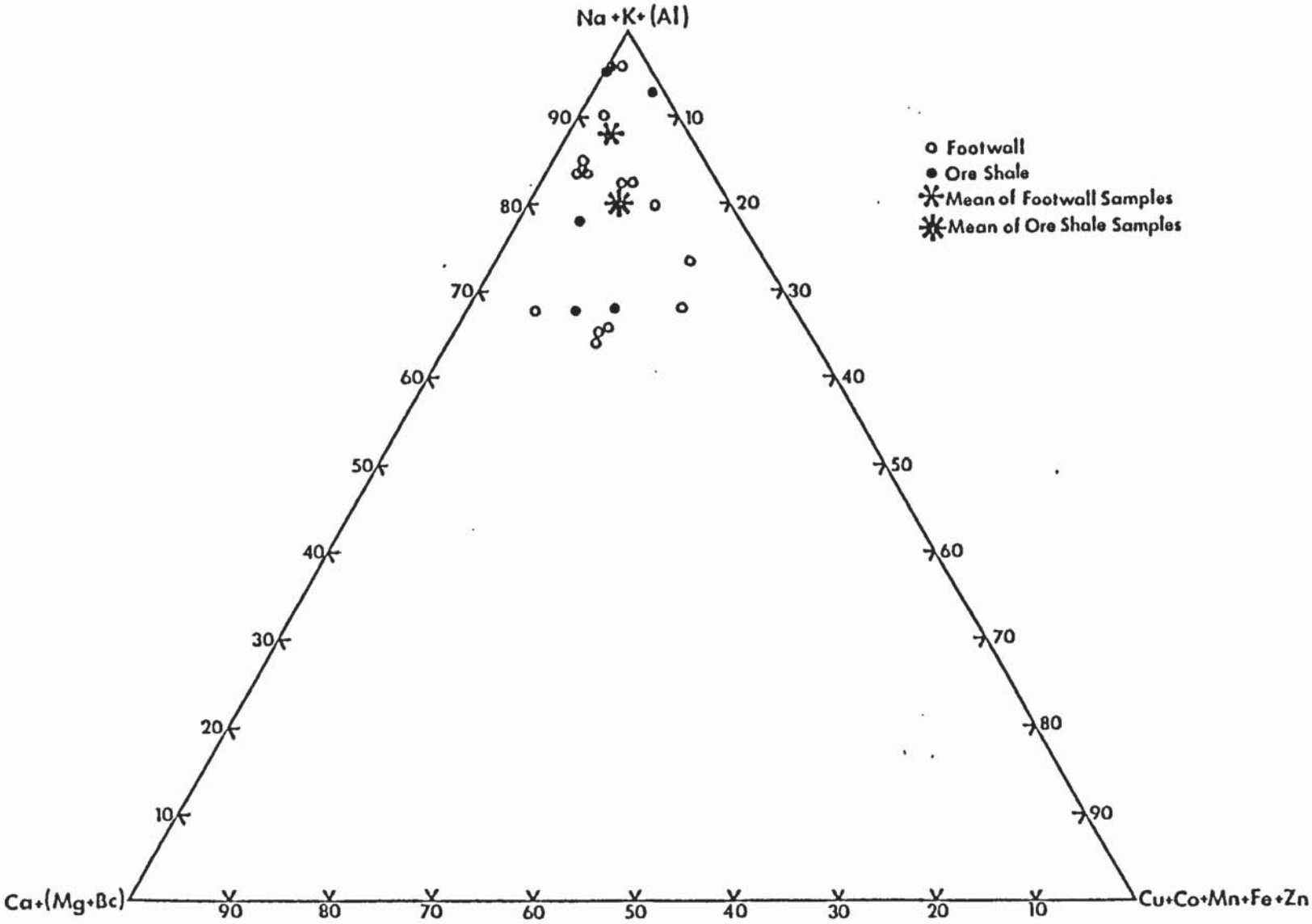

Fig. 7. 6

Plot of normalized cation totals for quartz vein fluid inclusions from the Ore Shale Footwall

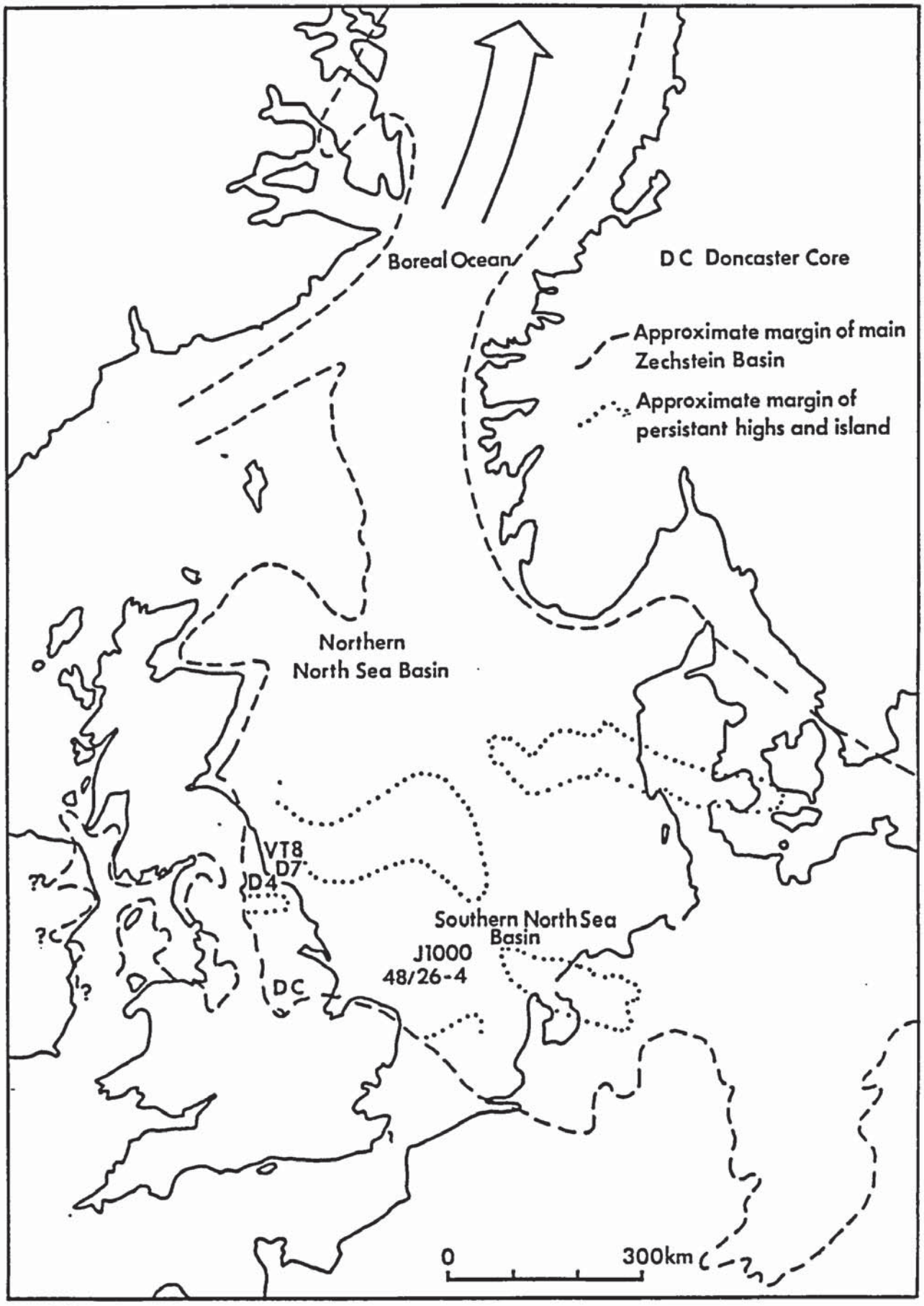

Fig 9.1

Generalized sketch map of the western parts of the Zechstein basin, showing location of boreholes sampled. (Adapted from Smith, 1980)

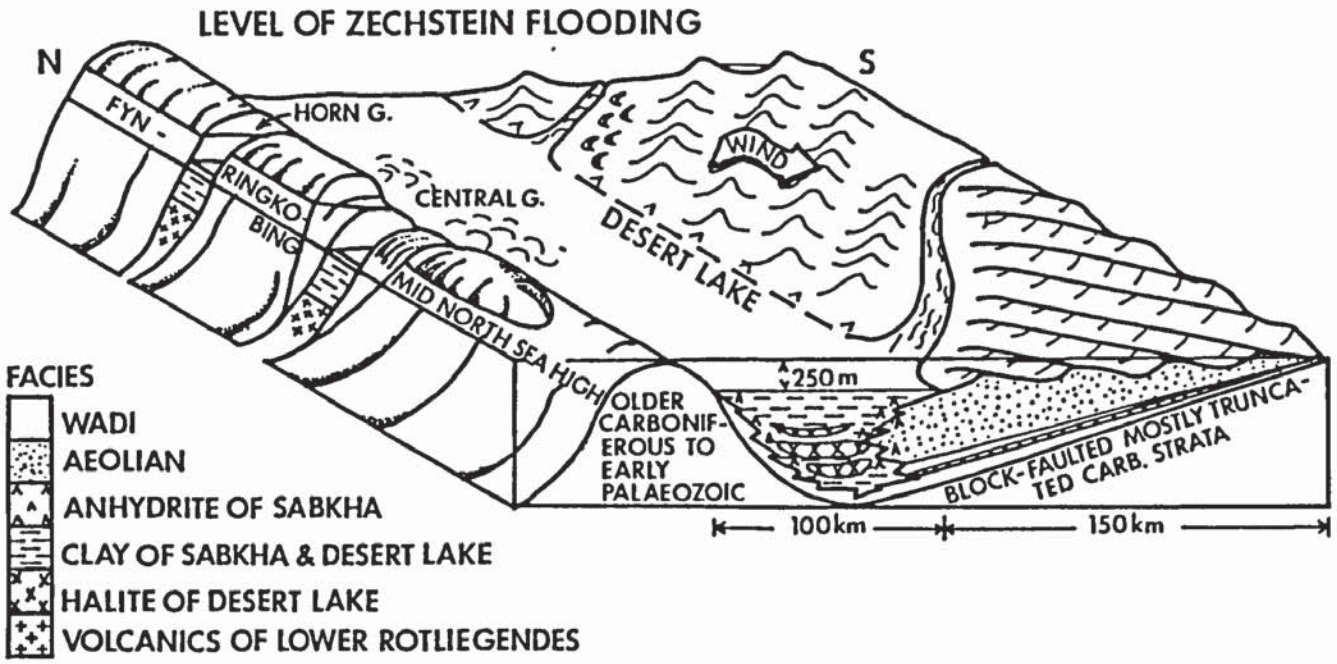

Fig.9.2

Schematic block diagram of the Southern Permian Basin and Central North Sea system of highs at the time of the Zechstein transgression. (After Glennie & Buller, 1983)

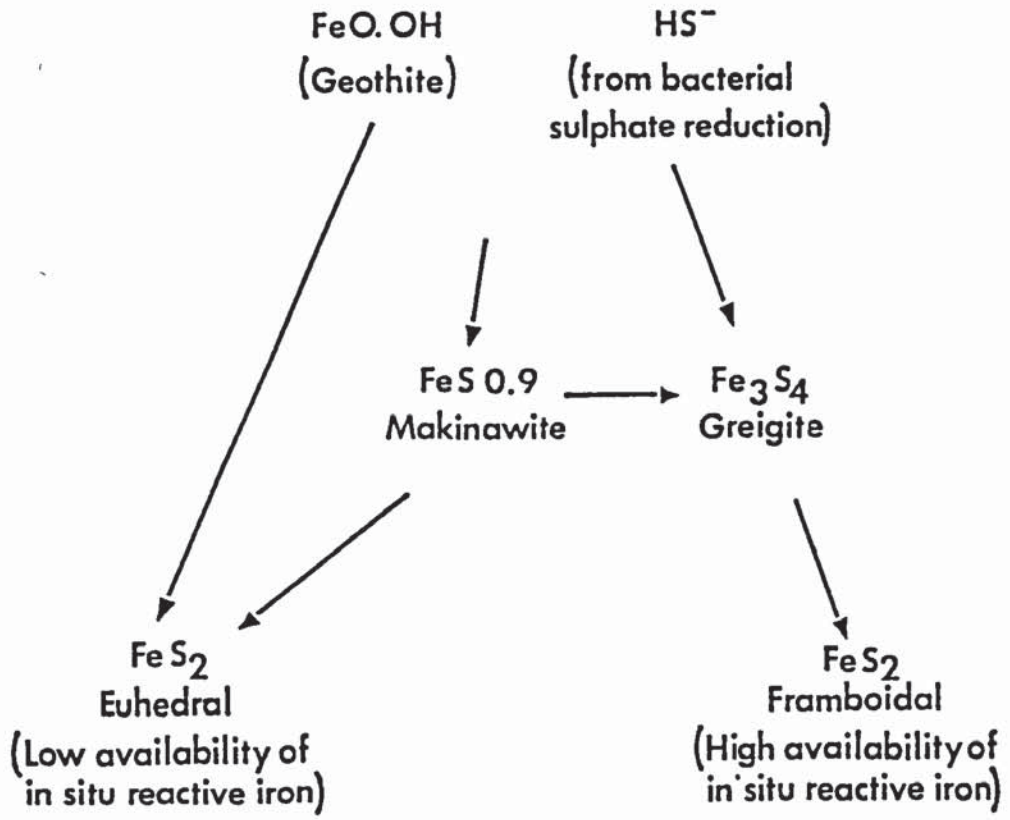

Fig. 9.3
Possible reaction pathways to framboidal and euhedral pyrite after Raiswell 1982

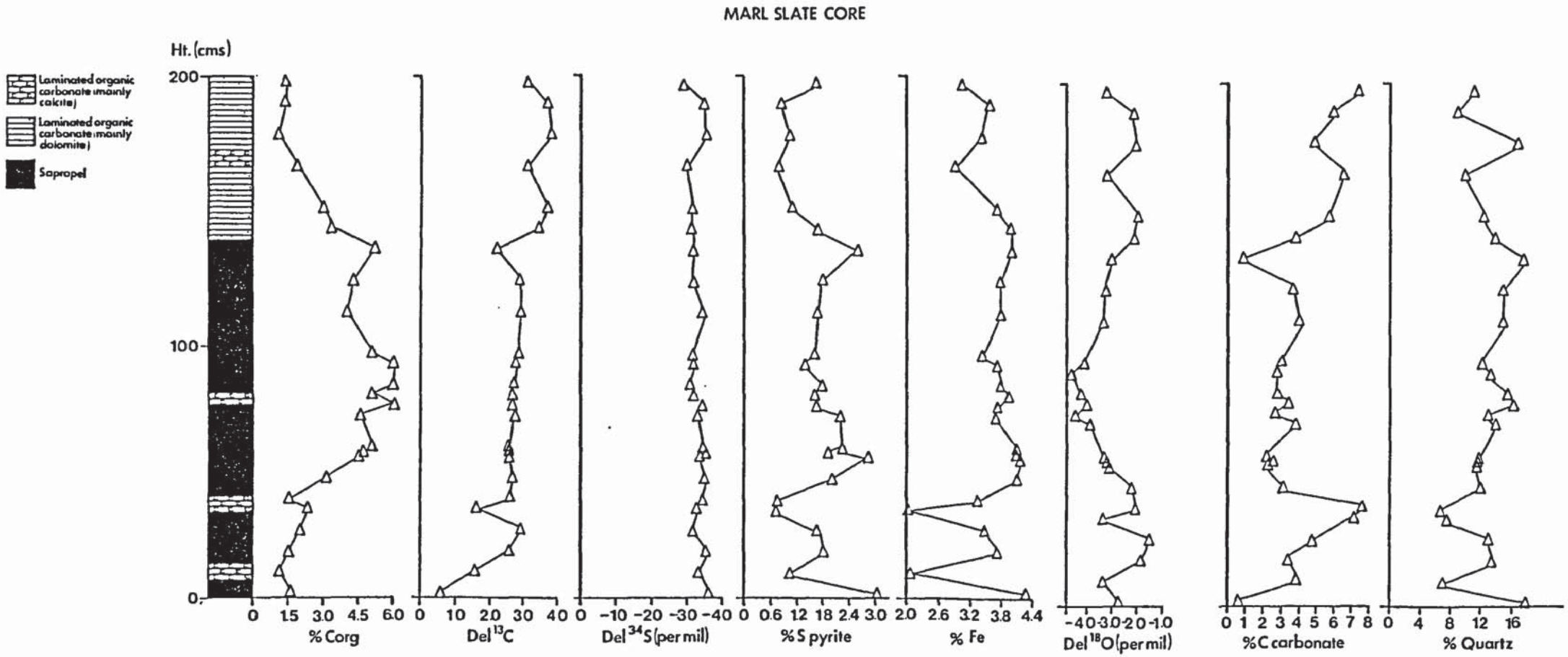

Fig 10.1 Vertical profiles of geochemical parameters of the Marl Slate Section of the Doncaster Core

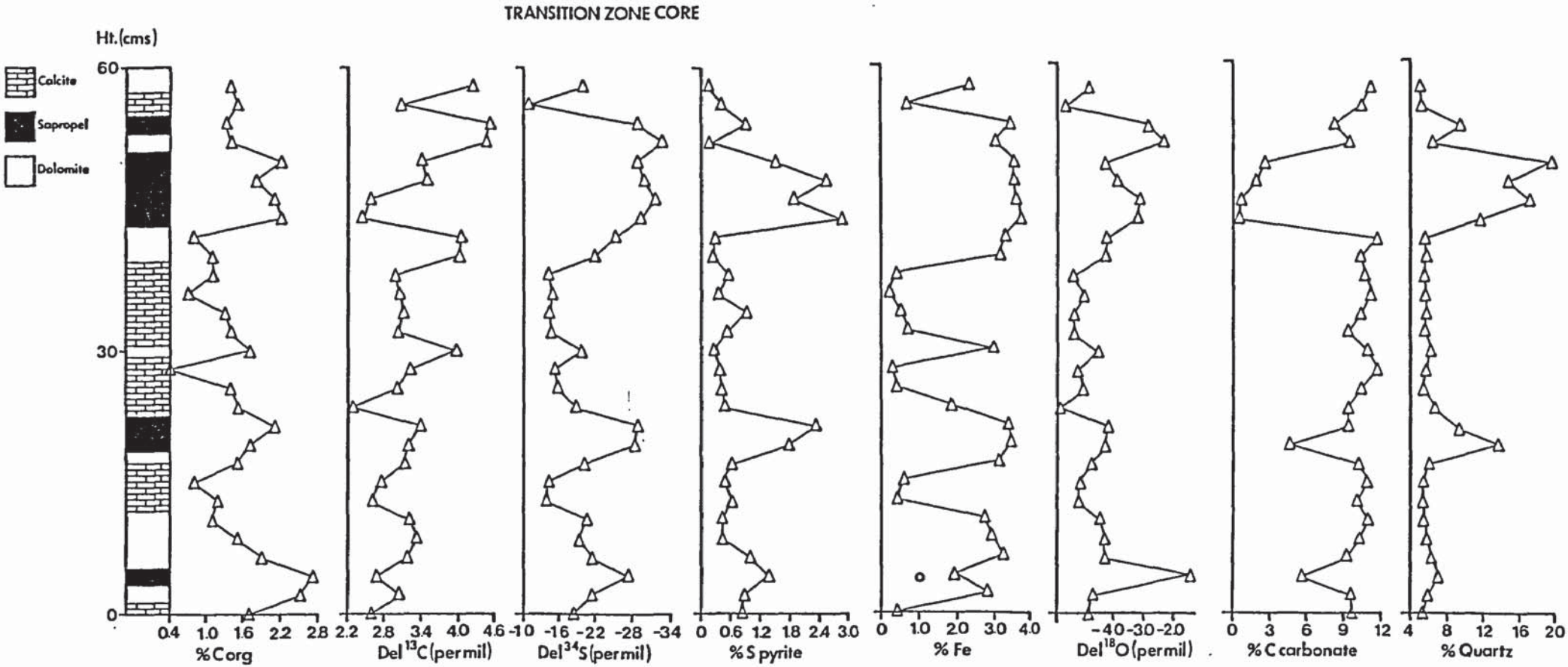

Fig 10.2

Vertical profiles of geochemical parameters of the Transition Zone Section of the Doncaster Core

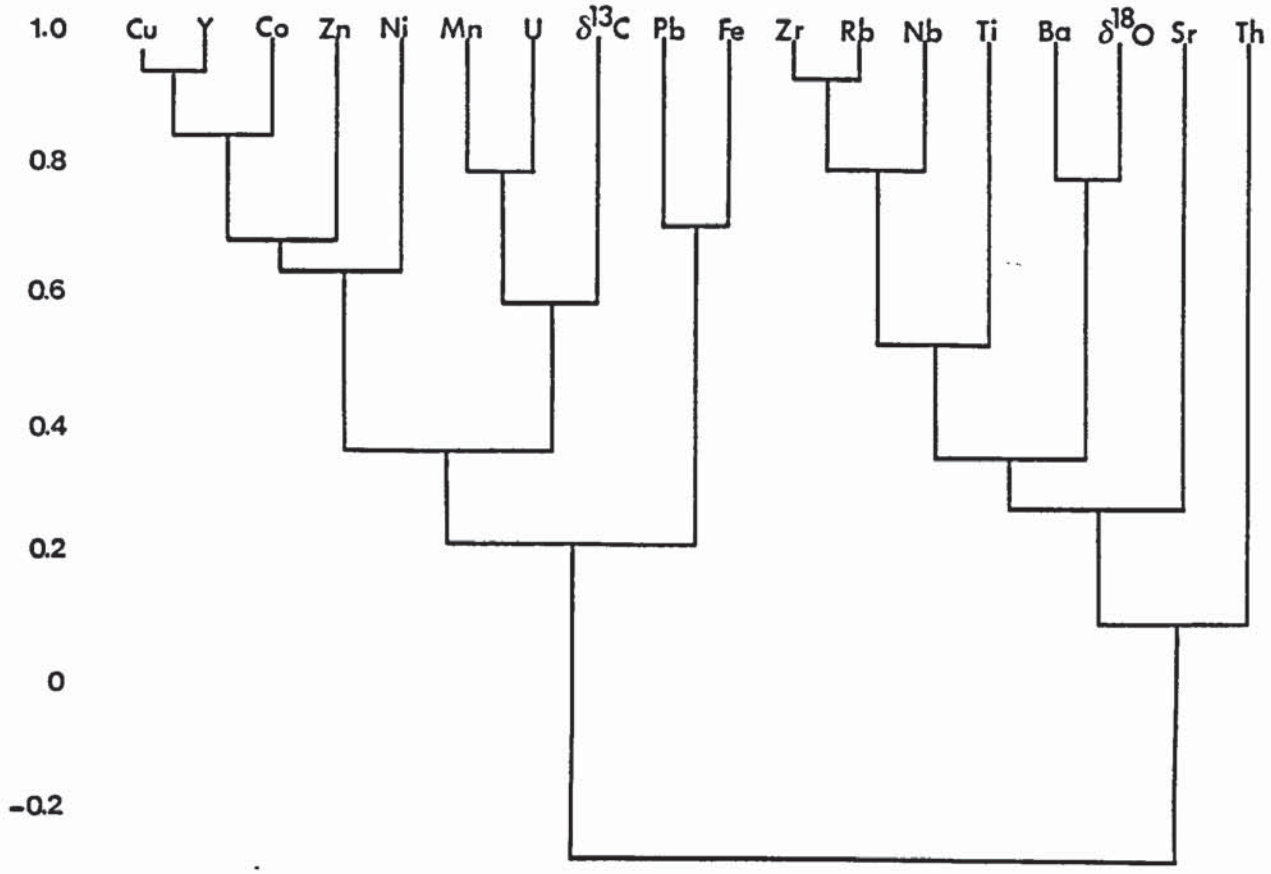

Borehole J1000

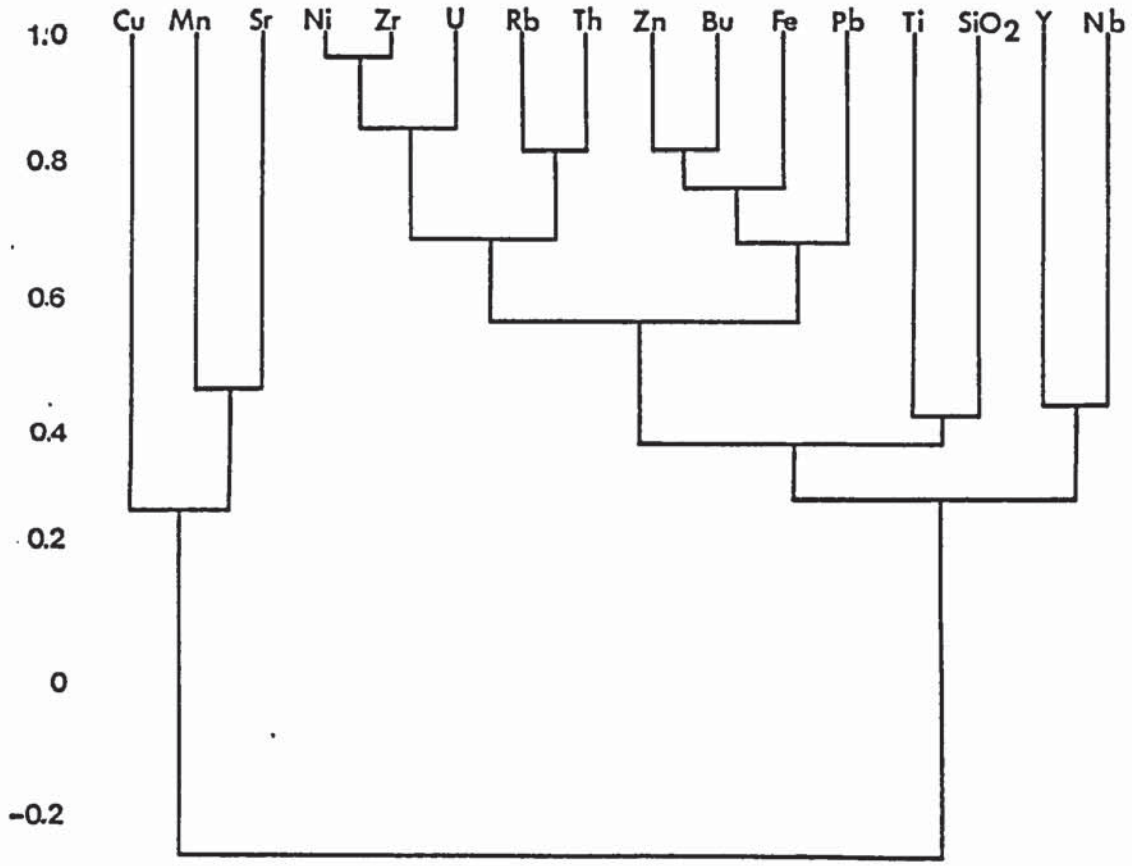

Borehole 49-26-4

Fig.10.3

Dendrograms for samples from the J1000 and the 49/26-4 cores

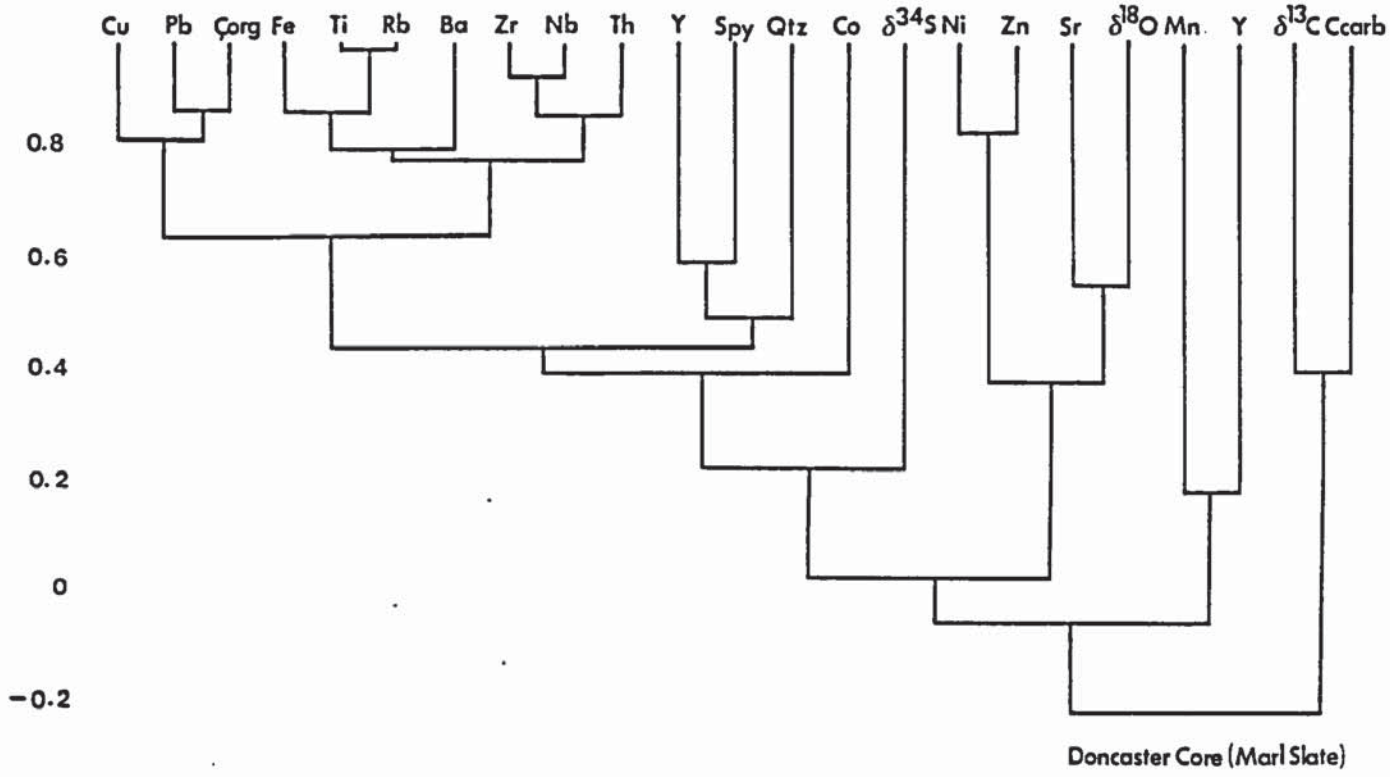

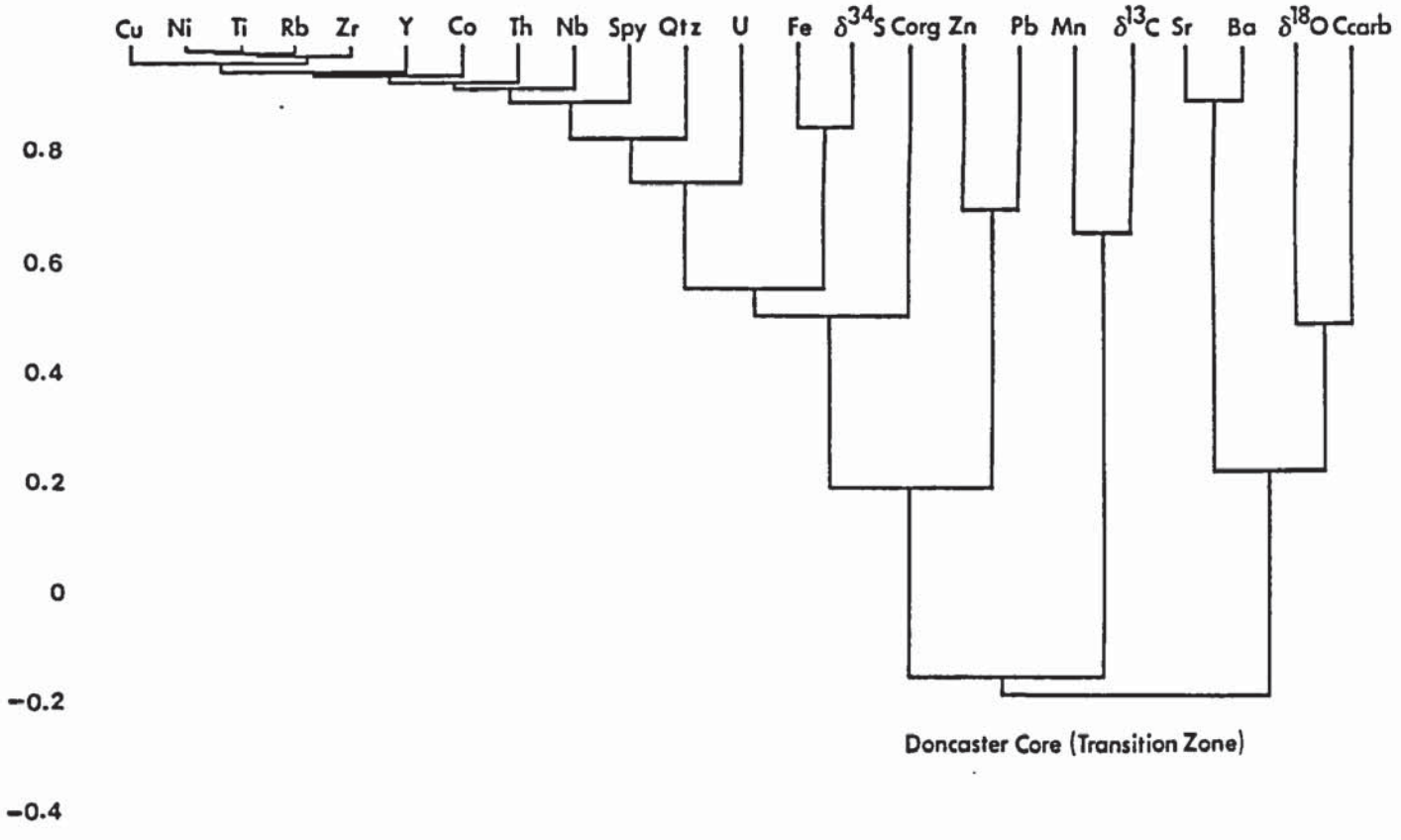

Fig 10.4

Dendrograms for samples from the Marl Slate and the Transition Zone section of tne Doncaster Core

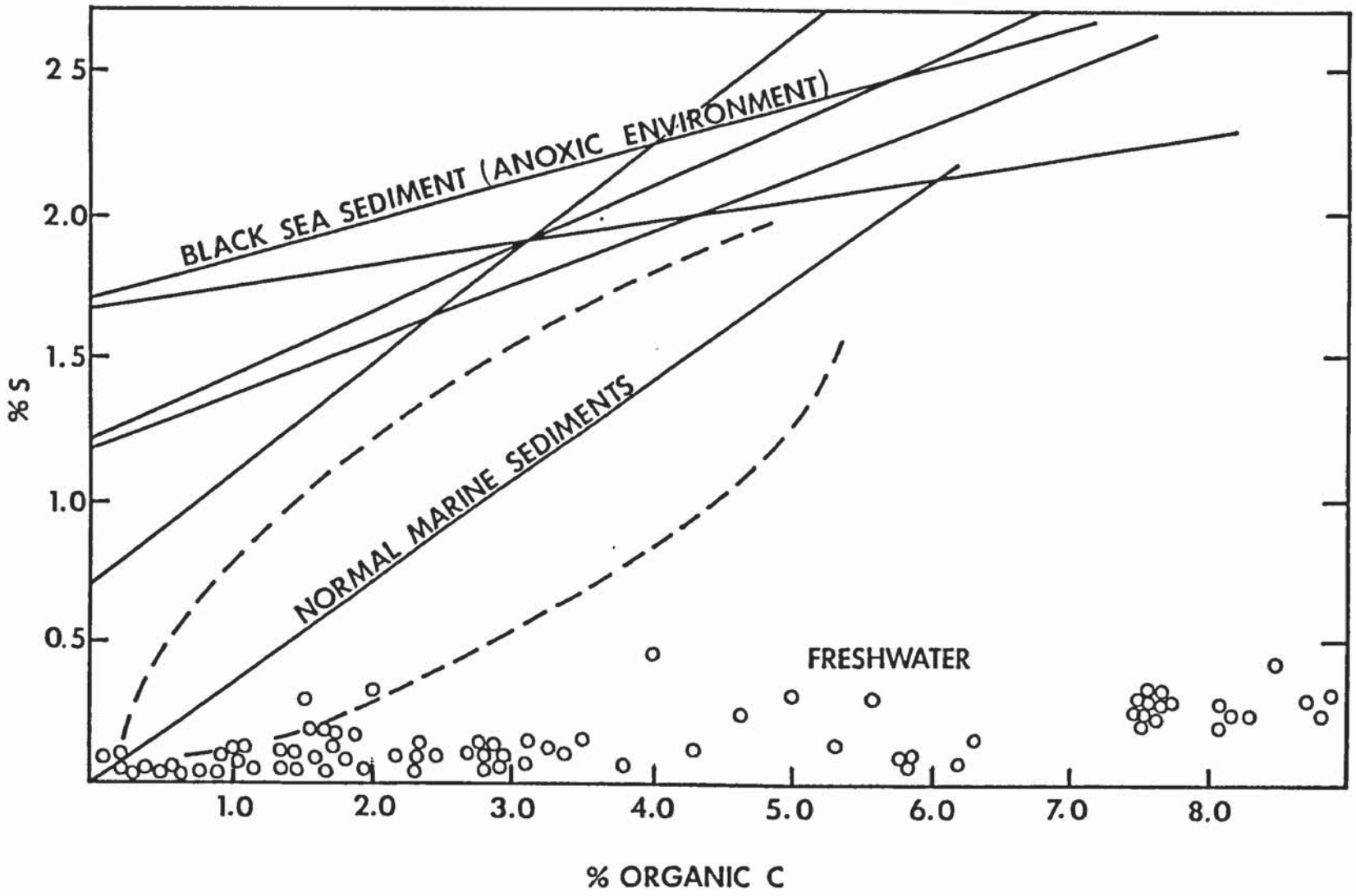

Fig. 10.6

Plot of weight percent organic carbon versus weight percent pyrite sulphur for freshwater, normal marine and anoxic sediments (Adapted from Leventhal 1983, Berner & Raiswell 1983)

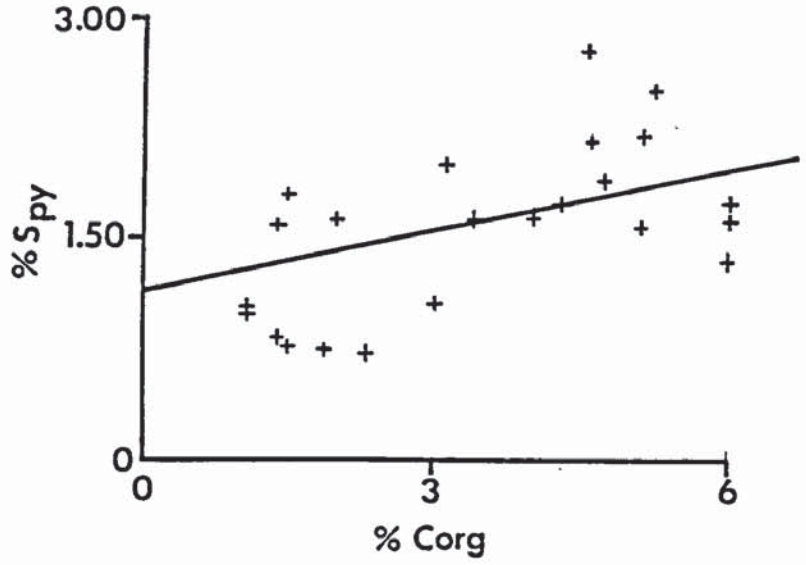

MARL SLATE SECTION
n = 24 Corr. Coef = 0.58

$\% S_{py} = 0.93 + 0.187 (\% Corg$

R Square = 0.34

C/S = 2.22

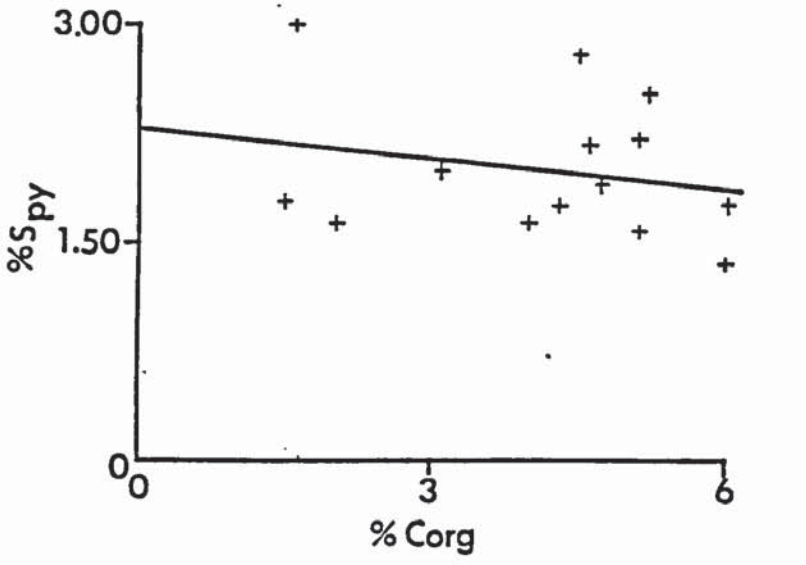

SAPROPELIC SAMPLES FROM THE MARL SLATE SECTION
n = 14 Corr Coef. = - 0.24

$\% S_{py} = 2.33 - 0.08 (\% Corg)$

R Square = 0.06

C/S = 1.80

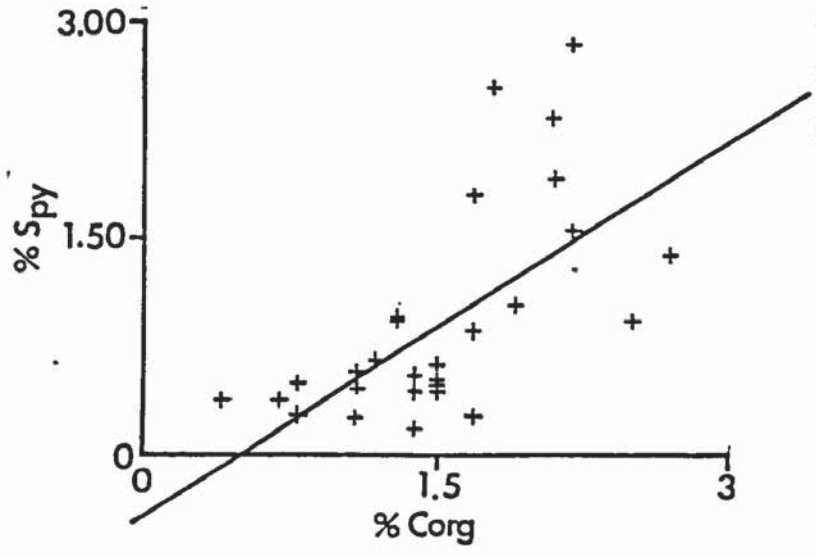

TRANSITION ZONE SECTION
n = 29 Corr Coef. = 0.63

$\% S_{py} = - 0.43 + 0.87 (\% Corg)$

R Square = 0.40

C/S = 1.72

Fig.10.7

Organic Carbon and Pyrite Sulphur Plots for samples from the Doncaster Core

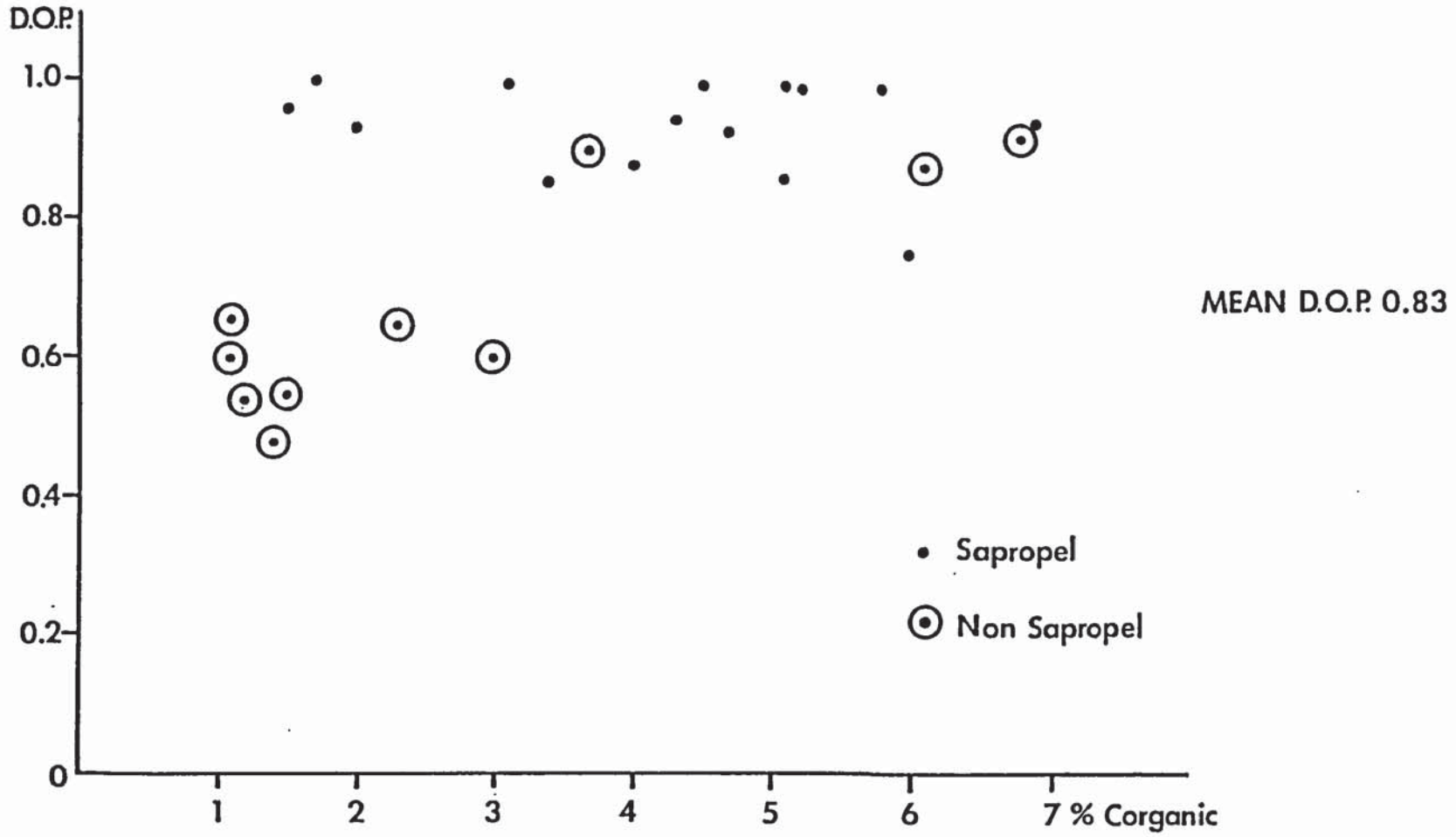

Fig. 10.8
Degree of pyritization plotted against organic carbon content for the Marl Slate section of the Doncaster Core

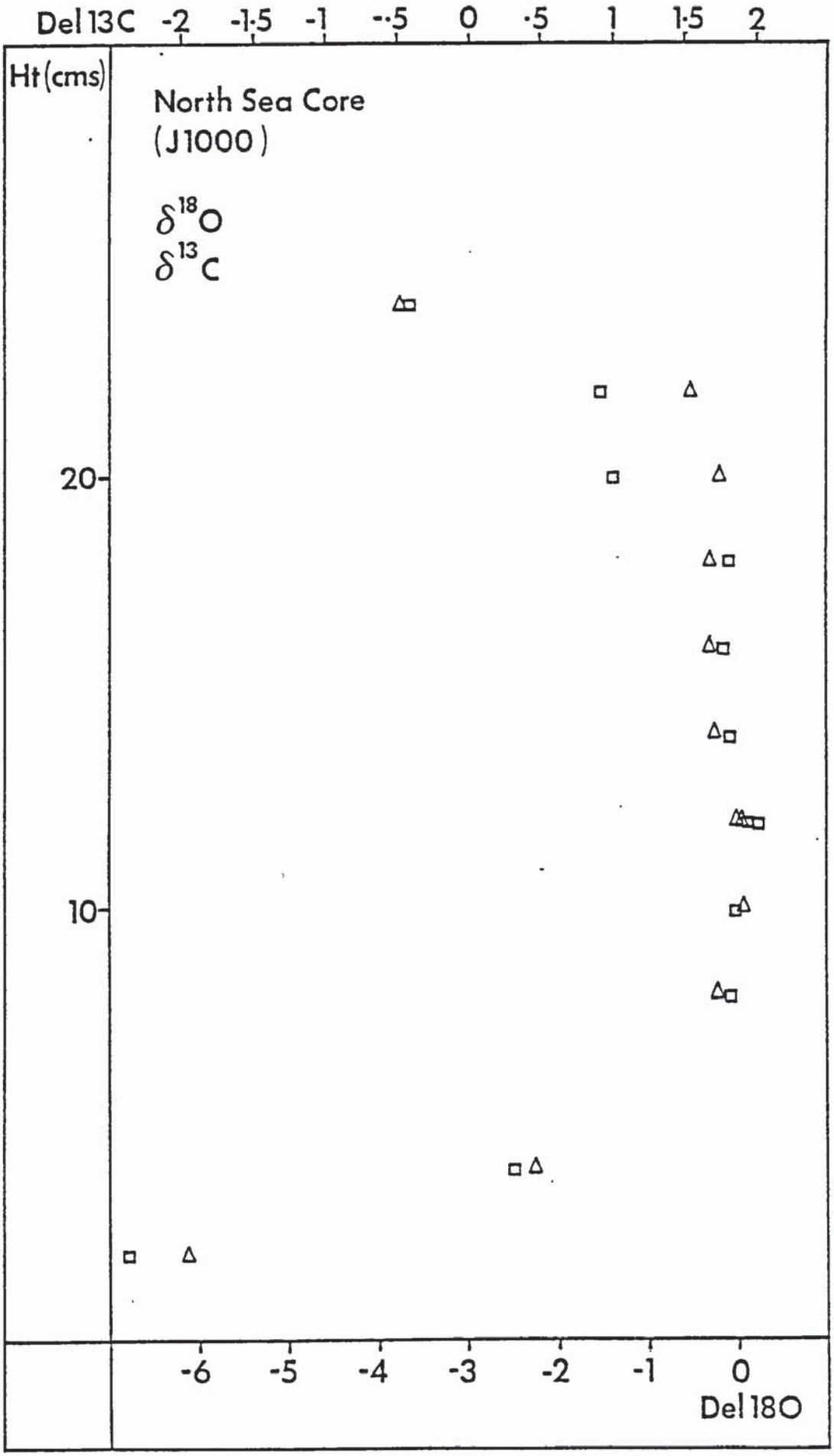

Fig.11.1 Plot of $\delta^{18}O$ and $\delta^{13}C$ values against height for Borehole J1000

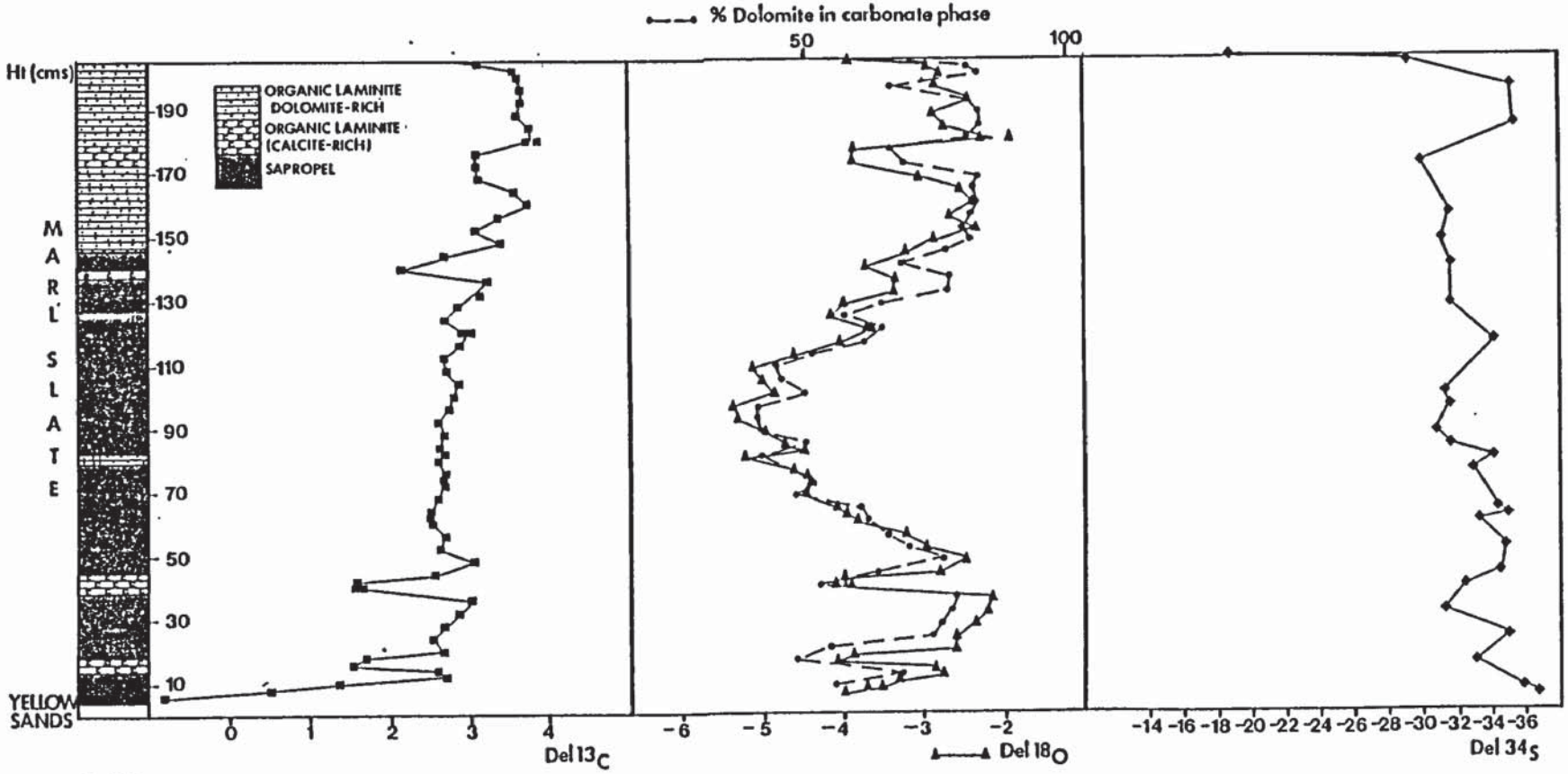

Fig.11.2

Plot of $\delta^{13}C$, $\delta^{18}O$, $\delta^{34}S$, and Percentage Dolomite in carbonate phase for the Marl Slate Section of the Doncaster Core

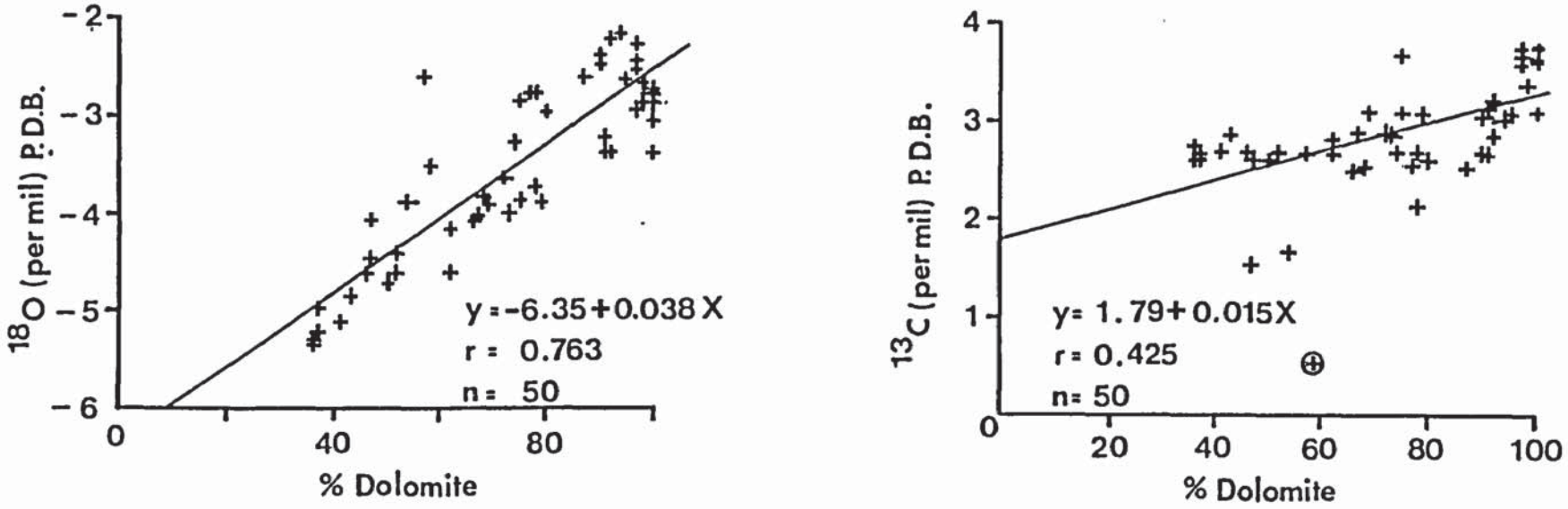

Fig.11.3

Plot of Percentage Dolomite in the sample Carbonate phase versus $\delta^{18}O$ and $\delta^{13}C$ values for the Marl Slate Section of the Doncaster Core

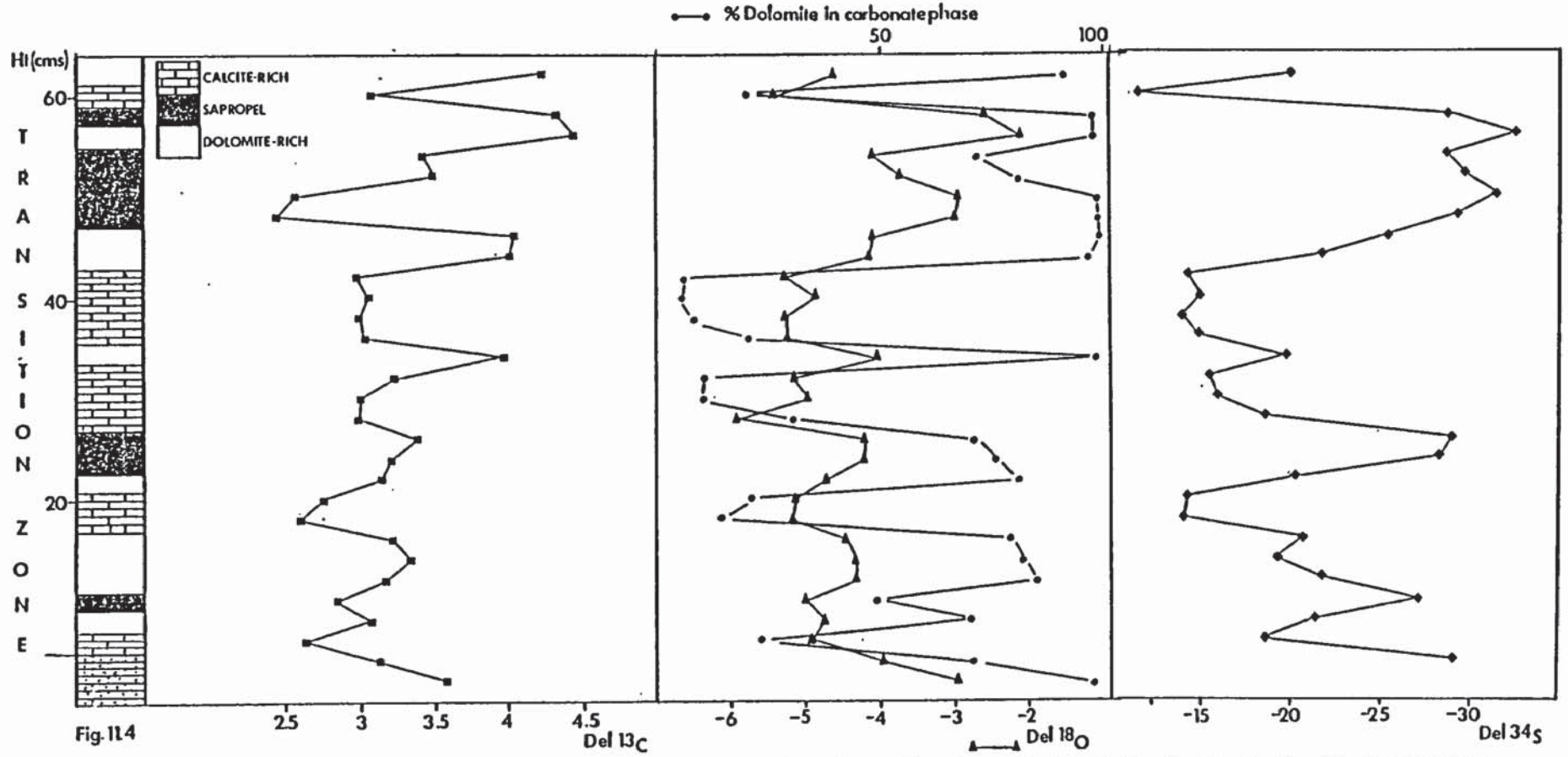

Fig. 11.4

Oxygen, Carbon and Sulphur isotype values and percentage dolomite in the carbonate phase for samples from the Transition Zone Section of the Doncaster Core

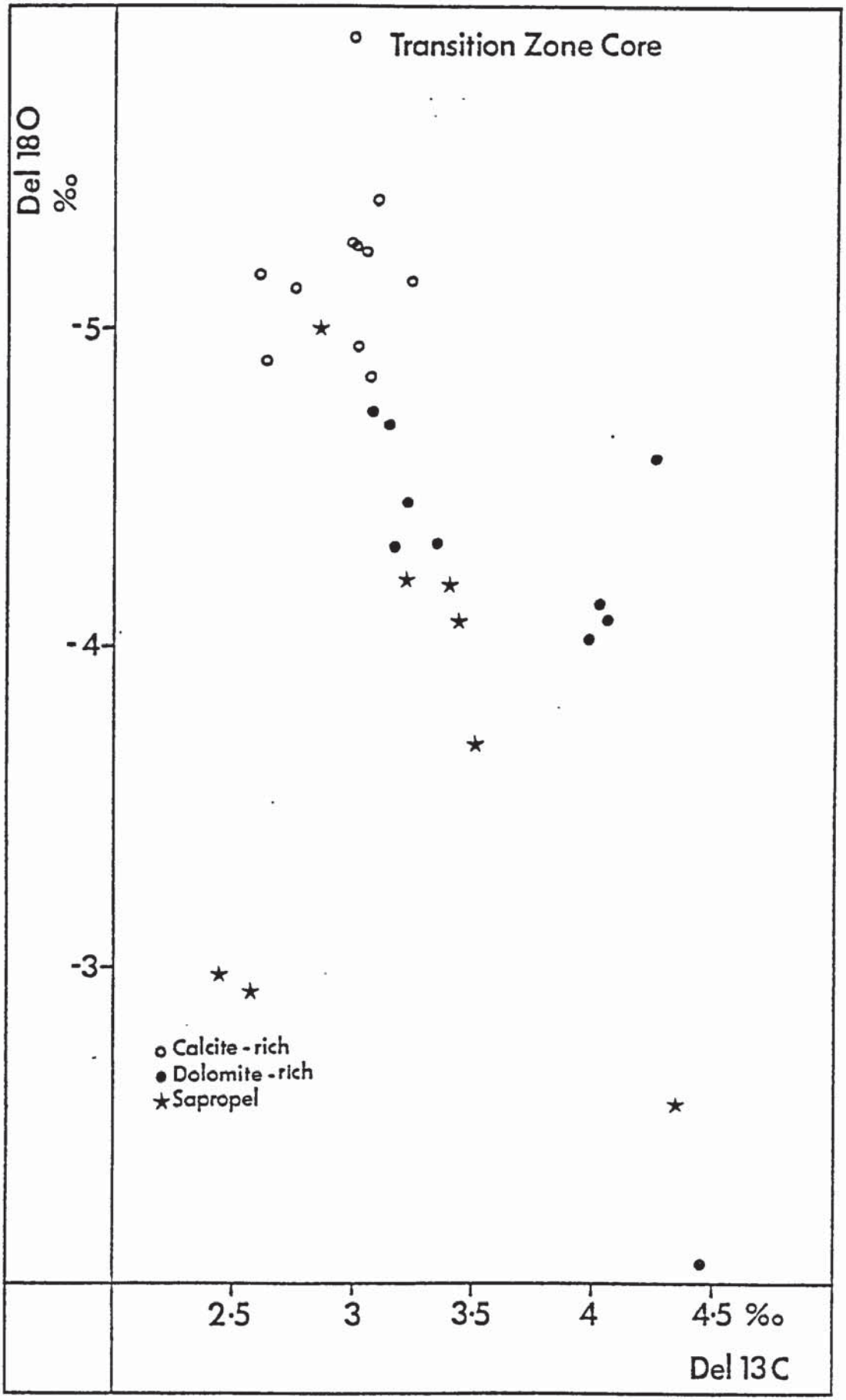

Fig.11.5
Plot of $\delta^{18}O$ versus $\delta^{13}C$ with lithology for the Transition Zone Core

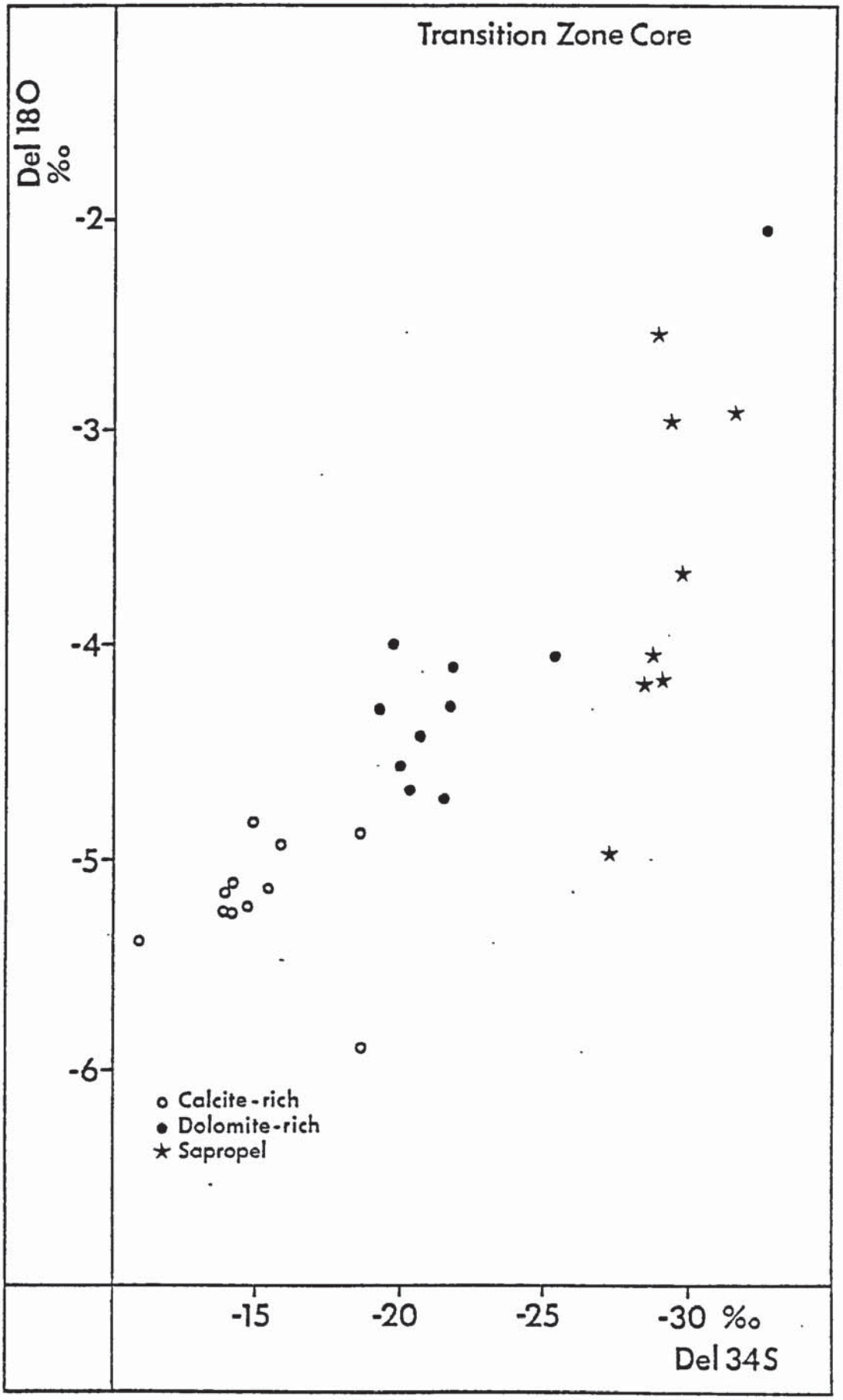

Fig. 11.6
Plot of $\delta^{18}O$ versus $\delta^{34}S$ with lithology for the Transition Zone Core

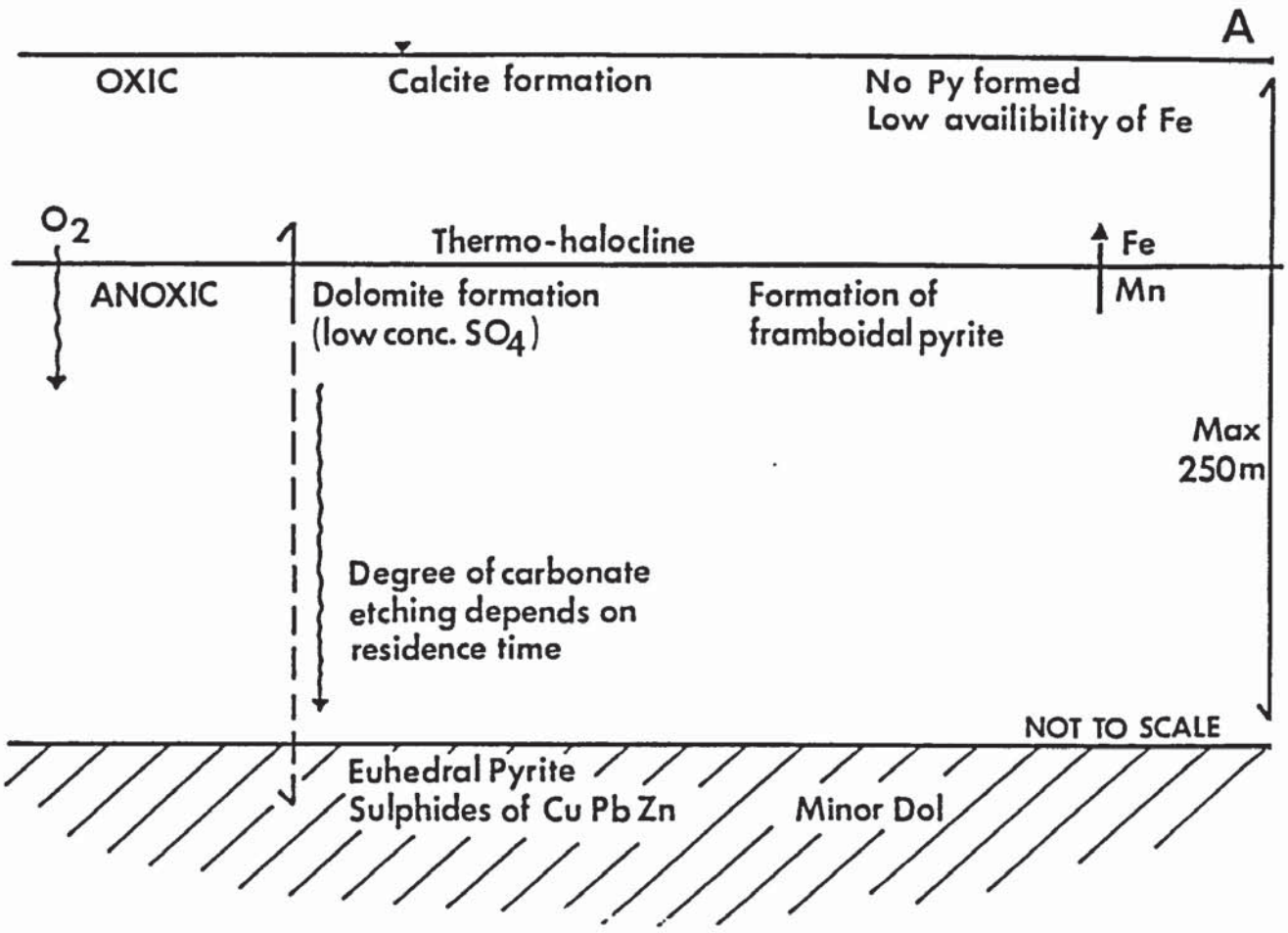

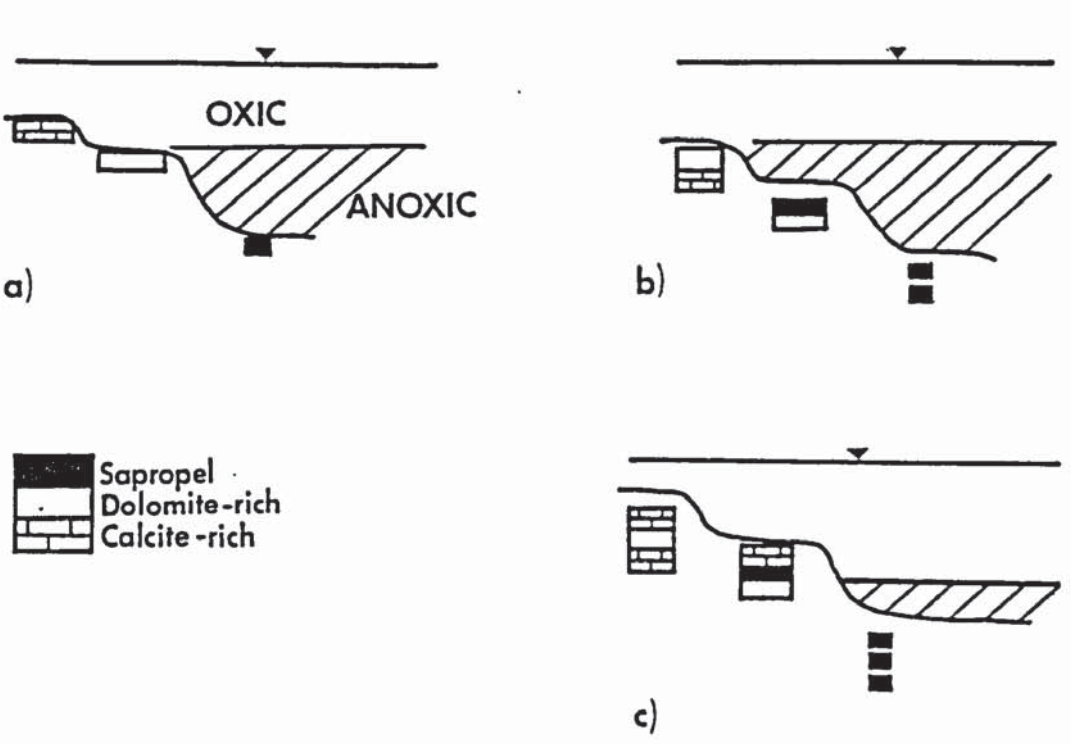

Fig. 12.1

Proposed model of Marl Slate Formation

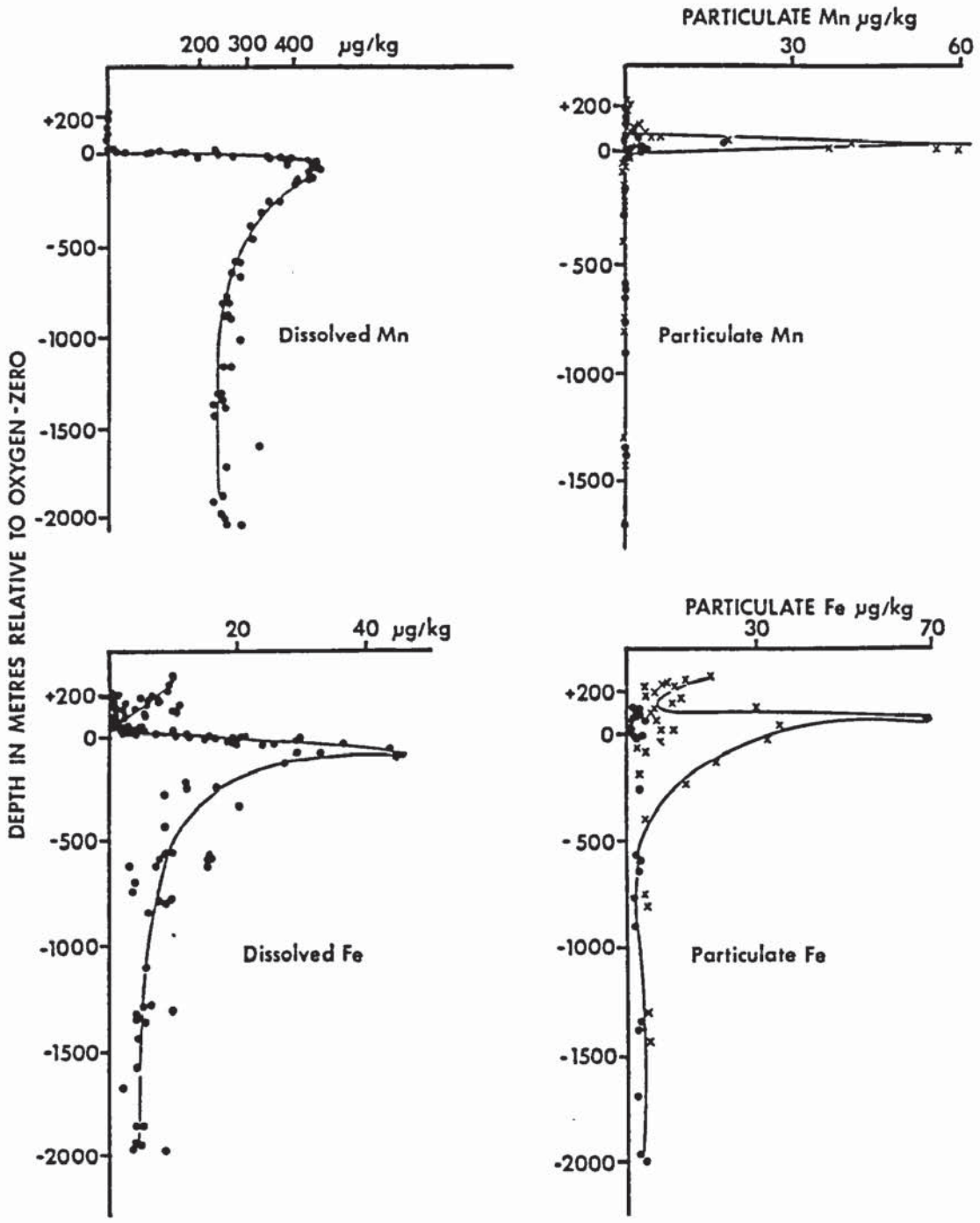

Fig. 12.2

Concentration of dissolved and particulate iron and manganese in the Black Sea (after Brewer & Spencer, 1974)

TABLES

Supergroup	Group	Formation	Member	Local Terminoglogy - Konkola	Approximate Thickness
KATANGA	Kundelugu	Upper		Shale	
		Middle		Sandstone	
		Lower		Kakontwe lst	250 m
	Upper	Grand Conglomerate		Tillite	10 m
		Mwashia		Mwashia	300 - 600 m
		Bancroft Dolomite		Upper Roan Dolomite	100 - 450 m
	Lower Roan	Kitwe	Antelope Clastics	Shale-with-Grit	40 - 165 m
			Chambishi Dolomites	Upper Hangingwall Aquifer	10 - 30 m
				Lower Hangingwall Aquifer	10 - 30 m
			Nchanga Quartzites	Hangingwall Quartzites	10 - 150 m
			Nokana Evaporites		
			Copperbelt Orebody	Ore-Shale E D C B A	5 - 20 m
		Mindola Clastics	Kafue Arenites	Footwall Conglomerate Footwall Sandstone Porous Conglomerate	20 - 40 m
			Bancroft Quartzite**	Argillaceous Sandstone Footwall Quartzites Lower Porous Conglomerate Pebble Conglomerate Boulder Congolmerate	400 m* 30 m 30 - 40 m 100 - 300 m
	Basement Complex			Schists and Gneiss with Muliashi Porphyry intrusions	

** Proposed name

Table 2.1 Stratigraphic succession of the Konkola Basin (classification modified after Clemmey, 1976).

Unit	Sedimentary Features	Comments
E	- Flaser bedding - Feldspathic layers	TRANSGRESSION
D	- Ripple marks - Load casts - Sulphidite layers	———————
		REGRESSION
C	- Ripple marks - Load casts - Desication cracks - Chicken wire texture	
B	- Siltstone with lower phase plane beds at base and upper phase plane beds towards the top - Moulds after gypsum	———————
		TRANSGRESSION
A	- Algal mats - Slump folding?	

EROSIONAL UNCONFORMITY

Table 3.1 Summary of sedimentary features in units of the Copperbelt Orebody Member (Ore-Shale).

%Mg	%Ca	%Mn	%Fe	%Co	%Cu	%Si	Total (%)
31.37	65.36	-	-	1.80	-	0.33	98.86
31.65	63.88	-	-	4.90	0.42	0.48	101.33
32.50	64.26	0.97	1.31	1.50	-	0.57	101.11
31.98	64.78	-	-	4.17	-	0.50	101.43
30.66	64.43	-	0.76	2.74	-	0.30	98.87
30.20	64.82	0.90	1.02	2.89	-	-	99.83
32.12	66.84	-	-	1.15	-	0.54	100.65
31.53	67.24	-	-	1.13	-	0.50	100.40
32.68	63.87	0.63	-	1.96	-	0.72	98.86
32.47	61.25	0.77	-	2.70	-	0.90	98.09

Table 4.1 Energy dispersive microprobe data for euhedral Footwall Dolomites (all metals calculated as percent carbonate).

Sample	%Cu	%Co	%Ni	%Fe	%S	Total (%)
Sample 638/6 Core	14.84	41.18	0.58	1.65	40.67	98.92
Rim	16.16	40.47	0.23	1.06	40.27	98.19
	14.81	41.32	0.63	1.67	40.63	99.05
(Hangingwall)	15.75	41.02	0.31	1.18	40.63	99.05
	16.56	41.26	0.56	0.09	40.53	99.00
	16.75	41.27	0.53	0.05	40.84	99.44
Ore-Shale (Borehole AP978)	16.94	40.91	0.71	0.07	40.17	98.80
	16.70	41.26	0.36	0.09	40.77	99.18
	16.29	41.81	0.31	0.05	40.82	99.28
(Footwall)	16.12	41.80	0.38	0.10	40.44	98.84
Average	16.09	41.23	0.46	0.60	40.55	98.93
Normalised Average	16.26	41.68	0.46	0.61	40.99	100.00
	18.13	40.25	0.26	0.16	40.99	99.79
FOOTWALL Samples	17.97	40.57	0.20	0.15	40.97	99.86
	17.44	40.03	0.07	0.01	41.17	98.72
	17.91	39.84	0.07	0.13	41.11	99.06
Average	17.86	40.17	0.15	0.11	41.06	99.35
Normalised Average	17.98	40.43	0.15	0.11	41.33	100.00

Table 4.2 Electron probe microanalysis of Carrollites

Grain No.	%SiO_2	%Al_2O_3	%K_2O	%Na_2O	%CaO	%CuO	%BaO	Total (%)
g 1	66.58	19.02	12.97	0.80	-	-	0.63	100.00
A	64.35	18.01	15.27	0.31	-	0.08	0.05	98.07
g 2	67.41	19.39	12.82	0.85	-	0.25	0.43	100.95
A	69.29	19.67	12.90	0.43	-	0.25	0.13	102.67
g 3	66.55	18.91	14.43	0.68	-	0.08	0.41	101.06
A	69.59	20.09	0.08	10.97	0.27	0.21	-	101.16
g 4	65.40	18.93	14.41	0.80	-	-	0.91	100.45
A	67.13	18.99	14.68	0.34	-	0.22	-	101.36
A	67.54	19.17	14.22	0.53	-	0.27	-	101.73
g 5	66.45	19.36	14.12	0.92	-	-	0.96	101.81
A	66.36	18.66	15.08	0.36	-	-	0.12	100.58
A	67.32	19.04	14.28	0.27	-	0.05	0.07	101.03
g 6	65.47	18.53	15.14	0.64	-	-	0.30	100.07
A	65.90	18.52	14.12	0.36	-	-	0.09	98.99
g 7	64.83	18.65	14.85	0.75	-	-	1.26	100.34
A	65.92	18.47	14.06	0.33	-	-	0.04	98.82
g 8	67.17	19.04	14.00	0.52	-	-	-	100.73
A	66.38	18.82	15.65	0.30	-	-	-	101.15
g 9	66.82	18.88	13.78	0.82	-	-	-	100.30
A	65.66	18.53	14.95	0.45	-	-	0.05	99.64
g 10	66.21	18.84	14.50	0.89	-	-	0.36	100.80
A	64.15	17.96	14.29	0.41	-	0.10	0.05	96.96

Table 4.3 Electron probe microanalysis of feldspar grains (g) and authigenic overgrowths (A) from the Ore-Shale.

Sample Number	$\delta^{34}S$	Comments
AP978/7L	-6.6	Lenticle chalcopyrite
AP978/7D	-6.3	Disseminated chalcopyrite, same sample as above
AP978/7C	-6.2	Carrollite, same sample as above
AP978/8L	-7.0	Lenticle chalcopyrite
AP978/9L	-6.6	Lenticle chalcopyrite
AP978/9C	-5.9	Carrollite, same sample as above
AP978/10L	-6.0	Lenticle chalcopyrite
AP978/10LC	-6.1	Chalcopyrite from lenticle core, same sample as above
AP978/10Le	-5.7	Chalcopyrite from lenticle edge, same lenticle as above
AP978/10D	-5.9	Disseminated chalcopyrite, same sample as above
AP978/10C	-6.1	Carrollite, same sample as above
AP978/12L	-4.2	Lenticle chalcopyrite
AP978/12D	-4.3	Disseminated chalcopyrite, same sample as above
AP978/13L	-2.8	Lenticle chalcopyrite
AP978/14D	-1.1	Disseminated chalcopyrite
AP978/15L	-0.4	Lenticle chalcopyrite
AP958/16L	+1.1	Lenticle chalcopyrite
AP978/16D	+0.9	Disseminated chalcopyrite, same sample as above
AP978/17L	+1.0	Lenticle chalcopyrite
AP978/18L	+1.2	Lenticle chalcopyrite
AP978/19L	-0.3	Lenticle chalcopyrite
AP978/19D	-0.4	Disseminated chalcopyrite, same sample as above
AP978/20D	-1.9	Disseminated chalcopyrite

Table 6.1 Sulphur isotope results for samples from Borehole AP978

Sample Number	$\delta^{34}S$	Comments
		FOOTWALL SAMPLES
Mbula Cp	+13.0	Chalcopyrite from Mbula Footwall Orebody Chingola
Mbula Bn	+12.3	Co-existing Bornite from above sample Temperature 330°C ± 20°C
KLB 136/Cp	+8.7	Chalcopyrite approx. 5m below GFW
KLB 136/Bn	+8.6	Co-existing Bornite from same sample as above
KLB 136/Bn	+8.7	Check sample
Carrollite 1	-1.1	Euhedral carrollite from Footwall Sandstone
Carrollite 2	-1.2	As above
Carrollite 2b	-1.3	Check sample
Carrollite 3	-2.5	Euhedral carrollite from Footwall Sandstone
Carrollite 4	-8.3	As above
FW2 Chalcocite	-1.0	Interstitial rim cement
197/1 Chalcocite	-3.8	Interstitial fined grained chalcocite
Chalcocite	-1.3	Chalcocite approx. 3cms below GFW
		UNIT A SAMPLES
197/2 Chalcocite	+0.8	Thin (3mm) chalcocite seam parallel to bedding
197/2 Chalcocite	+0.8	Check sample
		UNIT B SAMPLE
UB Carrollite	-4.0	Disseminated carrollite
		UNIT C SAMPLES
AP646/7 Cp	-4.6	Co-existing pair gives temperature of greater than 700°C
AP646/B Bn	-4.4	Probably no equilibriated
AP674/9 Cpy	-3.2	Chalcopyrite showing graded bedding
CP197/14 Cpy	+1.5	Co-existing pair gives temperature of 600°C ± 50°C
Cp197/14 Bn	+1.1	Probably not equilibriated
		UNIT D SAMPLES
Ch Cp	+2.6	Co-existing pair from partially
Ch Bn	+2.3	sulphide replaced anhydrite nodule gives
Ch Cp	+2.0	As above but different samples.
Ch Bn	+1.5	Temperature 350°C±30°C
Pod Vein Cpy	-1.4	Co-existing pair from quartz-feldspar
Bn	-0.7	vein. Temperature of formation 325°C±25°C
S/S Vein Cpy	-5.3	Co-existing set from quartz feldspar
Bn	-5.2	vein gives temperature of greater than
Carr	-4.1	700°C; probably not equilibriated.

Table 6.2 Sulphur isotope results from Ore-Shale and Footwall rock samples

Sample	$\delta^{13}C$ (PDB)	$\delta^{18}O$ (PDB)	$\delta^{18}O$(SMOW)	Comments
	FOOTWALL QUARTZITE SAMPLES (BANCROFT QUARTZITE MEMBER)			
FW1	+1.99	-19.17	11.10	Calcite from Footwall Quartzite
FW2	+1.81	-19.20	11.06	Calcite from Footwall Quartzite
	FOOTWALL SAMPLES (KAFUE ARENITE MEMBER)			
9463	-9.37	-9.74	20.82	Footwall Co Dolomite
9651	-6.56	-4.34	26.38	Footwall Co Dolomite
9652	-6.12	-4.35	26.37	Footwall Co Dolomite
9668	-6.43	-6.41	24.25	Footwall Co Dolomite
9669	-6 59	-6.79	23.86	Footwall Co Dolomite
9654	-4.42	-8.00	22.61	Footwall Dolomite
9771	-5.90	-4.82	25.89	Footwall Dolomite
	-4.42	-5.11	25.60	Footwall Dolomite
		ORE-SHALE SAMPLES		
Ua	-10.16	-15.50	14.88	Unit A Dolomite
Pc	-16.78	-14.68	15.23	Unit C Dolomite
Ld	-12.82	-14.44	15.98	Unit C layered Dolomite
946S	-9.22	-15.28	15.10	Lenticle core
9647	-8.77	-14.33	16.09	Lenticle core
9653	-9.70	-15.10	15.10	Lenticle core
9766	-10.11	-15.23	16.16	Lenticle core
6341	-10.50	-13.05		Lenticle core
9644	-20.52	-14.28	16.14	Lenticle edge
9646	-20.51	-15.81	14.56	Lenticle edge
9767	-13.13	-15.79	14.85	Lenticle edge
10678	-18.52	-13.64	16.80	Lenticle edge

Table 6.3 Carbon and Oxygen isotope results for Konkola carbonates

Sample	$\delta^{13}C$ (PDB)	$\delta^{18}O$ (PDB)	$\delta^{18}O$ (SMOW)	Comments
197/21	-13.27	-14.91	15.49	Hangingwall Quartzite
197/20	-13.42	-14.91	15.49	Hangingwall Quartzite
197/19	-15.01	-14.91	15.81	Unit E
197/18	-16.28	-13.79	16.65	Unit E
197/17	-16.69	-13.67	16.76	Unit D
197/16a	-17.08	-13.76	16.68	Unit D
197/16b	-17.95	-13.65	16.68	Unit D repeat sample
197/15	-17.78	-13.73	16.79	Unit D
197/14	-17.84	-13.78	16.65	Unit D/C
197/13	-17.67	-13.57	16.87	Unit D/C
197/12	-17.74	-13.70	16.74	Unit C
197/11	-17.42	-13.87	16.56	Unit C
197/10	-16.90	-13.98	16.45	Unit C
197/9	-16.64	-14.21	16.21	Unit C
197/7	-16.35	-14.58	15.84	Unit B
197/6	-15.15	-14.09	16.33	Unit B
197/5	-14.61	-14.54	15.87	Unit B
197/4	-13.61	-15.04	15.35	Unit B
197/3	-11.97	-12.96	17.50	Unit A
197/2	-5.04	-14.30	16.12	Unit A
197/1a	-5.55	-8.17	22.44	Footwall Conglomerate
197/1b	-5.62	-8.41	22.19	Repeat sample

Table 6.4 Carbonate isotope results for whole rock samples from Borehole CP197

Lenticle Dolomite Chemistry (Atomic Absorption Analysis)

LENTICLE DOLOMITE

Sr (ppm)		Na (ppm)	
Rim	Core	Rim	Core
134	250	211	258
150	192	128	300
35	115 (130)	125	210 (235)
169	336	179	336
122	204	161	268 mean

FOOTWALL DOLOMITE

Sr (ppm)	Na (ppm)
341	208
300	193
186	221
276	207

Electron-microprobe data (Normalised Percentage Carbonate)

%Mg	%Ca	%Fe	%Mn	%Co	
42.03	52.12	4.61	1.22	0.02	Core Dolomite n=10
41.73	52.10	4.61	1.45	0.09	Rim Dolomite n=15

Table 6.5 Atomic absorption analysis results of Footwall and Ore-Shale lenticle dolomites, and EPMA analysis of lenticle rim and core samples.

	No. 1 Shaft		No. 3 Shaft	
	Footwall Aquifer	Hanging Aquifer	Footwall Aquifer	Hanging Aquifer
pH	6.6-8.4	7.0-8.5	6.6-8.3	6.6-8.6
Eh(MV)	150-400	200-550	200-240	300-450
Mg/Ca ratio	1.:1.7	1:1.3	1:1.5	1:3

$\delta^{18}O$ Values (SMOW)

Footwall aquifer (220L 1000S drain drive)	-6.2 per mil
Hanging wall aquifer (1600L 200N D/W crosscut)	-6.2 per mil
Upper Roan dolomite (1600L 200N D/W crosscut)	-6.2 per mil
Kafue River	-3.6 per mil

Table 6.6 Compositional and isotopic data for mine waters at Konkola

Sample	Number	$\delta^{13}C$	$\delta^{18}O$ (PDB)	$\delta^{18}O$ (SMOW)	Comments
TB	1	-14.9	-6/7	23.9	Layered (5mm) malachite from the top of Unit B
TUB		-15.3	-8.7	21.9	As above but on re-examination sample found to be contaminated with Wad.
UB1	2b	-14.6	-6.1	24.6	Globular malachite partially filling a mould after gypsum
UB2	2a	-14.8	-6.4	24.2	Different sample but from same core sample as above
UA1	3a	-13.4	-7.6	23.1	Nodular malachite from Unit A
UA3	3b	-13.4	-7.4	23.3	Different sample but from same core specimen as above
UA2		-14.1	-9.2	-21.4	As above but on re-examination sample found to be contaminated with Wad.
GFWM	4	-13.5	-7.1	23.5	Layered malachite 2cm above the GFW contact
FWA	5	-12.6	-9.7	20.8	Nodular malachite (pore fill) 5cm below the GFW contact
FW1	6	-13.0	-8.0	22.6	Interstitial rim cement
FW3	7	-14.0	-7.6	23.0	Interstitial rim cement
FW4A	8b	-11.1	-12.8	17.6	Interstitial rim cement
FW4B	8a	-11.1	-12.4	18.2	As above. Check sample
FW5A	9	-7.8	-12.3	18.2	Interstitial rim cement
FW5B	10	-8.5	-13.5	16.9	Different sample but from same core specimen as above
FW6	11	-5.8	-11.4	19.1	Interstitial rim cement
SM	Sec Mal	-9.4	-4.4	26.3	Botroydal malachite from the same elevation (2200-2400L) as the above samples.

Table 6.7 Isotope results of Malachite samples (in descending stratigraphic order)

Sample	$\delta^{18}O$ (SMOW)			Mean	Comments
N/S Vein Quartz	17.51	17.28	17.58	17.45	Temperature 830°C
N/S Vein K Fds	16.78	16.61	16.66	16.68	
Pod Quartz	17.02	17.17	17.00	17.17	Temperature 830°C
Pod K Fds	16.46	16.36		16.41	
S/S Quartz	17.30	18.22		17.76	Temperature 570°C
S/S K Fds	16.05	16.78		16.42	
UA Quartz	22.0				
CH Quartz	16.69				

Table 6.8 Silicate oxygen isotope results

	%Fe	%S	%As	%Co	%Ni	%Cu	%Zn	%Pb	Totals(%)
Fine grained	30.47	34.74	0.86	-	-	32.6	-	0.12	98.81
	30.04	34.68	0.96	-	-	33.16	-	0.08	98.92
	29.82	34.99	0.86	-	-	34.09	-	0.08	99.84
	29.80	34.71	0.88	-	-	33.49	-	0.10	98.98
	30.46	34.81	0.96	-	-	32.22	-	0.11	98.58
	30.36	34.99	0.82	-	-	32.04	-	0.08	98.29
	30.41	34.46	0.92	-	-	32.90	-	0.08	98.77
	30.34	34.86	0.75	-	-	33.25	-	0.08	99.29
	30.43	35.01	0.94	-	-	32.65	-	0.06	99.09
	30.79	35.09	0.85	-	-	31.85	-	0.09	98.67
	30.64	35.72	0.77	-	-	32.67	-	0.10	99.90
	30.52	35.06	0.92	-	-	32.94	-	0.11	99.55
	30.43	34.98	0.78	-	-	33.30	-	0.09	99.58
	30.64	34.87	0.97	-	-	32.53	-	0.14	99.15
	30.50	34.62	0.89	-	-	32.67	-	0.13	98.81
Normalised Av:	30.66	35/23	0.88	-	-	33.13	-	0.10	100.00
Coarse grained (carbonate associated)	31.08	35.23	0.79	-	-	32.00	-	0.07	99.06
	30.98	35.47	0.98	-	-	31.81	-	0.08	99.32
	30.93	35.16	0.93	-	-	30.81	-	0.09	97.92
	30.84	35.21	0.89	-	-	32.08	-	0.09	99.11
	31.02	35.12	0.98	-	-	32.13	-	0.06	99.31
	30.90	35.32	0.77	-	-	32.19	-	0.12	99.28
	30.97	35.40	0.83	-	-	31.58	-	0.07	98.85
	30.87	35.10	0.98	-	-	31.98	-	0.07	99.00
	31.20	35.48	0.81	-	-	31.85	-	0.06	99.40
	31.28	35.26	1.01	-	-	31.53	-	0.06	99.14
	30.03	34.69	0.91	-	-	34.14	-	0.06	99.83
	31.14	35.56	0.80	-	-	31.88	-	0.10	99.48
	30.96	35.44	0.88	-	-	31.98	-	0.09	99.35
	30.73	35.21	0.95	-	-	32.34	-	0.13	99.36
Normalised Av:	31.17	35.50	0.97	-	-	32.28	-	0.08	100.00
Theoretical Assay Percent:	30.43	34.95				34.62			100.00

Table 7.1 Electron probe micro-analysis of fine grained and lenticular chalcopyrite.

	%Fe	%S	%As	%Co	%Ni	%Cu	%Zn	%Pb	Totals(%)
Fine grained:	11.40	25.81	1.53	-	-	59.27	-	-	98.02
	11.09	25.72	1.79	-	-	57.80	-	-	96.40
	11.22	25.90	1.77	-	-	58.47	-	-	97.36
	11.12	25.83	1.64	-	-	58.24	-	0.06	96.89
	11.25	25.92	1.56	-	-	58.12	-	0.05	96.90
	12.01	26.79	1.62	-	-	56.18	-	-	96.60
	11.22	25.59	1.74	-	-	58.13	-	0.07	96.75
	10.96	25.70	1.63	-	-	59.18	-	-	97.37
	11.27	25.31	1.71	-	-	58.39	-	-	96.69
	11.25	25.84	1.67	-	-	58.06	-	-	96.82
	11.81	26.04	1.48	-	-	57.85	-	0.07	97.25
	11.35	25.75	1.64	-	-	58.14	-	0.05	96.93
Normalised Av:	11.61	26.67	1.70	-	-	59.99	-	0.03	100.00
Coarse grained (carbonate associated)	11.50	25.99	1.57	-	-	58.89	-	0.07	98.02
	11.58	25.87	1.56	-	-	58.18	-	0.08	97.27
	11.29	25.59	1.63	-	-	59.16	-	0.05	97.72
	11.45	25.87	1.80	-	-	58.28	-	-	97.40
	11.37	25.97	1.71	-	-	58.68	-	0.06	97.79
	11.59	26.03	1.76	-	-	58.10	-	0.06	97.54
	11.56	26.02	1.69	-	-	58.24	-	0.05	97.56
	11.41	25.92	1.73	-	-	57.93	-	-	96.99
	11.46	2590	1.78	-	-	57.53	-	0.05	96.72
	11.52	25.92	1.67	-	-	57.30	-	-	96.41
	11.55	26.44	1.65	-	-	57.73	-	0.05	97.43
	11.95	26.09	1.84	-	-	57.70	-	0.07	97.65
Normalised Av:	11.83	26.67	1.75	-	-	59.70	-	0.05	100.00
Theoretical Assay Percent:	11.13	25.56				63.31			100.00

Table 7.2 Electron probe micro-analysis of fine grained and lenticular bornite.

Rutile Samples

Sample	$\%T_1O_2$	$\%Fe_2O_3$	$\%Nb_2O_5$	$\%ZrO_2$	$\%U_3O_8$	$\%ThO_2$	Total(%)
CP337/6/1 Auth	100.55	-	0.26	0.05	-	0.01	100.87
/2 Auth	99.15	0.42	0.37	0.26	0.21	0.01	100.42
/3 Auth	99.56	0.49	0.59	0.06	-	-	100.70
CP337/S/1 Auth	99.24	0.46	0.54	0.08	0.09	0.13	100.54
/2 Auth	101.02	0.45	0.33	0.14	0.08	0.13	102.15
/3 Auth	101.11	0.41	0.34	0.02	-	-	100.88
/4 Det	94.70	0.58	0.59	0.06	-	0.07	96.00
/5 Det	98.20	0.47	0.68	0.08	-	0.06	99.49
/6 Det	97.70	0.45	0.63	0.07	0.01	0.04	98.80
CP337/B/1 Auth	101.2	0.35	0.28	0.01	-	-	101.86
/2 Auth	99.37	0.69	0.58	-	-	0.09	100.73

Auth - authigenic or have a detrital core plus authigenic overgrowth - all have euhedral crystal forms.

Det - Detrital - boxwork pseudomorph after FeT_1O_3.

Zircon Samples

	$\%S_1O_2$	$\%ZrO_2$	$\%Nb_2O_5$	$\%V_3O_8$	$\%ThO_2$	$\%Fe_2O_3$	Totals(%)
337/6/1	32.73	67.64	-	0.16	0.12	0.34	100.99
/2	32.67	67.80	-	-	-	0.61	101.08
/3	32.94	67.80	-	-	-	0.10	101.51
/4	32.51	67.53	-	0.16	0.32	0.17	100.69

Table 7.3 Electron probe micro-analysis of rutile and zircon.

Element	Positive Correlation	Negative Correlation
Cu	Pb Ba Y Th	Fe Zr Ti Rb Nb
Co	Zn Fe Mn	Zr Ti Ba Y Nb
Ni	Zn Zr Ti Rb Y Nb Th	Mn Sr
Zn	Co Ni Pb Fe Zr Ti Rb Th U	
Pb	Cu Zn Ba Th	
Fe	Co Zn Mn Ti Rb	Cu Sr Ba U
Mn	Co Fe Sr	Ni Zr Ti Rb Ba Zr Y Nb Th
Zr	Ni Zn Ti Y Nb Th	Cu Co Mn Sr
Ti	Ni Zn Rb Zr Y Nb Th Fe	Cu Co Mn Sr
Rb	Ni Zr Ti Zr Y Nb Th Fe	Cu Mn Sr
Sr	Mn Ba	Ni Fe Zr Ti Rb Y Nb Th
Ba	Cu Pb Rb Sr Y U	Co Fe Mn Sr
Y	Cu Ni Zr Ti Rb Ba Nb Th	Co Sr Mn
Nb	Ni Zr Ti Rb Y Th	Cu Co Mn Sr
Th	Cu Ni Zn Pb Zr Ti Rb Y Nb	Mn Sr
U	Zn Ba	Fe

Table 7.4 Correlation between elements at the 95% confidence limit for combined borehole samples (n=243).

%Na	%Mg	%Al	%Si*	%S	%U	%k	%Ca	%Mn	%Fe	%Co	%Cu	%Zn	%Ba	Total %
Ore Shale Samples														
28.5	-	0.2	43.4	0.2	20.6	-	2.2	1.1	1.2	-	0.2	0.4	0.8	98.9
32.4	0.3	0.3	27.0	0.2	22.3	-	4.6	0.6	0.4	0.7	-	-	-	78.8
35.7	0.2	0.2	22.5	0.3	20.1	-	2.7	-	0.4	-	-	0.5	-	82.5
43.2	0.5	0.3	75.6	0.4	25.9	-	5.3	-	1.1	-	-	0.2	1.2	93.7
28.5	-	0.2	45.6	0.1	20.5	-	2.2	1.1	1.1	-	0.2	0.4	1.0	99.9
33.9	0.2	0.2	20.3	0.3	18.1	-	2.4	0.5	0.3	-	-	0.4	-	76.6
42.8	0.3	-	8.6	0.2	34.8	1.3	1.0	0.2	0.2	-	-	-	-	89.4
30.7	-	0.3	18.4	0.3	22.6	-	3.1	4.0	3.3	-	-	0.7	-	83.4
34.2	0.3	0.2	14.3	0.3	27.3	3.0	5.5	-	0.7	-	-	0.5	-	86.3
26.5	1.5	1.0	14.8	0.3	23.3	-	8.3	-	0.7	1.3	-	-	0.5	78.2
14.3	-	0.3	53.3	0.1	12.7	2.5	3.6	1.6	1.8	-	-	-	1.6	91.8
14.2	-	0.4	55.0	0.1	12.1	2.4	3.5	1.4	2.0	-	-	0.5	1.4	93.0
21.5	-	0.4	36.6	0.3	28.7	5.8	2.6	0.4	0.7	-	-	-	1.4	98.4
15.1	-	0.3	21.4	0.2	20.3	7.7	7.7	2.0	2.2	-	-	1.0	-	77.9
Footwall Samples														
8.9	-	0.4	80.6	-	6.9	1.2	3.2	0.7	0.6					102.5
3.1	-	0.3	77.5	-	2.0									82.9
20.2	-	0.3	50.9	0.7	10.8	-	0.8							83.7
6.8	-	0.2	63.6	0.2	5.2	-	0.3							76.3
7.7	-	0.2	55.9	0.3	7.2	-	-	-	0.1					71.4
1.6	-	0.2	75.7	-	2.3	1.8	-	-	0.1					81.7
2.5	-	0.2	66.7	-	5.1	1.2	0.8	-	0.3					76.8
3.4	-	0.2	56.5	1.5	5.3	5.2	0.8	0.4						73.3
2.6	-	0.2	61.4	-	5.1	2.2	1.3	0.6	0.5					73.9
3.2	-	15.0	79.1	-	3.1	0.7	0.2	0.1	1.1					102.5
2.5	-	15.0	74.7	-	2.3	0.1	0.1	-	0.4					95.1

* Calculated as S_1O_2.

Table 7.5 Results of energy dispersive analysis of decrepitation products from Footwall and Ore-Shale Quartz veins.

%Na	%Mg	%Al	%k	%Ca	%Mn	%Fe	%Co	%Cu	%Zn	%Ba
Ore-Shale Samples										
82.3	-	0.5	-	6.4	3.2	3.4	0.3	0.5	1.2	2.2
82.6	0.8	0.8	-	11.6	1.6	0.9	1.7	-	-	-
89.9	0.6	0.6	-	6.8	-	0.9	-	-	1.2	-
83.4	0.9	0.6	-	10.2	-	2.1	-	-	0.5	2.3
82.0	-	0.6	-	6.4	3.2	3.2	-	0.6	1.1	2.9
89.3	0.6	0.6	-	6.5	1.3	0.7	-	-	1.0	-
93.5	0.7	-	2.9	2.1	0.4	0.4	-	-	-	-
72.8	-	0.8	-	7.4	9.4	7.9	-	-	1.7	-
77.1	0.6	0.5	6.8	12.3	-	1.6	-	-	1.1	-
65.6	3.6	2.4	-	20.6	1.3	1.8	3.2	-	-	1.4
55.6	-	1.2	9.7	14.0	6.2	7.1	-	-	1.9	6.2
55.0	-	1.6	9.3	13.6	5.4	7.8	-	-	1.9	5.4
65.5	-	1.2	17.6	7.9	1.1	1.2	-	-	1.2	4.3
41.9	-	0.8	21.3	21.3	5.5	6.1	-	-	2.7	-
Footwall Samples										
59.4	-	2.6	8.0	21.3	4.7	4.0				
91.2	-	8.8								
94.8	-	1.4	-	3.8						
93.2	-	2.7	-	4.1						
96.2	-	2.5	-	-	-	1.3				
43.2	-	5.4	48.6	-	-	2.8				
50.0	-	4.0	24.0	16.0	-	6.0				
34.0	-	2.0	52.0	8.0	4.0					
35.1	-	2.7	29.7	17.6	8.1	6.7				
15.8	-	73.9	3.4	1.0	0.5	5.4				

Table 7.6 Normalised cation totals for decrepitated Ore-Shale and Footwall sample fluid inclusions.

Borehole J1000	49-26-4	D.C. Marl Slate	D.C. Trans.	Trans Sap.	Trans Cal.	Trans Dol.	Black Shale**
Cu 1560*	914*	34	7	20	4	1	0.007
Co 343*	N.M.	34*	6	18*	1	1	0.001
Ni 183*	108*	88*	16	48	3	5	0.005
Zn 52	54	224	44	42	10	162*	0.03
Pb 116*	65*	184*	74*	125*	64*	44*	0.002
Fe 32800*	62400*	36150*	21900*	33700*	6030	29900*	2.000
Mn 334*	1200*	1530*	1310*	1040*	700*	2230*	0.015
Zr 152*	108*	114*	51*	125*	24	22	0.007
Ti 4450*	7170*	3440*	1130	3750*	45	229	0.2
Rb 159	138	96	37	102	10	13	
Sr 352*	145	204*	208*	148	294*	164	0.02
Ba 341*	303*	271	585*	373*	774*	550*	0.03
Y 30	29	21	10	16	8	8	0.003
Nb 16	17	11	5	11	2	3	
Th 14	13	13	5	12	2	2	
U 19	8	3	.2	4	1	1	

NM = Not Measured * = Enriched relative to average black shale. ** = In percent, after Vine and Tourtelot (1970

Table 10.1 Mean trace element composition of Marl Slate Borehole samples.

Transition Zone

Dolomite (rich) Unit	Calcite (n=8)	$Ca_{0.99}$	Mg_{-}	$Fe_{0.001}$	Mn_{-}	CO_3
	Dolomite (n=12)	$Ca_{0.60}$	$Mg_{0.25}$	$Fe_{0.14}$	$Mn_{0.01}$	CO_3
Calcite (rich) Unit	Calcite (n=12)	$Ca_{0.60}$	Mg_{-}	$Fe_{0.01}$	$Mn_{0.01}$	CO_3
	Dolomite (n=16)	$Ca_{0.58}$	$Mg_{0.26}$	$Fe_{0.15}$	$Mn_{0.01}$	CO_3
Sapropel	Calcite (n=15)	$Ca_{0.99}$	Mg_{-}	$Fe_{0.01}$	Mn_{-}	CO_3
	Dolomite (n=16)	$Ca_{0.60}$	$Mg_{0.25}$	$Fe_{0.14}$	$Mn_{0.01}$	CO_3

	% Calcite	% Dolomite
Calcite (rich) unit	85	15
Sapropel	27	80
Dolomite (rich) unit	8	92

Marl Slate

Sapropel	Calcite (n=14)	$Ca_{0.98}$	Mg_{-}	$Fe_{0.01}$	$Mn_{0.01}$	CO_3
	Dolomite (n=15)	$Ca_{0.58}$	$Mg_{0.25}$	$Fe_{0.16}$	$Mn_{0.01}$	CO_3

percentage calcite and dolomite highly variable.

Table 10.2 Normalised carbonate compositional data and percentage Calcite/Dolomite for the Doncaster Core.

%Fe	%S	%As	%Co	%Zn	%Ni	%Cu	%Pb	%Mn	Total	Comments
					Transition Zone					
45.80	57.42	-	-	-	-	-	0.18	-	98.40	Calcite Unit
45.54	51.18	-	-	-	-	-	0.16	-	96.88	Calcite Unit
46.14	52.55	-	-	-	-	-	0.11	-	98.80	Calcite Unit
45.62	52.62	-	-	-	-	-	0.20	-	98.44	Dolomite Unit
45.44	53.00	-	-	-	-	-	0.28	-	98.72	Dolomite Unit
45.79	53.30	-	-	-	-	-	0.23	-	99.32	Dolomite Unit
45.57	52.72	-	-	-	-	-	0.19	-	98.48	Dolomite Unit
46.11	53.39	-	-	-	-	-	0.27	-	99.77	Dolomite Unit
46.31	53.22	-	-	-	-	-	0.15	-	99.68	Dolomite Unit
45.51	52.88	-	-	-	-	-	0.16	-	98.55	Dolomite Unit
45.97	53.33	-	-	-	-	-	0.29	-	99.59	Dolomite Unit
43.03	51.45	-	-	-	-	0.05	0.70	0.40	95.63	Sapropel Unit
42.76	51.95	-	-	0.14	0.04	0.05	0.51	0.52	95.97	Sapropel Unit
43.75	51.44	-	-	0.09	0.06	0.07	0.39	0.26	96.06	Sapropel Unit
43.95	52.29	-	-	-	0.04	0.06	0.32	0.55	97.21	Sapropel Unit
43.92	51.87	-	-	-	0.07	-	0.38	0.31	96.55	Sapropel Unit
46.55	53.33	-	-	-	-	-	0.18	-	100.60	Vein Centre
46.38	53.49	-	-	-	-	-	0.75	-	100.12	Vein Centre
46.53	53.50	-	-	-	-	-	0.14	-	99.97	Vein Centre
46.66	53.44	-	-	-	-	-	0.16	-	100.26	Vein Centre
46.39	53.29	0.29	-	-	-	-	0.38	-	100.30	Vein Margin
46.50	53.38	0.37	-	-	-	-	0.19	-	100.44	Vein Margin
46.29	53.01	0.41	-	-	-	-	0.20	-	99.91	Vein Margin
45.58	52.92	0.26	-	-	-	-	0.19	-	98.93	Vein Margin
46.31	53.20	-	-	-	-	-	0.19	-	99.70	Dolomite Matrix
45.97	52.54	-	-	-	-	-	0.27	-	98.60	Dolomite Matrix
					Marl Slate					
45.51	53.22	-	-	-	0.68	-	0.15	-	99.56	Sapropel Unit
46.60	53.44	-	-	-	-	-	0.15	-	100.19	Sapropel Unit
45.52	52.58	-	-	-	0.13	-	0.31	-	98.56	Sapropel Unit
46.06	51.01	-	-	-	0.14	0.10	0.17	-	97.48	Sapropel Unit

Figure 10.3 Compositional variation of pyrite from the Doncaster Core.

Sample	$\delta^{13}C$ (PDB)	$\delta^{18}O$ (PDB)	Comments
J12	-0.40	-3.70	Dirty Sample
J11	0.94	-0.52	
J10	1.03	-0.17	
J9	1.84	-0.27	
J8	1.80	-0.29	
J7	1.84	-0.25	SAPROPEL
J6	2.04	0.05	
J6 R	1.95	0.03	
J5	1.89	-0.07	
J4	1.84	-0.20	
J3	-	-	Sample lost in extraction
J2	0.34	-2.25	
J1	-2.36	-6.12	

Table 11.1 Carbon and Oxygen Isotope Results from Borehole J1000.

Sample	$\delta^{13}C$ (PDB)	$\delta^{18}O$ (PDB)	$\delta^{34}S$	Comments
46	2.60	-5.31		Sapropel
44	2.67	-4.96	-30.7	
42	2.62	-4.72	-31.6	Laminated organic
40	2.69	-4.44	-34.0	carbonate, mainly
40 R	2.60	-4.81		calcite.
38	2.70	-4.62	-32.9	
36	2.67	-4.45		Sapropel
36 R	2.69	-4.41		(Repeat Sample)
34	2.60	-4.48		
32	2.51	-4.08	-34.3	
31	2.50	-3.97	-34.1	
30	2.53	-3.83	-33.2	
28	2.69	-3.29		
26	2.63	-2.96	-34.7	
24	3.05	-2.47		
22	2.56	-2.78	-34.4	Laminated organic
21	1.58	-4.00		carbonate, mainly
20	1.56	-4.11	-32.4	calcite
20 R	1.65	-3.90		
18	3.02	-2.16		
16	2.87	-2.22	-31.2	Sapropel
14	2.69	-2.38		
12	2.53	-2.61	-34.9	
10	2.67	-2.62		Laminated organic
9	1.70	-3.73		carbonate, mainly
8	1.53	-4.07	-32.9	calcite
7	2.59	-2.86		
6	2.70	-2.77		
5	1.37	-3.12		Sapropel
4	0.52	-3.53	-35.7	
4 R	0.50	-3.69		
3	-0.81	-3.70	-36.7	
2			-2.6	
2 R			-2.4	Yellow Sands
Q4a	-3.06	-10.93		Calcite rug in the Marl Slate, Quarrington Quarry.
Q4b	-2.71	-11.55	-24.1	As above sulphide is sphalerite
			+11.6	As above barytes from a rug

Table 11.2 Carbon, oxygen and sulphur isotope results from the Marl Slate section of the Doncaster Core

Sample	$\delta^{13}C$ (PDB)	$\delta^{18}O$ (PDB)	$\delta^{34}S$	Comments
102	3.12	-.393	-29.1	Laminated organic
101	3.57	-2.94		carbonate mainly
100	3.63	-2.79		dolomite
98	3.67	-2.86	-35.7	
96	3.68	-2.44		
94	3.62	-2.87		
92	3.78	-2.73	-35.3	
90	3.89	-1.93		
90 R	3.14	-2.29		Laminated organic
88	3.08	-3.87		carbonate mainly
86	3.09	-3.88	-29.8	calcite
84	3.12	-3.05		
82	3.57	-2.54		Laminated organic
80	3.75	-2.38		carbonate mainly
78	3.67	-2.68	-31.5	dolomite
76	3.08	-2.65		
74	3.40	-2.86	-31.1	
72	2.68	-3.21		
70	2.14	-3.72	-31.6	
68	3.22	-3.35		Sapropel
66	3.14	-3.37		
64	2.85	-3.99	-31.6	
62	2.68	-4.16		
60	2.90	-3.65		
60 R	3.02	-3.70		(Repeat sample)
58	2.88	-4.04	-34.1	
56	2.67	-4.61		
54	2.70	-5.13		
52	2.86	-4.99		
50	2.80	-4.86	-31.3	
48	2.74	-5.37	-31.6	

Table 11.2 continued Carbon, oxygen and sulphur isotope results from the Marl Slate section of the Doncaster Core.

Sample	$\delta^{13}C$ (PDB)	$\delta^{18}O$ (PDB)	$\delta^{34}S$	Comments
131	4.25	-4.58	-20.0	Dolomite-rich unit
130	3.09	-5.39	-11.0	Calcite-rich unit
129	4.52	-1.94	-28.8	Sapropel
128	4.46	-2.06	-32.6	Dolomite-rich unit
127	3.43	-4.07	-28.6	Sapropel
126	3.50	-3.68	-29.7	Sapropel
125	2.57	-2.92	-31.5	Sapropel
124	2.44	-2.97	-29.3	Sapropel
123	4.05	-4.07	-25.3	Dolomite-rich unit
122	4.02	-4.12	-21.8	Dolomite-rich unit
122 R	4.00	-4.17		Repeat Sample
121	2.98	-5.26	-14.2	Calcite-rich unit
120	3.06	-4.84	-14.9	Calcite-rich unit
119	3.11	-5.21	-14.8	Calcite-rich unit
119 R	2.97	-5.29	-14.3	Repeat Sample
118	3.04	-5.23	-14.7	Calcite-rich unit
117	3.97	-4.40	-19.7	Dolomite-rich unit
117 R	3.90	-4.28		Repeat Sample
116	3.23	-5.13	-15.4	Calcite-rich unit
115	3.02	-4.94	-15.8	Calcite-rich unit
114	2.78	-5.78	-18.8	Calcite-rich unit
114 R	2.98	-5.89	-18.5	Repeat Sample
113	3.349	-4.18	-29.0	Sapropel
112	3.21	-4.20	-28.4	Sapropel
111	3.14	-4.69	-20.3	Dolomite-rich unit
110	2.75	-5.12	-14.2	Calcite-rich unit
109	2.60	-5.16	-13.9	Calcite-rich unit
108	3.22	-4.44	-20.7	Dolomite-rich unit
107	3.34	-4.31	-19.3	Dolomite-rich unit
106	3.18	-4.30	-21.7	Dolomite-rich unit
105	2.68	-5.67	-27.2	Sapropel
104	3.07	-4.75	-21.5	Dolomite-rich unit
104 R	3.07	-4.73		Repeat Sample
103	2.60	-4.89	-18.4	Calcite-rich unit
103 R	2.67	-4.90		Repeat Sample
Mean	2.68	-5.18	-15.0	Calcite-rich unit
Mean	3.67	-4.17	-22.3	Dolomite-rich unit
Mean	3.22	-3.78	-29.1	Sapropel
Vein Dolomite	2.30	8.18	-23.3	Cross cuts sample 104

Table 11.3 Carbon, oxygen and sulphur isotope results from the Transition Zone section of the Doncaster Core.

Feature	Calcite-rich horizons	Dolomite-rich horizons	Sapropel horizon (including Marl Slate)	Comments
Degree of Pyritization (DOP)	High	Low	High (low during framboidal growth)	Low DOP indicates low availability of Fe during pyrite formation.
C_{org}/S_{py} Intercept	+ve C_{org}	+ve S_{py}	+ve S_{py}	+ve S_{py} intercept implies that pyrite formed in an anoxic water column. +ve C_{org} intercept implies that sulphate supply may be a limiting factor in pyrite formation
Fractionation Factor (Sulphur)	29 per mil (partially open system)	37 per mil	44 per mil (open system)	Open system fractionation indicates abundant supply of sulphate.
Pyrite Form	Euhedral	Framboid + Euhedral	Framboid (minor euhedral)	Framboidal - high iron availability. Euhedral - low iron availability
Pyrite Composition	Fe, S, Pb	Fe, S, Pb	Fe,S,Pb,Cu,Zn,Ni,Mn	Increased trace elements content in sapropel pyrites
% Dolomite	15	92	80	
$\%C_{carbonate}$	10.3	10.3	3.8	Considerably less carbonate in the sapropel
Carbonate Composition	Calcite $Ca_{0.98}Mg_{-}Fe_{0.01}Mn_{0.01}CO_3$	Dolomite $Ca_{0.59}Mg_{0.25}Fe_{0.15}Mn_{0.01}CO_3$		Composition of carbonate phases is remarkably uniform
Calcite Texture	Euhedral	Very slightly etching	Etching	

Table 12.1 Characteristic features of different lithological types associated with the Marl Slate.

PLATES

PHOTOGRAPHIC PLATES

NOTE Plates are shown in chapter order as used in the text.

Where no scale appears in the plate, the approximate field of view (F.O.V.) is given in the accompanying caption.

Key

PPL	Plane Polarised Light
XN	Crossed Nicols
Refl. Light	Reflected Light.

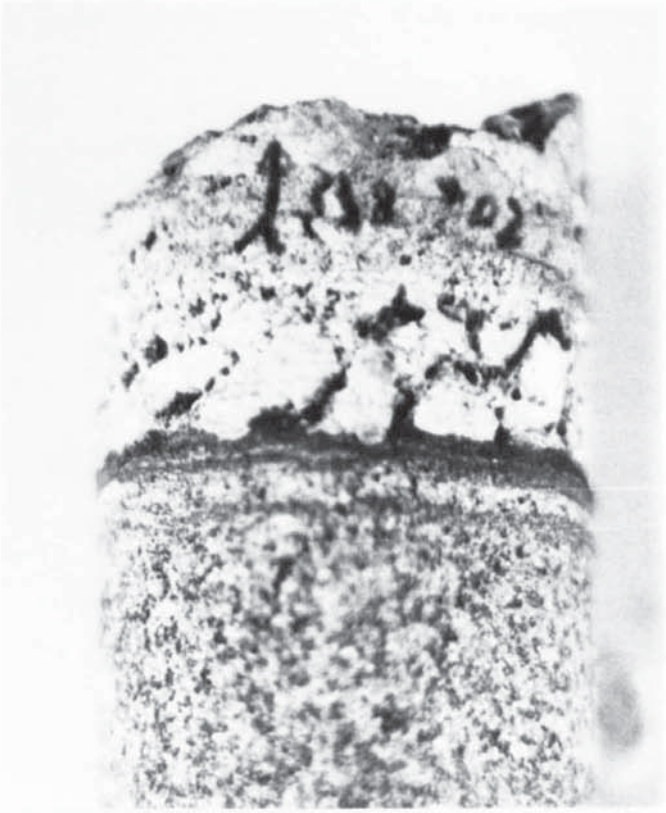

Plate 3.1a Haematite rich laminae of probable detrital origin occur parallel to bedding and in this example is deformed by clasts of the overlying conglomerate horizon. Core diamater is 7 cms.

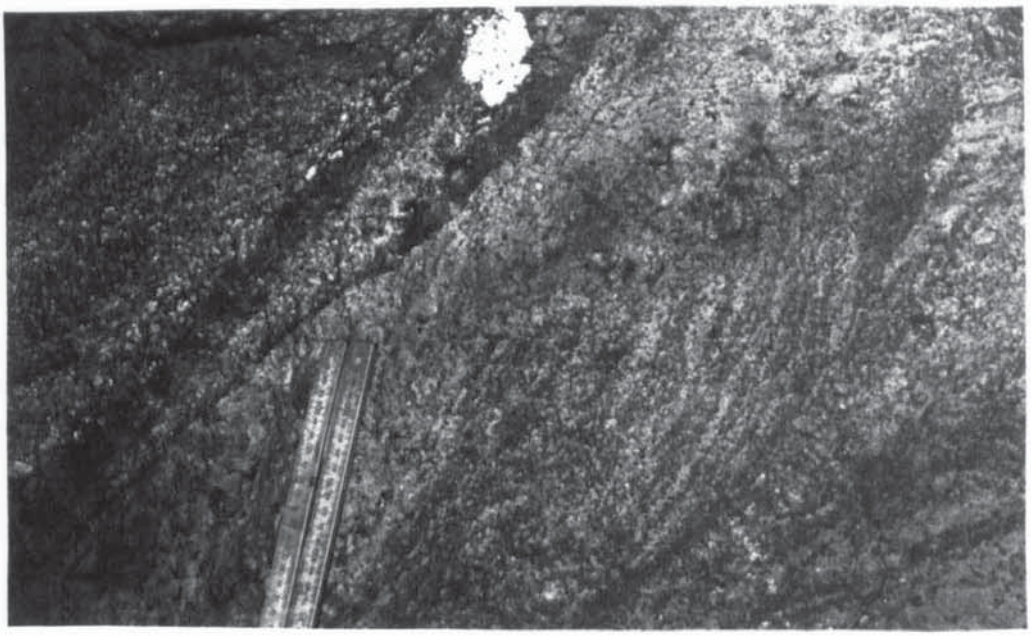

Plate 3.1b An example of truncated cross-bedding and graded bedding in the Footwall Sandstone from the 2030 level, 260 mS Area of No. 1 Shaft. Orebody Scale, in centimetres is given by the clino-rule.

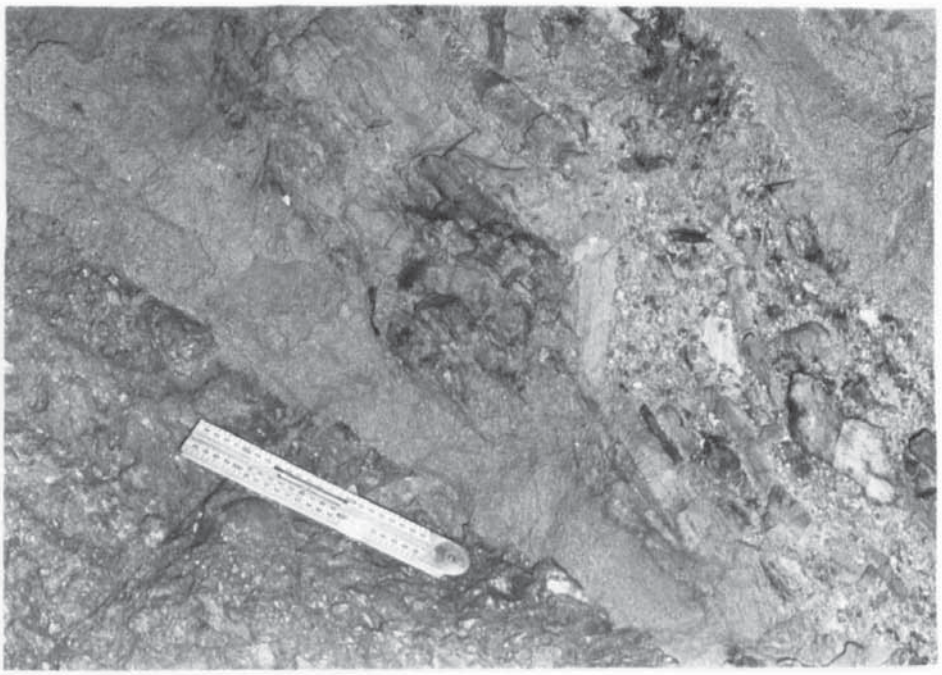

Plate 3.2a Longitudinal section through an erosional channel at the Footwall Conglomerate/Ore-Shale contact from the 2060L, 1000 mN Area of the No. 1 Shaft Orebody.

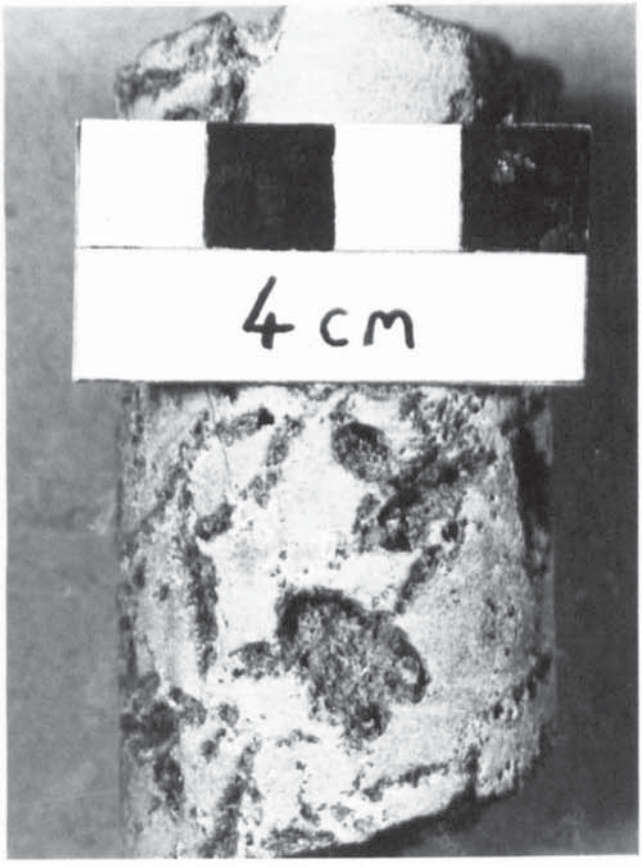

Plate 3.2b Moulds after gypsum seen in unit B of the Ore-Shale. A mould after a swallowtail twin can be seen towards the base of the core.

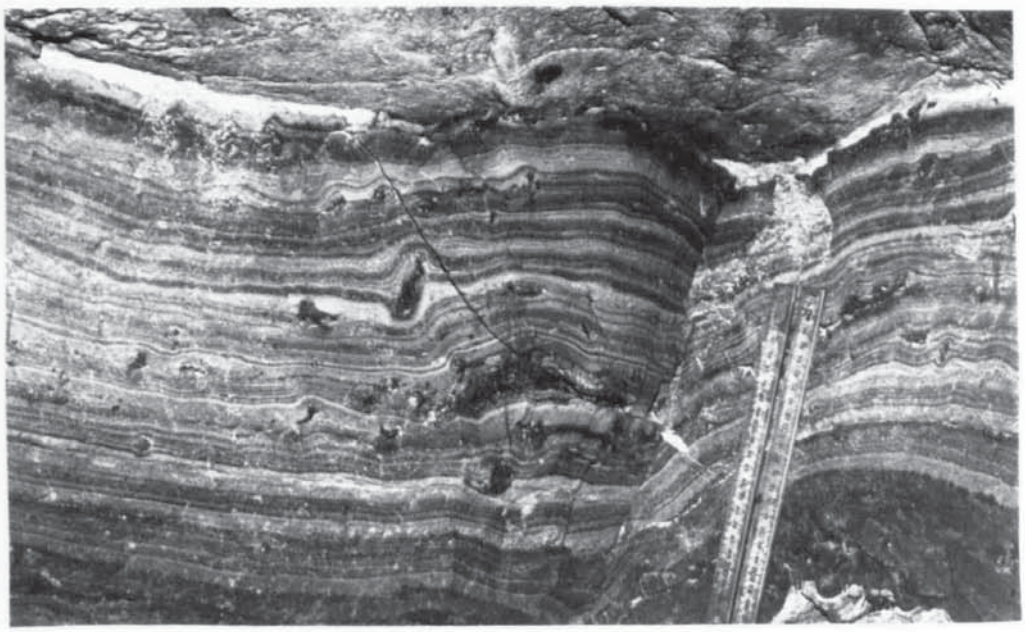

Plate 3.3a Dolomite and sulphide pseudomorphs after sulphate from unit C of the Ore-Shale. The lenticles clearly displace bedding a feature indicative of their 'early' soft sediment formation.

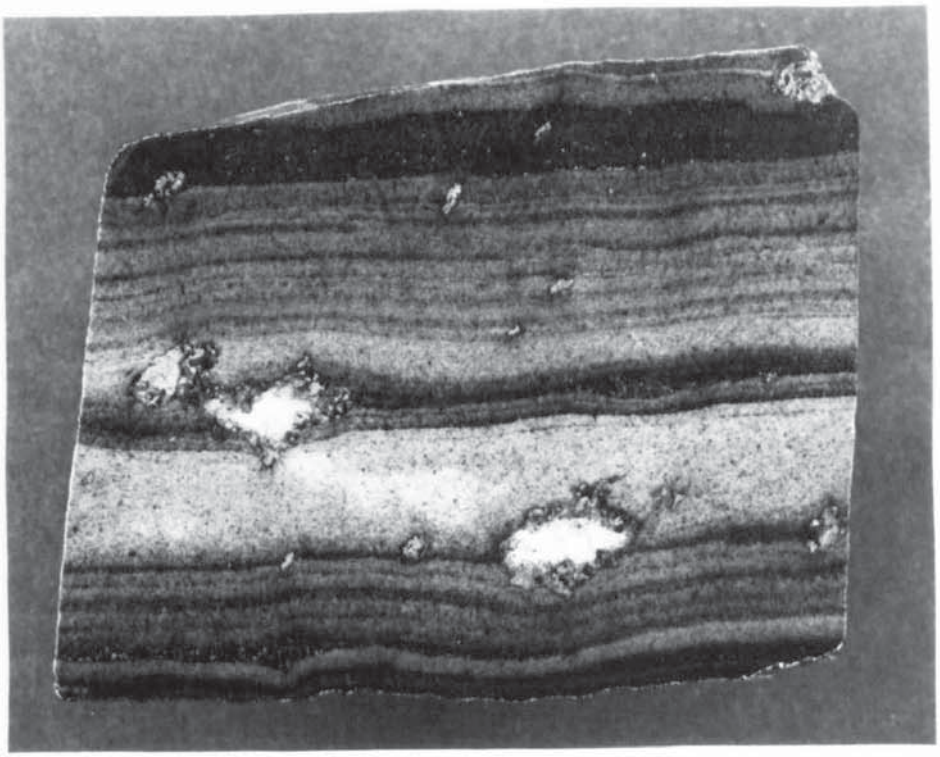

Plate 3.3b Lenticles of carbonate after sulphate from unit D of the Ore-Shale. Quartz and feldspar along with chalcopyrite rim the lenticle perimeter. Note also the soft sediment deformation of bedding around, the lenticles. Width of core is 7 cms.

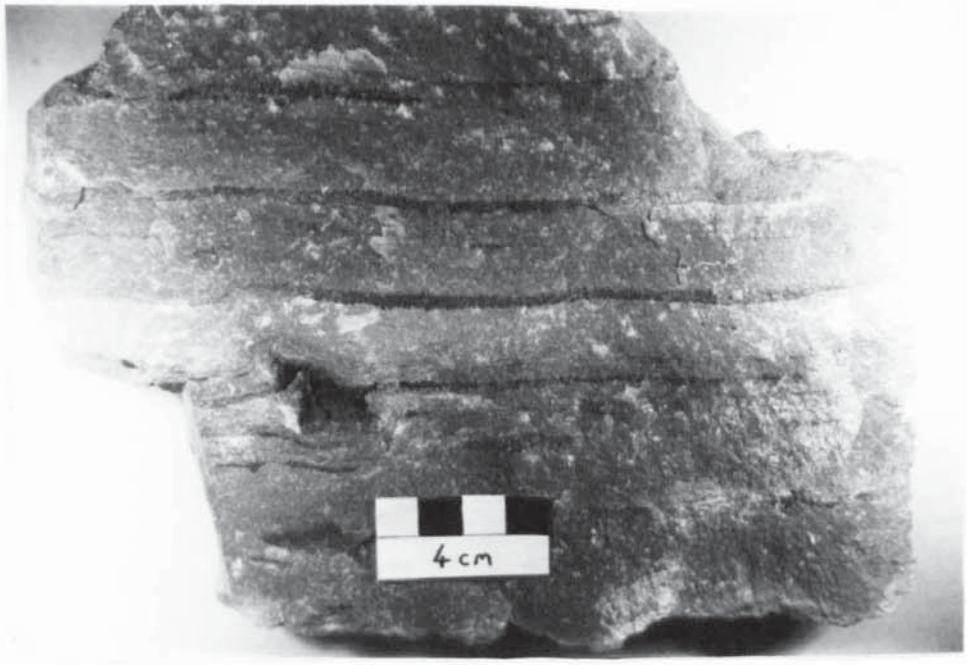

Plate 3.4a Sulphudite layers of chalcopyrite from unit D of the Ore-Shale. From the 2060 Level, 1000 mS Area of the No. 1 Shaft Orebody.

Plate 3.4b White carbonate after sulphate, forming an almost wiremesh texture. Thin rims of sulphide (Bornite) line the perimeter of the lenticles. Sample from unit D of the Ore-Shale, 2120 Level, 500 mS Area of the No. 1 Shaft Orebody.

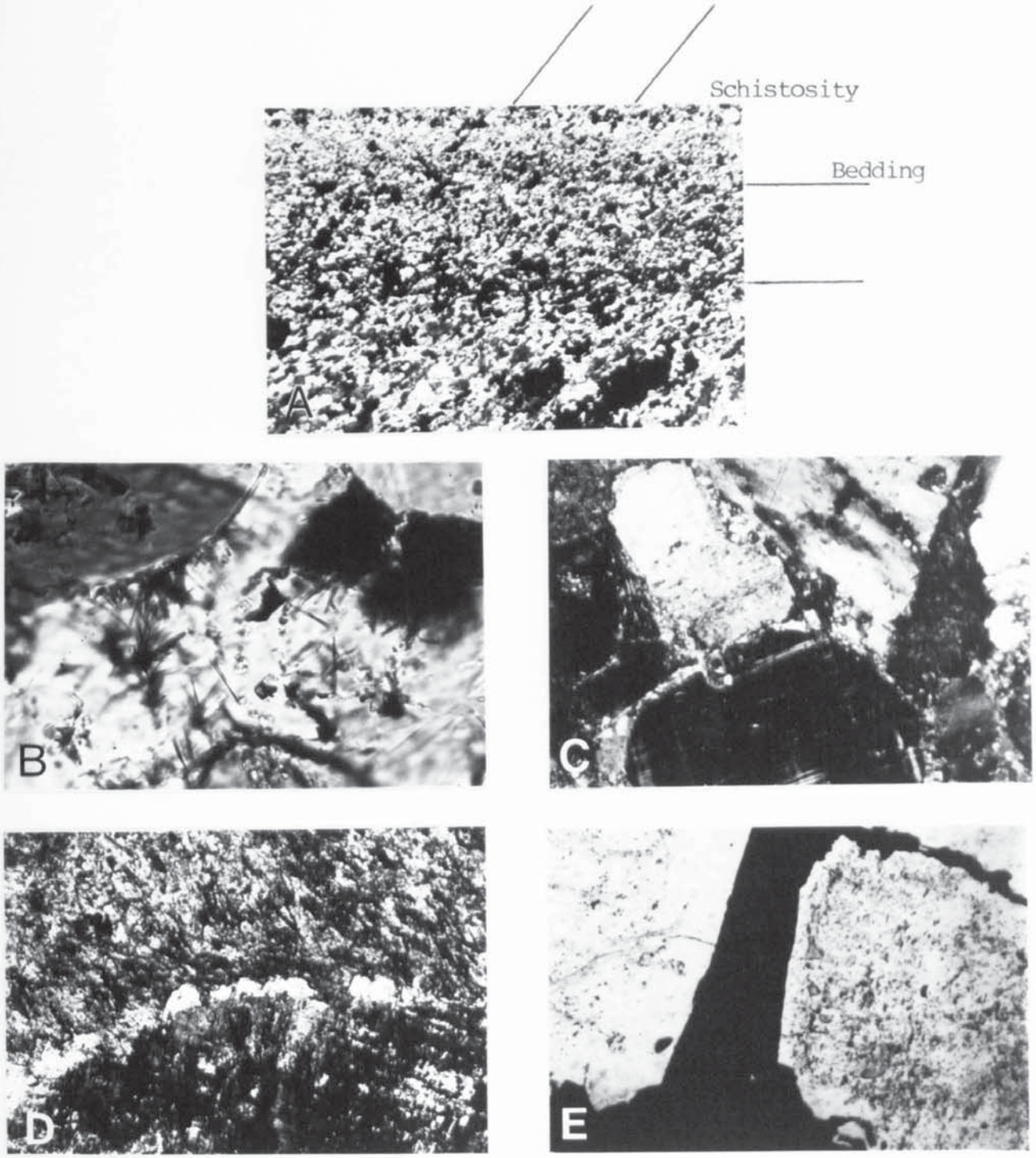

Plate 4.1

A. Schistosity-bedding relationship in unit B. F.O.V. 5.8 mm. PPL.

B. Rutile nucleated on rounded detrital grains. Pore space filled with quartz. Footwall Sandstone 500mS 2120L, No. 1 Shaft F.O.V. 360 microns. PPL.

C and D Optically discontinuous feldspar overgrowth, note the rounded nature of the host grains. Footwall Conglomerate 50 mN 2320L, No. 1 Shaft, F.O.V. 1.2 mm. XN.

E. Feldspar overgrowth, note euhedral tendency and pre-sulphide pore fill age. Footwall Conglomerate 50 mS 2120L, No. 1 Shaft. F.O.V. 0.9 mm. PPL.

Plate 4.2

A. 'Clay' coating on detrital quartz grain is pre-haematite overgrowth. Footwall Sandstone 50 mS 2200L, No. 1 Shaft. F.O.V. 1.2 mm, XN.

B. 'Clay' coating (white specks) is pre-feldspar overgrowth. Feldspar overgrowth is in optical continuity with the host grain. Footwall Sandstone 50 mN 2120L, No. 1 Shaft, F.O.V. 0.9 mm, XN.

C. 'Clay' coating on rutile rich detrital quartz grain. Note rutile free quartz overgrowth. Nicols slightly uncrossed. Footwall Sandstone 500 mS 2200L, No. 1 Shaft, F.O.V. 0.7 mm, XN.

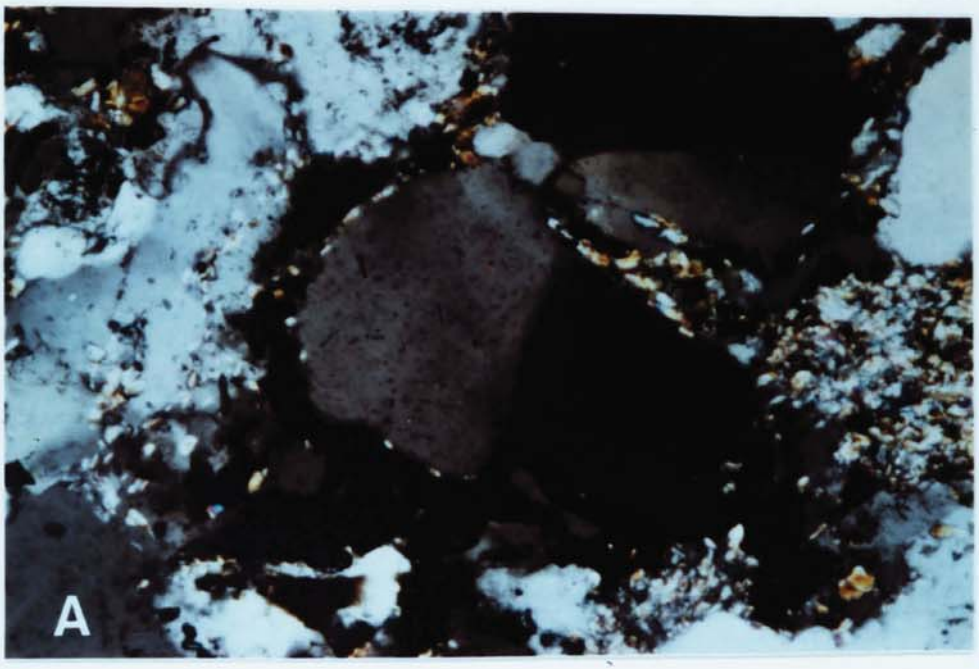

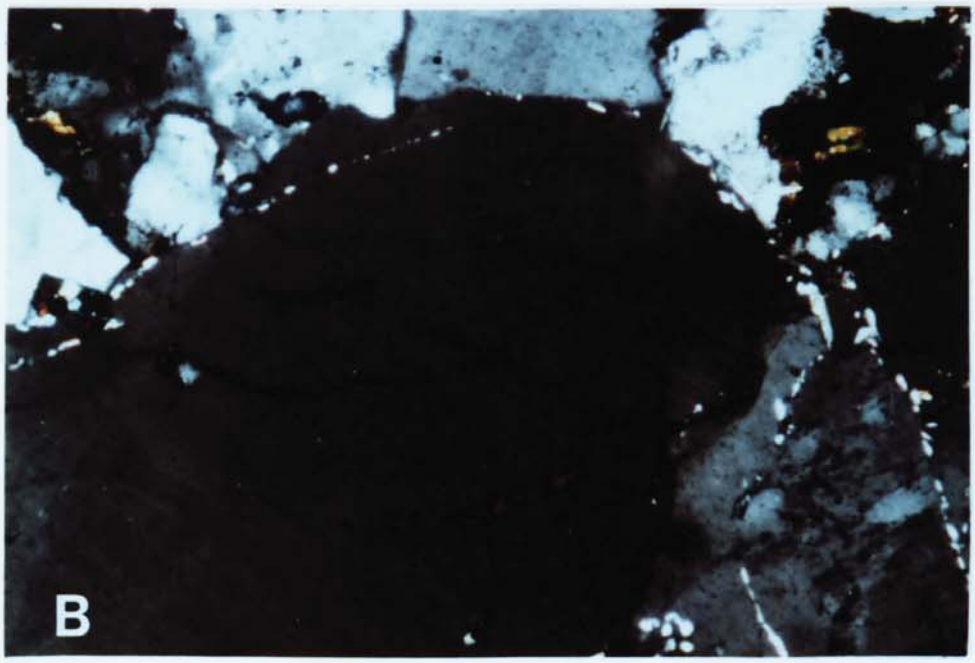

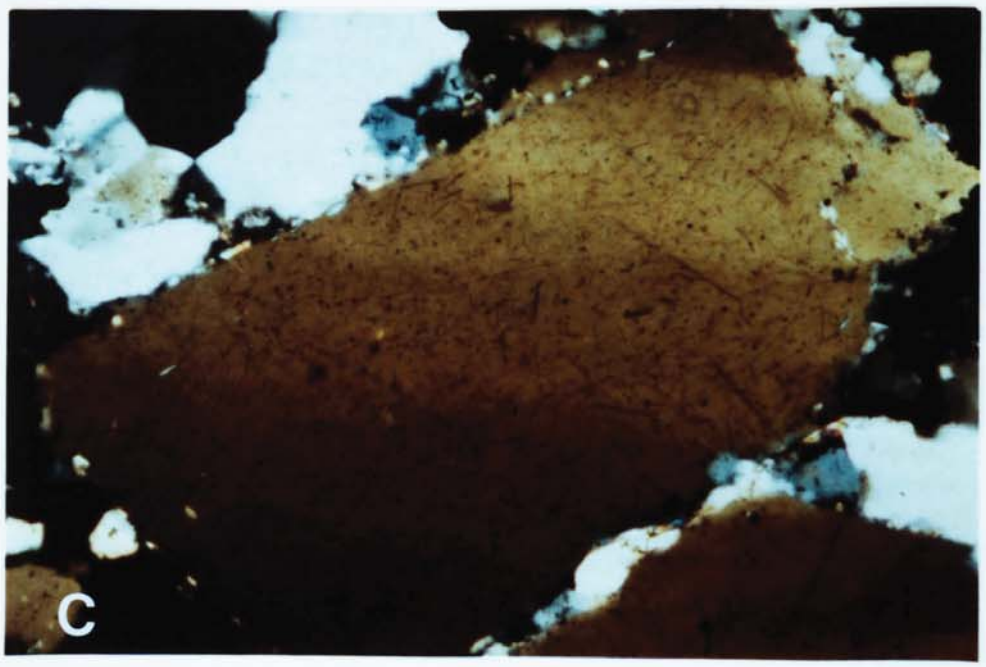

PLATE 4.2

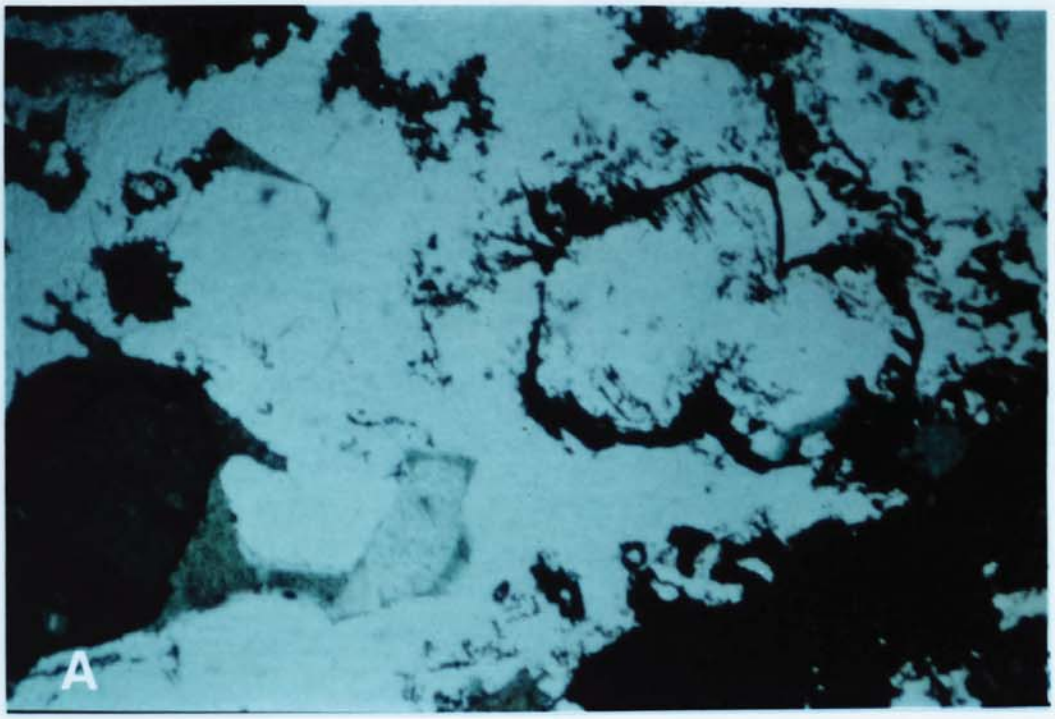

Plate 4.3A Relect structure of detrital grains (hornblend) preserved by haematite coating. Footwall Conglomerate 50 mS 2120L, No. 1 Shaft, F.O.V. 1.2 mm, PPL.

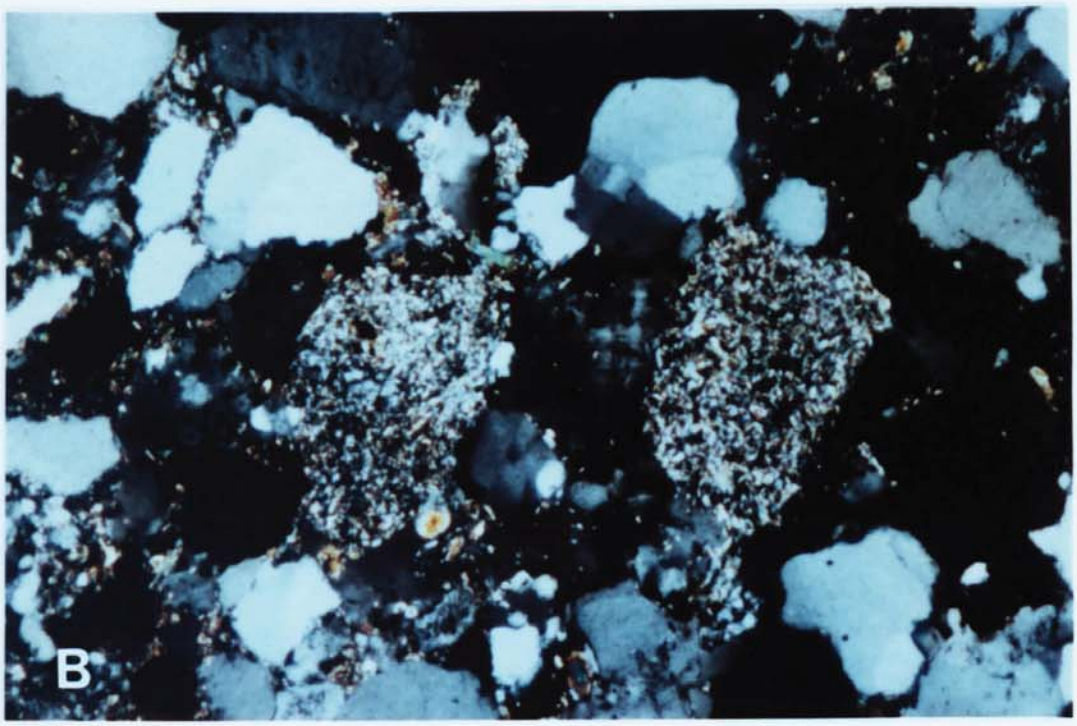

Plate 4.3B Replacement of feldspar, particularly plagioclase is common, and can lead to the production of clay ball pseduomorphs. Here the clays (now serecite) maintain the original feldspar grain shape. Footwall Sandstone 50 mS 2060L, No. 1 Shaft, F.O.V. 1.2 mm, XN.

Plate 4.4

A and B Yellow luminescent tourmaline. Note the rounded detrital core and a tendency to euhedral form in the overgrowth. Samples from the Ore-Shale sample numbers 197/7 and 638/10 respectively. F.O.V. approximately 0.9 mm.

C. Euhedral cobalt rich dolomite crystal nucleated on a quartz grain. The dolomite crystal is replaced by later malachite pore fill. Carbonate replacement along fractures also occurs. Chyrsocolla lines a fracture in the lower left hand corner of the quartz grain. Footwall Conglomerate, 50 mS 2260L No. 1 Shaft, F.O.V. 3.6 mm, XN.

D. Yellow-orange luminescent pore fill dolomite is post the karki-brown overgrowth on the blue luminescent feldspar. Footwall Conglomerate, 50 mS 2120L No. 1 Shaft, F.O.V. 1.8 mm.

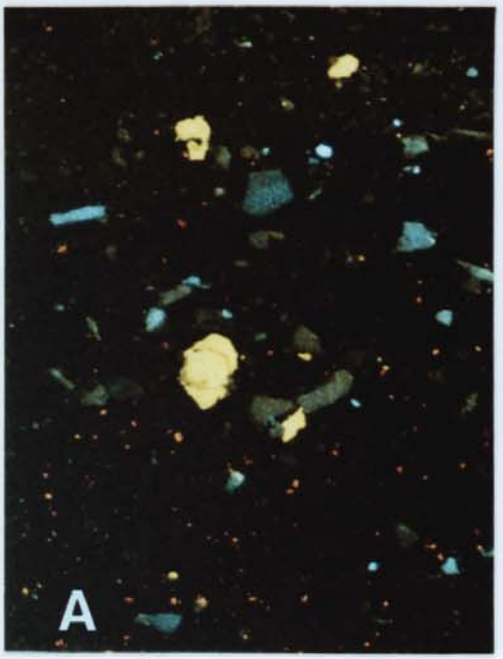

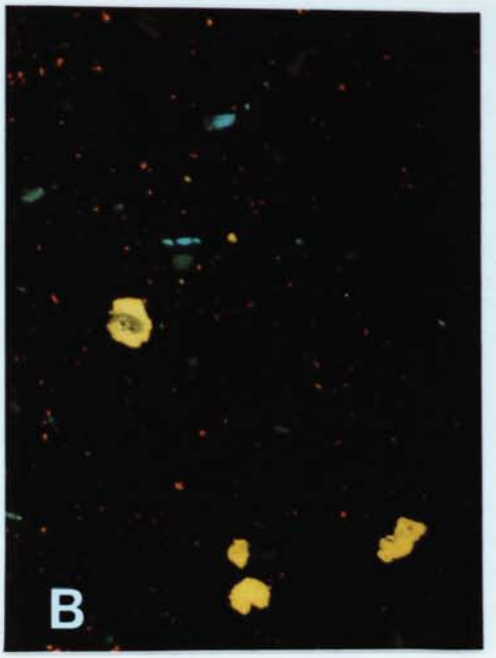

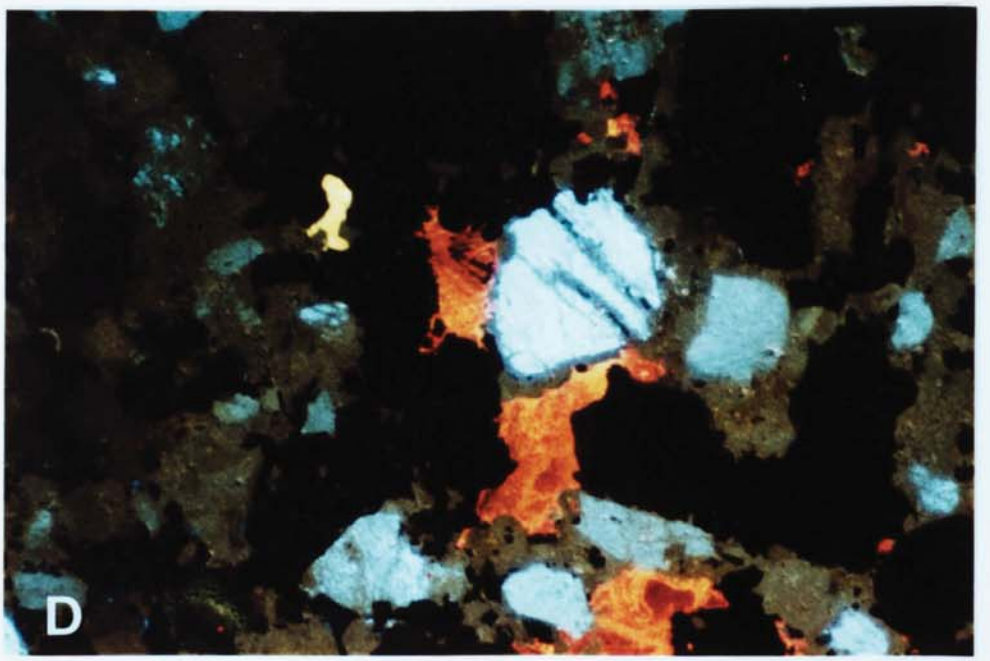

PLATE 4.4

Plate 4.5

A. Optically continuous overgrowth on a rounded (dashed line) plagioclase feldspar core. Footwall Sandstone, 50 mN 2260L, No. 1 Shaft, F.O.V. 0.7 mm. XN.

B. Carbonate lenticles after anhydrite. Note sulphide (bornite and chalcopyrite) replacement towards lenticle perimeters. Unit D of the Ore-Shale, 50 mS 2120L, No. 1 Shaft. Sticker is 2.2 cms by 1.5 cms.

C. Elongate crystals of Rim dolomite aligned approximately perpendicular to the lenticle edge. A mosaic of sparry dolomite fills the lenticle core (right-handside of photo). Unit D of the Ore-Shale. F.O.V. 2.8 mm, XN.

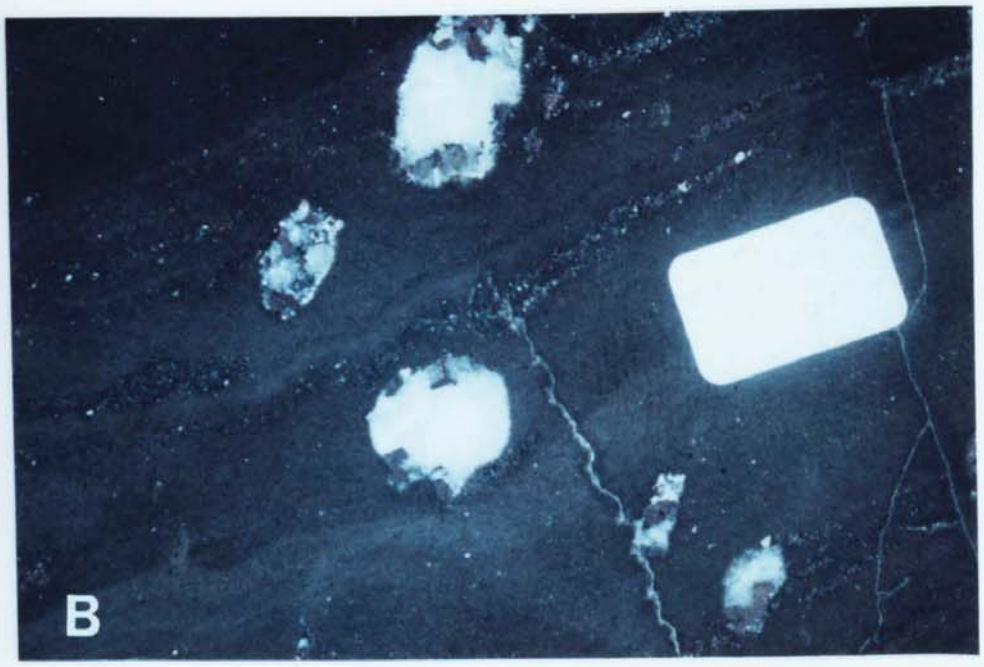

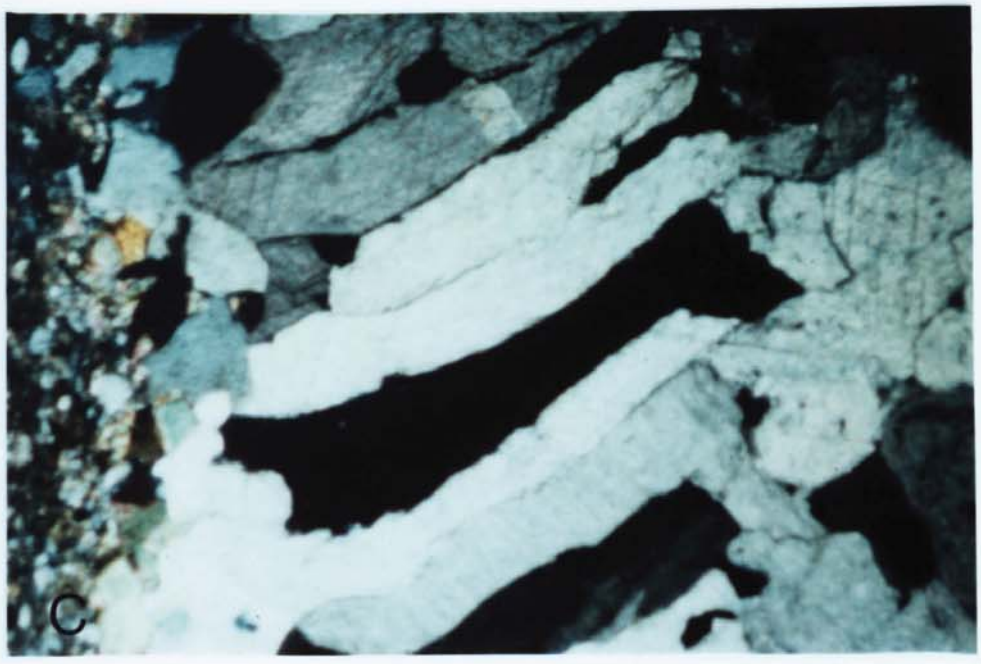

PLATE 4.5

Plate 4.7

A. Crystal of authigenic quartz with triangular pits suggesting its co-precipitation with carbonate. Sample from carbonate lenticle 600 mS 2320L No. 1 Shaft.

B. Development of rhombic crystal form in potassium feldspar overgrowth. Note that the overgrowth is relatively clean compared with the host. Overgrowth is pre-sulphide (black) Sample KLB 136, F.O.V. 0.7 mm, PPL.

C. Euhedral albite overgrowth on a microcline core (analysis on Table 4.3). Sulphide (black) is chalcopyrite. Sample 197/18. F.O.V. 1.2 mm.

D. Euhedral authigenic microcline crystal from the edge of a carbonate lenticle barren of sulphide.

E. Euhedral albite crystal associated with chalcopyrite from the edge of a carbonate lenticle.

F. Euhedral outline of pyrite (white) partially replaced by chalcopyrite (grey) and totally enclosed in a grain of carrollite (dark grey). Sample AP978/18. F.O.V. 0.6 mm, Refl. Light.

G. Carrollite with chalcopyrite filled fractures, bornite forms an incomplete rim. Sample AP638/6. F.O.V. 1.8 mm, Refl. Light.

H. Tectonically (?) induced fractures in carrollite. Note the way in which the carrollite mosaic could be rebuilt. Specimen AP638/10, F.O.V. 1.8 mm, Refl. Light.

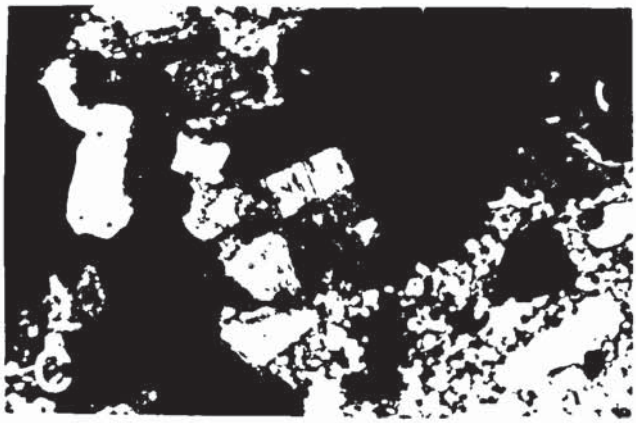

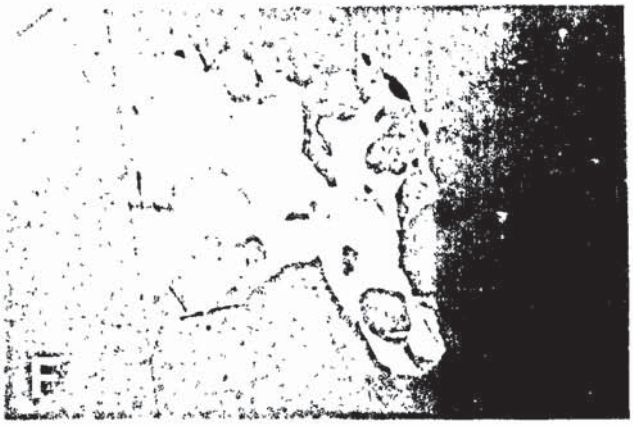

PLATE 4.7

Plate 4.8

A and B Transmitted Light (XN) and cathodoluminescence plates of a detrital feldspar grain (blue luminescence) with an euhedral overgrowth (karki-brown luminescence). Note crystallographically aligned leaching of detrital grain infilled with later feldspar. Compositional data (Table 4.3 analysis 10) suggests that the blue luminescence is caused by the presence of barium. Sample 638/15. F.O.V. approximately 0.6 mm.

C and D. Transmitted light (XN) and chathodoluminescence plates of detrital feldspar (blue luminescence) with euhedral overgrowth (karki-yellow luminescence). The brown luminescent mineral is quartz. Compositional data are given in Table 4.3 analysis 1. Sample 197/18. F.O.V. approximately 0.9 mm.

E. Cathodoluminescent plate of Footwall Conglomerate, 250 mS 2260L, No. 1 Shaft. Chathodoluminescence allows the easy determination of original grain boundaries, which because of metamorphism can be difficult in transmitted light. Blue and karki-gray luminescent grains are potassium feldspars, while the dark brown grains are quartz. Note the rectangular nature of many of the feldspar grains, suggesting a local provenance. F.O.V. approximately 2.8 mm.

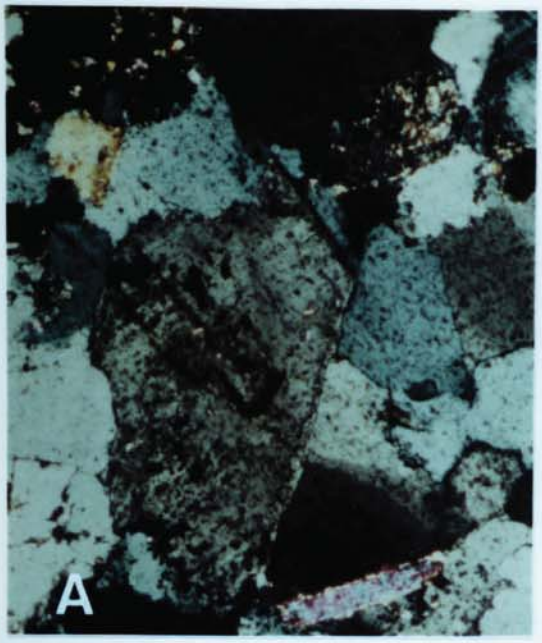

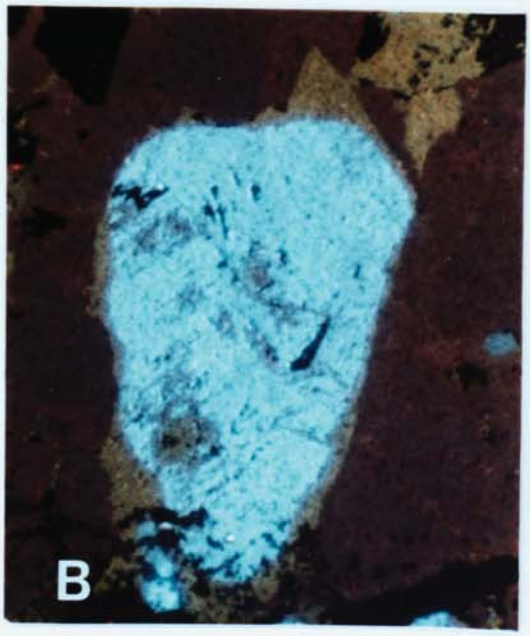

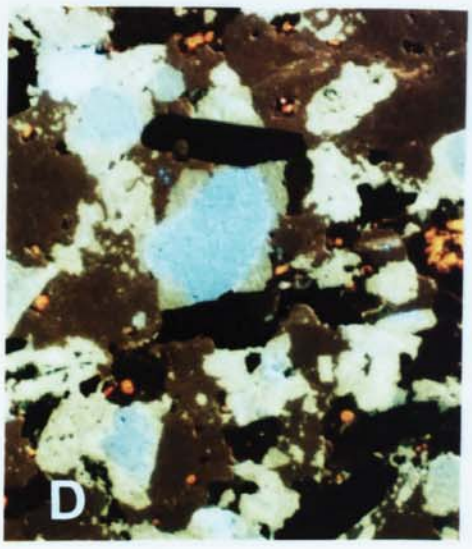

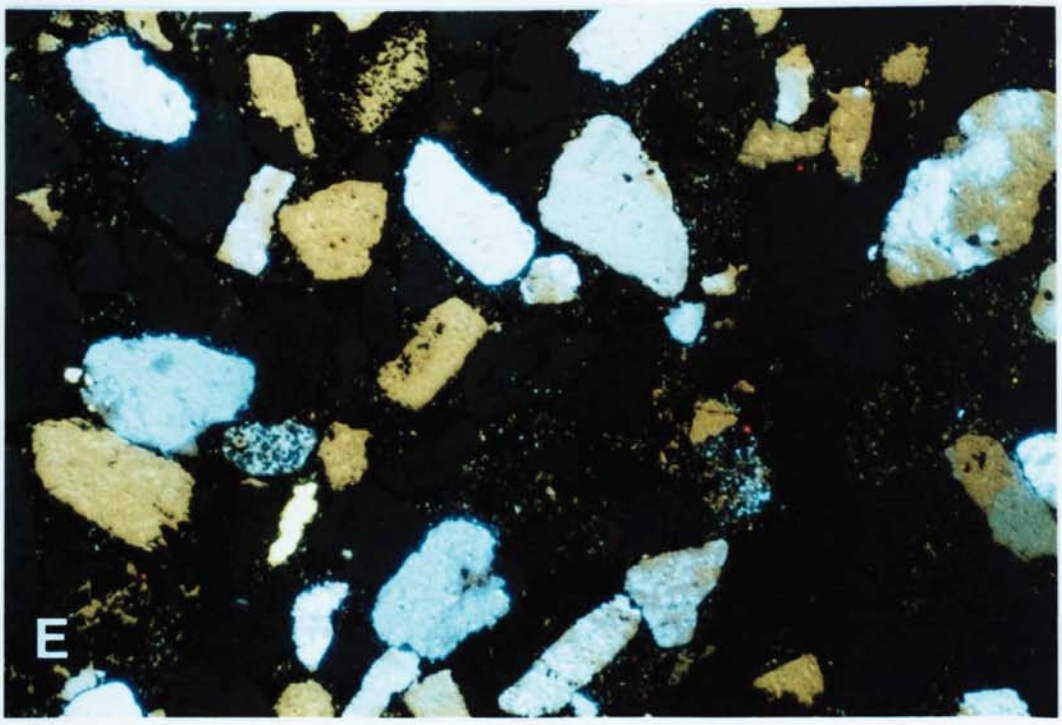

PLATE 4.8

Plate 4.9

A. Carrollite (white) grain with chalcopyrite (grey). Note the silicate inclusion rich core compared with the clean rim, also the occurrence of chalcopyrite along this boundary. Core and Rim carrollites also have different compositions, see Table 4.2. Sample AP638/6.

B, C and D. X-Ray density maps of above grain, for sulphur, copper and cobalt respectively. Note the occurrence of copper between rim and core carrollites.

E. Malachite noduals probably pseduomorphing sulphate. A later silicification event result in quartz crystals lining pores (upper left-hand margin) and in some replacement of malachite. Length of core approximately 10 cms.

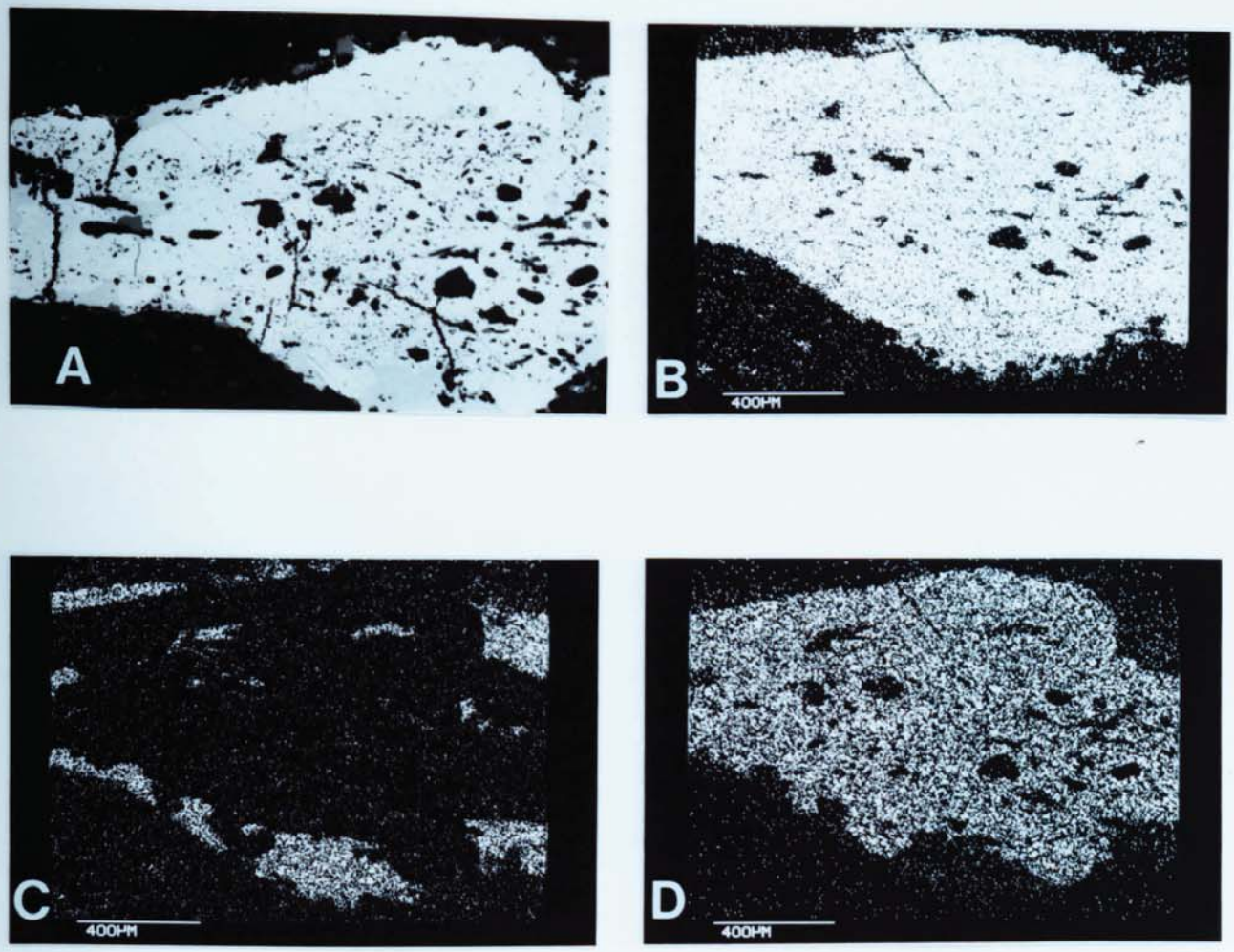

PLATE 4.9

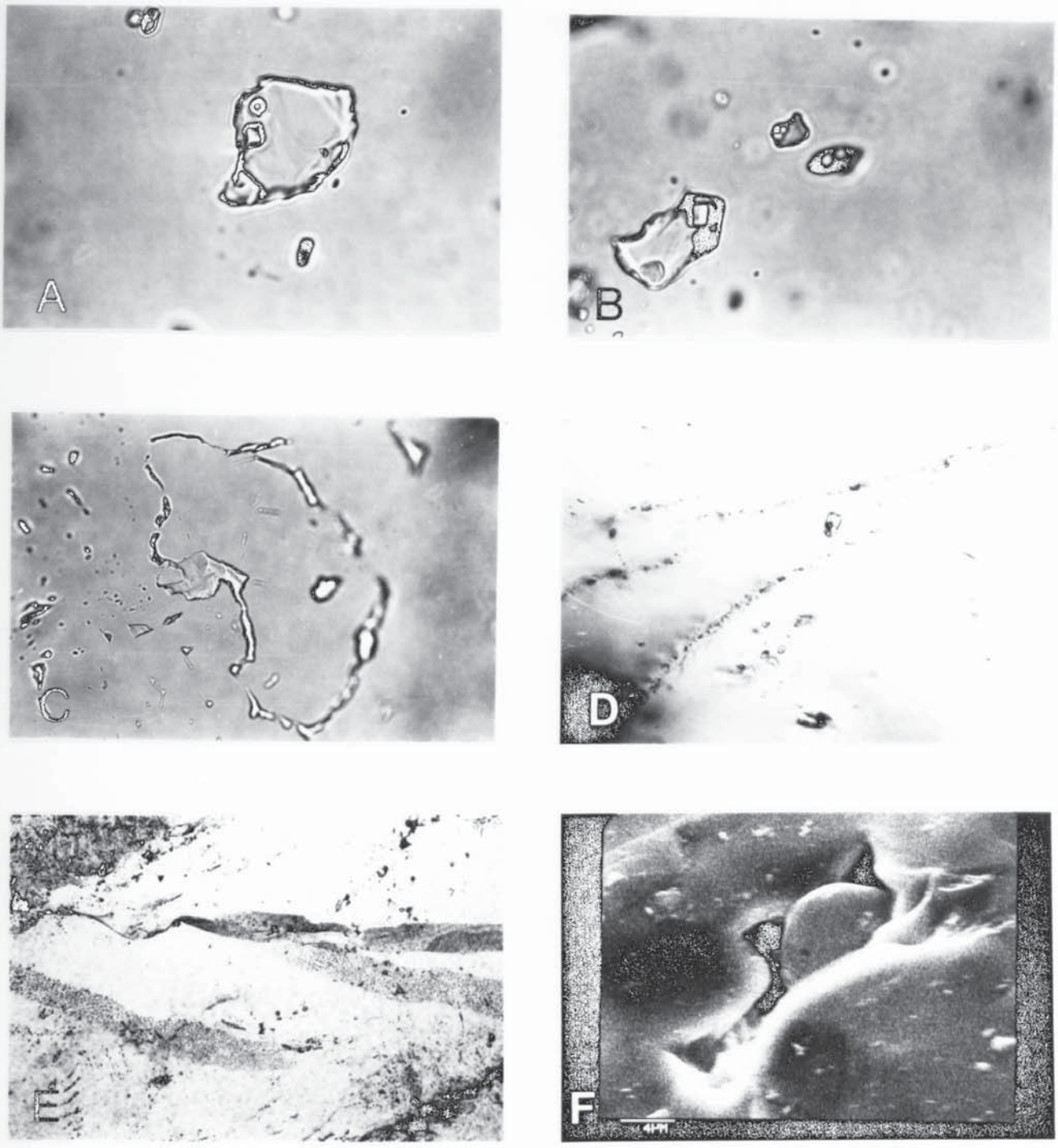

Plate 7.1 (a) and (b) Fluid inclusions of relative high salinity, containing halite, sylvite and a vapour phase. Ore-Shale vein quartz F.O.V360 μ .
(c) Necked inclusion from Footwall vein quartz. F.O.V.360 μ .
(d) and (e) Inclusion trails in Ore-Shale vein quartz. Note high salinity and necking in d. F.O.V. 360 μ and 4 mm.
(f) 'Broken Open' inclusion with large sylvite crystal. Evidence of necking is apparent towards the upper right hand corner of the inlcusion.

Plate 7.2

A. Large inclusions from Ore-Shale vein quartz. The overall triangular nature of the void indicates that it probably formed at quartz crystal boundaries. The phase at the bottom left hand corner is probably a mixture of halite and sylvite, as suggested by on line E.D.S. anlaysis. B and D, close up of inclusion phases showing a small microcline crystal attached to the inclusion sidewall by quartz. A native copper crystal growing outward from the side wall quartz overgrowth is shown in Plate D.

PLATE 7.2

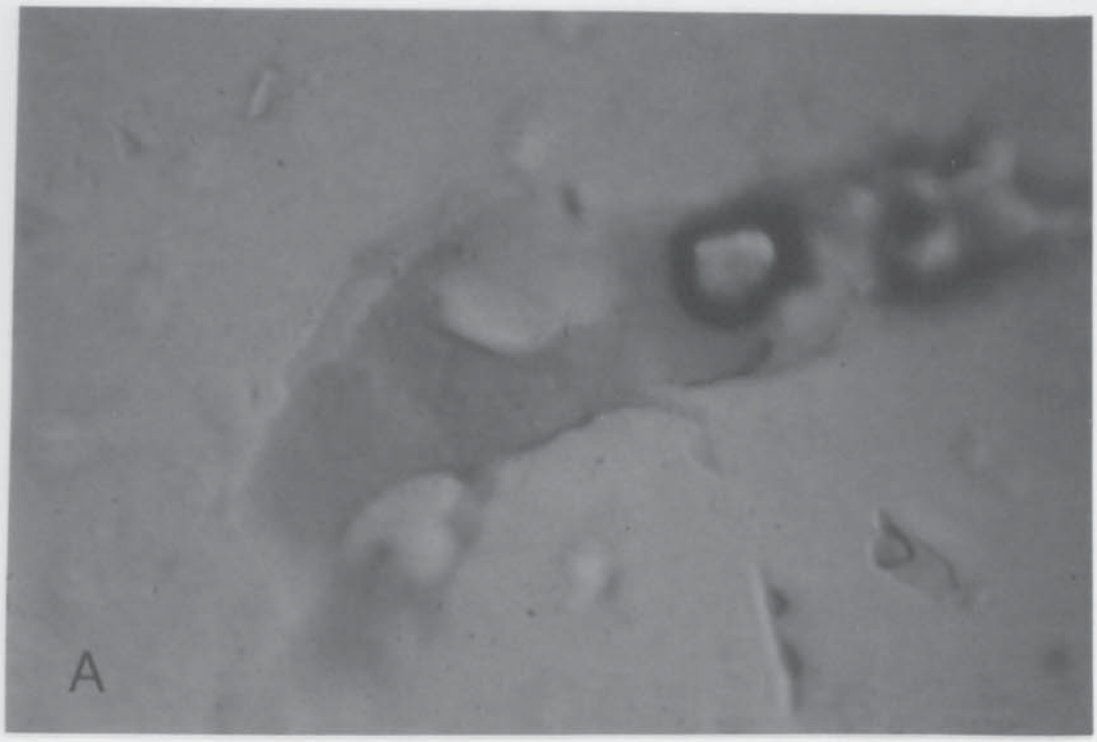

Plate 7.3 (a) Ore-Shale vein quartz inclusion, containing halite, sylvite, a vapour phase and hydrocarbon. The occurrence of hydrocarbon is confirmed by long wave U.V. (485 Nm) excitation (b). F.O.V. 360 microns.

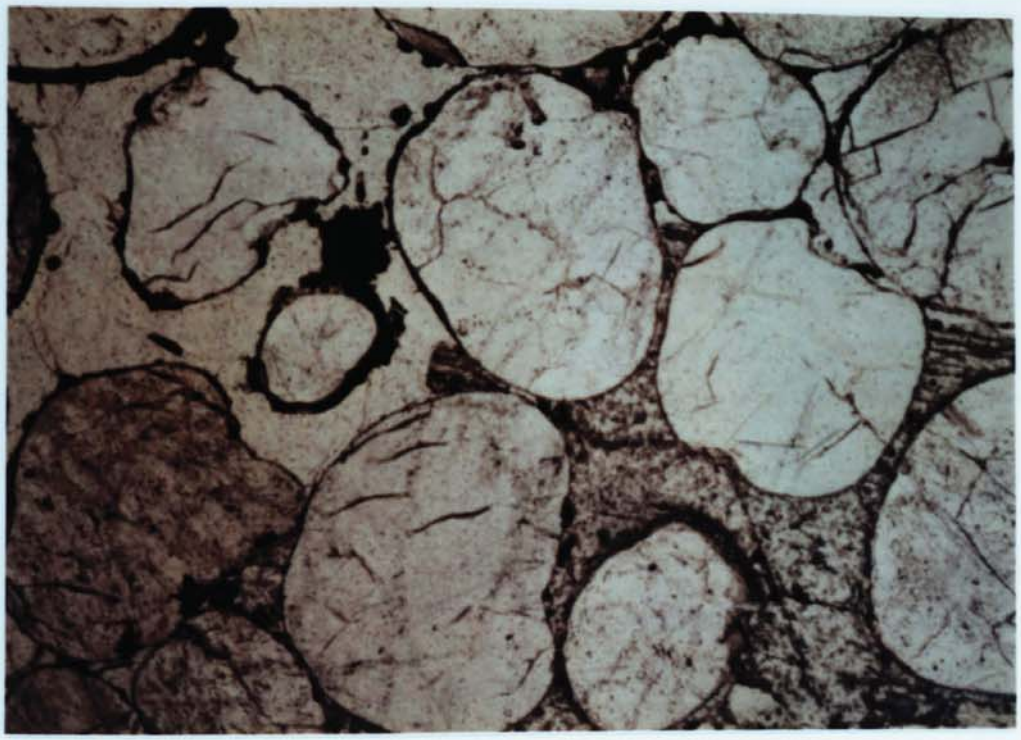

Plate 9.1A Quartz grains from the Yellow Sands, displaying rounded forms typical of aeolian sandstones, from Quarrington Quarry. Note that where the calcite cement is absent, the quartz grains are coated in manganese oxide which frequently shows a meniscus textures. F.O.V. 3.6 mm, PPL.

Plate 9.1B Marl Slate (arrowed) thins over a ridge of underlying Yellow Sands, Quarrington Quarry (N2 326 381).

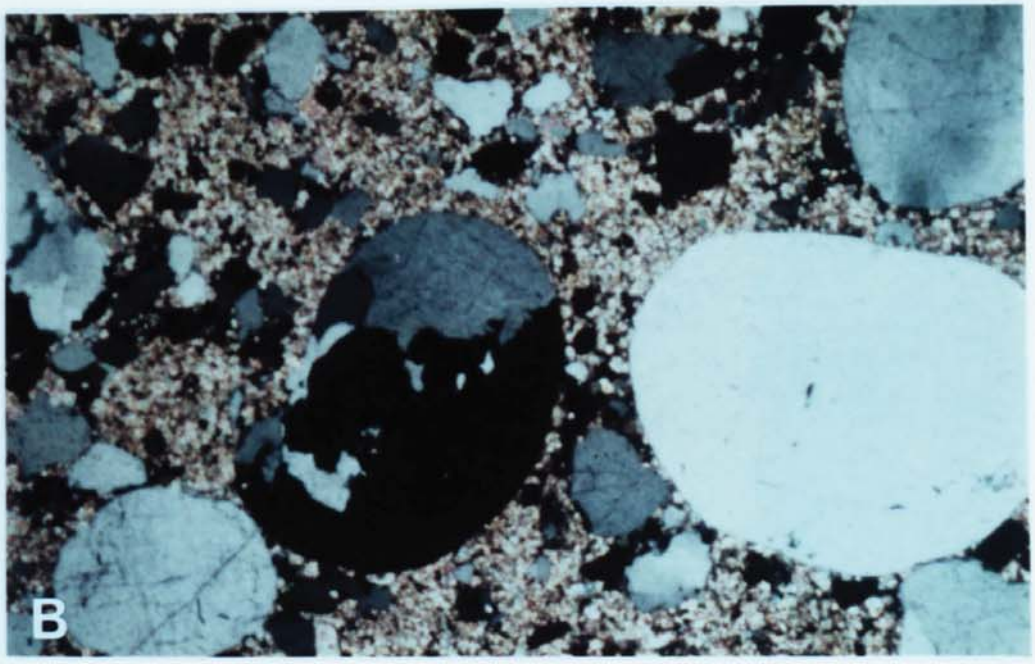

Plate 9.2A

A Cross-bedded Yellow Sands with marine reworked top (horizontally bedded unit below hammer) overlain by Marl Slate. Raisby Quarry. (NZ 3435).

B Photomicrograph of reworked Yellow Sands from the above locality. Note the occurrence of angular quartz fragments in the carbonate matrix. Compare with the unworked Yellow Sands in Plate 9.1A. F.O.V. 3.6 mm, XN.

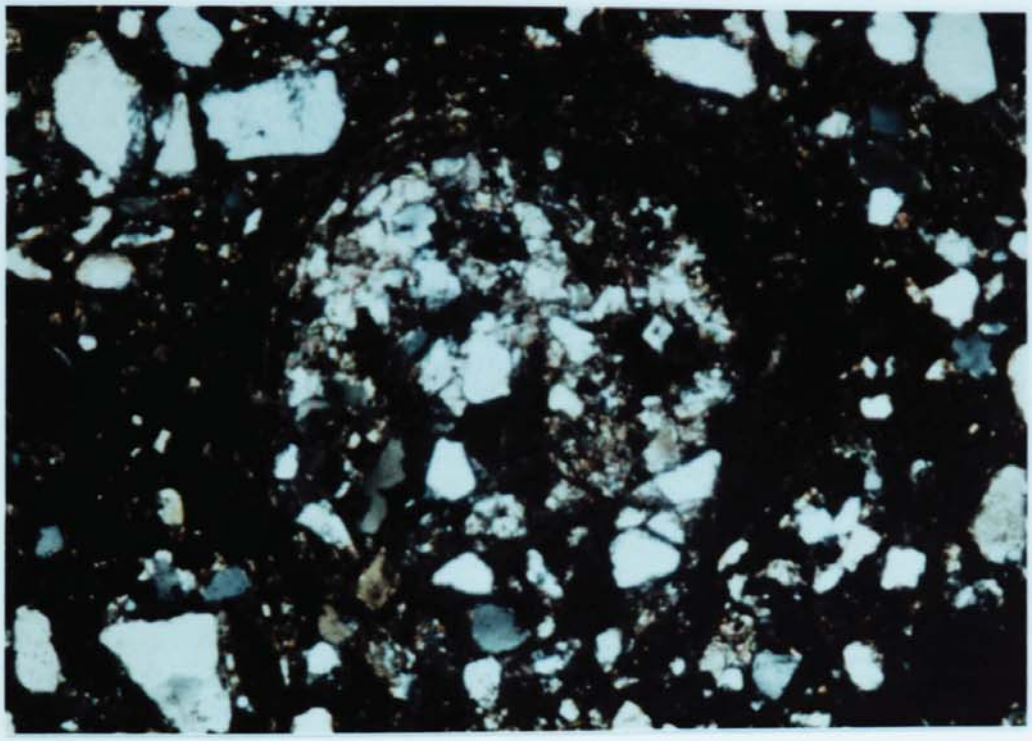

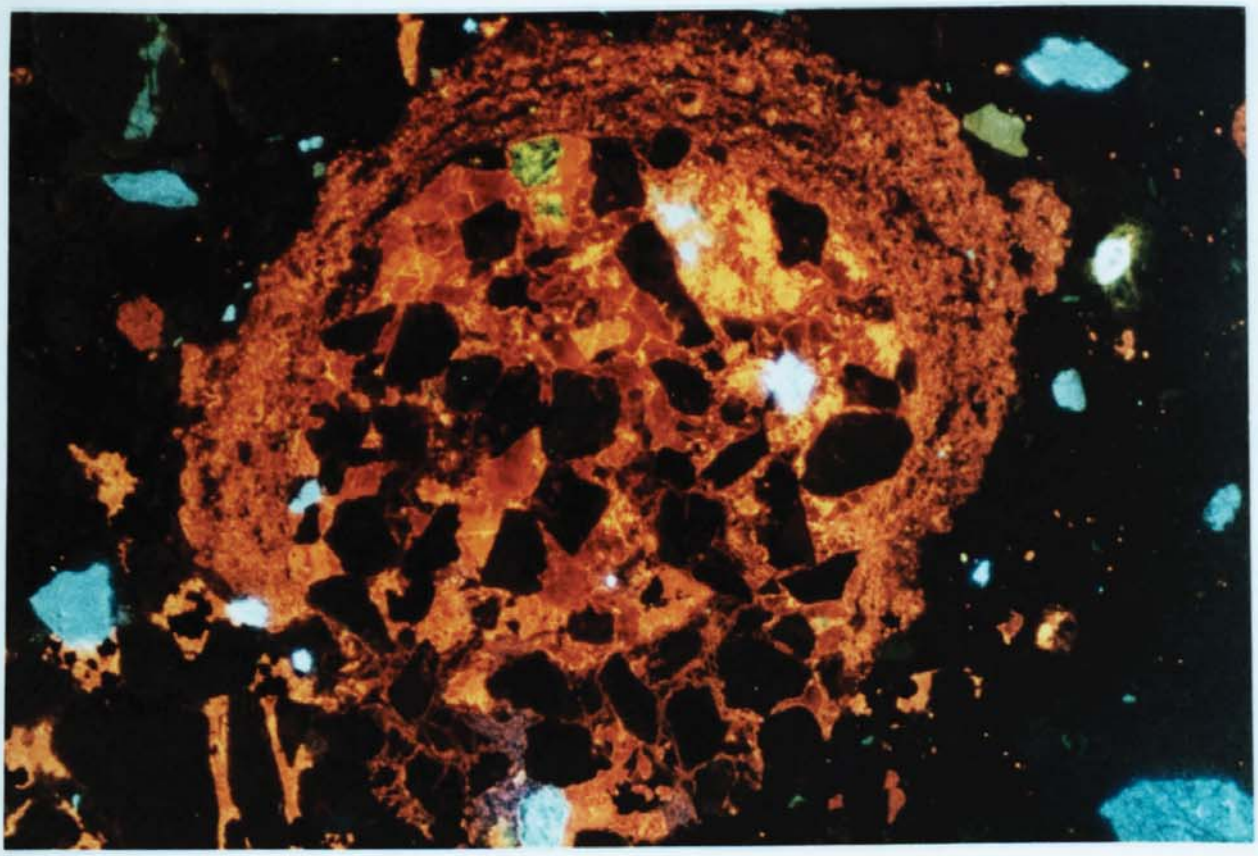

Plate 9.3 Cathodoluminescence and transmitted light (XN) photomicrographs of an algal coated, calcite cemented, clast of reworked Yellow Sands fragments. The algal coated clast has itself been reworked, which suggests the possibility of an earlier period of flooding prior to the main transgressive event. Doncaster Core. F.O.V. approximately 3.4 mm.

Plate 9.4

A Marl Slate, Quarrington Quarry (N2 326 381), note the ease with which the Marl Slate weathers, and the occurrence of thin carbonate laminae parallel to bedding. Leached vugs after carbonate can be seen in the area around the coin, see also Plate 9.9B.

B Photomicrograph of the basal organic rich section of the Marl Slate. Note the occurrence of carbonate as discontinuous streaks. Doncaster Core sample D.C. 14.
F.O.V. 3.0 mm. PPL.

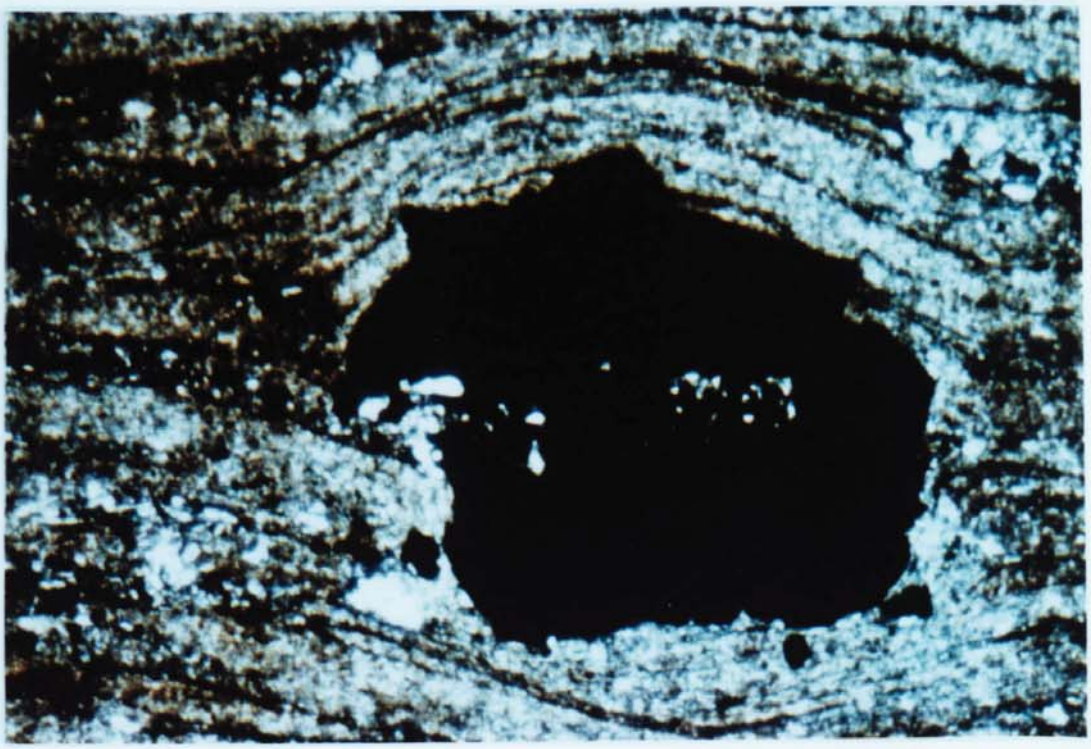

Plate 9.5

A. Silt horizon in bitumen-rich Marl Slate, sample J12 from core J1000. Sulphide grains (most of the black grains) are relatively abundant. Note that this core contains significantly less carbonate than the sapropelic section of the Doncaster Core (Plate 9.4B). F.O.V. 3.0 mm, XN.

B Pyrite filling a nodual after carbonate. Silicate trails run through the centre of the grain and the pyrite which is subhedral deforms bedding, suggesting that the replacement was pre-significant burial. Sample Q4. F.O.V. 1.8 mm, XN.

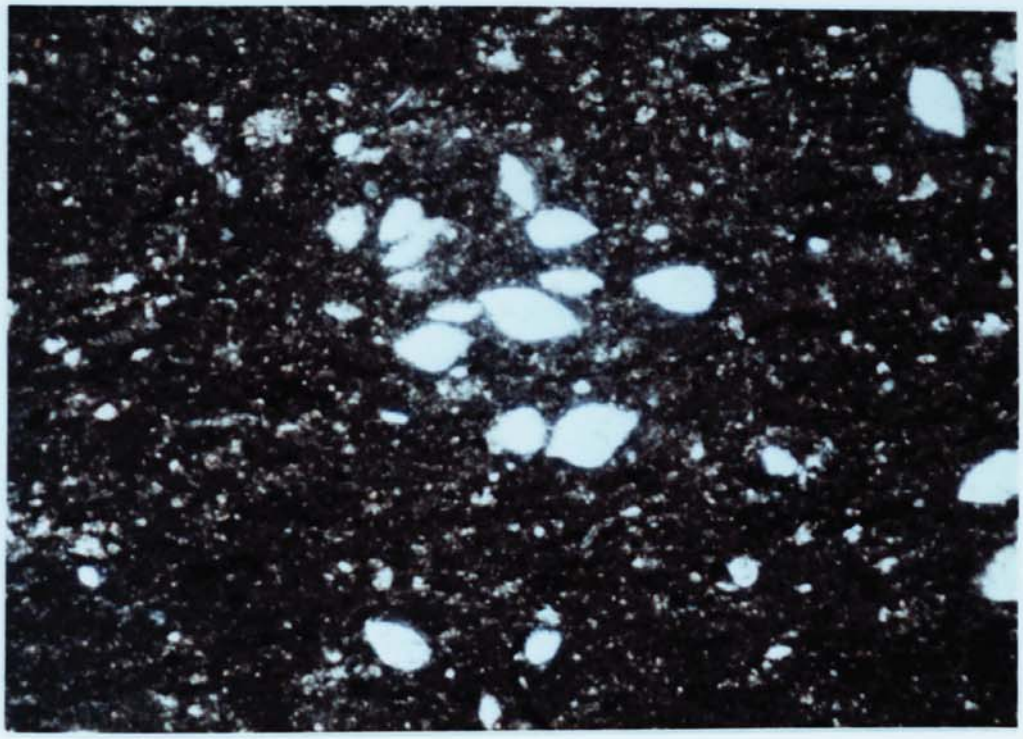

Plate 9.6

A Poorly laminated organic carbonate (mainly calcite) from the base of the Doncaster Core, Sample D.C.8. Ostracods occur throughout these horizons. F.O.V. 3.6 mm, PPL.

B Well laminated organic carbonate (mainly dolomite) from the upper section of the Marl Slate (Doncaster Core) Sample D.C. 90. F.O.V. 3.6 mm, PPL.

Plate 9.7

A. Yellow orange luminescent calcite showing evidence of corrosion, from a sapropelic section of the Transition Zone core, sample D.C. 113. F.O.V. 1.8 mm.

B. Yellow orange luminescent calcite from a calcite-rich horizon of the Transition Zone core, sample D.C. 119. Note that the crystals are frequently zoned and are euhedral even though they are in contact with dolomite (non-luminescent). F.O.V. 1.8 mm.

C. SEM micrograph of etched calcite crystals from a sparopelic section of the Transition Zone core, sample D.C. 113.

D. SEM micrograph of a dolomite-rich horizon from the Transition Zone core, sample D.C. 117. Note that although calcite (euhedral) and dolomite (matrix) are in intimate contact, the calcite crystals remain uncorroded. This is particularly well seen in the lower left hand corner of the micrograph.

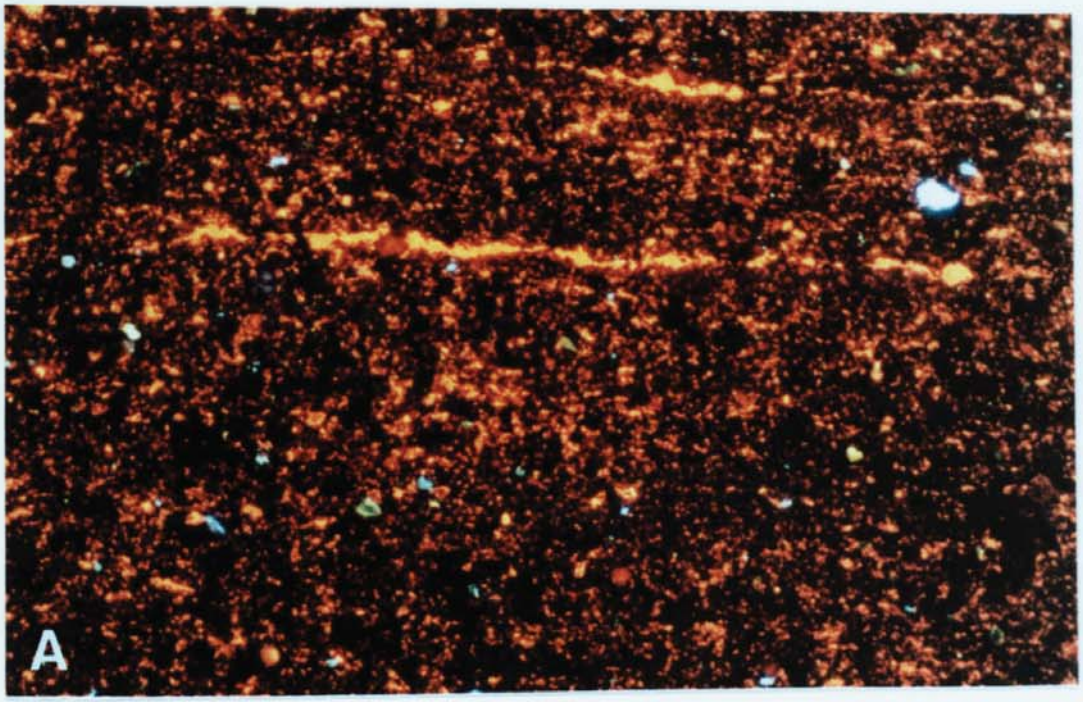

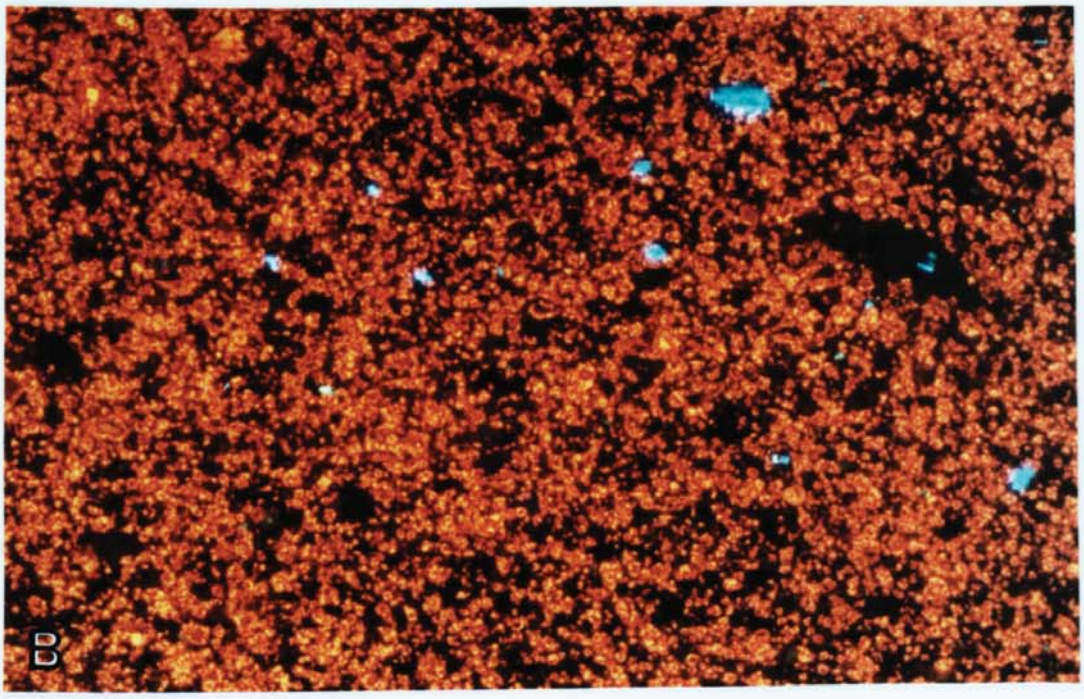

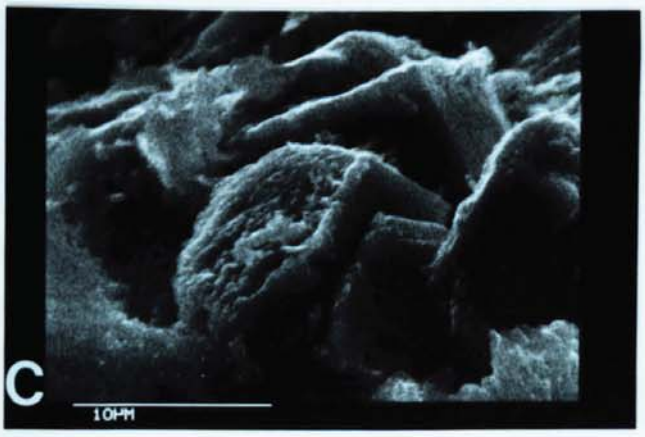

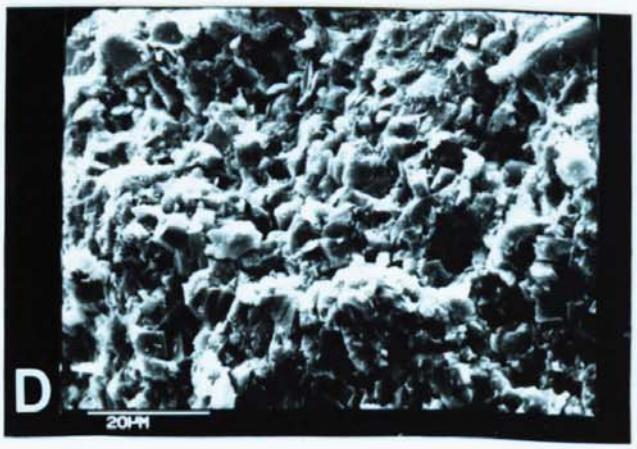

PLATE 9.7

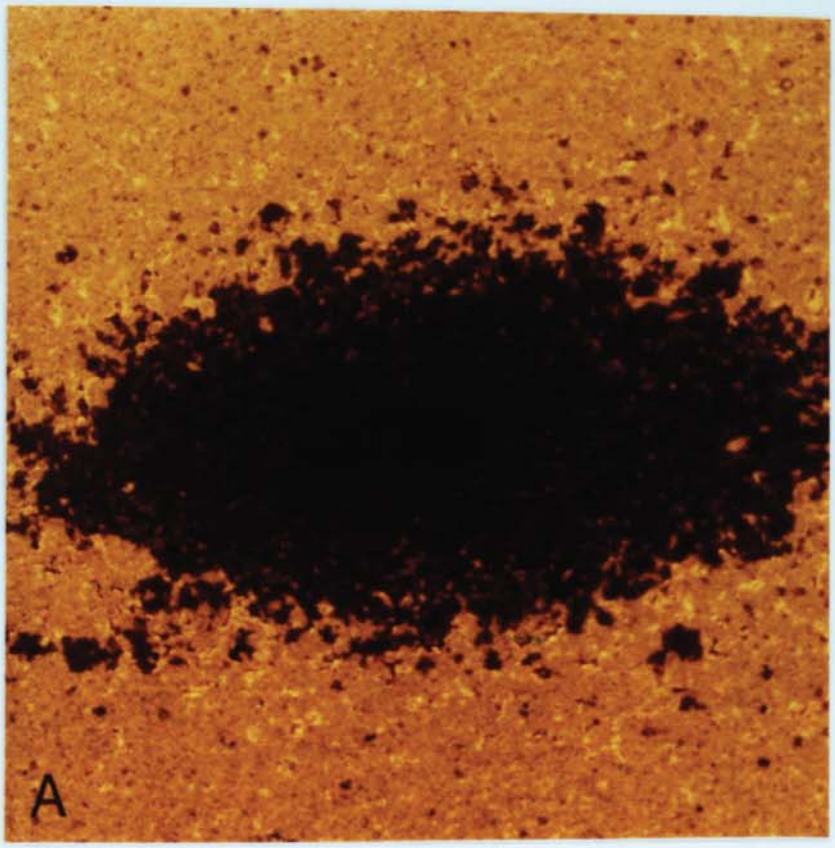

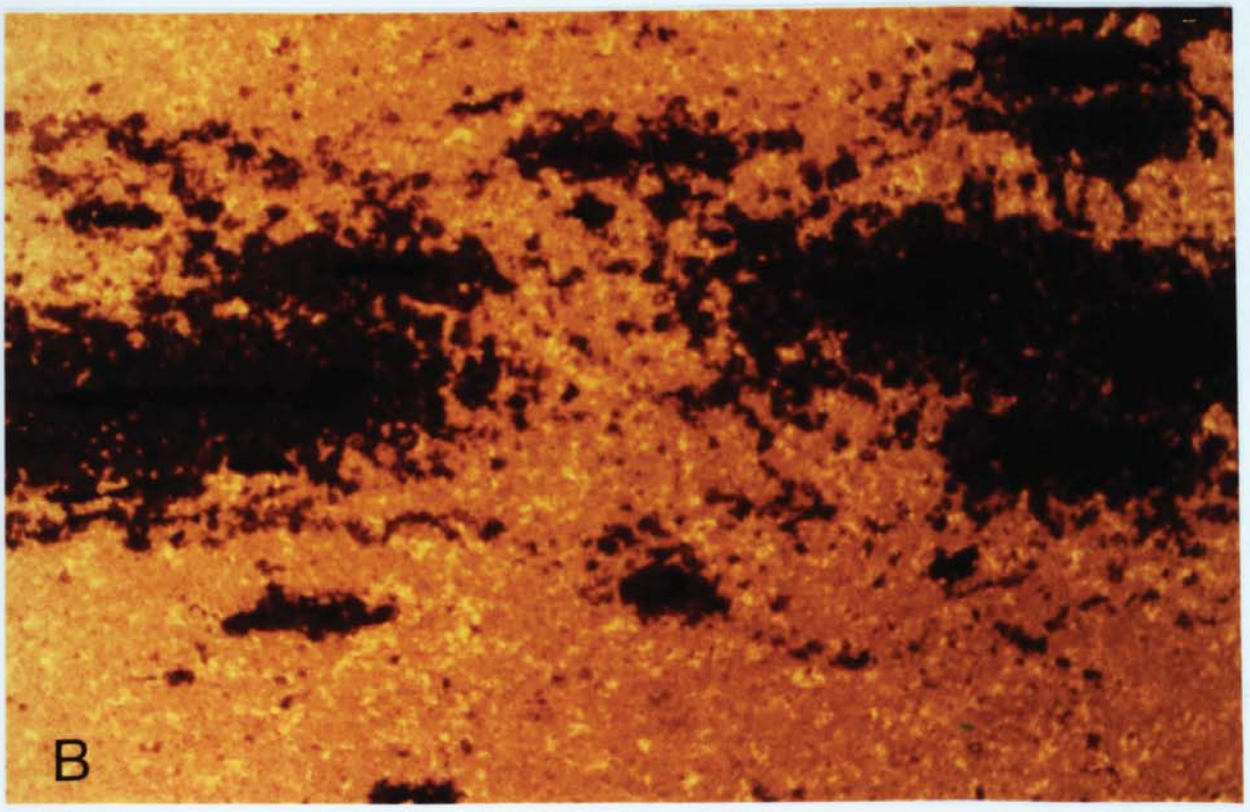

Plate 9.8 A Zone of non-luminescent dolomite apparently nucleated on organic matter (black) in a matrix of yellow-orange luminescent calcite. An increase in porosity can be seen towards the edge of the dolomitizing front. If sufficient dolomite centres are nucleated, it is possible that a thin horizon of dolomite may form within the calcite matrix. This may have been in the process of happening in (B). F.O.V. approximately 1.2 mm and 2.8 mm.

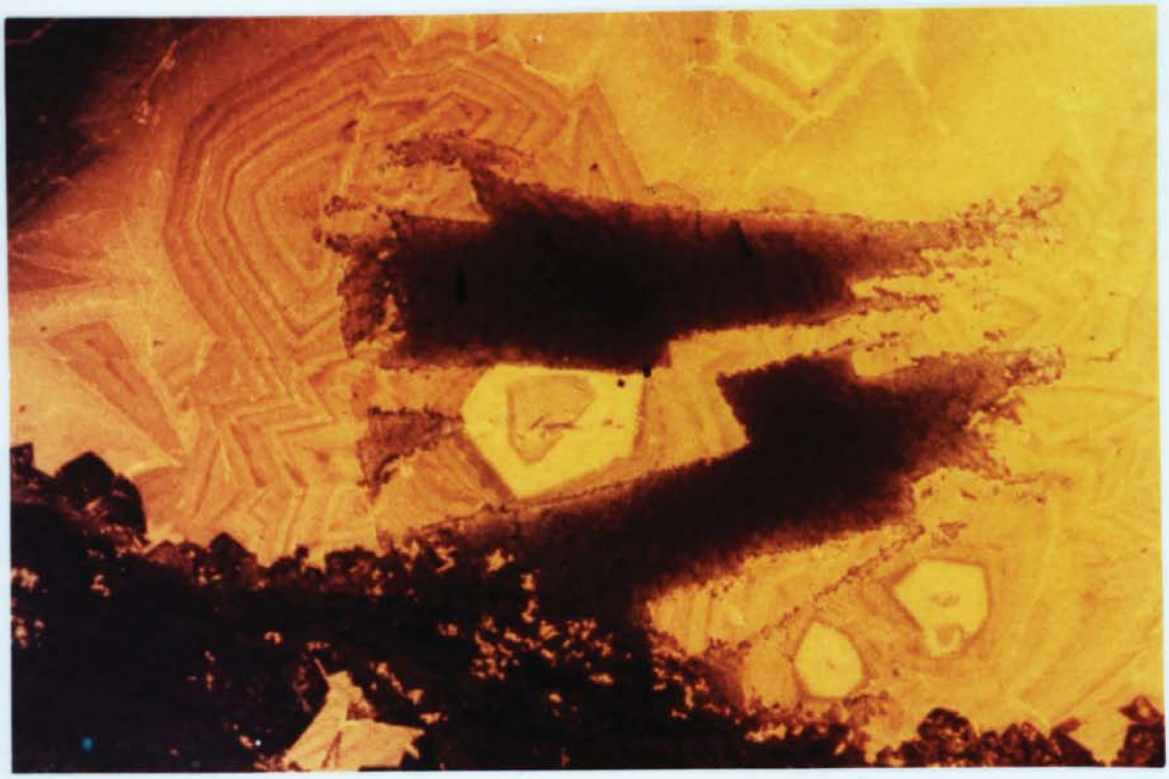

Plate 9.9

A Crystals of saddle dolomite, showing characteristic sweeping extinction. Sample from a cross-cutting vein from the lower part of the Transition Zone Core. F.O.V. 3.6 mm, XN.

B. Cathodoluminescence micrograph of part of a calcite filled vug from the Marl Slate, Quarrington Quarry. The fractures sphalerite (non-luminescent) is cemented by later zoned yellow-orange calcite, a non-luminescent euhedral calcite lines the vug perimeter. F.O.V. 2.8 mm.

Plate 9.10

A. SEM micrograph of an iron sulphide sphere, possibly greigite with a pyrite (cubic) overgrowth. Sample from core 49/26-4.

B and C. SEM micrograph showing isolated pyrite farmboids from the Marl Slate section of the Doncaster Core.

D. Reflected light micrograph showing isolated pyrite spheres and framboids with 'clover leaf' combination of spheres towards the centre of the field of view. Sample SR3. F.O.V. 240 microns, Oil immersed.

E and F. SEM micrographs of groups of well formed compound crystal framboids from the J1000 core. In plate E the framboids in the centre of the field of view appear to have suffered soft deformation.

G and H. SEM micrographs of euhedral 'nests' of cubic pyrite crystals. The crystals are closely associated with organic matter and fossil debris. Samples from the Marl Slate section of the Doncaster Core and the J1000 core.

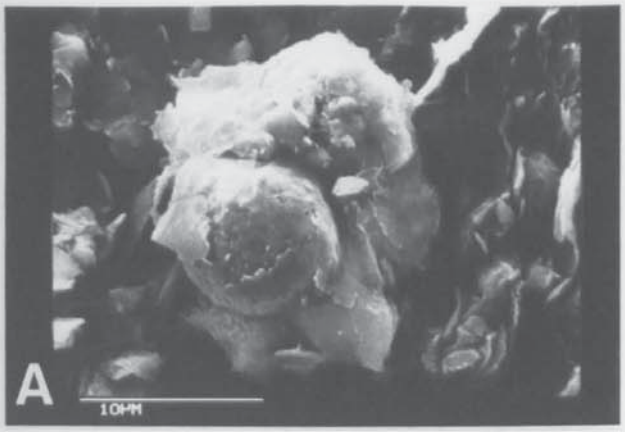

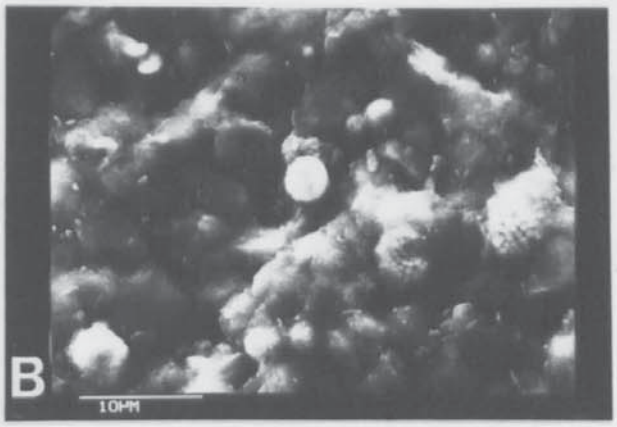

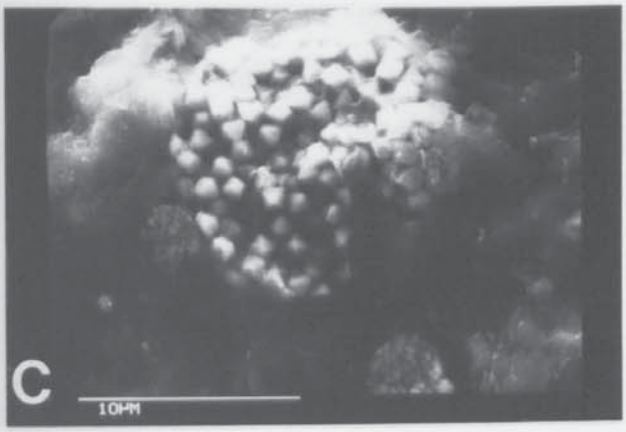

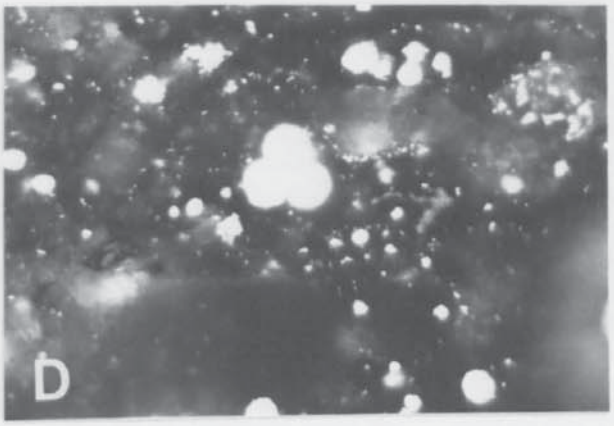

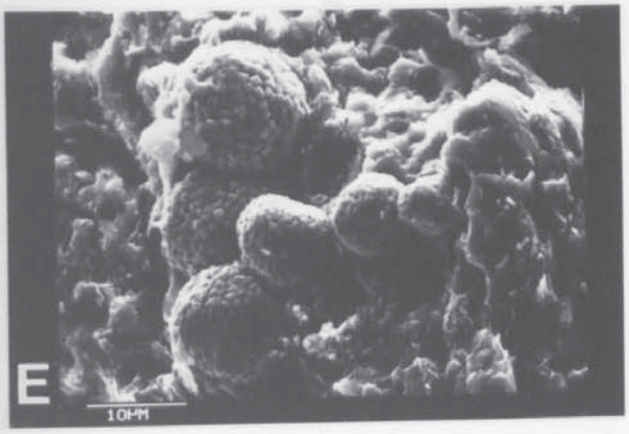

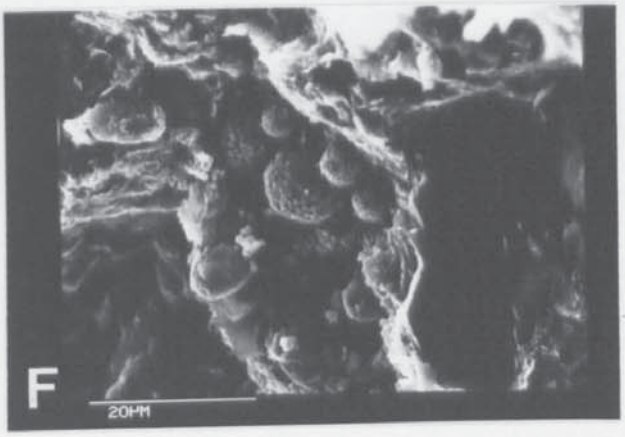

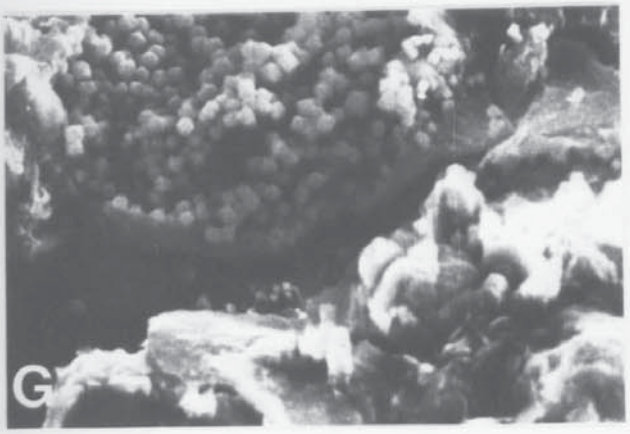

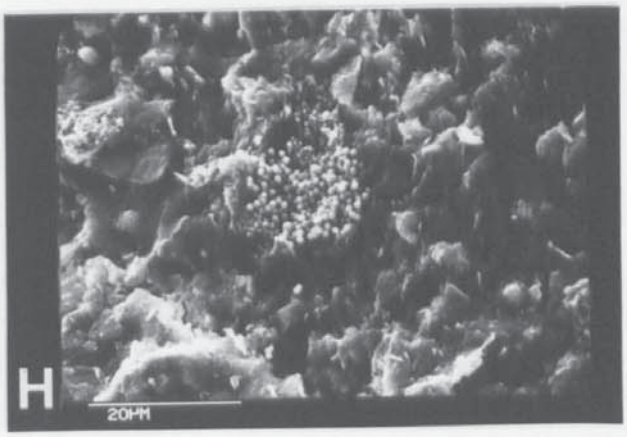

PLATE 9.10

Plate 9.11

A. Pyrite framboids with partial euhedral overgrowths (arrowed). The framboids contain 'holes' while the overgrowths are 'clean'. Sample SR3. F.O.V. 240 microns. Refl. Light (in oil).

B. Pyrite framboids (white) enclosed in chalcopyrite (yellow). Sample form the J1000 core. F.O.V. 0.9 mm. Refl. Light.

C. Rounded, probably detrital grains of pyrite in the Yellow Sands immediately underlying the Marl Slate of the Doncaster Core. F.O.V. 0.9 mm. Refl. Light.

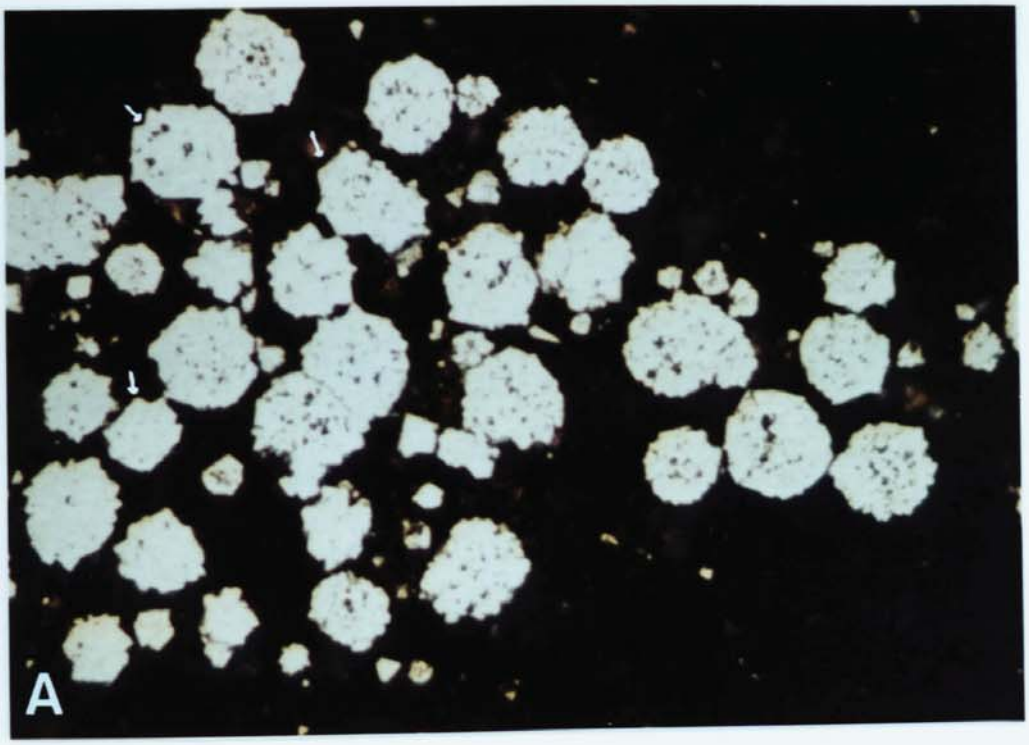

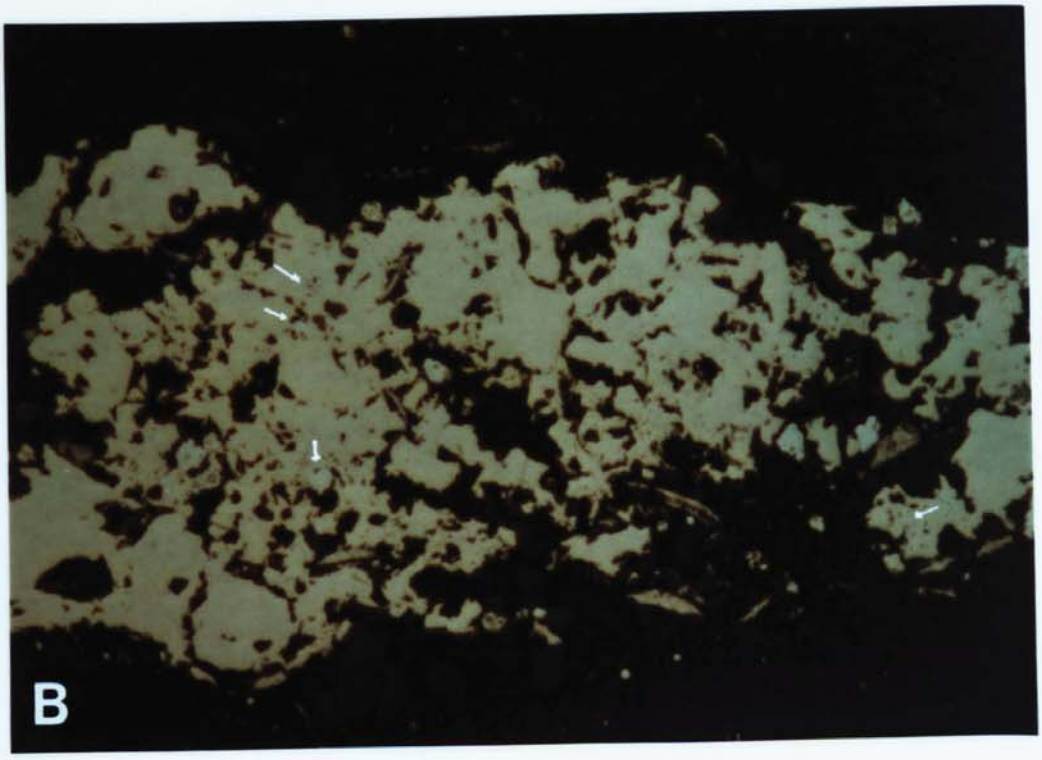

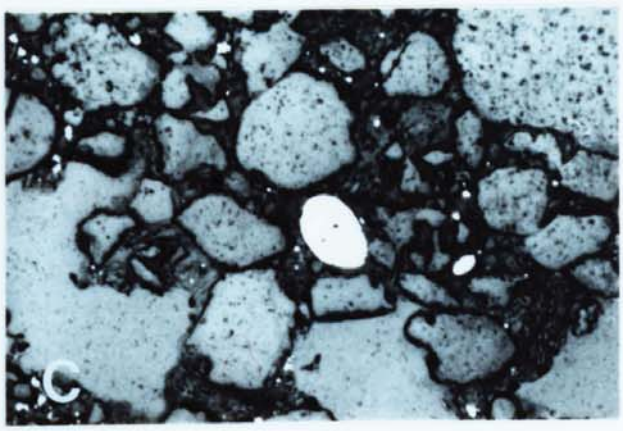

PLATE 9.11

APPENDICES

APPENDIX 1

CATHODOLUMINESCENCE TECHNIQUES

Cathodoluminescence was achieved using a Technosyn cold cathode luminescence model 8200 Mk 2 instrument. An accelerating voltage of between 15 - 20 kV with a current of 0.2 - 0.4 mA and a beam area of approximately 100 mm^2 was applied to polished thin sections. Non-polished sections were used during preliminary investigation, but lacked the detail of well polished sections.

To reduce exposure time while recording observations, and thus reduce problems associated with vibrations and drifting 'standard' conditions, 1000 ASA Kodacolour VR colour slide film was used. Exposure times were variable, being typically 8 - 30 seconds for yellow-orange carbonates and 5 - 15 minutes for poorly luminescing silicates.

APPENDIX 2

METHOD OF DETERMINATION OF WHOLE-ROCK CARBONATE CARBON AND ORGANIC CARBON CONTENT

Samples were finely crushed, homogenised and air dried in a warm (approximately 30°C) oven. Total carbon and organic carbon contents were determined on a Carlo Erba 1106 gas chromatograph using an ignition temperature of 1040°C. To determine the organic carbon content, the carbonate fraction of the sample was dissolved off in 10% warm hydrochloric acid and the residue washed, dried and analysed. The quoted weight percent organic carbon were corrected for the sample weight loss due to the acid treatment. Carbonate carbon content was calculated by subtracting the organic carbon value from the determined total carbon value for the sample. All samples were analysed twice, with check samples being analysed up to six times. Repeated analysis rarely showed a variation of greater than 0.1% carbon.

APPENDIX 3

TECHNICAL DETAILS OF SULPHUR ISOTOPE ANALYSIS AND SAMPLE PREPARATION

(i) Sulphur Isotope Analysis

To prepare a gas from sulphides, samples were oxidised at 1070°C with cuprous oxide (Robinson and Kusakbe, 1975). Sulphate samples were treated by the method of Coleman and More (1978). The sulphur dioxide produced from a sample was measured on a V.G. double collector mass spectrometer. This has an inlet system heated to 110°C to avoid memory effects between successive samples.

All samples were analysed relative to an internal laboratory standard of chalcopyrite (CP1). This has an isotopic composition of $\delta^{34}S = -4.56$ per mil relative to the international standard C.D.T.

CP1 standard gas samples were prepared and analysed at the beginning and end of each batch of six samples.

The raw data were corrected for instrumental and isotopic effects (Craig 1957, Deines 1970 and Coleman 1980). The final values were not accepted if two times the standard error exceeded 0.06 per mil. All sample values are quoted relative to the international standard,

Canyon Diablo Troilite.

(ii) Sample Preparation

A flow chart for Copperbelt sample preparation is shown in Figure A3.1. All samples were checked for purity by X.R.D. It was found from test runs that upwards of 2% by weight of Bornite and 5% by weight of carrollite impurity in chalcopyrite could be detected. Only samples with no detectable impurity were used in isotope analysis.

In order to determine the pyrite sulphur content of the Marl Slate, whole rock samples were analysed. The samples had carbonate and organic carbon content removed by acidification with 10% acetic acid, and plasma treatment respectively. This was done to avoid gas separation problems and possible contamination. Polished thin sections were used to check that pyrite was the only potential source of sulphide sulphur.

Undoubtedly minor contamination occurs, but in view of the sample preparation techniques this is not considered a major source of error. One sample from the Transition Zone core was separated by heavy liquid techniques. This was analysed after microscopic examination and X.R.D. checks for purity. The values of -14.8 per mil for whole rock, and -14.3 per mil for the pure pyrite sample are considered to be in good

agreement. The difference is small compared with the major difference in facies. A contamination due to sulphate of another sulphide is therefore considered unlikely.

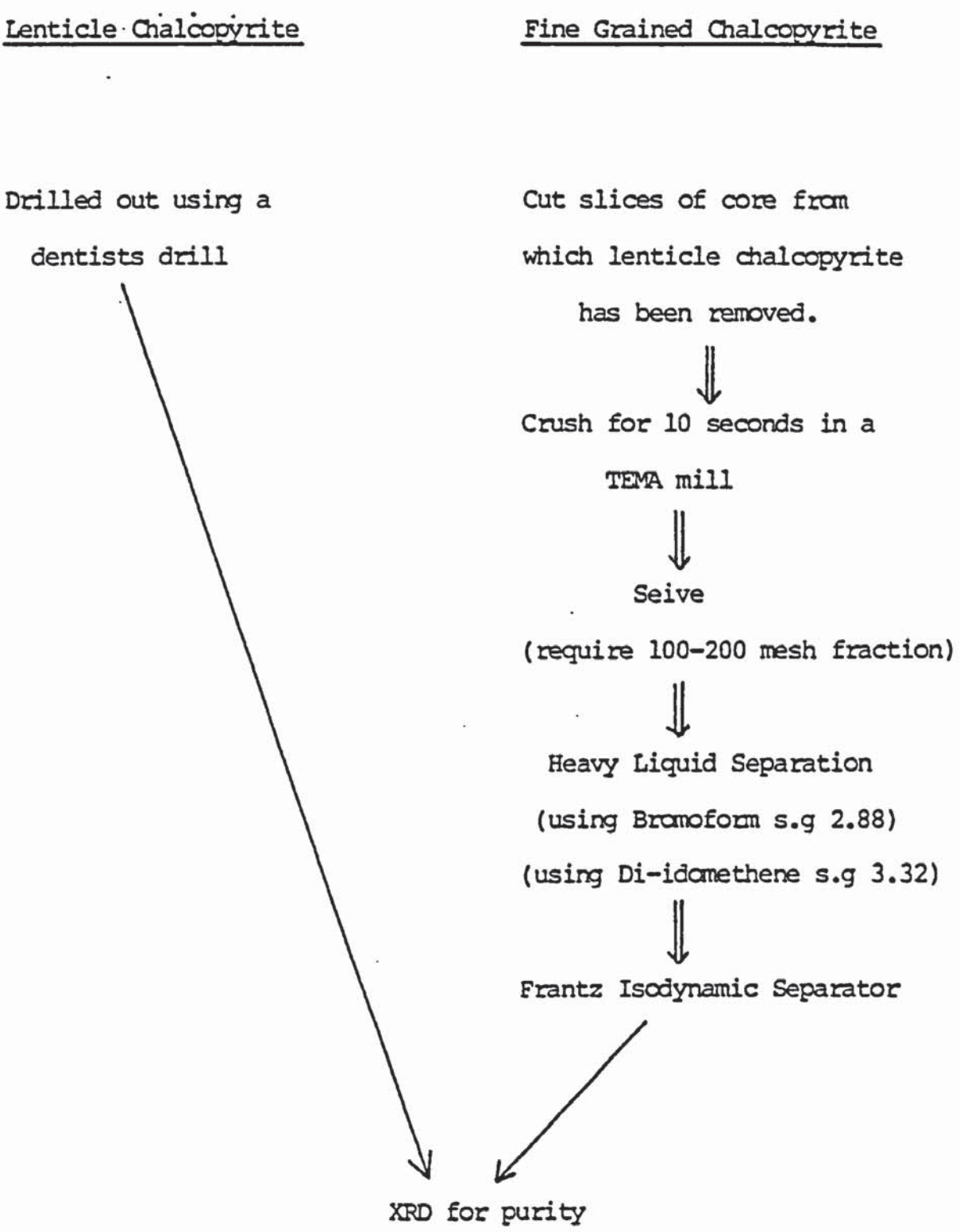

Figure A3.1 Flow Chart for Sample Preparation for Copperbelt Samples.

APPENDIX 4

TECHNICAL DETAILS OF CARBONATE ISOTOPE ANALYSIS AND SAMPLE PREPARATION

(I) Carbon and Oxygen Isotope Analysis

Carbon Dioxide was extracted from the samples by reaction in vacuo with 100% orthophosphoric acid (McCrea, 1950) at 22.2°C. The Copperbelt samples were reacted for 10 days and the Marl Slate samples for a minimum of 4 days. In each case the reaction had gone to completion.

The carbon dioxide gas produced was collected and measured in a tripple collector Micromass 903 mass spectrometer. Samples were analysed relative to an internal laboratory standard of calcite (M.C.S.). This has an isotopic composition of $\delta^{13}C = -0.70$ per mil and $\delta^{18}O = 9.12$ per mil relative to P.D.B. (a Cretaceous belemnite-Belemnitella americana from the Pedee Formation, S. Carolina, USA).

MCS standard gas samples were prepared and analysed at the beginning and end of each batch of six samples.

The raw data were corrected for instrumental and isotopic effects (Craig, 1957 and Deines, 1970). The final values were not accepted if twice the standard error exceeded 0.06 per mil. The fractionation factors used

were 1.01110 for dolomite, and 1.01025 for calcite and malachite.

Nine repeat samples were processed from the crushing through to the analytical stage. Linear regression plots for original values (x axis) against repeat samples are shown in Figure A4.1. The results show an extremely good correlation.

(ii) Sample Preparation

The Copperbelt samples were extracted by drilling using a dentists drill. In the case of lenticle samples, material was obtained by drilling from thin slices of clean drill core. Some whole rock analysis (CP197 samples) of crushed whole rock samples was also undertaken.

Large amounts of organic matter in samples can interfere with the measurement of the isotopic composition of CO_2, by producing organic molecules of masses 45 and 46 (Weber et al., 1976). Since some Marl Slate samples contain up to 6% organic carbon, this was removed prior to reacting the samples to produce CO_2. To do this, all samples were oxidised for up to 8 hours in a Nanotech Plasmaprep P100 low temperature oxygen plasma unit. Goreau (1977), and checks on internal laboratory standards (J. Rouse pers. comm.) have shown that this treatment does

not affect the isotopic composition of carbonates or sulphides. The removal of organic matter may also have served to remove organic sulphur from the samples, although this is not thought to be a significant source of sulphur contamination.

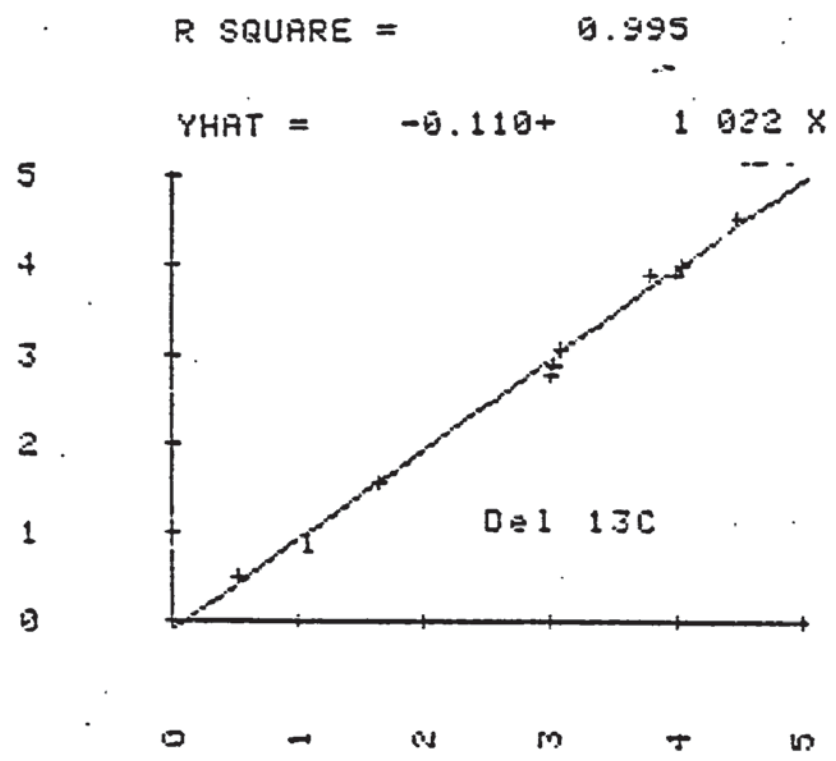

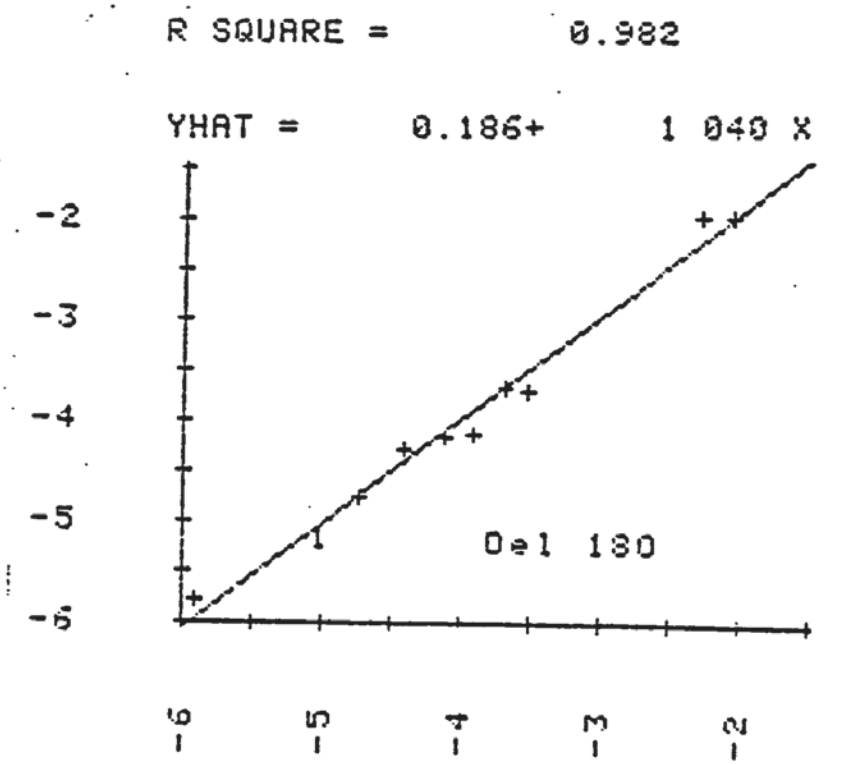

Figure A4.1 Linear regression plots for repeat carbonate samples.

APPENDIX 5

TRACE ELEMENT DETERMINATION BY X-RAY FLUORESCENCE

Sample Preparation

Samples were first washed to remove any extraneous material, and were then crushed in a jaw crusher and finally ground in a TEMA mill for a total of three minutes. Ground samples were then dried overnight at a temperature of 110°C.

Pressed Powder Pellets

To 8.5g of a sample was added 1.5g of Bakelite (RO214/1) binding agent. This was then placed on a shaking table for 30 minutes to ensure homogenisation. The homogenised material was then placed in a steel mould and pressed to a pressure of 20 tons/in^2 for 10 seconds. The pellets produced were then cured overnight in an oven at a temperature of 120°C.

Fused Glass Discs

To prepare fused glass discs, samples were crushed, ground and dried as above. To 0.75g of a carefully weighed sample was added 5.3333 times the measured weight of Johnson and Matthey Spectroflux 105. This was then placed in an oven at 1100°C for 20 minutes. When

completely cooled the weight loss (loss on ignition) was made up with spectroflux. A meker burner was then used to remelt and homogenise this.

A preheated (220°C) disc-shaped graphite mould was used to form the fused glass disc. Gentle hand pressure was applied via a steel rod to ensure an even spread of the melt.

Cooled fused discs were stored in individual plastic envelopes in a dessicator.

Analysis

International standards of approximately the same matrix as the samples were used for calibration. No international standards of suitably high Cu and Co values were available. Spiked standards using Johnson and Matthey spec-pure Cu and Co were made using a non-mineralised granite base.

Samples were run against both international and internal standards. For values of Cu less than 0.5% and less than 0.08% Co, the values obtained from international standard callibration were considered more reliable, and are the values quoted.

A Philips PW1400 System X-ray Spectrometer was used

for all analysis. Duplicate samples were made every four samples, and correlated with the original samples at the 99.9% Confidence Limit.

The high sulphide content of the Copperbelt ores, forbade the use of platinum ware, and only a few test fused discs were made. As a result all Copperbelt samples were analysed using only pressed power pellets. As a consequence the values obtained for iron, manganese and titanium are subject to large errors due to absorption effects. Some 50 samples were analysed for these elements by Atomic Absorption Analysis. The results were in good agreement; within 10% of each other, with the XRF values tending to be lower. The results are therefore considered to be good enough for inclusion with the bulk of the chemical analysis.

APPENDIX 6

SAMPLE PREPARATION AND ANALYSIS OF FLUID INCLUSION GAS/LIQUID PHASES

Samples of vein quartz were first crushed in a jaw crusher and then in a steel mortar and pestle. The crushed sample was then sieved and the fraction less than 1 mm and greater than 500 μ was retained. This portion was then sorted under a binocular microscope, and only pure single phase quartz grains were chosen for analysis. Between a half and one gram of sample was then weighed and placed in the apparatus shown in Figure A6.

The sample was then degassed and preheated at 100°C to remove any surface moisture and contaminant. Without going into too much detail, the sample is then decrepitated at 550°C and the condensable component frozen in a cold trap (CTI) with liquid nitrogen. The volume of the non-condensable component was then measured and passed to a mass spectrometer for analysis. Thus the argon, methane, hydrogen and nitrogen components were measured, and the system was then pumped clean. The liquid nitrogen was then removed from the cold trap (CTI) and replaced with a mixture of dry ice, acetone and liquid nitrogen (-78°C) which allowed CO_2 to evolve. The CO_2 pressure was allowed to stabilise and its pressure (and thus volume) was measured. The system was again pumped clean. By this time only water remained in the collecting vessel (CTI)

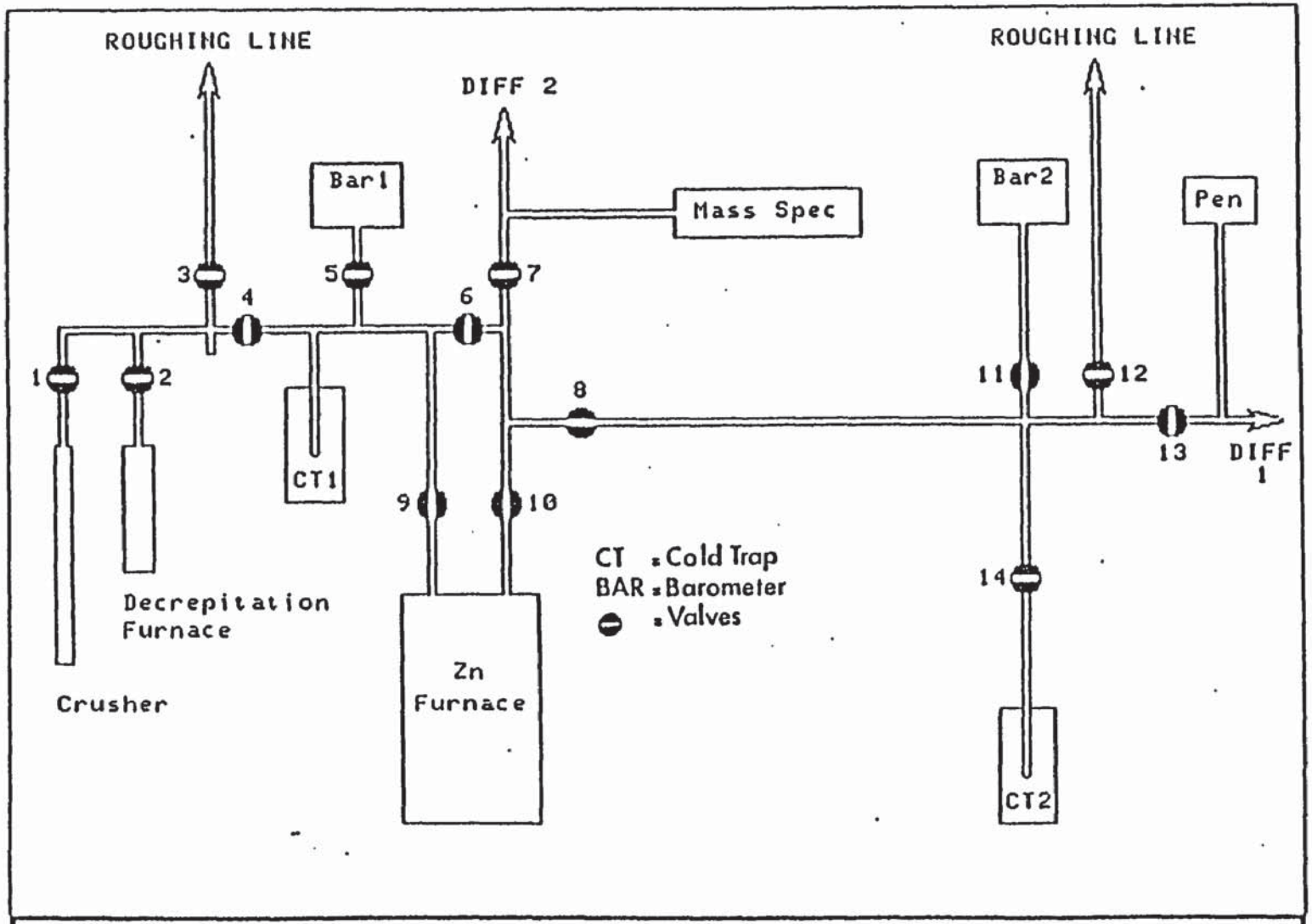

Fig. A6. Schematic Diagram of Equipment used in the Analysis of Fluid Inclusion Gas/Liquid Phases

and the dry ice mixture was slowly removed. In order to avoid moisture contamination (which is difficult to pump out) to the measuring side of the apparatus, the water was reduced to hydrogen by passing over warm zinc wire. The volume of hydrogen produced was then measured and corrected to appropriate volume of water. All necessary corrections (temperature, pressure, etc.) were calculated by on line computer facilities, and the results printed out as shown in Figures A6.1 - A6.5.

Sample no.= FWC 1
Date= 10th. March 1984

Weight of sample= 2.03 g
Gases collected in temperature interval 100 to 550 °C.

Lab. temp.= 21 °C

"Non-condensable" components:

Pressure of non-condensed gases in extraction-line system= .090 torr in 6
= .0077 cm^3 at

Sample spectrum, corrected for background measurements:

Channel	Mass	Peak height	Acc. code
1	0	1.26E-06	2
2	1	4.70E-11	2
3	2	2.27E-07	5
4	12	7.83E-09	2
5	13	4.78E-09	2
6	14	1.15E-08	2
7	15	8.18E-08	2
8	16	9.27E-08	2
9	17	1.09E-09	2
10	18	2.66E-10	2
11	28	4.28E-07	5
12	32	1.70E-11	2
13	40	3.42E-10	2
14	44	6.95E-09	2

CH_4/N_2 ratio= .44 H_2/N_2 ratio= .78 Ar/N_2 ratio= .00

"Condensable" components:

Pressure of CO_2 contained in 69cm^3 = .181 torr

H_2 pressure from H_2O reduction, expanded into 158 cm^3 = 2.319 torr

Total H_2O content= .18 mg per gram of sample.
= 9.83E-06 moles/gram of sample

Total CO_2 content= 3.35E-07 moles per gram of sample.

H_2O/CO_2 mole ratio for the given temp. interval= 29

Fluid Inclusions - gas composition data summary:

Results given are mole percent values:

H_2O= 95.13 CO_2= 3.24 H_2= .73 CH_4= .32
H_2= .57 Ar= .00

Element mole percentage values:

Mole percent C= 1.19 Mole percent H= 64.37
Mole percent O= 33.95 Mole percent N= .49

Figure A6.1 Fluid Inclusion gas/liquid phase geochemistry - Footwall Sample 1 South

Sample no.= FWC 2
Date= 10th. March 1984

Weight of sample= .86 g
Gases collected in temperature interval 100 to 550 °C.

Lab. temp.= 21 °C

"Non-condensable" components:

Pressure of non-condensed gases in extraction-line system= .038 torr in 69cm^
= .0032 cm^3 at STP

Sample spectrum, corrected for background measurements:

Channel	Mass	Peak height	Acc. code
1	0	1.16E-06	2
2	1	6.20E-11	2
3	2	2.69E-07	5
4	12	6.51E-09	2
5	13	4.20E-09	2
6	14	9.17E-09	2
7	15	6.35E-08	2
8	16	6.79E-08	2
9	17	1.10E-09	2
10	18	4.83E-10	2
11	28	3.85E-07	5
12	32	1.90E-11	2
13	40	5.01E-10	2
14	44	5.75E-09	2

CH_4/N_2 ratio= .38 H_2/N_2 ratio= 1.02 Ar/N_2 ratio= .00

"Condensable" components:

Pressure of CO_2 contained in 69cm^3 = .085 torr

H_2 pressure from H_2O reduction, expanded into 158 cm^3 = .843 torr

Total H_2O content= .15 mg per gram of sample.
= 8.43E-06 moles/gram of sample

Total CO_2 content= 3.71E-07 moles per gram of sample.

H_2O/CO_2 mole ratio for the given temp. interval= 23

Fluid Inclusions - gas composition data summary:

Results given are mole percent values:

H_2O= 93.99 CO_2= 4.14 N_2= .78 CH_4= .30
H_2= .80 Ar= .00

Element mole percentage values:

Mole percent C= 1.48 Mole percent H= 63.80
Mole percent O= 34.20 Mole percent N= .52

Figure A6.2 Fluid Inclusion gas/liquid phase geochemistry - Footwall Sample 2 South

Sample no.= O/S Bn/Carr

Original data obtained on 03.03.84
Data re-printed on 10th. March 1984

Weight of sample= 1 g

Gases collected in temperature interval 100 to 550 °C.

Lab. temp.= 22 °C

"Non-condensable" components:

Pressure of non-condensed gases = .047 torr in 41 cm^3
= .0023 cm^3 at STP

Sample spectrum, corrected for background measurements:

Channel	Mass	Peak height	Acc. code
1	0	9.84E-07	2
2	1	3.20E-11	2
3	2	2.06E-07	5
4	12	2.46E-09	2
5	13	1.51E-09	2
6	14	1.34E-08	2
7	15	2.23E-08	2
8	16	2.31E-08	2
9	17	3.91E-10	2
10	18	3.13E-10	2
11	28	4.21E-07	5
12	32	1.40E-11	2
13	40	3.17E-09	5
14	44	6.17E-09	2

CH_4/N_2 ratio= .12 H_2/N_2 ratio= .71 Ar/N_2 ratio= .00

"Condensable" components:

Pressure of CO_2 contained in 69 cm^3 = .122 torr

H_2 pressure from H_2O reduction, expanded into 158 cm^3 = 8.188 torr

Total H_2O content= 1.26 mg per gram of sample.
= 7.02E-05 moles/gram of sample

Total CO_2 content= 4.57E-07 moles per gram of sample.

H_2O/CO_2 mole ratio for the given temp. interval= 153

Fluid Inclusions - gas composition data summary:

Results given are mole percent values:

H_2O= 99.21 CO_2= .65 N_2= .08 CH_4= .01
H_2= .06 Ar= .00

Element mole percentage values:

Mole percent C= .22 Mole percent H= 66.21
Mole percent O= 33.51 Mole percent N= .05

Figure A6.3 Fluid Inclusion gas/liquid phase geochemistry
Ore-Shale Sample 1 - South

Sample no.= O/S RUT N/SIDE
Date= 10th. March 1984

Weight of sample= .9 g
Gases collected in temperature interval 100 to 550 °C.

Lab. temp.= 21 °C

"Non-condensable" components:

Pressure of non-condensed gases in extraction-line system= .038 torr in 69cm^
= .0032 cm^3 at STP

Sample spectrum, corrected for background measurements:

Channel	Mass	Peak height	Acc. code
1	0	1.38E-06	2
2	1	4.30E-11	2
3	2	2.63E-07	5
4	12	4.54E-09	2
5	13	1.47E-09	2
6	14	1.73E-08	2
7	15	2.46E-08	2
8	16	3.02E-08	2
9	17	3.81E-10	2
10	18	3.60E-10	2
11	28	6.50E-07	5
12	32	1.50E-11	2
13	40	4.67E-09	2
14	44	5.82E-09	2

CH_4/N_2 ratio= .09 H_2/N_2 ratio= .59 Ar/N_2 ratio= .00

"Condensable" components:

Pressure of CO_2 contained in 69cm^3 = .105 torr

H_2 pressure from H_2O reduction, expanded into 158 cm^3 = 5.572 torr

Total H_2O content= .96 mg per gram of sample.
= 5.33E-05 moles/gram of sample

Total CO_2 content= 4.40E-07 moles per gram of sample.

H_2O/CO_2 mole ratio for the given temp. interval= 121

Fluid Inclusions - gas composition data summary:

Results given are mole percent values:

H_2O= 98.89 CO_2= .82 N_2= .17 CH_4= .02
H_2= .10 Ar= .00

Element mole percentage values:

Mole percent C= .28 Mole percent H= 66.07
Mole percent O= 33.54 Mole percent N= .12

Figure A6.5 Fluid Inclusion gas/liquid phase geochemistry
Ore-Shale Sample 1 - North

APPENDIX 7

R-MODE CORRELATION MATRICES FOR BOREHOLE ELEMENT PAIRS. COPPERBELT BOREHOLES

R-mode correlation matrices for all element pairs were carried out on the trace element results from sixteen boreholes, and on the combined data from all these boreholes, and are shown in Tables A7.1 - A7.17. The tables are shown in the borehole order displayed in Figure 7.1, starting with Borehole AP 644 on the north limb of the North Orebody and moving anticlockwise.

	Cu	Co	Ni	Zn	Pb	Fe	Mn	Zr	Ti	Rb	Sr	Ba	Y	Nb	Th	U
Cu																
Co	-0.02															
Ni	0.06	0.51														
Zn	0.13	0.75	0.43													
Pb	0.06	0.47	0.50	0.46								Number of samples = 20				
Fe	-0.87	0.13	0.16	0.15	0.12							99.9% Fit at 0.68				
Mn	0.06	-0.47	-0.59	-0.61	-0.47	-0.30						99% Fit at 0.56				
Zr	-0.38	0.61	0.20	0.39	0.36	0.48	-0.35					95% Fit at 0.44				
Ti	-0.55	0.39	0.67	0.34	0.44	0.73	-0.56	0.57								
Rb	-0.43	0.50	0.78	0.41	0.44	0.63	-0.61	0.58	0.95							
Sr	0.37	-0.72	-0.46	-0.67	-0.49	-0.62	0.77	-0.70	-0.68	-0.70						
Ba	0.14	-0.50	0.31	-0.34	-0.17	-0.08	0.06	-0.59	-0.02	0.08	0.34					
Y	0.48	0.09	-0.04	-0.22	-0.28	-0.61	0.24	-0.20	-0.50	-0.37	-0.26	-0.02				
Nb	-0.32	0.01	0.20	-0.17	0.35	0.28	-0.11	0.22	0.54	0.40	-0.12	-0.07	-0.46			
Th	0.40	0.31	0.43	0.07	0.40	-0.36	-0.06	0.16	0.21	0.28	-0.01	0.01	0.18	0.54		
U	0.28	-0.15	-0.42	-0.22	-0.01	-0.25	0.38	-0.28	-0.24	-0.34	0.22	-0.26	0.14	0.24	0.44	

Table A7.1 Correlation coefficients for all element pairs in Borehole AP 644.

	Cu	Co	Ni	Zn	Pb	Fe	Mn	Zr	Ti	Rb	Sr	Ba	Y	Nb	Th	U
Cu								Number of Samples = 17								
Co	-0.11							99.9% Fit at 0.72								
Ni	0.20	0.65						99% Fit at 0.61								
Zn	0.52	0.50	0.49					95% Fit at 0.48								
Pb	0.30	0.37	0.31	0.51												
Fe	-0.69	0.35	0.31	-0.03	0.04											
Mn	-0.41	-0.02	-0.41	-0.06	0.32	0.22										
Zr	0.08	0.45	0.55	-0.06	-0.26	0.26	-0.53									
Ti	-0.32	0.35	0.59	-0.08	-0.02	0.67	-0.37	0.51								
Rb	-0.28	0.56	0.63	0.11	-0.04	0.52	-0.45	0.58	0.85							
Sr	-0.18	-0.65	-0.73	-0.38	-0.05	-0.26	0.51	-0.59	-0.57	-0.54						
Ba	0.41	-0.06	-0.27	0.29	0.27	-0.68	0.18	-0.35	-0.63	-0.31	0.42					
Y	0.37	0.09	-0.11	-0.03	0.14	-0.49	-0.01	0.01	-0.43	-0.43	-0.19	027				
Nb	-0.32	0.05	0.08	-0.28	-0.22	0.21	-0.32	0.61	0.36	0.553	0.05	-0.05	-0.31			
Th	0.66	-0.06	0.49	0.29	0.04	-0.35	-0.66	0.25	0.20	0.22	-0.41	0.07	0.17	0.03		
U	-0.14	-0.38	-0.25	-0.46	-0.08	-0.18	0.27	-0.32	-0.03	-0.25	0.23	0.03	0.11	-0.15	0.02	

Table A7.2 Correlation coefficients for all element pairs in Borehole AP 643.

	Cu	Co	Ni	Zn	Pb	Fe	Mn	Zr	Ti	Rb	Sr	Ba	Y	Nb	Th	U
Cu																
Co	-0.50															
Ni	0.09	0.50							Number of samples = 17							
Zn	0.07	0.48	0.29						99.9% Fit at 0.72							
Pb	-0.05	0.31	-0.15	0.57					99% Fit at 0.61							
Fe	-0.79	0.72	0.28	0.13	0.12				95% Fit at 0.48							
Mn	-0.18	-0.41	-0.85	-0.38	0.08	-0.22										
Zr	-0.13	0.60	0.48	0.42	0.09	0.40	-0.45									
Ti	-0.23	0.48	0.78	0.14	-0.22	0.55	-0.60	0.39								
Rb	-0.07	0.67	0.89	0.52	0.08	0.49	-0.81	0.55	0.85							
Sr	0.08	-0.51	-0.66	0.15	0.21	-0.46	0.65	-0.38	-0.50	-0.54						
Ba	0.33	0.04	0.33	0.75	0.26	-0.04	-0.57	0.35	0.20	0.47	0.10					
Y	0.15	0.18	0.51	0.28	0.17	0.09	-0.54	0.53	0.43	0.56	-0.25	0.47				
Nb	0.13	0.17	0.38	-0.28	-0.26	0.16	-0.28	0.42	0.19	0.16	-0.74	-0.12	0.24			
Th	0.80	-0.17	0.36	0.36	0.05	-0.56	-0.53	0.13	-0.03	0.29	-0.08	0.59	0.51	0.06		
U	0.39	-0.13	0.36	0.17	0.34	-0.09	-0.25	0.02	0.33	0.38	-0.02	0.03	0.42	0.03	0.34	

Table A7.3 Correlation coefficients for all element pairs in Borehole AP 647.

	Cu	Co	Ni	Zn	Pb	Fe	Mn	Zr	Ti	Rb	Sr	Ba	Y	Nb	Th	U
Cu																
Co	0.47															
Ni	0.44	0.88														
Zn	-0.18	0.33	0.40													
Pb	-0.28	0.21	0.23	0.63												
Fe	0.12	0.65	0.71	0.32	0.25											
Mn	-0.23	-0.64	-0.63	-0.09	0.02	-0.24										
Zr	-0.21	0.43	0.60	0.51	0.34	0.60	-0.39					Number of Samples = 17				
Ti	0.22	0.83	0.92	0.52	0.40	0.72	-0.65	0.79				99.9% Fit at 0.72				
Rb	0.09	0.77	0.88	0.51	0.34	0.76	-0.68	0.79	0.97			99% Fit at 0.61				
Sr	-0.45	-0.53	-0.42	0.24	0.23	-0.07	0.82	-0.05	-0.39	-0.40		95% Fit at 0.48				
Ba	-0.29	0.24	0.29	0.56	0.32	0.14	-0.45	0.47	0.46	0.51	0.03					
Y	-0.34	-0.11	0.15	0.57	0.42	0.19	0.13	0.56	0.30	0.31	0.50	0.63				
Nb	0.28	0.77	0.89	0.47	0.31	0.63	-0.67	0.76	0.98	0.93	-0.45	0.44	0.27			
Th	0.72	0.90	0.89	0.17	0.06	0.58	-0.66	0.35	0.79	0.71	-0.64	0.14	-0.11	0.80		
U	0.25	0.37	0.39	-0.01	-0.34	0.30	-0.56	0.16	0.27	0.36	-0.63	0.09	-0.22	0.31	0.43	

Table A7.4 Correlation coefficients for all element pairs in Borehole BV 25C.

	Cu	Co	Ni	Zn	Pb	Fe	Mn	Zr	Ti	Rb	Sr	Ba	Y	Nb	Th	U
Cu																
Co	0.57															
Ni	0.73	0.79														
Zn	-0.23	-0.03	0.04													
Pb	0.13	0.39	0.26	0.20												
Fe	0.16	0.78	0.48	-0.05	0.28						Number of Samples = 19					
Mn	0.13	0.10	-0.14	-0.14	-0.05	0.26					99.9% Fit at 0.69					
Zr	-0.45	0.04	0.13	0.28	-0.07	0.14	-0.44				99% Fit at 0.58					
Ti	0.29	0.65	0.72	0.40	0.24	0.52	-0.34	0.55			95% Fit at 0.46					
Rb	0.20	0.71	0.68	0.23	0.22	0.62	-0.42	0.56	0.94							
Sr	-0.17	-0.16	-0.28	-0.13	-0.24	0.08	0.85	-0.07	-0.35	-0.43						
Ba	-0.12	0.03	0.12	-0.02	-0.15	-0.13	-0.45	0.59	0.39	0.46	-0.16					
Y	-0.44	-0.14	-0.01	0.32	-0.20	-0.10	-0.61	0.84	0.38	0.38	-0.30	0.43				
Nb	0.16	0.38	0.61	0.36	0.08	0.14	-0.53	0.74	0.84	0.77	-0.34	0.64	0.63			
Th	0.90	0.67	0.85	-0.11	0.18	0.23	-0.14	-0.16	0.54	0.50	-0.33	0.19	-0.22	0.45		
U	-0.04	0.08	0.18	0.24	0.25	0.02	-0.36	0.29	0.38	0.38	-0.18	0.24	0.29	0.28	0.12	

Table A7.5 Correlation coefficients for all element pairs in Borehole BV 26C

	Cu	Co	Ni	Zn	Pb	Fe	Mn	Zr	Ti	Rb	Sr	Ba	Y	Nb	Th	U
Cu																
Co	0.46															
Ni	0.71	-0.20									Number of Samples = 16					
Zn	0.16	0.11	0.11								99.9% Fit at 0.74					
Pb	0.06	0.24	-0.37	0.13							99% Fit at 0.62					
Fe	-0.60	0.39	-0.09	0.11	-0.30						95% Fit at 0.50					
Mn	-0.78	0.10	-0.87	-0.05	0.10	0.17										
Zr	0.40	0.24	0.69	0.29	-0.21	0.17	-0.72									
Ti	0.35	0.13	0.73	0.36	-0.34	0.39	-0.75	0.74								
Rb	0.40	0.25	0.80	-0.02	-0.35	0.14	-0.78	0.69	0.77							
Sr	-0.07	-0.30	-0.40	-0.45	0.22	-0.44	0.39	-0.77	-0.64	-0.51						
Ba	0.81	-0.42	0.68	0.09	0.06	-0.40	-0.79	0.62	0.39	0.38	-0.28					
Y	0.58	-0.15	0.24	-0.05	0.55	-0.57	-0.49	0.29	-0.02	0.02	0.08	0.71				
Nb	0.62	-0.02	0.83	0.23	-0.10	0.01	-0.93	0.73	0.87	0.77	-0.44	0.69	0.41			
Th	0.82	-0.47	0.79	0.13	0.34	-0.29	-0.70	0.41	0.47	0.55	-0.13	0.66	0.13	0.58		
U	0.63	-0.14	0.28	0.23	0.62	-0.44	-0.56	0.30	0.21	0.05	0.04	0.68	0.87	0.55	0.24	

Table A7.6 Correlation coefficients for all element pairs in Borehole BP 58N.

	Cu	Co	Ni	Zn	Pb	Fe	Mn	Zr	Ti	Rb	Sr	Ba	Y	Nb	Th	U
Cu																
Co	0.55															
Ni	-0.18	-0.43								Number of Samples = 16						
Zn	0.26	0.65	-0.17							99.9% Fit at 0.74						
Pb	-0.46	-0.53	0.04	0.01						99% Fit at 0.62						
Fe	0.79	0.49	0.08	0.49	-0.26					95% Fit at 0.50						
Mn	0.57	0.63	-0.68	0.50	-0.30	0.46										
Zr	-0.27	-0.63	0.74	0.45	-0.46	-0.46	-0.85									
Ti	-0.58	-0.65	0.80	-0.30	0.28	-0.35	-0.87	0.93								
Rb	-0.79	-0.49	0.35	-0.07	0.26	-0.67	-0.59	0.74	0.62							
Sr	0.10	-0.24	-0.41	-0.65	-0.13	-0.23	0.25	-0.37	-0.37	-0.32						
Ba	-0.28	-0.45	0.70	-0.54	0.20	-0.24	-0.84	0.70	0.81	0.23	-0.07					
Y	-0.04	-0.18	0.64	-0.11	0.18	0.01	-0.64	0.54	0.51	0.22	-0.47	0.56				
Nb	-0.43	-0.60	0.88	-0.26	0.26	-0.18	-0.81	0.87	0.95	0.51	-0.41	-0.14	-0.52			
Th	0.40	0.49	-0.38	0.46	-0.23	0.06	0.59	-0.50	-0.56	-0.03	0.04	0.18	0.19	0.04		
U	0.39	-0.24	0.23	-0.51	-0.17	0.06	-0.16	-0.02	0.16	-0.26	0.46	0.20	0.64	-0.69	-0.05	

Table A7.7 Correlation coefficients for all element pairs in Borehole BP 55N

	Cu	Co	Ni	Zn	Pb	Fe	Mn	Zr	Ti	Rb	Sr	Ba	Y	Nb	Th	U
Cu																
Co	0.68															
Ni	-0.26	0.39								Number of Samples = 13						
Zn	-0.10	0.01	0.44							99.9% Fit at 0.80						
Pb	-0.15	0.20	0.40	0.07						99% Fit at 0.68						
Fe	0.33	0.06	-0.30	0.12	0.11					95% Fit at 0.55						
Mn	0.71	0.28	-0.60	-0.47	-0.15	0.56										
Zr	-0.72	-0.41	0.46	0.39	0.33	-0.36	-0.84									
Ti	-0.63	-0.38	0.47	0.49	0.33	-0.36	-0.85	0.96								
Rb	-0.53	-0.37	0.50	0.71	0.20	-0.19	-0.79	0.87	0.93							
Sr	0.53	0.19	-0.61	-0.68	-0.06	0.45	0.94	-0.78	-0.85	-0.87						
Ba	-0.27	0.07	0.35	-0.03	0.41	-0.71	-0.60	0.52	0.55	0.30	-0.45					
Y	-0.37	-0.10	0.35	0.16	-0.34	-0.59	-0.56	0.40	0.36	0.28	-0.53	0.35				
Nb	-0.68	-0.30	0.44	0.35	0.41	-0.40	-0.85	0.96	0.92	0.80	-0.77	0.64	0.35			
Th	-0.05	0.03	0.50	0.71	0.20	-0.12	-0.53	0.55	0.63	0.77	-0.68	0.20	-0.07	0.46		
U	-0.48	-0.47	0.33	0.14	0.11	-0.43	-0.41	0.48	0.52	0.48	-0.37	0.25	0.43	0.32	0.20	

Table A7.8 Correlation coefficients for all element pairs in Borehole AP 674.

	Cu	Co	Ni	Zn	Pb	Fe	Mn	Zr	Ti	Rb	Sr	Ba	Y	Nb	Th	U
Cu																
Co	-0.41															
Ni	0.21	-0.07									Number of Samples = 10					
Zn	-0.84	0.23	0.11								99.9% Fit at 0.87					
Pb	0.07	0.42	0.04	0.18							99% Fit at 0.77					
Fe	-0.50	0.46	0.25	0.70	0.26						95% Fit at 0.63					
Mn	0.23	-0.02	-0.55	-0.45	-0.42	-0.06										
Zr	-0.48	0.01	0.49	0.70	0.27	0.24	-0.91									
Ti	-0.11	-0.24	0.73	0.39	-0.01	0.23	-0.59	0.73								
Rb	-0.14	-0.03	0.77	0.44	-0.04	0.58	-0.31	0.50	0.86							
Sr	0.48	-0.13	-0.27	-0.66	-0.49	-0.18	0.93	-0.92	-0.45	-0.19						
Ba	0.81	-0.50	-0.16	-0.73	0.01	-0.58	0.37	-0.50	-0.28	-0.30	0.48					
Y	-0.50	0.11	0.08	0.40	0.01	-0.17	-0.61	0.69	0.23	-0.01	-0.68	-0.25				
Nb	0.30	-0.17	0.39	-0.30	-0.20	-0.02	0.03	-0.02	0.37	0.37	0.21	0.25	-0.02			
Th	0.87	-0.38	0.31	-0.65	0.19	-0.45	-0.05	-0.22	-0.09	-0.12	0.18	0.81	-0.12	0.35		
U	-0.13	-0.13	0.03	0.09	0.11	-0.43	-0.48	0.53	0.48	0.06	-0.47	-0.12	0.44	-0.13	-0.21	

Table A7.9 Correlation coefficients for all element pairs in Borehole AP 646.

	Cu	Co	Ni	Zn	Pb	Fe	Mn	Zr	Ti	Rb	Sr	Ba	Y	Nb	Th	U
Cu																
Co	-0.69															
Ni	-0.02	0.57									Number of Samples = 15					
Zn	-0.54	0.74	0.29								99.9% Fit at 0.76					
Pb	0.24	-0.24	0.12	-0.18							99% Fit at 0.64					
Fe	-0.18	-0.51	-0.62	-0.49	0.19						95% Fit at 0.51					
Mn	-0.36	-0.18	-0.72	-0.26	-0.44	0.66										
Zr	-0.43	0.75	0.40	0.86	-0.08	-0.50	-0.37									
Ti	-0.43	0.87	0.79	0.69	-0.15	-0.72	-0.51	0.67								
Rb	-0.41	0.87	0.87	0.63	0.06	-0.63	-0.58	0.68	0.95							
Sr	0.02	-0.20	-0.28	-0.40	-0.55	0.14	0.58	-0.58	-0.20	-0.37						
Ba	0.51	-0.03	0.58	-0.13	0.33	-0.33	-0.66	0.23	0.16	0.31	-0.47					
Y	0.73	-0.42	-0.08	-0.21	0.29	-0.10	-0.20	-0.02	-0.34	-0.27	-0.22	0.48				
Nb	-0.46	0.51	-0.06	0.70	-0.20	-0.20	-	0.86	0.31	0.29	-0.53	0.02	0.55			
Th	0.61	-0.72	-0.10	-0.68	0.58	0.45	-0.16	-0.53	-0.57	-0.44	-0.15	0.41	0.20	-0.52		
U	0.53	-0.21	0.49	-0.60	0.14	-0.15	-0.34	-0.46	0.03	0.10	0.20	0.57	0.23	-0.68	0.53	

Table A7.10 Correlation coefficients for all element pairs in Borehole AP 629.

	Cu	Co	Ni	Zn	Pb	Fe	Mn	Zr	Ti	Rb	Sr	Ba	Y	Nb	Th	U
Cu																
Co	0.40															
Ni	-0.01	-0.03								Number of Samples = 17						
Zn	0.35	0.49	0.48							99.9% Fit at 0.72						
Pb	0.06	-0.30	-0.02	-0.10						99% Fit at 0.61						
Fe	-0.73	-0.43	0.13	-0.04	-0.04					95% Fit at 0.48						
Mn	0.07	-0.03	-0.88	-0.46	-0.08	-0.09										
Zr	-0.18	0.17	0.55	0.14	-0.24	0.39	-0.38									
Ti	-0.58	-0.25	0.71	0.14	0.07	0.54	-0.70	0.51								
Rb	-0.43	0.24	0.78	0.24	-0.10	0.65	-0.67	0.75	0.85							
Sr	0.24	0.14	-0.81	-0.19	-0.02	-0.40	0.82	-0.65	-0.76	-0.88						
Ba	-0.02	-0.39	0.71	-0.02	0.02	-0.08	-0.55	0.14	0.53	0.44	-0.48					
Y	-0.23	-0.47	0.44	-0.03	0.07	0.41	-0.42	0.31	0.37	0.57	-0.57	0.47				
Nb	-0.32	-0.45	0.72	-0.12	0.06	0.43	-0.62	0.59	0.80	0.81	-0.79	0.70	0.60			
Th	0.67	0.23	0.56	0.49	-0.10	-0.39	-0.42	0.05	-0.04	0.12	-0.31	0.49	0.10	0.20		
U	0.51	0.52	0.02	0.16	-0.05	-0.54	-0.03	-0.07	0.37	-0.33	0.14	-0.06	-0.35	-0.34	0.44	

Table A7.11 Correlation coefficients for all element pairs in Borehole AD 203.

	Cu	Co	Ni	Zn	Pb	Fe	Mn	Zr	Ti	Rb	Sr	Ba	Y	Nb	Th	U
Cu																
Co	-0.31															
Ni	-0.41	0.20								Number of Samples = 12						
Zn	-0.61	0.21	0.26							99.9% Fit at 0.82						
Pb	-0.19	0.08	-0.42	0.25						99% Fit at 0.71						
Fe	-0.07	0.46	0.09	-0.37	-0.23					95% Fit at 0.58						
Mn	-0.06	0.84	-0.12	0.21	0.06	0.51										
Zr	-0.23	-0.69	-0.07	0.21	0.24	-0.36	-0.51									
Ti	-0.20	-0.62	-0.08	0.24	0.18	-0.27	0.36	0.98								
Rb	-0.61	-0.39	0.44	0.53	0.10	-0.28	-0.42	0.81	0.78							
Sr	-0.57	0.50	0.23	0.46	0.26	-0.15	0.16	-0.35	0.45	0.03						
Ba	-0.69	-0.31	0.22	0.49	0.25	-0.43	-0.45	0.68	0.57	0.83	0.41					
Y	-0.17	-0.40	-0.46	-0.04	0.01	0.02	-0.14	0.48	0.51	0.17	-0.30	0.28				
Nb	-0.19	-0.53	0.08	0.19	0.18	-0.33	-0.37	0.84	0.82	0.76	-0.17	0.66	0.30			
Th	0.63	-0.68	-0.60	-0.57	-0.17	-0.05	-0.32	0.41	0.43	-0.10	-0.75	-0.17	0.44	0.26		
U	0.13	0.17	0.12	0.05	0.11	-0.29	-0.07	-0.35	-0.44	-0.18	0.50	0.06	-0.62	-0.32	-0.23	

Table A7.12 Correlation coefficient for all element pairs in Borehole AP 982.

	Cu	Co	Ni	Zn	Pb	Fe	Mn	Zr	Ti	Rb	Sr	Ba	Y	Nb	Th	U
Cu																
Co	0.38															
Ni	0.11	0.47								Number of Samples = 21						
Zn	0.21	0.36	0.31							99.9% Fit at 0.66						
Pb	0.30	0.62	0.39	0.32						99% Fit at 0.55						
Fe	-0.01	-0.12	0.05	-0.45	-0.05					95% Fit at 0.43						
Mn	0.12	0.29	-0.56	0.05	-	0.04										
Zr	-0.29	-0.44	0.12	-0.31	-0.35	0.21	-0.58									
Ti	-0.22	-0.66	0.19	-0.37	-0.45	0.45	-0.70	0.73								
Rb	-0.01	-0.50	0.31	-0.13	-0.19	0.20	-0.81	0.66	0.86							
Sr	-0.38	0.12	-0.33	0.31	-0.10	-0.60	0.46	-0.35	-0.66	-0.65						
Ba	0.20	-0.43	0.20	0.04	-0.19	-0.12	-0.71	0.53	0.60	0.87	-0.39					
Y	-0.30	-0.34	0.28	-0.36	-0.48	0.43	-0.44	0.74	0.67	0.49	-0.24	0.38				
Nb	-0.10	-0.58	0.18	-0.36	-0.43	0.37	-0.70	0.81	0.95	0.85	-0.67	0.64	0.68			
Th	0.25	0.28	0.62	0.15	0.17	-0.37	-0.60	0.30	0.11	0.30	-0.14	0.42	0.22	0.27		
U	0.09	0.13	0.16	0.53	-0.01	-0.35	-0.01	0.04	-0.18	-0.08	0.32	0.08	-0.12	-0.08	0.37	

Table A7.13 Correlation coefficients for all element pairs in Borehol CP 197.

	Cu	Co	Ni	Zn	Pb	Fe	Mn	Zr	Ti	Rb	Sr	Ba	Y	Nb	Th	U
Cu																
Co	-0.32															
Ni	0.59	-0.08								Number of Samples = 29						
Zn	0.44	-0.59	0.73							99.9% Fit at 0.58						
Pb	0.19	-0.21	-0.13	-0.02						99% Fit at 0.47						
Fe	0.77	-0.39	0.77	0.73	-0.06					95% Fit at 0.37						
Mn	-0.05	0.25	-0.29	-0.50	0.14	-0.28										
Zr	0.68	-0.29	0.45	0.44	0.38	0.53	-0.20									
Ti	0.71	-0.43	0.66	0.70	0.13	0.81	-0.34	0.86								
Rb	0.51	-0.48	0.80	0.88	-0.02	0.78	-0.56	0.62	0.86							
Sr	-0.30	-0.01	-0.50	-0.38	0.51	-0.64	0.42	-0.04	-0.39	-0.49						
Ba	-0.53	0.39	-0.56	-0.67	0.03	-0.80	0.21	-0.54	-0.80	-0.70	0.35					
Y	0.66	-0.26	0.5	0.44	0.32	0.39	-0.05	0.73	0.58	0.42	0.13	-0.38				
Nb	0.62	-0.28	0.53	0.51	0.26	0.62	-0.29	0.92	0.75	-0.22	-0.59	0.58				
Th	0.79	-0.08	0.49	0.23	0.17	0.71	0.04	0.52	0.54	0.34	0.03	0.55	0.45	0.51		
U	-0.76	0.30	-0.52	-0.37	-0.25	-0.56	-0.01	-0.78	-0.73	-0.49	0.03	-0.21	-0.70	-0.71	-0.61	
C	0.59	-0.34	0.37	0.32	0.28	0.38	0.05	0.76	0.59	0.38	0.16	-0.32	-0.67	0.63	0.37	-0.7

Table A7.14 Correlation coefficients for all element pairs in Borehole CP 337.

	Cu	Co	Ni	Zn	Pb	Fe	Mn	Zr	Ti	Rb	Sr	Ba	Y	Nb	Th	U
Cu																
Co	0.34															
Ni	0.03	0.73								Number of Samples = 20						
Zn	-0.13	-0.09	0.27							99.9% Fit at 0.68						
Pb	0.13	0.42	0.53	0.31						99% Fit at 0.56						
Fe	0.22	-0.12	-0.19	0.21	0.29					95% Fit at 0.44						
Mn	-0.15	-0.32	-0.18	0.69	0.15	0.54										
Zr	0.46	-0.22	-0.32	-0.21	-0.30	0.17	-0.20									
Ti	-0.28	-0.14	-0.04	-0.25	-0.38	-0.39	-0.43	0.38								
Rb	-0.13	0.26	0.53	0.21	0.30	-0.03	-0.25	0.01	0.26							
Sr	0.62	0.02	-0.33	-0.17	-0.37	0.24	-.013	0.37	0.17	-0.15						
Ba	0.69	-	-0.17	-0.20	-0.28	0.07	-0.28	0.74	0.28	0.04	0.85					
Y	0.65	0.21	-0.19	-0.36	-0.21	0.20	-0.11	0.44	0.16	-0.17	0.64	0.59				
Nb	0.01	-0.17	-0.28	-0.18	-0.44	-0.06	-0.08	0.35	0.51	-0.15	0.51	0.31	0.35			
Th	0.34	-0.02	-0.03	-0.08	0.11	0.13	-0.33	0.36	0.28	0.28	0.34	0.36	0.15	0.19		
U	-0.55	-0.08	0.16	0.36	0.12	-0.38	0.32	-0.40	0.01	0.01	-0.39	-0.36	-0.48	0.03	-0.41	

Table A7.15 Correlation cofficients for all element pairs in Borehole AP 978.

	Cu	Co	Ni	Zn	Pb	Fe	Mn	Zr	Ti	Rb	Sr	Ba	Y	Nb	Th	U
Cu																
Co	0.22															
Ni	0.51	0.10								Number of Samples = 17						
Zn	0.52	0.18	0.75							99.9% Fit at 0.72						
Pb	-0.18	-0.04	-0.50	-0.46						99% Fit at 0.61						
Fe	0.15	0.38	-0.12	0.16	0.23					95% Fit at 0.48						
Mn	-0.27	0.37	-0.43	0.03	0.03	0.54										
Zr	0.35	-0.07	0.47	0.32	0.19	-0.02	-0.33									
Ti	0.23	0.21	0.13	0.11	0.28	0.56	0.19	0.72								
Rb	0.56	-0.13	0.62	0.46	-	0.11	-0.21	0.90	0.72							
Sr	-0.21	0.12	0.21	o.3o	-0.65	-0.29	0.16	-0.57	-0.69	-0.42						
Ba	0.30	-0.42	0.51	0.31	0.24	-0.68	-0.66	0.43	-0.25	0.33	0.12					
Y	0.11	-0.09	0.19	0.04	0.39	-0.15	-0.21	0.81	0.60	0.71	-0.67	0.22				
Nb	0.04	-0.41	0.14	-0.17	0.34	-0.27	-0.48	0.57	0.28	0.49	-0.61	0.34	0.76			
Th	0.47	0.14	0.39	0.42	0.26	-0.05	-0.22	0.89	0.56	0.79	-0.54	0.48	0.76	0.48		
U	0.60	0.23	0.18	0.14	0.10	-0.09	-0.16	0.57	0.48	0.37	-0.46	0.22	0.57	0.33	0.60	

Table A7.16 Correlation coefficients for all element pairs in Borehole AP 972.

	Cu	Co	Ni	Zn	Pb	Fe	Mn	Zr	Ti	Rb	Sr	Ba	Y	Nb	Th	U
Cu																
Co	0.110															
Ni	0.034	0.109								Number of Samples = 278						
Zn	0.082	0.241	0.263							99.9% Fit at 0.194						
Pb	0.156	0.041	0.030	0.304						99% Fit at 0.153						
Fe	-0.231	0.193	0.090	0.260	0.009					95% Fit at 0.117						
Mn	-0.104	0.125	-0.307	-0.024	-0.072	0.239										
Zr	-0.223	-0.255	0.351	0.154	0.055	0.094	-0.335									
Ti	0.226	-0.171	0.433	0.158	-0.023	0.329	-0.301	0.771								
Rb	-0.182	-0.103	0.529	0.266	0.060	0.202	-0.459	0.661	0.786							
Sr	0.064	0.029	-0.258	-0.062	0.005	-0.171	0.475	-0.373	-0.483	-0.415						
Ba	0.145	-0.155	0.065	0.015	0.184	-0.284	-0.130	0.065	-0.074	0.118	0.207					
Y	0.157	-0.198	0.168	0.012	0.086	0.019	-0.230	0.463	0.318	0.243	-0.208	0.147				
Nb	-0.173	-0.236	0.278	-0.041	-0.071	0.026	-0.435	0.690	0.658	0.581	-0.470	0.070	0.376			
Th	0.422	-0.039	0.326	0.127	0.140	0.003	-0.319	0.376	0.322	0.345	-0.367	-0.013	0.338	0.341		
U	0.080	0.053	0.048	0.147	0.085	-0.241	-0.110	0.032	0.044	0.081	-0.090	0.177	-0.062	0.060	0.079	

Table A7.17 Correlation coefficients for all element pairs in all Boreholes.

APPENDIX 8

TRACE ELEMENT CONCENTRATION PROFILES - COPPERBELT BOREHOLE CORES

Trace element concentration profiles for the sixteen borehole cores analysed are shown in Figures A8.1 - A8.16. The figures refer to the boreholes in the order shown in the borehole location plan (Figure 7.1), and are comparable with the figure numbers in Appendix 7. All the results are quoted in parts per million and the sample interval is approximately 0.5 m. All boreholes were drilled approximately perpendicular to strike, and intersect the plane of the orebody at right angles. Abbreviations used in describing lithologies are shown below.

Abbreviations	Lithology
HWQ	Hangingwall Quartzite
E	Unit E
D	Unit D
C	Unit C
B	Unit B
A	Unit A
FWC	Footwall Conglomerate

APPENDIX 9

R-MODE CORRELATION MATRICES FOR BOREHOLE ELEMENT PAIRS

MARL SLATE BOREHOLES

R-mode correlation matrices for all element pairs were carried out on four borehole cores from the Marl Slate, and are shown in Tables A9.1 - A9.4.

	Cu	Co	Ni	Zn	Nb	Fe	Mn	Zr	Ti	Nb	Sr	Ba	Y	Nb	Th	U	$\delta^{13}C$	$\delta^{18}O$
Cu																		
Co	0.93																	
Ni	0.68	0.60																
Zn	0.85	0.71	0.64															
Nb	-	-0.10	0.28	-0.14														
Fe	0.18	0.15	0.16	0.06	0.70													
Mn	0.57	0.77	0.32	0.25	0.12	0.44												
Zr	0.65	-0.80	-0.44	-0.36	-0.37	-0.56	-0.91											
Ti	-0.40	-0.37	-0.48	-0.47	-0.38	-0.36	-0.29	0.41										
Nb	-0.50	-0.63	-0.33	-0.19	-0.48	-0.72	-0.91	0.95	0.42									
Sr	0.34	0.18	0.03	0.36	-0.64	-0.58	-0.37	0.35	0.15	0.53								
Ba	-0.32	-0.46	-0.26	-0.13	-0.22	-0.46	-0.69	0.65	0.27	0.70	0.49							
Y	0.90	0.89	0.62	0.59	-0.13	0.19	0.66	-0.65	-0.33	-0.53	0.34	-0.40						
Nb	-0.70	-0.73	-0.30	-0.43	-0.33	-0.39	-0.65	0.86	0.32	0.74	0.11	0.54	0.54					
Th	-0.14	-0.15	-0.19	-0.06	-0.37	0.06	-0.16	0.26	0.53	0.23	0.17	-0.25	-0.02	0.15				
U	0.76	0.78	0.44	0.44	0.40	0.51	0.76	-0.92	-0.39	-0.83	-0.20	-0.49	0.62	-0.92	-0.28			
$\delta^{13}C$	0.57	0.72	0.34	0.27	0.02	0.43	0.91	-0.78	-0.33	-0.81	-0.20	-0.80	0.74	-0.51	0.02	0.61		
$\delta^{18}O$	-0.52	-0.71	0.27	0.28	-0.12	0.37	-0.90	-0.71	-0.29	-0.75	-0.25	-0.70	0.71	-0.41	0.03	0.32	0.97	

Number of Samples = 13
99.9% Plt at 0.80
99% Plt at 0.68
95% Plt at 0.55

Table A9.1 Correlation coefficients for all element pairs in Borehole J1000.

	Cu	Ni	Zn	Pb	Fe	Mn	Zr	Ti	Rb	Sr	Ba	Y	Nb	Th	U	SiO_2
Cu																
Ni	-0.37															
Zn	-0.18	0.76							Number of Samples = 16							
Pb	-0.33	0.68	0.83						99.9% Fit at 0.94							
Fe	-0.06	0.60	0.79	0.66					99% Fit at 0.62							
Mn	0.43	-0.53	-0.60	-0.59	-0.66				95% Fit at 0.50							
Zr	-0.49	0.97	0.78	0.74	0.55	-0.58										
Ti	-0.37	0.52	0.40	0.47	0.51	-0.55	0.49									
Rb	-0.64	0.78	0.80	0.81	0.43	-0.66	0.85	0.50								
Sr	0.66	-0.71	-0.67	-0.78	-0.34	0.51	-0.82	-0.34	-0.87							
Ba	0.19	0.53	0.84	0.66	0.74	-0.37	0.54	0.09	0.47	-0.37						
Y	0.14	0.50	0.20	-0.08	0.36	-0.25	0.35	0.38	0.08	0.09	0.13					
Nb	-0.03	0.59	0.29	0.44	0.36	-0.33	0.57	0.31	0.34	-0.30	0.21	0.41				
Th	-0.45	0.77	0.56	0.60	0.23	-0.49	0.81	0.34	0.80	-0.76	0.25	0.21	0.53			
U	-0.29	0.83	0.64	0.54	0.63	-0.42	0.83	0.36	0.60	-0.63	0.59	0.39	0.43	0.48		
SiO_2	-0.25	0.32	0.46	0.43	0.32	-0.55	0.40	0.43	0.50	-0.23	0.39	0.26	0.30	0.21	0.11	

Table A9.2 Correlation coefficients for all element pairs in Borehole 49/26-4.

	Cu	Co	Ni	Zn	Pb	Fe	Mn	Zr	Tl	Rb	Sr	Ba	Y	Nb	Th	U	$\alpha_{C_{org}}$	$\alpha_{\delta^{13}C}$	$\alpha_{\delta^{34}S}$	$\alpha_{S_{py}}$	$\alpha_{\delta^{18}O}$	$\alpha_{C_{carb}}$	α_{Qtz}
Cu																							
Co	0.66																						
Ni	0.93	0.56																					
Zn	0.68	0.18	0.70																				
Pb	0.74	0.21	0.72										Number of Sample			Trace Elements n = 100				α others		n = 25	
Fe	0.63	0.47	0.61	0.36	0.64																		
Mn	-0.65	-0.39	-0.64	-0.50	-0.61	-0.41										99.9%	Fit at 0.32				0.62		
Zr	0.64	0.43	0.68	0.36	0.69	0.72	-0.72									99%	Fit at 0.26				0.51		
Tl	0.77	0.60	0.78	0.44	0.70	0.86	-0.67	0.91								95%	Fit at 0.20				0.40		
Rb	0.85	0.63	0.84	0.51	0.74	0.81	-0.69	0.97															
Sr	0.54	0.43	0.44	0.16	-0.19	-0.34	-0.05	0.06	0.18														
Ba	0.49	0.36	0.52	0.26	0.54	0.68	-0.62	0.87	0.84	0.81	-0.09												
Y	0.73	0.65	0.63	0.36	0.33	0.24	-0.58	0.48	0.47	0.56	0.61	0.25											
Nb	0.64	0.49	0.69	0.29	0.66	0.76	-0.66	0.93	0.67	0.86	-0.09	0.78	0.48										
Th	0.74	0.43	0.76	0.53	0.80	0.76	-0.67	0.85	0.87	0.87	0.07	0.75	0.45	0.82									
U	0.20	0.26	0.17	0.06	-0.02	0.09	-0.17	0.16	0.17	0.20	0.19	0.17	0.29	0.18	0.12								
$\alpha_{C_{org}}$	0.83	0.35	0.78	0.77	0.89	0.63	-0.44	0.65	0.69	0.71	0.27	0.48	0.36	0.68	0.74	0.11							
$\alpha_{\delta^{13}C}$	0.07	-0.13	0.15	0.19	0.38	0.36	-0.12	0.30	0.29	0.30	-0.41	0.51	-0.57	0.19	0.28	-0.26	0.15						
$\alpha_{\delta^{34}S}$	-0.07	-0.40	-0.01	0.14	0.08	-0.12	-0.11	0.08	-0.09	-0.06	-0.18	0.12	-0.23	0.03	-0.04	0.18	0.17	0.30					
$\alpha_{S_{py}}$	0.70	0.63	0.57	0.39	0.50	0.64	-0.17	0.60	0.70	0.66	0.17	0.53	0.59	0.69	0.63	0.12	0.49	-0.31	0.13				
$\alpha_{\delta^{18}O}$	-0.42	0.08	-0.41	-0.63	-0.52	-	0.33	-0.19	-0.12	-0.16	-0.53	-0.06	-0.28	-0.12	-0.35	-0.11	-0.63	0.16	0.23	0.19			
$\alpha_{C_{carb}}$	-0.71	-0.55	-0.61	-0.43	-0.52	-0.54	0.33	-0.65	-0.68	-0.68	-0.29	-0.42	-0.80	-0.71	-0.69	-0.22	-0.55	0.40	-0.30	-0.82	-0.32		
α_{Qtz}	0.16	0.06	0.26	0.31	0.25	0.27	-0.18	0.45	0.33	0.27	-0.16	0.27	0.34	0.33	0.36	-0.15	0.14	-0.08	-0.14	0.36	0.02	-0.34	

Table A9.3 Correlation coefficients for all element pairs in the Marl Slate Section of the Doncaster core

	Cu	Co	Ni	Zn	Pb	Fe	Mn	Zr	Tl	Rb	Sr	Ba	Y	Nb	Th	U	C_{org}	$\delta^{13}C$	$\delta^{34}S$	S_{py}	$\delta^{18}O$	C_{carb}	Qtz
Cu																							
Co	0.34																						
Ni	0.62	0.77																					
Zn	0.22	0.06	-0.01																				
Pb	0.54	0.63	0.69	0.52									Number of Samples = 29										
Fe	-0.15	0.68	0.61	-0.03	0.38								99.9% Fit at 0.58										
Mn	-0.65	0.09	-0.14	-0.07	-0.17	0.60							99% Fit at 0.47										
Zr	0.73	0.72	0.91	0.20	0.72	0.42	-0.36						95% Fit at 0.37										
Tl	0.18	0.67	0.77	0.01	0.42	0.81	0.32	0.62															
Rb	0.67	0.79	0.97	0.06	0.72	0.53	-0.25	0.97	0.69														
Sr	0.24	-0.52	-0.40	0.57	-0.10	-0.66	-0.41	-0.11	-0.47	-0.31													
Ba	0.37	0.04	0.14	0.80	0.38	-0.03	-0.18	0.39	0.18	0.20	0.71												
Y	0.63	0.78	0.93	0.23	0.80	0.55	-0.21	0.91	0.72	0.93	-0.30	0.27											
Nb	0.49	0.70	0.90	0.08	0.72	0.55	-0.17	0.88	0.69	0.90	-0.30	0.22	0.88										
Th	0.23	0.53	0.65	-0.13	0.53	0.50	0.04	0.53	0.56	0.61	-0.55	-0.21	0.63	0.66									
U	0.62	0.37	0.61	0.06	0.27	0.23	-0.25	0.67	0.52	0.66	0.03	0.31	0.53	0.48	0.27								
C_{org}	0.18	0.37	0.61	0.10	0.62	0.56	0.09	0.51	0.46	0.56	-0.26	0.17	0.53	0.68	0.41	0.27							
$\delta^{13}C$	-0.50	0.22	-0.07	-0.35	-0.29	0.37	0.64	-0.24	0.15	-0.13	-0.50	-0.47	-0.18	-0.12	0.16	-0.20	-0.18						
$\delta^{34}S$	-0.16	-0.78	-0.77	0.01	-0.54	-0.82	-0.30	-0.66	-0.72	-0.75	0.54	-	-0.69	-0.74	-0.74	-0.43	-0.50	-0.29					
S_{py}	0.69	0.56	0.78	0.22	0.74	0.27	-0.40	0.84	0.39	0.81	-0.06	0.33	0.84	0.82	0.38	0.38	0.57	-0.44	-0.45				
$\delta^{18}O$	0.12	0.71	0.53	-0.02	0.35	0.56	0.16	0.46	0.49	0.55	-0.42	-0.08	0.44	0.45	0.48	0.32	0.18	0.46	0.72	0.13			
C_{carb}	-0.61	-0.73	-0.92	-0.06	-0.70	-0.50	0.36	-0.94	-0.62	-0.96	0.31	-0.19	-0.92	-0.90	-0.60	-0.57	-0.60	0.22	-0.68	-0.83	0.46		
Qtz	0.55	0.71	0.86	0.01	0.61	0.48	-0.27	0.88	0.58	0.89	-0.33	0.14	0.84	0.82	0.56	0.53	0.47	-0.07	-0.67	0.71	-0.43	-0.91	

Table A9.4 Correlation coefficients for all element pairs in the Transition Zone Section of the Doncaster Core.

APPENDIX 10

TRACE ELEMENT CONCENTRATION PROFILES - MARL SLATE BOREHOLE CORES

Trace element concentration profiles for the four borehole cores analysed are shown in Figures A10.1 - A10.4. The figures refer to boreholes in the order; J1000, 49/26-4, and Marl Slate and Transition Zone cores of the Doncaster Core. All results are quoted in parts per million, and the sample interval is approximately two centimetres. Borehole cores J1000 and 49/26-4 are sapropelic throughout their length. The different lithology types in the Doncaster Core are colour coded in the figures as shown below.

Transition Zone Section

Lithology	Colour in Figure
Calcite-rich	Yellow
Sapropel	Red
Dolomite-rich	Blank

Marl Slate Section

Lithology	Colour in Figure
Laminated organic carbonate (mainly dolomite)	Blue
Laminated organic carbonate (mainly calcite)	Yellow
Sapropel	Red

APPENDIX 11

ELECTRON MICROPROBE ANALYSIS

Three different electron microscopes were employed during the course of this study, they were:-

(a) Scanning electron microscope with a Link 850 energy dispersive analysing unit.

(b) Cambridge Microscane Mk 5 microprobe

(c) C.A.M.E.C.H. CAMBEX microprobe.

Samples were coated under vacuum by either carbon (a 20 nm layer) for polished sections, or gold palladium in the case of rock chips.

The scanning electron microscope (SEM) was used to analyse both rock chips and polished sections. All fluid inclusion mineral phases and decrepitation products were analysed using the SEM with on line Link 850 energy dispersive analysis. The Link 850 analysing unit was also employed to confirm the composition of mineral phases observed during the examination of rock chips, and to determine the composition of Footwall dolomites (polished sections). All corrections including the matrix correction factors (ZAF) were made using a program patented by Link Systems Limited. A count time of 100 seconds was used for all analysis.

The Cambridge Microscan Mk 5 microprobe was used to analyse carrollite and cobaltiferous pyrite samples. An accelerating voltage of 15 kV, current of approximately 5 nA and a count time of 100 seconds was used during all anlayses. Peak and background counts were corrected for dead time before calculation of the unknown value by comparison with the standard counts. The uncorrected value was then corrected for atomic number, absorption and flourescence effects using the program devised by Sweatman and Long (1969).

The remaining microprobe analyses, which constitutes the bulk of the microprobe data presented were made using the Manchester University C.A.M.E.C.A. CAMBEX system. This machine is fitted with two wavelength dispersive spectrometers (WDS) and a Link 850 - 500 energy dispersive system (EDS), it has on-line correction facilities and is fully automated. For any mineral, the major element composition was determined using energy dispersive system analysis, while trace element concentration was determined by wavelength dispersive analysis. The count time used was 200 seconds for EDS anlaysis and 150 seconds for WDS analysis. An accelerating voltage of 15 kV and a beam current of 14.5 nA was used for all analyses. The ZAF correction program used was modified after that of Duncomb and Reed (1968) and Yakowitz et al. (1973).